

GABRB3 Point Mutations Cause a Range of Epilepsy:
Genetic Cases of Lennox-Gastaut Syndrome and Childhood Absence Epilepsy

By

Mackenzie Alice Catron

Dissertation

Submitted to the Faculty of the
Graduate School of Vanderbilt University

in partial fulfillment of the requirements

for the degree of

DOCTOR OF PHILOSOPHY

In

Neuroscience

August 7, 2020

Nashville, Tennessee

Approved:

Martin J Gallagher, M.D., Ph.D.

Fiona Harrison, Ph.D.

Brad Greuter, Ph.D.

Kevin Currie, Ph.D.

Robert L. Macdonald, M.D., Ph.D.

Copyright © 2020 by Mackenzie Alice Catron
All Rights Reserved

TABLE OF CONTENTS

| | Page |
|---------------------------------------------------------------|------|
| LIST OF FIGURES | ix |
| LIST OF TABLES..... | xii |
| Chapter | |
| 1. Introduction | 1 |
| Seizures and epilepsy | 1 |
| Definition of epilepsy | 1 |
| Introduction to epileptic encephalopathies | 2 |
| Types of seizures in epileptic encephalopathies | 5 |
| Types of epileptic encephalopathy | 9 |
| GABA _A receptors..... | 13 |
| General function..... | 13 |
| Structure..... | 17 |
| Common dysfunction | 19 |
| Drug binding domains | 21 |
| The $\beta 3$ subunit of the GABA _A receptor | 23 |
| Overview..... | 23 |
| Variants 1 and 2..... | 25 |
| Genomic interactions..... | 26 |
| Disorders associated with chromosome 15q11-13..... | 29 |
| Information gathered from <i>Gabrb3</i> mouse studies | 30 |
| Need for mouse models..... | 32 |
| Typical absence models..... | 32 |
| Atypical absence seizure (AAS) models | 35 |
| Moving forward | 36 |
| Bibliography | 37 |
| 2. Materials and Methods..... | 43 |
| Mouse husbandry and data fidelity | 43 |
| Video-EEG recordings and analysis | 44 |
| Behavioral testing..... | 46 |
| Elevated zero maze..... | 47 |
| Locomotor activity tests | 48 |
| 3-chamber socialization test (3CST) | 49 |
| Barnes maze | 51 |
| Sense of smell | 55 |
| Biochemistry | 60 |
| Electrophysiology | 61 |

| | |
|-------------------------------------------------------------------------------------------------------------------------------------------------------------------------------------------------|-----|
| Whole-cell slice recording | 61 |
| Thalamocortical oscillations | 62 |
| Statistical analysis | 63 |
| Bibliography | 64 |
| | |
| 3. A Knock-in Mouse Harboring a Patient-Derived Disease-Associated Mutation, <i>Gabrb3</i> ^{+D120N} , Recapitulates the Full Triad of Features of the Lennox-Gastaut Syndrome | 66 |
| | |
| Introduction | 66 |
| Lennox-Gastaut syndrome | 69 |
| General information | 69 |
| Genetics of LGS | 70 |
| Seizures associated with LGS | 70 |
| Cognitive dysfunction in LGS | 71 |
| Treatments used in LGS | 73 |
| Outcomes for patients with LGS | 78 |
| The D120N patient | 78 |
| The D120N mutation | 79 |
| <i>In vitro</i> data | 80 |
| Materials and methods | 82 |
| Generation of the <i>Gabrb3</i> ^{+D120N} KI mouse | 82 |
| RT-PCR | 83 |
| Postnatal spasm observations | 83 |
| Behavioral testing | 83 |
| AED treatment of LGS KI mice | 84 |
| Statistical analysis and data availability | 85 |
| Generating the mouse | 85 |
| Genetic approach | 85 |
| <i>Gabrb3</i> ^{+D120N} mice had increased mortality, reduced body weight, and other abnormalities | 88 |
| Seizure phenotype of the mouse | 89 |
| <i>Gabrb3</i> ^{+D120N} mice had seizure semiologies and ictal EEG patterns consistent with LGS | 89 |
| Behavioral phenotype of the KI mouse | 97 |
| <i>Gabrb3</i> ^{+D120N} mice had impaired spatial learning and memory | 97 |
| Addressing potential confounding factors in behavioral testing | 108 |
| Cellular profile in wild type and KI mice | 115 |
| Electrophysiological findings | 117 |
| mIPSCs recorded from SS cortex layer V/VI pyramidal neurons of <i>Gabrb3</i> ^{+D120N} mice had reduced amplitude | 117 |
| Thalamocortical oscillations recorded from VBn neurons of <i>Gabrb3</i> ^{+D120N} mice had prolonged duration | 120 |
| Therapeutics in mice | 122 |
| Discussion | 126 |
| The <i>Gabrb3</i> ^{+D120N} KI mouse is a model of human LGS | 126 |
| <i>Gabrb3</i> ^{+D120N} mice had seizure semiologies like those of LGS patients. | 127 |
| <i>Gabrb3</i> ^{+D120N} mice exhibited behavioral comorbidities like those of LGS patients.. | 128 |

| | |
|------------------------------------------------------------------------------------------------------------------------------------------------------------------------------------------------|-----|
| Cortical layer V/VI neurons in thalamocortical slices from <i>Gabrb3</i> ^{+D120N} mice showed decreased inhibition..... | 129 |
| Existing relevant mouse models..... | 131 |
| How this mouse fits into future of LGS therapies..... | 133 |
| Network disturbances in <i>Gabrb3</i> ^{+D120N} mice provide opportunities for discovery.... | 135 |
| Bibliography | 136 |
| 4. A Knock-in Mouse Harboring a Patient-Derived Disease-Associated Mutation, <i>Gabrb3</i> ^{+P11S} , Recapitulates Both Childhood Absence Epilepsy and Autism Spectrum Disorder | 143 |
| Introduction..... | 143 |
| Childhood absence epilepsy | 145 |
| Overview..... | 145 |
| Genetics of CAE..... | 146 |
| ASD in CAE..... | 147 |
| GABA _A receptors: an overlap between ASD and CAE genetics..... | 147 |
| Treatment of CAE | 148 |
| Outcome and prognosis of CAE..... | 148 |
| Thalamocortical circuitry in TASs and CAE..... | 149 |
| Patient background..... | 150 |
| Location and functional impact of mutation..... | 154 |
| Materials and methods..... | 155 |
| Generation of <i>Gabrb3</i> ^{+P11S} knock-in mice | 155 |
| Published <i>in vitro</i> data..... | 157 |
| Seizure phenotype of the P11S KI mouse | 158 |
| Behavioral phenotype of mouse..... | 160 |
| <i>Gabrb3</i> ^{+P11S} mice displayed abnormal social preferences..... | 160 |
| <i>Gabrb3</i> ^{+P11S} mice did not have additional cognitive deficits..... | 163 |
| Cellular profile in mouse | 167 |
| Electrophysiology in <i>ex vivo</i> slices | 169 |
| <i>Gabrb3</i> ^{+P11S} mice had reduced mIPSC amplitudes in SS cortex layer V/VI pyramidal neurons..... | 169 |
| Discussion | 171 |
| The P11S mutation is involved in the pathogenesis of CAE..... | 171 |
| Bibliography | 174 |
| 5. Conclusions and Future Directions..... | 177 |
| Summary of findings..... | 177 |
| The role of GABA _A receptor β3 subunits..... | 179 |
| Thalamocortical circuitry and the hippocampus..... | 181 |
| Future directions: viral gene therapy..... | 182 |
| Introduction to lentivirus (LV) and adeno-associated virus (AAV) | 183 |
| Introduction to CRISPR..... | 185 |
| Viral gene therapy | 187 |
| Future directions: using viruses to further scientific knowledge..... | 188 |

| | |
|-------------------------------------------|-----|
| Introduction to rabies virus | 189 |
| Introduction to the Cre/loxP system | 190 |
| Proposed experiments | 194 |
| Bibliography | 208 |

LIST OF FIGURES

| Figure | Page |
|---------------------------------------------------------------------------------------------------------------------------------------|------|
| Chapter 1 | |
| 1: GABA _A receptor structure overview | 16 |
| 2: <i>GABRB3</i> expression in humans and <i>Gabrb3</i> expression in mice (Allen Brain Atlas)..... | 25 |
| 3: Chromosome 15q11-13 genetic regulation schematic..... | 27 |
| 4: Comparison of wild-type mouse of $\beta 3$, $\beta 1$, and $\beta 2$ subunit RNA expression at P56 (from Allen Brain Atlas)..... | 31 |
| 5: Thalamocortical oscillations in TASs are facilitated by low-threshold T-type calcium channel bursting..... | 34 |
| Chapter 2 | |
| 1: Headmount implantation location..... | 45 |
| 2: Headmount diagram..... | 45 |
| 3: Elevated zero maze | 47 |
| 4: Locomotor activity chambers diagram (image adapted from Med Associates)..... | 48 |
| 5: 3CST diagram..... | 50 |
| 6: Barnes maze diagram..... | 52 |
| 7: Search strategy examples | 54 |
| 8: Sense of smell..... | 56 |
| 9: TreadScan..... | 57 |
| 10: Rotarod..... | 58 |
| 11: Tail suspension test (TST) schematic | 59 |

Chapter 3

| | |
|------------------------------------------------------------------------------------------------------------------------------------------------------------------|-----|
| 1: GABA _A receptor structure with D120 highlighted..... | 79 |
| 2: The $\beta 3$ (D120N) subunit amino acid substitution disrupts GABA _A receptor function and tertiary structure..... | 81 |
| 3: Generating the <i>Gabrb3</i> ^{+/<i>D120N</i>} mouse..... | 87 |
| 4: Spontaneous TAS in wild type mice and AASs in <i>Gabrb3</i> ^{+/<i>D120N</i>} mice..... | 90 |
| 5: AASs were distinguishable from NREM sleep by power spectral density analysis. | 92 |
| 6: Myoclonic, tonic, and GTC seizures in <i>Gabrb3</i> ^{+/<i>D120N</i>} mice. | 93 |
| 7: Quantification of seizure incidence and timing in <i>Gabrb3</i> ^{+/<i>D120N</i>} mice..... | 95 |
| 8: Spontaneous spasms in young <i>Gabrb3</i> ^{+/<i>D120N</i>} mice..... | 96 |
| 9: Barnes maze timeline..... | 98 |
| 10: <i>Gabrb3</i> ^{+/<i>D120N</i>} mice had spatial learning deficits..... | 99 |
| 11: <i>Gabrb3</i> ^{+/<i>D120N</i>} mice had spatial memory deficits..... | 100 |
| 12: <i>Gabrb3</i> ^{+/<i>D120N</i>} mice had a mild hyperactive phenotype at P49, which became more pronounced at P200..... | 102 |
| 13: Stage 2 of the 3CST: <i>Gabrb3</i> ^{+/<i>D120N</i>} mice had mild social deficits..... | 104 |
| 14: Stage 3 of the 3CST: <i>Gabrb3</i> ^{+/<i>D120N</i>} mice had severe social deficits. | 105 |
| 15: <i>Gabrb3</i> ^{+/<i>D120N</i>} mice had elevated anxiety that worsened with age..... | 107 |
| 16: <i>Gabrb3</i> ^{+/<i>D120N</i>} mice did not show any deficits in the sense of smell..... | 111 |
| 17: <i>Gabrb3</i> ^{+/<i>D120N</i>} mice did not exhibit a depression-like phenotype..... | 112 |
| 18: <i>Gabrb3</i> ^{+/<i>D120N</i>} mice did not display motor deficits on the Rotarod..... | 113 |
| 19: <i>Gabrb3</i> ^{+/<i>D120N</i>} mice displayed minor motor abnormalities using TreadScan..... | 114 |
| 20: Biogenesis and trafficking of receptors containing mutant $\beta 3$ (D120N) subunits were unaltered in <i>Gabrb3</i> ^{+/<i>D120N</i>} KI mice. | 116 |
| 21: mIPSCs recorded from KI mouse SS cortex layer V/VI neurons were altered..... | 119 |
| 22: Spontaneous thalamocortical network oscillations from KI mice were longer and more frequent than those from wild type littermate mice..... | 121 |
| 23: The AEDs ethosuximide and clobazam, but not topiramate, reduced total AAS duration in KI mice..... | 124 |
| 24: Cannabinoid therapy was effective at reducing AASs..... | 125 |

Chapter 4

| | |
|---------------------------------------------------------------------------------------------------------------------------------------------|-----|
| 1: P11S was found in four families with CAE in Central America..... | 151 |
| 2: P11S is found in a French-Canadian family with a history of CAE..... | 152 |
| 3: P11S was found in 17 families with ASD..... | 153 |
| 4: Peptide sequences resulting from translation of exons 1a and 2 in both wild type and P11S transcripts. | 154 |
| 5: P11S reduced peak current amplitude and current density in HEK cells. | 158 |
| 6: <i>Gabrb3</i> ^{+P11S} mice had frequent TASs..... | 159 |
| 7: <i>Gabrb3</i> ^{+P11S} mice had more TASs per hour as well as longer TASs than wild type..... | 159 |
| 8: Stage 2 of the 3CST: <i>Gabrb3</i> ^{+P11S} mice had mild social deficits. | 161 |
| 9: Stage 3 of the 3CST: <i>Gabrb3</i> ^{+P11S} mice had severe social deficits. | 162 |
| 10: <i>Gabrb3</i> ^{+P11S} mice were not hyperactive..... | 163 |
| 11: <i>Gabrb3</i> ^{+P11S} mice did not have elevated anxiety. | 164 |
| 12: <i>Gabrb3</i> ^{+P11S} mice did not have spatial learning deficits. | 165 |
| 13: <i>Gabrb3</i> ^{+P11S} mice did not have impaired spatial memory..... | 166 |
| 14: Neither total nor surface expression of GABA _A receptor subunits was changed in <i>Gabrb3</i> ^{+P11S} mice..... | 168 |
| 15: <i>Gabrb3</i> ^{+P11S} had mIPSCs with decreased amplitude and increased spontaneous thalamocortical network oscillations. | 170 |

Chapter 5

| | |
|---------------------------------------------------------------------------|-----|
| 1: What role does the hippocampus play in thalamocortical circuitry?..... | 180 |
|---------------------------------------------------------------------------|-----|

LIST OF TABLES

| Table | Page |
|--------------------------------------------------------------------------------------------------------------------------------------------------------------------------------------------------------------------------------------------------|------|
| 1: Commercially available (via Jackson Labs, www.jax.org) promoter-driven Cre mouse lines relevant to the LGS and CAE mouse models, listed according to the gene canonically controlled by that promoter. | 193 |

Chapter 1

Introduction

Seizures and epilepsy

Definition of epilepsy

Epilepsy is a common, chronic neurologic disorder defined as any seizure disorder in which unprovoked seizures reoccur [1]. Epilepsy affects 1-3% of the population [1], totaling 2.2 million people in the United States and 65 million people world-wide [2]. Psychogenic or non-epileptic seizures affect about 10% of the population [1]. The direct annual medical care cost of epilepsy in the United States is about \$10 billion. However, indirect costs are estimated to be much higher and include community costs and individual losses in quality of life and productivity [2]. Additionally, the risk of psychiatric illness is approximately doubled in epileptic patients and 20-50% of individuals with epilepsy have cognitive impairment severe enough to interfere with daily life [2].

Seizures are paroxysmal events resulting from abnormal, involuntary, neuronal discharges in the brain [1]. There are many types of seizures and their classification is crucial for diagnosing an epilepsy syndrome. Diagnosis of an epilepsy syndrome is also dependent on age of onset, family history, EEG, and neuroimaging, and provides information about prognosis and potential response to therapies [1]. 68% of epilepsies are likely genetic, and the rest are of

remote symptomatic causes, such as cerebrovascular disease, head trauma, brain tumor, infection, or neuronal degeneration [1]. Some causes of provoked seizures include electrolyte disorders, toxins, acute head injury, infectious disease, vascular abnormalities, and tumors [3]. Treatment of epilepsy can be difficult, and 30% of patients will not respond to any antiepileptic drug (AED) [2]. Of those whose seizures are successfully managed with an AED, 10% will become refractory [2].

Introduction to epileptic encephalopathies

Epileptic encephalopathies are a severe subset of epilepsies associated with a high probability of impaired development and cognition [4-6]. Epileptic encephalopathy onset is generally associated with developmental delay or regression, psychomotor dysfunction and movement disorders, and cognitive, behavioral, or neurological deficits that are difficult to manage [4, 7-10]. Patients typically experience frequent, multiple types of pharmacoresistant seizures, abundant epileptiform activity on EEG, and sometimes early death [4, 5, 7]. In general, epileptic encephalopathies are associated with poor clinical outcomes [7]. It is worth noting that a patient does not have to have an epilepsy identified as an epileptic encephalopathy to have encephalopathic features, nor does diagnosis of an epileptic encephalopathy guarantee a patient will have encephalopathic features; an epileptic encephalopathy diagnosis indicates that the risk is substantially higher for having encephalopathic features [5].

Epileptic encephalopathies have a broad range of disease mechanisms, including channelopathies, synaptic dysfunction, transporter defects, transcriptional dysregulation, impaired DNA repair, impaired chromatin remodeling, and metabolic defects. Epilepsy-

associated genes show phenotypic pleiotropy, meaning mutations in each of these genes can cause multiple epilepsy syndromes. Human genotyping and phenotyping have revealed that mutations in a single gene can be associated with anything from a benign epilepsy to an epileptic encephalopathy. For example, *KCNQ2* mutations appear in 20% of patients with the epileptic encephalopathy Ohtahara syndrome but are also associated with benign familial neonatal epilepsy, which has an excellent prognosis. Genetic abnormalities (mutations, truncations, copy number variation) in *SCN1A* occur in 90% of patients with the epileptic encephalopathy Dravet syndrome and have been identified in other epileptic encephalopathies such as Lennox-Gastaut syndrome. However, *SCN1A* mutations are also associated with less severe conditions such as autism spectrum disorder and genetic epilepsy with febrile seizures plus; even some unaffected relatives of Dravet syndrome patients carry *SCN1A* mutations. Regardless of severity, epilepsies in these patients typically appear around the time of onset of the mutant gene expression and while some may resolve, others persist with devastating outcomes. [7]

There are several genetic phenomena that explain some of the patient phenotypic heterogeneity. Mosaicism explains a small amount of the phenotypic pleiotropy, and mosaicism factors include epigenetics, if the mutation was gonadal or somatic, when in development the mutation occurred, and how many and what type of cells contained the mutation [7]. This was clearly shown in a Dravet syndrome study in which parents of Dravet syndrome patients were analyzed and each parent carried an *SCN1A* mutation in 0.04 – 85% of their blood DNA. The severity of the disorder each parent had, ranging from neurotypical to severely afflicted, was associated with the mutational load of that individual [11]. At least 30 other diseases have demonstrated varying severity linked to somatic mosaicism [11]. These factors can influence the type, timing, and location of mutations during development. *SCN1A* and *KCNQ2* mutations, for

example, usually result in disease onset that coincides with the onset of expression of the mutant gene. Additionally, epilepsy syndromes show genetic heterogeneity, meaning that they can be caused by abnormalities in multiple genes. For example, mutations thought to be causative for Ohtahara syndrome have been repeatedly identified in the genes *STXBPI*, *KCNQ2*, and *SCN2A*, as well as individual cases in over a dozen other genes. While 90% of Dravet syndrome cases are thought to be caused by abnormalities in *SCN1A*, mutations in other genes such as those encoding the $\alpha 1$ and $\gamma 2$ subunits of the GABA_A receptor have also been identified in patients with Dravet syndrome. Dysfunction of various genes has been suggested to lead to disruption of common pathways or mechanisms at a specific age that converge to produce a specific epilepsy phenotype. For example, both gain-of-function mutations in *SCN2A* and loss-of-function mutations in *GABRB1* and *GABRB3* can lead to West syndrome as they all disrupt the balance between excitatory and inhibitory neurotransmission. There are common pathways that appear with causative mutations, including regulation of synaptic transmission, abnormalities of interneuron development, migration, or function and activity-driven protein synthesis. [7] For example, *ARX* is critical for interneuron migration and differentiation and mutations in *ARX* can disrupt interneuron function and connectivity leading to disorders such as West syndrome [12, 13], and mutations in the GABAergic synaptic genes *GABRB1* and *GABRB3* can also lead to West syndrome [7]. Genetic heterogeneity can make identifying genetic causes and treatment of a disorder more difficult. Despite the phenotype, whether causative mutations cause gain or loss of function is essential for design of targeted therapies. Many patients with epileptic encephalopathies do not fit neatly into a specific syndrome; however, careful phenotyping has resulted in the recognition of many new epileptic encephalopathies. [7]

For about 30% of epilepsy patients, their seizures are treatment resistant. This occurs after failure to achieve remission after trials of at least two AEDs because there is a <5% chance of responding positively to a third AED after two have failed [2, 14]. These patients have severe morbidity and increased mortality, with sudden unexpected death in epilepsy (SUDEP) being the leading cause of death [15, 16]. Sudden death is about 25-times more likely to occur in people with chronic epilepsy than in normal populations, a risk that increases with age and that is even higher in patients with treatment resistant epilepsy [15, 16]. Changes in brain connectivity and decreased neurogenesis have been identified in patients with epileptic encephalopathies, which likely contributes to their refractoriness to treatment, and there are few disease-specific treatments for epileptic encephalopathies [4]. Those caused by *SLC2A1* (blood-brain-barrier glucose transporter) mutations are well controlled with a ketogenic diet [7]. Most patients, however, undergo trial and error with available AEDs. If a potentially causative mutation is identified, it may be possible to pharmacologically target the affected gene, protein, or pathway. For genetic causes, drugs will not address the underlying mechanism and are likely to have only limited efficacy [7]. Neuronal function may also be affected by processes other than the genetic abnormality or seizures, such as development of abnormal neuronal migration and formation of abnormal neuronal networks, which can contribute to cognitive impairment and are unlikely to be rescued with conventional therapies [7].

Types of seizures in epileptic encephalopathies

Patients with epilepsy can experience generalized and/or partial seizures. Generalized seizures are characterized by a loss of consciousness and bilateral involvement of the entire cortex at seizure onset [2]. Partial seizures are initially limited to one brain region or one

hemisphere and may result in focal symptoms such as motor or sensory phenomena [3], but they are not associated with loss of consciousness [1]. Partial seizures can progress to generalized seizures [3]. EEG is often helpful in confirming if seizures are partial or generalized at onset [1]. Since epileptic encephalopathies are usually associated with generalized seizures, only those will be discussed further. The International League Against Epilepsy (ILAE) identifies 7 types of generalized seizures that occur in patients with epileptic encephalopathies. They are separated into two groups: those with major motor symptoms (generalized tonic-clonic, tonic, clonic, and myoclonic seizures) and those without major motor symptoms (typical absence, atypical absence, and atonic seizures) [1].

Generalized tonic-clonic seizures (GTCS) were previously known as *grand mal seizures* but were renamed to be more specific as they contain both tonic and clonic components. GTCS begin with a tonic phase in which the whole body stiffens and progress to a clonic phase involving repetitive (clonic) muscle contractions. These seizures last 2-3 minutes followed by several minutes to several hours of post-ictal unresponsiveness or confusion. Patients may also sleep for several hours after a GTCS. Due to the long duration and severe motor component of these seizures, GTCS often lead to significant injuries. [1]

In tonic seizures, the tonic, whole-body stiffening is due to a sustained and widespread increase in muscle contraction. Tonic seizures can last for a few seconds or for several minutes. The repetitive contractions of tonic-clonic seizures are due to repetitive, generalized muscle contractions. The frequency of clonic contractions is typically between 2-3 Hz [4], and they can last seconds up to a few minutes [17]. Myoclonic seizures involve only one or a few such contractions. Myoclonic seizures are rapid muscle jerks lasting less than 100 ms (much briefer than clonic seizures). They can be unilateral or bilateral, often affecting the hands or arms, but

they can affect any body part [1, 4]. If multiple myoclonic seizures occur, they are distinguishable from clonic seizures in that they are arrhythmic. Myoclonic movements are only considered seizures if they originate in the cortex; however, physiological myoclonus can arise from subcortical regions or the spinal cord in healthy people [18]. Myoclonic seizures are so brief that the loss of consciousness is often not observable [1].

Absence seizures (ASs) are generalized seizures without a strong motor component. There are two types of ASs: typical absence seizures (TASs) and atypical absence seizures (AASs). TASs, previously termed *petit mal seizures*, are a brief (average 9 seconds, range 1-44 seconds [19]) loss of consciousness with staring, unresponsiveness, and minimal motor activity such as eye blinking or automatisms [1]; however, there is no aura or postictal state [20]. The EEG signature of TASs is a well-formed, high-amplitude, around 3 Hz (2.5-4 Hz) spike-and-wave discharge (SWD) [1, 20, 21]. TASs are commonly treated with ethosuximide, valproic acid, or benzodiazepines [20]. TASs usually occur in children with remission during adolescence and are fairly benign [20]. Patients have minimal to no long-term cognitive impairment [21]; however, frequent seizures can interfere with learning and have a negative impact on school performance [22]. It is important to note that while the majority of TASs are brief, longer TASs do occur, and TASs can progress to status epilepticus [23] (see below for more on status epilepticus).

AASs are similar to TASs; however, they are longer, often have motor components, and are associated with more negative outcomes. The EEG signature of AASs is a SWD that is slower than seen in TASs with a frequency around 2.5 Hz [1, 20]. This slower activity is termed a slow spike-and-wave discharge (SSWD) and is often asymmetrical and less well-formed or less rhythmic than the SWD associated with TASs [21]. Behavioral arrest is gradual at both onset

and offset and is not necessarily time locked with SSWDs on EEG. Additionally, patients may retain some ability to move, including talking or walking during the seizures [20]. AASs are frequently associated with significant cognitive and neurodevelopmental deficits [20, 21]; therefore, recognition and diagnosis of AASs is of great clinical importance. AEDs have only a modest impact on AASs [21].

Atonic seizures are another generalized seizure type present in epileptic encephalopathies. Atonic seizures involve a sudden loss in muscle tone, lasting 1-2 seconds. They can affect the head, trunk, jaw, or limbs [4]. The colloquial term for these seizures is “drop attacks” because the patients fall or “drop” to the ground, often resulting in injury [1, 24]. If atonic seizures occur, they are often the most critical to control due to the physical risk they impose [25].

Epileptic spasms (or “infantile spasms”) are an important component of the epileptic encephalopathy West syndrome (see: *Types of epileptic encephalopathies* below). These are not classified as a generalized seizure by the ILAE because they typically occur in infants, and there is insufficient understanding of these seizures to classify them as either generalized or focal [2]. Epileptic spasms are sudden flexion, extension, or flexion-extension movements lasting 0.2-2 seconds (longer than a myoclonic seizure, shorter than a tonic seizure), and they often occur in clusters [1, 4]. The flexion movement is referred to as a “jackknife pattern” and occurs in about 40% of cases. Extensor spasms occur in about 10% of cases and involve a backwards movement of the head and hyperextension of the body. Flexion-extension spasms are the most common, occurring in about half of cases, and involve flexion of the upper body, usually the trunk or arms, and extension of the legs [4]. Spasms are usually bilateral and symmetrical [4]. On EEG, ictal

epileptic spasms are accompanied by interictal electrodecrement (a reduction in EEG voltage) [1, 26].

Status epilepticus (SE) is not a class of seizure but rather describes prolonged or rapidly recurrent seizures of several types. Generalized convulsive SE can describe either a single seizure lasting over 5 minutes, or several seizures occurring in succession without regaining consciousness between the seizures [3, 27, 28]. Convulsive SE is accompanied by tonic, clonic, or tonic-clonic motor activity [27, 29], polyspike activity on EEG [29], and represents a medical emergency as these seizures are difficult to stop and can lead to progressive cell death and excitotoxicity in the brain [28, 30, 31]. Nonconvulsive SE (NCSE) presents with little or no motor activity despite ongoing EEG abnormalities [27, 28]. NCSE is difficult to diagnose as there is impaired consciousness and continuous epileptiform activity on EEG, but little to no obvious motor component [32, 33]. One type of NCSE, absence SE (ASE), can be very long in duration, lasting hours or even days [34], though it is not thought to be associated with neuronal damage [32]. EEG shows continuous SWD [33], and consciousness can vary from mild confusion to complete loss of consciousness [32]. Tonic or clonic activity may occur in any extremity, and some patients experience automatisms of the face, hands, or arms [32]. ASE can be either typical or atypical, with atypical ASE usually being associated with severe cognitive impairment [34]. There are other forms of NCSE, most of which are partial in origin, but which may progress to be generalized [33].

Types of epileptic encephalopathy

While there are many disorders classified as epileptic encephalopathies, the focus here will be on early onset epileptic encephalopathies (EOEEs), or those with perinatal, neonatal, or early childhood onset. Some epileptic encephalopathies are “self-limited”, meaning that they

have high probability of spontaneous remission at a predictable age [5]. These include Landau-Kleffner syndrome (acquired epileptic aphasia) and epilepsy with continuous SWD during slow-wave sleep, both of which are known to remit around the age of 15 [4]. While self-limiting epilepsies usually remit in adolescence, the cognitive effects may remain [4]. EOEEs that are not known to remit will be discussed in further detail. The epilepsy syndromes included as EOEEs often differ among investigators; however, the most common “core” epileptic encephalopathies include early myoclonic encephalopathy (EME), Ohtahara syndrome (OS), West syndrome (WS), Lennox-Gastaut syndrome (LGS), and Dravet syndrome (DS).

EME has an age of onset of less than 3 months and consists of three types of intractable seizures/spasms: myoclonic seizures, focal seizures, and tonic epileptic spasms. Patients may also have hypsarrhythmia, which is seen on EEG as chaotic high-amplitude slow waves with intermixed multifocal spikes [35, 36]. Cognitive dysfunction is commonly associated with EME and includes severe psychomotor and developmental problems, as well as severe mental and neurological deficits. There is no effective treatment for EME, and around half of patients die within weeks or months of onset of EME [4].

OS is the first step in a common disease progression, in which OS may evolve into WS at 4-6 months, which may evolve into LGS at 2-3 years [4, 7]. OS itself begins in the first two months of life, usually around 10 days old. Patients have tonic flexion epileptic spasms in long clusters, with 10-300 clusters per day. Spasms can occur both during wakefulness and sleep. Malformations of the cerebrum during development are a common cause. OS is associated with encephalopathic morbidity, with permanent and severe mental and neurological deficits [4]. No AED is known to have any benefit for OS. OS has high mortality, with about one-half of

patients dying within weeks or months of onset [4], and up to 75% of surviving patients with OS progress to a diagnosis of WS [35].

WS, or infantile spasms, is the most common EOEE [7]. The onset of WS is at 3-12 months of age with a peak at 5 months of age [4]. Patients have epileptic spasms and interictal hypersarrhythmia on EEG [7], experiencing 1-30 clusters of spasms per day with 20-150 spasms per cluster. During clusters of spasms, 60% patients may experience altered or lack of breathing. After a cluster, the postictal state can last up to 90 seconds during which the patient may be unresponsive. In WS, there is also interictal hypersarrhythmia between spasms. There are several known causes of West syndrome, including hypoxia-ischemia, infection, intracranial hemorrhage, and genetic abnormalities, although for some patients the cause is unknown. Only about 1/3 of patients have normal development prior to seizure onset, and most experience arrest or regression of psychomotor development at onset. Around half of WS patients progress to a diagnosis of LGS [4]. While prognosis is generally poor, it has not been found to be related to frequency or severity of spasms. Adrenocorticotrophic hormone (ACTH), oral steroids, and vigabatrin are the most effective treatment for improving outcome, reducing seizures in 2/3 of patients. However, no treatment has been shown to positively affect intellectual development.

LGS is characterized by a triad of features: multiple seizure semiologies, SSWD on EEG, and encephalopathies including cognitive and behavioral abnormalities [37]. LGS has a low birth incidence but represents 5-10% of children with seizures due to its intractable and non-remitting nature [4]. LGS has an age of onset between 1-9 years of age with a peak at 3-5 years of age [4, 7, 38]. LGS patients experience a high seizure frequency, with all patients experiencing multiple types of seizures, including GTC, tonic, clonic, myoclonic, atypical absence, and atonic seizures. NCSE of prolonged AASs, tonic seizures, or mixed AASs and

tonic seizures is common and frequent, may last days or weeks [4], and may be difficult to stop with AEDs [34]. There is little data on the effects of prolonged AAS NCSE in LGS patients. In 67-75% of patients, the cause of LGS is identifiable and can include genetic mutation, brain damage, perinatal complications, and infection; the remainder of cases are cryptogenic, meaning their etiology is likely genetic or unknown [38, 39]. Up to 60% of LGS patients had a previous epileptic encephalopathy diagnosis [4, 34], and around 30% had a previous WS diagnosis [40]. It is rare for patients to achieve normal mental and motor development [4]. Cognitive dysfunction includes varying degrees of developmental delay, moderate to severe intellectual impairment, hyperactivity, autism spectrum disorder (ASD), and mood instability [41]. LGS often requires polytherapy, which is rarely successful [4]. Seizures in LGS are highly resistant to AEDs, which may provide only temporary relief from seizures, lasting a few weeks or months. Often AEDs are only effective when the AEDs or their levels are changed. A permanent seizure-free state is considered unachievable with current therapies, and the prognosis of LGS has been referred to as “appalling.” Eighty to 90% of LGS patients continue to have seizures into adulthood. [4] For more information on LGS, see *Chapter 3*.

DS (previously “severe myoclonic epilepsy in infancy”) is the second most common EOEE with an incidence of 1 per 22,000 births [7]. DS has an age of onset around 5 months of age and typically begins with febrile seizures, often lasting more than 10 minutes, and progressing to SE. Patients continue to experience febrile clonic convulsions, myoclonic jerks, AASs, complex partial seizures, and NCSE [4]. Patients may experience short AASs (5-6 seconds) with myoclonic jerks [4]. DS is most often caused by *de novo* mutations in the sodium channel gene *SCN1A* [4], half of which are missense mutations and half of which are truncation mutations [7]. At onset of DS, patients experience a halting or regression of cognitive

development and neuropsychological abilities [42, 43]. Seizures may improve or abate in early adolescence (11-12 years old), but patients are left with persistent and serious mental and neurological abnormalities. Seizures in DS are very resistant to treatment. AEDs may reduce seizure frequency, but full seizure control is not achieved, and long-term outcome is not improved with therapy. A ketogenic diet has been particularly helpful in reducing seizures associated with DS. [4]

While not classified as an epileptic encephalopathy, childhood absence epilepsy (CAE) is relevant to introduce here. CAE is a genetic generalized epilepsy [44] with an age of onset between 4 and 9 year of age and multiple daily TAs [1, 21]. The definition of genetic generalized epilepsies requires that patients are not accompanied by abnormal cognition [44], and the classical reporting of CAE indicates that these patients have normal cognition [21]. Additionally, for 57-75% of patients, CAE remits around adolescence [19, 21]. However, there are reports of CAE overlapping with ASD in family pedigrees and with CAE being associated with significant cognitive dysfunction. See *Chapter 4* for more details.

GABA_A receptors

General function

GABA is a neurotransmitter that is released primarily from GABAergic interneurons and binds to either GABA_A receptors or GABA_B receptors. GABA_B receptors are coupled to G $\alpha_{i/o}$ -type G proteins, which act to inhibit adenylyl cyclase in a slow form of both pre- and post-

synaptic inhibition [45]. Ionotropic GABA_A receptors are the main mediators of fast inhibitory neurotransmission in the central nervous system [46, 47] and will be the focus of GABA-mediated inhibition in this section.

GABA_A receptors are ligand-gated chloride ion channels [48, 49] and are developmental regulators for neuronal growth and differentiation [50]. In the developing brain, GABA and GABA_A receptor synapses emerge before glutamatergic synapses [50], with the first signs of GABA immunoreactivity around E10 in mice [49]. At early stages of neuronal development (embryonic through early postnatal ages), the neuronal intracellular and extracellular chloride ion concentrations are opposite to those of adult neurons with the chloride concentration outside the cell being lower than inside the cell, which results in depolarizing excitatory responses to GABA when chloride ions flow out of the cell through GABA_A receptors [49-51]. Thus, GABAergic interneurons are likely the first neurons to generate network-driven activity in the brain [52]. In humans, while the GABAergic system emerges towards the end of the first trimester of gestation, it continues developing through the first few years of life [49]. When GABA binds to GABA_A receptors in mature neurons, they evoke inward chloride ion currents and stabilize neurons near the resting potential, acting to inhibit action potential generation [50], dampen neuronal electrical excitability, regulate spike timing, and control circuit function [48]. From a systemic perspective, GABA_A receptors are involved in regulating excitability of the brain, anxiety, vigilance, and learning and memory [53].

There are 19 GABA_A receptor subunit genes: *GABRA1-6* (encoding α 1-6 subunits), *GABRB1-3* (encoding β 1-3 subunits), *GABRG1-3* (encoding γ 1-3 subunits), *GABRD* (encoding the δ subunit), *GABRE* (encoding the ϵ subunit), *GABRR1-3* (encoding ρ 1-3 subunits), *GABRP* (encoding the π subunit), and *GABRQ* (encoding the θ subunit) [48, 53]. Alternative splicing of

some genes increases heterogeneity [47, 51, 53]. There is large spatial and temporal variation in subunit expression [47, 48], with some subunits having broad expression and others having very restricted expression [51], even down to the single neuron level [48]. Up to eight subunits have been found to be expressed in a single neuron [51]. There are two broad groups of assembled receptors: synaptic and extrasynaptic. Synaptic receptors provide brief, strong phasic inhibition, whereas extrasynaptic receptors provide long-lived, tonic inhibition in response to ambient GABA [48]. These different responses to GABA are partly due to receptor composition; $\alpha 1$ and $\gamma 2$ subunits are exclusively expressed synaptically, and $\alpha 4$, $\alpha 6$, and δ subunits are primarily expressed extrasynaptically; expression of the remaining subunits can vary [49].

Complete GABA_A receptors are assembled in the endoplasmic reticulum (ER) with the help of chaperone molecules [53]. If not properly assembled, receptors are retained in the ER by these chaperones and are rapidly degraded; only properly assembled receptors are trafficked to the cell surface [47, 53]. Canonical pentameric assembly of GABA_A receptors contains two α subunits, two β subunits, and a third subunit, usually γ or δ [49, 54]. The most abundant receptor subtypes in the brain are $\alpha 1\beta 2\gamma 2$ and $\alpha 1\beta 3\gamma 2$ [51, 55]. When viewed from the extracellular space, synaptic subunit arrangement is $\alpha\beta\alpha\beta\gamma$, clockwise [51, 53, 55] (Figure 1A).

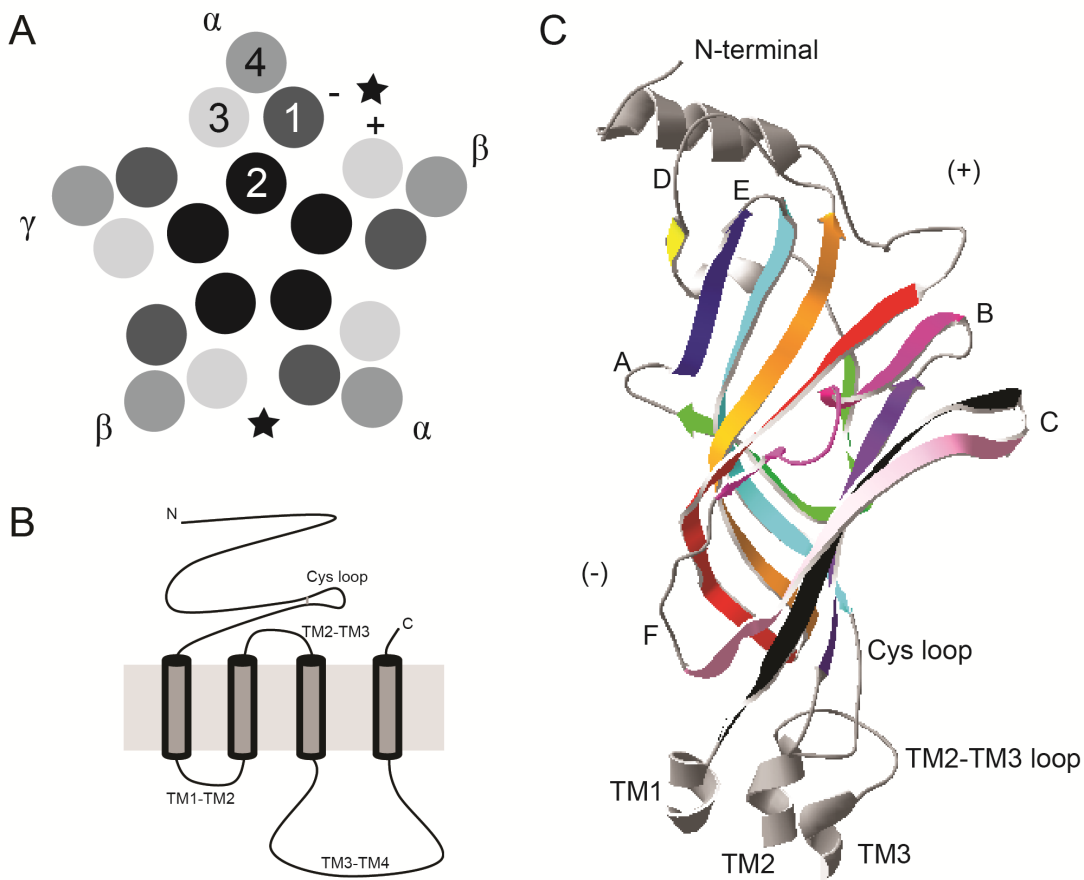


Figure 1: GABA_A receptor structure overview

A) View down through the GABA_A receptor from the extracellular space. GABA_A receptor subunits are arranged in a heteropentamer around a central chloride ion conducting pore. TM2 of each subunit lines the pore and is buffered from the lipid membrane by an aqueous cavity formed by TM1, TM3, and TM4. The most common subunit arrangement is $\alpha, \beta, \alpha, \beta, [\gamma \text{ or } \delta]$ (γ is shown), in a clockwise direction from this view. Black stars indicated GABA binding sites. **B)** Simplified GABA_A subunit structure. Each subunit has a long ECD which contains the Cys loop, four TM domains, the TM2-TM3 loop, which interacts with the ECD in the process of signal transduction, and the long ICD (TM3-TM4), which interacts with intracellular partners. **C)** 3D model of the ECD of a GABA_A receptor subunit based on the crystal structure [56]. There is an N-terminal α -helix and 10 β -sheets in the ECD of each subunit. The β -sheets are colored in the following order: red (1), orange (2), yellow (3), green (4), navy (5), cyan (6), purple (7), magenta (8), pink (9), black (10). The β -sheets arrange to form two surfaces, or a "sandwich". The three loops from the β subunit that make up the (+) interface of the GABA binding pocket are A, B, and C (from this view loop A is rotated around, appearing to be on the (-) side). The three loops from the α subunit that make up the (-) interface of the GABA binding pocket are E, D, and F. The Cys loop and the TM2-TM3 loop are also involved in signal transduction.

Structure

GABA_A receptors are a pentameric Cys-loop subtype of the superfamily of ligand-gated ion channels, which also includes nicotinic and 5-HT serotonergic cationic receptors, and glycine anionic receptors [57]. As with all Cys-loop receptors, each of the five subunits of a GABA_A receptor contains a long N-terminal extracellular domain (ECD) encompassing the ligand-binding domain, four α -helical transmembrane domains (TMDs, termed TM1-TM4) arranged in a pentamer around the ion-conducting pore that is composed of the 5 TM2 domains, and a highly-variable large intracellular domain (ICD) between TM3 and TM4 [46, 51, 53, 57] (Figure 1B). While primary structure may vary highly amongst Cys-loop receptors, secondary, tertiary and quaternary structure are all highly conserved [57].

Cys-loop receptors are so-named because they have a sequence of 13 amino acids flanked by cysteines, which form a covalent bond and thus a closed loop between them [58]. The extreme N-terminus of the ECD contains sequences important for assembly and trafficking [53]; however, the ECD is composed primarily of β -sheets and the loops between them [58]. (Figure 1C) These 10 β -sheets are arranged in a 3D structure that resembles a sandwich [59, 60] and form the agonist-binding pocket. Agonists bind at the interface between two subunits, one α and one β , with each subunit contributing three discontinuous loops between β -sheets to the binding pocket [58]. The two interfaces that comprise the GABA binding pocket are termed the (+) face and the (-) face. The (+) face formed by the β subunit contains loops A, B, and C, and the (-) face formed by the α subunit contains loops D, E, and F. Together these loops form the GABA binding pocket. The binding pocket for benzodiazepines, GABA_A positive allosteric modulators (see: *Drug binding domains*) are similar to the GABA binding pocket; however, they are formed between the γ (- interface) and α (+ interface) subunits. [55]

Each transmembrane domain is about 20 amino acids long [55] and continues for some distance beyond the hydrophobic core of the membrane on the extracellular side [60]. The transmembrane domains from each of the five subunits are arranged symmetrically [59] such that TM2 from each subunit lines the pore (Figure 1A), and together they form the GABA_A receptor channel gate and ion selectivity filter [51, 60]. The TM2 sequence lining the pore is highly conserved across all Cys-loop receptors (TTVLTMTT, 5 of which line the pore). The chloride selectivity filter and gate are located towards the intracellular end of TM2 [55]. TM1, TM3, and TM4 coil around each other and shield the inner TM2 ring from the lipid membrane [59].

Signal transduction of Cys-loop receptors is composed of three processes: agonist binding, channel gating, and the coupling of binding to gating [58]. The binding pocket is buried in the receptor, with loop C functioning as a cap to close off the pocket when the agonist is bound [58]. Channel gating primarily involves motion in TM2, which rotates after agonist binding allowing the pore to open [58, 60]. In order for TM2 to freely move, it has minimal interactions with the other three transmembrane domains [60]. There are several structural components to the coupling of binding and gating: a subset of loops that form the binding domain, the Cys loop, the TM2-TM3 loop, and the link between β -sheet 10 and TM1. Closing of loop C and movement of loop B after agonist binding locks the agonist in the binding pocket [51, 59] and weakens an interaction with the Cys loop and the final β sheet (β 10), which is connected to TM1 [58]. The Cys loop then interacts with the TM2-TM3 loop [59], which may function to encourage movement of TM2 thereby opening the pore.

The ICD connects TM3 and TM4 and contains between 85 and 255 amino acid residues [56]. While it contains a substantial α -helix [58], the remaining structure is difficult to predict and had to be removed for successful crystallization [56]. The ICD functions to modify the

receptor [61] and undergoes modification via phosphorylation [51]. It also interacts with intracellular structural partners that have roles in anchoring GABA_A receptors to the cytoskeleton and trafficking of receptors [51]. Gephyrin, a widely-expressed microtubule-binding protein, helps anchor GABA_A receptors at the synapse [55] by binding to the ICD of the γ 2 subunit [62]. Other proteins have been identified that interact with the ICD of specific GABA_A receptor subunits [51].

GABA_A receptor subunits vary in size from 45 kD to 85 kD [46]. There is 70-80% sequence homology within each subunit family and 30-40% homology across all families [46]. The expression of subunits is age-, region-, and subcellular location-specific [55]. Individual subunits portray overlapping but distinct expression patterns [53]. Varying subunit composition in turn alters the biophysical properties of GABA_A receptors [55], including pharmacology and electrophysiology [53]. Specific subunits are phosphorylated to affect surface stability or trafficking of the whole receptor [51]. Structural differences in individual subunits account for differences in assembled receptor pharmacology, subcellular localization, and intrinsic channel kinetics [48]. In addition to subunit composition, other factors influence the response of GABA_A receptors to GABA, including: density of receptors, phosphorylation state, chloride equilibrium potential, and the quantity of GABA released [55].

Common dysfunction

Inherited familial and *de novo* mutations in channels can lead to channelopathies, diseases that arise due to a defect in an ion channel. Channelopathies have been associated with many diseases including diabetes, hypertension, cardiac arrhythmia, asthma, cystic fibrosis, and

many neurological diseases including epilepsy [48]. Missense mutations, those which encode a different amino acid at a specific position, can result in misfolded or unincorporated proteins, or in intact receptors that incorporate mutant subunits and have altered GABA binding or impaired channel conductance and/or kinetic properties [48]. Despite a single mutation, channelopathies often result in dysfunction beyond the one channel directly affected as secondary neurobiological problems can occur such as altered circuitry. This complicates treatment as symptoms can be independent of the initial genetic abnormality [48]. Additionally, mutations in different channels can lead to similar diseases [48]. It is important to identify the channel or channels affected as this helps inform treatment options.

While most channelopathies involve voltage-gated ion channels, GABA_A receptor mutations have been associated with various neurologic and psychiatric diseases [48], including epilepsy, ASD, impulsivity, schizophrenia, addiction, altered mood, and chronic pain [48, 63]. Mutations in GABA_A receptors have been described to disrupt protein structure, conformation, abundance, or localization [48]. These disruptions impact inhibition, which can lead to hypersynchronous excitatory firing, abnormal burst generation, neuropathology, and seizures [48].

Many rare and *de novo* *GABR* mutations have been directly associated with diseases [48]. Altered GABAergic signaling has been associated with ASD pathogenesis and several ASD patients have shown reduced GABA_A receptor binding in frontal cortex as well as reduced expression of the $\beta 3$ subunits and of the GABA synthesis enzymes GAD65 and GAD67 [64]. Many epilepsy syndromes including generalized epilepsy with febrile seizures plus and genetic generalized epilepsies (including childhood absence epilepsy, juvenile absence epilepsy and juvenile myoclonic epilepsy) have been linked to rare inherited *GABR* mutations [48, 65]. *De*

novo mutations in *GABRs* have been previously associated with several epilepsies, including CAE, DS, generalized epilepsy with febrile seizures plus, and juvenile myoclonic epilepsy [65]. In addition to mutations, untranslated region and intronic mutations are commonly reported to lead to a reduction in human brain *GABR* transcription and RNA processing [48].

Drug binding domains

GABA_A receptors are targeted by many signal-modifying compounds, both intrinsic and extrinsic, and subunit composition and arrangement can determine drug selectivity [45, 46, 48-51]. GABA_A receptors are activated by GABA and by GABA_A receptor agonists such as muscimol and are blocked completely by GABA_A receptor antagonists such as bicuculline and SR95531. Picrotoxin non-competitively blocks GABA_A receptors, likely by binding in the pore. There are several groups of positive and negative allosteric GABA_A receptor modulators (PAMs and NAMs). Allosteric modulators preserve the location and timing dynamics of activation by changing the shape of a receptor to alter the efficacy of channel opening. They generally only function in the presence of GABA and when the GABA concentration is below the receptor's maximal activating concentration. [51, 55]

PAMs are used widely in medicine as anesthetics and in the treatment of anxiety, epilepsy, or sleep disorders [55]. One of the best-described classes of PAMs are benzodiazepines, which are useful for sedation, controlling anxiety and seizures, and muscle relaxation [55]. Binding of benzodiazepines leads to a conformational change in the receptor, which increases affinity for GABA. The GABA concentration response curve is thus shifted left but the maximal current remains unchanged [51]. The binding pocket for benzodiazepines is similar to that of GABA; however, it is formed between the γ (- interface) and α (+ interface)

subunits, and it communicates more directly with the Cys-loop of the α subunit, which interacts with the M2-M3 loop of that subunit [51, 55]. Benzodiazepines are therefore selective for $\alpha\beta\gamma$ -containing receptors; however, different α subunits can also affect the sensitivity of some benzodiazepines. Diazepam, for example, is a classic benzodiazepine and cannot bind the extrasynaptic α subunits $\alpha 4$ and $\alpha 6$. Even though it is chemically different from benzodiazepines, zolpidem (brand name Ambien) also binds the benzodiazepine site and is selective for $\alpha 1$ subunit-containing $\alpha\beta\gamma$ receptors. Flumazenil is a competitive antagonist at the benzodiazepine binding site and is used in the event of benzodiazepine overdose. [55]

General anesthetics bind several ion channels, and their main targets include two pore domain potassium channels. However, volatile anesthetics like isoflurane are GABA_A receptor PAMs [55]. Intravenous anesthetics (barbiturates, steroids, propofol, etomidate) are also GABA_A receptor PAMs at low concentrations and can directly activate GABA_A receptor activity at high concentrations. Propofol and etomidate act through M2 and M3 transmembrane domains of the $\beta 2$ subunit (possibly the sedative effect) and $\beta 3$ subunit (possibly the loss of consciousness effect) [55].

Zinc and neurosteroids are both natural allosteric modulators of GABA_A receptors. Cys-loop receptors all undergo allosteric modulation by zinc [57], which reduces amplitude, slows the rise time, and accelerates the decay of inhibitory post-synaptic currents (IPSCs) [55]. Zinc is 3400x more potent on $\alpha\beta$ receptors than $\alpha\beta\gamma 2$ receptors [55]. Several naturally occurring neurosteroids act on GABA receptors by various, poorly-described mechanisms [55], although some neurosteroids have been shown to specifically amplify extrasynaptic GABA_A receptor activity [48]. Some neurosteroids can be both allosteric modulators and agonists at high concentrations by binding to the transmembrane regions of α and β subunits [51]. Female sex

hormones are neurosteroids that can bind GABA_A receptors and may function to reduce anxiety and seizure susceptibility [51]. Ethanol acts on many receptors including GABA_A and glutamate receptors [55]. GABA_A receptors containing β 3 undergo the strongest ethanol potentiation at high concentrations of ethanol, although extrasynaptic δ subunit-containing receptors are potentiated by very low concentrations of ethanol [55]. Both ethanol and anesthetics likely bind in water-filled cavities behind TM2 [60]. Finally, endocannabinoids have been shown to positively modulate GABA_A receptors by binding to TM4 of the β 2 subunit [51].

GABA_A receptor negative allosteric modulators (NAMs) are less-well described. These include beta-carbolines and DMCM, which may be cognitive enhancers [55] and are being used in clinical trials for treatment of ASD, Down's syndrome, and schizophrenia [66]. Partial GABA_A receptor agonists and subtype specific agonists are being developed to be fast-acting and have minimal side effects, a common complication of benzodiazepine therapy [55].

The β 3 subunit of the GABA_A receptor

Overview

The β 3 subunit is important for GABA_A receptor assembly and trafficking, brain development, and cell proliferation [67]. β 3 subunits emerge at E14-17 [50], which correlates to about 12-16 weeks in utero in humans [68]. Its expression is strongest in the perinatal period [50, 67] when β 3 subunits are important in neurogenesis and neural development [50]. β 3

subunits remain a main component of GABA_A receptors in most brain regions throughout childhood, including many thalamic nuclei [50]. By adulthood, $\beta 3$ subunit expression decreases to moderate levels in cortex but remains high in both hippocampus and nucleus reticularis of the thalamus (nRT) [50]. Although it is not expressed in thalamic regions besides the nRT in adulthood, the nRT is the main location of thalamic inhibitory drive and $\beta 3$ subunits are important in thalamocortical circuitry, particularly for sensory processing [50].

GABRB3 and *Gabrb3* are responsible for encoding the $\beta 3$ subunit in humans and mice, respectively. Sequence alignment between translated *GABRB3* and *Gabrb3* yields a 97.25% homology between the two amino acid sequences. Twelve of the thirteen amino acid changes are located in the large M3-M4 ICD [69, 70], and the final amino acid change is located in the cleaved signal peptide domain. The principle functional domains of $\beta 3$ subunits are fully conserved between mouse and human and conclusions drawn from murine studies are highly applicable to human $\beta 3$ subunits. Expression in key areas, such as the cortex and hippocampus (Figure 2), are similar between humans and mice, allowing for mice to represent a faithful model of human $\beta 3$ expression.

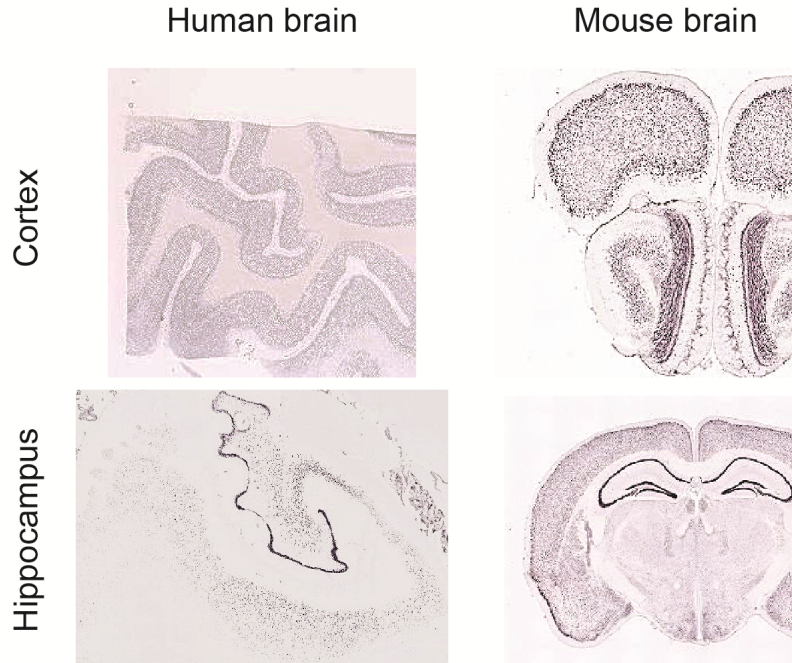


Figure 2: Expression of *GABRB3* in humans and *Gabrb3* in mice (Allen Brain Atlas)

$\beta 3$ subunit mRNA expression in humans and mice is similar. *In situ* staining for $\beta 3$ subunit RNA is shown in both human (adult) and mouse (adult, P56) in the cortex and hippocampus, as examples.

Variants 1 and 2

GABRB3 has 10 exons; however, the first exon in each gene is alternatively spliced and called exon 1 and exon 1A [50, 64]. Exons 1 and 1A result in the protein products $\beta 3$ -variant 1 subunit ($\beta 3$ -V1) and $\beta 3$ -variant 2 subunit ($\beta 3$ -V2), respectively, which have the same number of amino acids but different signal peptides and different N-terminus sequences in the mature peptide after signal peptide cleavage [50, 64]. $\beta 3$ -V2 subunits are abundantly expressed in the fetal brain but have low expression in the adult brain, suggesting a role in embryonic

neurogenesis. β 3-V1 subunits, however, are more highly expressed in the adult brain indicating a role in mature neuron function [50].

Genomic interactions

Genetic regulation of *GABRB3* is complex (Figure 3) and has been implicated in several disease processes. *GABRB3* is located on chromosome 15q12, in the middle of the region 15q11-13, an area which is known for disease-causing genomic rearrangements. Other genes in this region include *UBE3A*, *GABRA5*, *GABRG3*, and *OCA2* [48, 67]. Several genes within 15q11-13 are either paternally or maternally imprinted, and genomic abnormalities in this region are associated with Angelman syndrome, Prader-Willi syndrome, ASD, schizophrenia, addiction, and albinism [64, 71]. There is conflicting evidence as to whether or not *GABRB3* is imprinted (a form of inherited epigenetic control usually involving silencing of one gene by methylation [72, 73]); however, the strongest evidence suggests that it is not and is instead biallelically expressed in the brain [50].

Chromosome 15q11-13

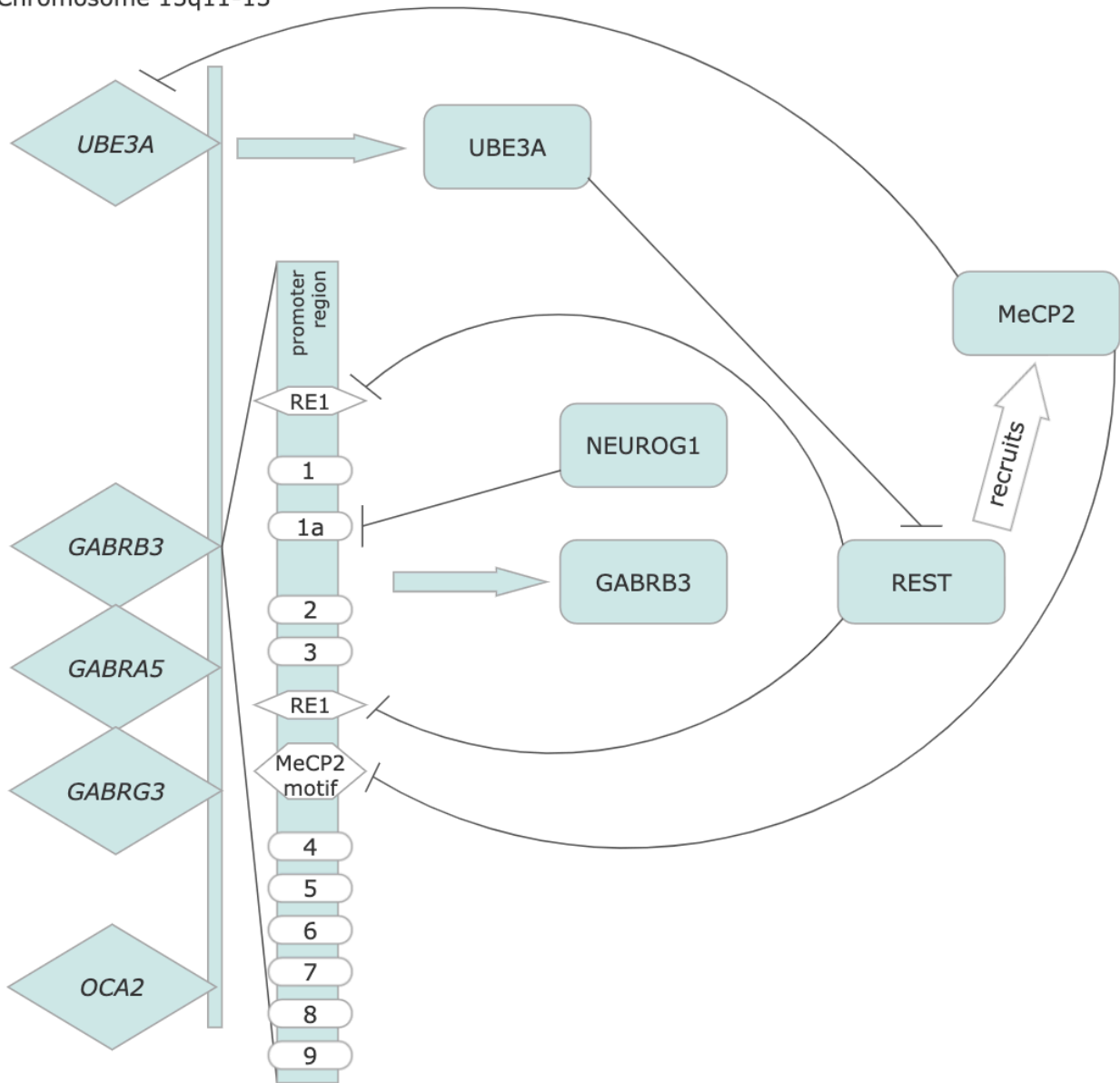


Figure 3: Chromosome 15q11-13 genetic regulation schematic

This region of human chromosome 15 is known for having disease-causing genetic abnormalities. Genetic regulation of this region is complex and intertwined. The sequence of genes on human chromosome 15q11-13 and their regulation are homologous to those on mouse chromosome 7.

Neurogenin 1 (NEUROG1) is a basic helix-loop-helix transcription factor that binds to the signal peptide domain in exon 1A of *GABRB3*. As is detailed above, exon 1A is the first exon encoding $\beta 3$ -V2 subunits, which are expressed highly in neurogenesis. NEUROG1 encourages glutamatergic neuron specification by binding to *GABRB3* and suppressing transcription during this critical window. Located within the NEUROG1 binding motif is a mutation that has been implicated in both CAE and ASD pathogenesis, GABRB3(P11S). This non-conservative mutation may affect the ability of NEUROG1 and other transcription factors to bind to *GABRB3* and is thought to disrupt the balance between glutamatergic and GABAergic neurons. [50] The P11S mutation is the subject of *Chapter 4*.

Located in both intron 3 and the 5' end of *GABRB3* are two repressor element-1 (RE1) binding motifs. An epigenetic modulator, RE1-silencing transcription factor (REST), binds to the RE1 domains to modulate *GABRB3* expression through recruitment of cofactors like methyl CpG binding protein 2 (MeCP2) and other silencing machinery [50]. Adjacent to the RE1 domain in intron 3 of *GABRB3* is a MeCP2 binding site. MeCP2 binds methylated DNA and recruits histone modifiers resulting in heterochromatinization and silencing of target genes. REST and MeCP2 modulate *GABRB3* expression in an age-dependent and tissue-specific fashion in both stem cells and mature neurons [50]. MeCP2 also binds the *GABRB3*-adjacent gene, *UBE3A*, which in turn, modulates REST activity. Without the MeCP2 binding, antisense *UBE3A* is transcribed, resulting in reduced UBE3A activity [50]. In mice, *Gabrb3* is on chromosome 7 along with the rest of the orthologs of the human chromosome 15q11-13 region [63, 74].

Disorders associated with chromosome 15q11-13

Adult neurogenesis is promoted by *GABRB3* via modulation of *REST* activity, which has been implicated to have roles in neuronal differentiation, gene expression, homeostasis, and plasticity. Dysregulation of REST has been implicated in cancer, neurodegenerative diseases, neurodevelopmental disorders, and epilepsy. Dysregulation of MeCP2 has been identified as crucial in the pathogenesis of Rett syndrome which results in severe psychomotor dysfunction and cognitive impairment. Despite intact *UBE3A* and *GABRB3* genes, Rett syndrome patients have reduced *UBE3A* and *GABRB3* expression and often also have epilepsy. A *de novo* deletion of *UBE3A* occurs in 70% of Angelman syndrome cases, a disorder which is characterized by severe mental retardation, motor dysfunction, and early onset intractable epilepsy (mostly AASs and myoclonic seizures). In some Angelman syndrome patients with severe epilepsy, *GABRB3* was also deleted on the maternal chromosome. [50]

Recall that mutations in *GABRB3* have been associated with epileptic encephalopathies, CAE, and ASD. Disruption of *GABRB3* expression has been identified in both Angelman and Rett syndromes, despite other genes being responsible for those syndromes. In particular, it is common for Angelman syndrome, Rett syndrome, and ASD patients to have reduced *GABRB3* expression in the prefrontal cortex. Angelman syndrome, Rett syndrome, ASD, and epileptic encephalopathies all share neurodevelopmental delay and epilepsy as part of their phenotypic profile. Therefore, *GABRB3* mutations may indicate a convergence of these disorders on genetic and epigenetic regulation of the GABA_A receptor β 3 subunit. [50]

Information gathered from *Gabrb3* mouse studies

A lot of work has been done to characterize the *Gabrb3* knock-out (KO) mouse by studying both homozygous (hom) KO and heterozygous (het) KO mice. The het KO mouse has a mild phenotype with elevated seizure susceptibility when injected with pro-convulsant drugs [50]. However, the hom KO is highly neonatal lethal. The mice that survive have cleft palate, spontaneous myoclonic seizures, impaired cognition and motor coordination, and elevated sensory responsiveness [50, 74]. Additionally, hom KO mice display spatial learning and memory deficits, social deficits, and abnormal attention. The neurochemical, electrophysiological, and behavioral phenotype of the hom KO mouse has substantial overlap with ASD [64].

Importantly, several studies have shown a lack of compensatory expression by $\beta 1$ and $\beta 2$ subunits when the $\beta 3$ subunit is compromised. RNA expression patterns for each of the β subunits are overlapping but distinct (Figure 4). Autoradiographic studies in the $\beta 3$ subunit KO mouse indicate substantially reduced binding of GABA and benzodiazepines across many brain regions [74], indicating a global inability of $\beta 1$ and $\beta 2$ subunits to compensate for the loss of $\beta 3$ subunits. Additionally, GABA_A receptor expression is globally reduced in hom $\beta 3$ subunit KO mice [74]. In the hippocampus, $\beta 3$ subunits are more highly expressed than $\beta 1$ or $\beta 2$ subunits, although all three are expressed there (Figure 4G-I). Of the three β subunits, CRISPR studies have shown that $\beta 3$ subunit expression is both necessary and sufficient for normal synaptic and extrasynaptic inhibitory transmission in the hippocampus. Removal of $\beta 3$ subunits greatly impairs GABAergic activity, and expression of only $\beta 3$, without $\beta 1$ and $\beta 2$, subunits is sufficient to restore GABAergic activity [54].

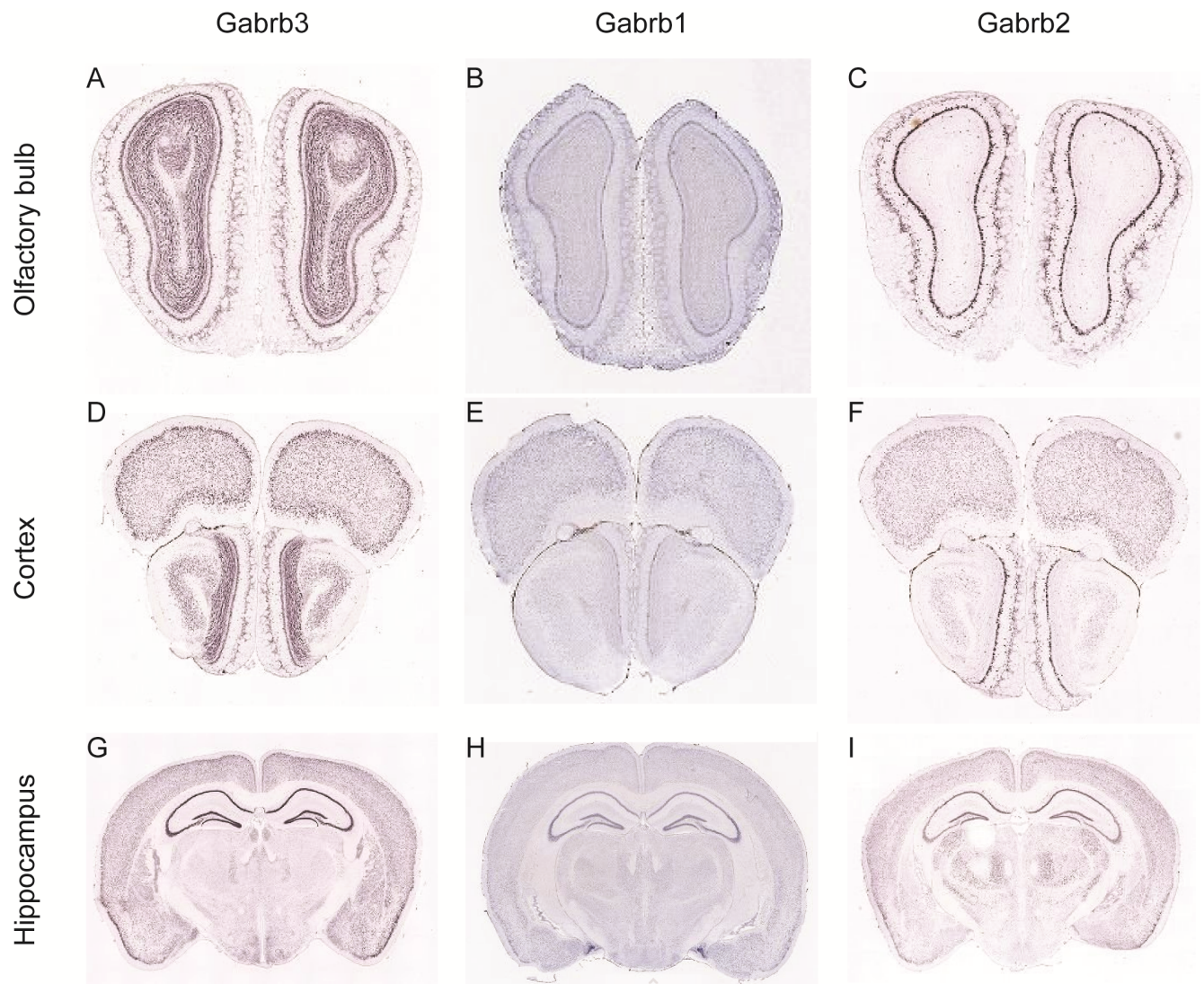


Figure 4: Comparison of wild-type mouse of $\beta 3$, $\beta 1$, and $\beta 2$ subunit RNA expression at P56 (from Allen Brain Atlas).

The $\beta 1$ -3 subunits have unique expression patterns in mice. *In situ* RNA staining of each of the three β subunits at P56 is shown at three levels of coronal sectioning which include some of the brain regions where $\beta 3$ is known to express highly. (A – C) olfactory bulb, (D – F) anterior cortex (including motor cortex), and (G – I) posterior cortex (including somatosensory cortex), hippocampus, and thalamus.

Need for mouse models

There exist several rodent models for various types of seizures or epilepsy. However, a standard approach for characterizing seizures in animal models does not exist, either by electrophysiology or by behavior [23]. Seizure characterization can vary widely among labs and often arbitrary criteria have diverged from the clinical approach [23]. Specifically, duration- and motor-based definitions of seizures in rodents are wide-spread, and while practical, they often have little to no basis for clinical practice [23]. Additionally, full characterization of an epilepsy syndrome is rare in epilepsy research. Often times researchers have used pre-existing classification systems, such as the Racine scale, while ignoring other phenomena [23]. The need for fully characterized rodent models of complex epilepsies remains high.

Typical absence models

Several rodent models of TASs have been well-characterized, including two rat models and several genetic mouse models [20]. Rodent TASs show bilateral, synchronous SWD with a peak spectral frequency of 6-9 Hz and an average duration of 0.3-10 seconds [20, 75, 76]. This reflects a shift in SWD frequency, with rodents having faster SWD than humans (around 3 Hz [19]). Rodents exhibit similar EEG time-locked behavioral arrest during TASs as humans, and rodent TASs have a similar pharmacological profile [20], with rodent TASs responding well to ethosuximide, the first-line therapy for TASs in humans [77].

Rodent TASs have informed much of our knowledge on thalamocortical circuitry. Rodent SWDs emanate from the cortex and thalamus but do not involve the hippocampus or

temporal lobe [20, 21], although the hippocampus may play a modulatory role [21]. SWDs have primarily been shown to initiate in the somatosensory cortex and propagate to the ventrobasal nucleus (VBn) of the thalamus [21]. There is some debate over whether the thalamus can also initiate thalamocortical SWDs [78]. The VBn receives the majority of its inhibitory drive from the nRT [21], which houses the majority of all thalamic GABAergic neurons [78] (Figure 5). GABAergic nRT cells are excited by both cortical projections and thalamic relay cells, such as those in the VBn [78]. Low-threshold T-type calcium channels in the VBn are de-inactivated at membrane potentials more negative than the resting potential [72, 73, 75-78], such as after an inhibitory post-synaptic potential (IPSP) is received from a GABAergic nRT neuron. Once de-inactivated, these calcium channels cause action potential bursting in the VBn when the membrane potential increases above the resting potential but below the typical action potential threshold. The VBn sends excitatory projections to the cortex, stimulating it to again project to the nRT, elucidating the mechanism for thalamocortical oscillation propagation. [78] Of particular interest, $\beta 3$ subunit expression is high in the nRT even in adulthood. When $\beta 3$ subunit signaling is compromised, this decreases inhibitory input to the nRT (which projects back to itself [22], terminating its own firing and therefore priming it to be stimulated again), thereby increasing nRT output. This leads to larger de-inactivating IPSPs in the VBn and subsequently stronger rebound bursting projecting to the cortex. [79] Thus it is clear how $\beta 3$ subunits are critical for control of thalamocortical oscillations and why the $\beta 3$ subunit KO mouse is reported to have increased oscillatory activity [79].

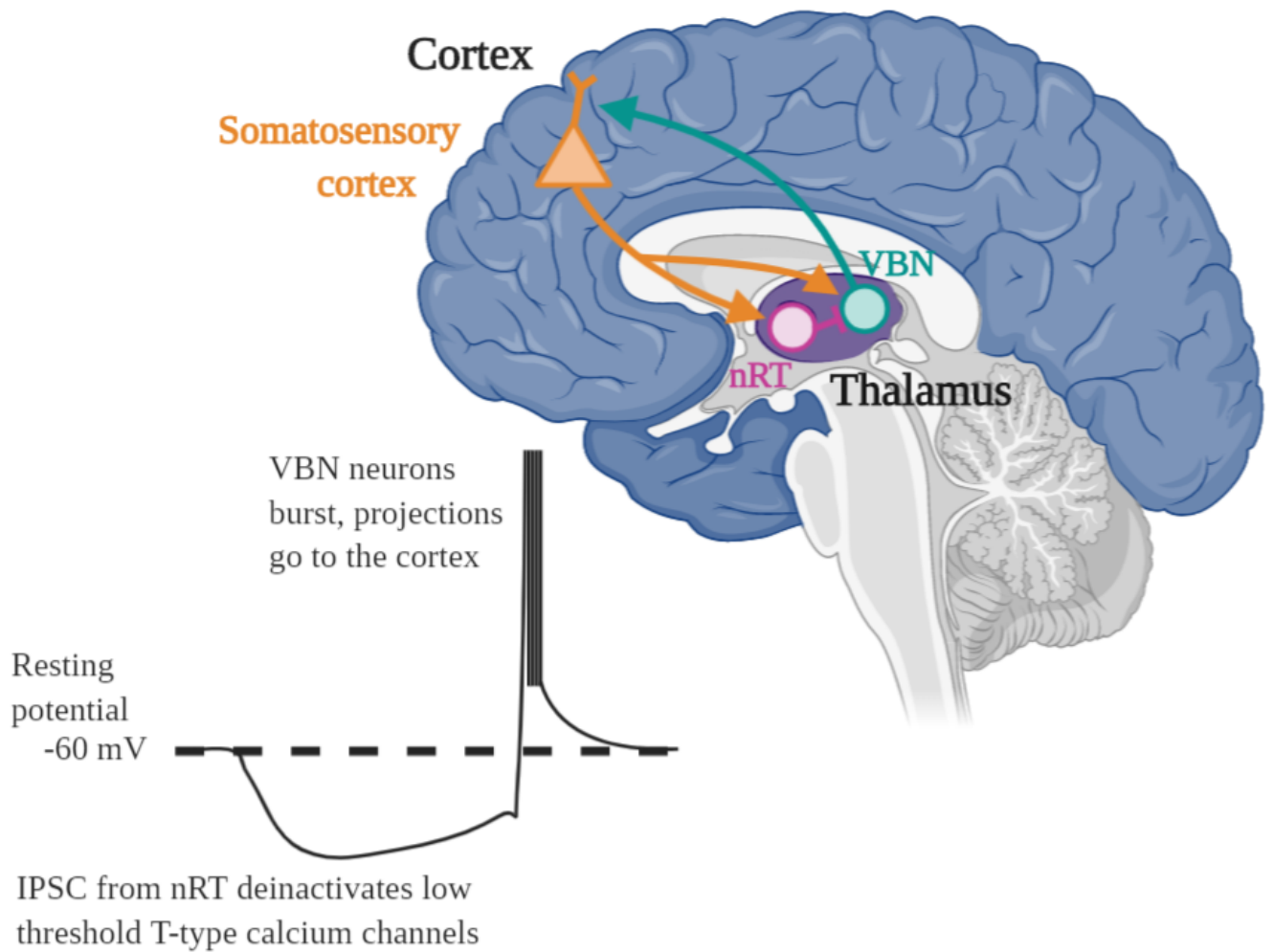


Figure 5: Thalamocortical oscillations in TASs are facilitated by low-threshold T-type calcium channel bursting.

Cortical pyramidal neurons (orange) project to the thalamus (purple), synapsing on both the nRT (pink) and the VBN (green). The nRT is comprised of GABAergic neurons which also synapse on the VBN. Cells in the VBN express low-threshold T-type calcium channels, which deactivate after a hyperpolarizing current like those received from the nRT. After they are deactivated, when the cell is only slightly depolarized these calcium channels initiate burst firing. The bursting VBN neurons project to the cortex (blue). A stronger projection from the cortex, like that which occurs after receiving bursting input from the VBN, more strongly stimulates the nRT which then drives a stronger inhibitory current from the nRT to the VBN, increasing burst firing.

Rat TAS models have shown no evidence of neurodevelopmental impairment [20], as would be expected or ideal for the canonical definition of CAE [21, 44]. However, some CAE patients report having significant encephalopathies in conjunction with TASs, primarily ASD [80]. TAS models that do not reflect encephalopathies, or ASD in particular, likely do not fully reflect the neurological changes experienced by these patients. A genetic model that incorporated both TASs and ASD would be particularly useful for exploring circuitry changes that lead to an overlap of these conditions. Additionally, the existing rodent TAS models also display abnormalities not commonly associated with TASs in humans, including lethargy, ataxia, and movement disorders [20], indicating that there may be abnormal circuitry in these rodent models that is not reflective of the human condition.

Atypical absence seizure (AAS) models

There are two existing rodent models of AASs: the cholesterol biosynthesis inhibitor AY-9944 induction rat model and the GABA_B receptor R1a subunit overexpression mouse model. Both models confirm that the SSWD associated with AAS is faster in rodents than in humans but slower than the SWD observed in TAS models at 5-6 Hz [20, 81]. The average duration of AASs in AY-9944 treated female rats was 7.9 minutes [20]. While the onset and offset of SSWD was abrupt, AY-9944 treated rats displayed behavioral arrest that was not time-locked to the SSWD and the rats occasionally moved during AASs [20]. Pro- and anti-convulsant drugs had a similar effect in AY-9944 treated rats as on humans. AEDs exhibited a short half-life, with seizures returning to baseline after the AED had worn off and the AEDs had no lasting effects [20]. Rats exhibited peaks in SSWD occurrence and duration at the day-to-night and night-to-

day transitions [82], as humans do [83]. The GABA_B receptor mouse model has provided evidence of recruitment of the hippocampus to the corticothalamic network during AAS activity [21]. Interestingly, GABA_B receptor agonists exacerbate AASs while antagonists suppress seizures in both of the rodent models, indicating that the AY-9944 model may also work through the GABA_B receptor [84]. Neither of these models show increased susceptibility to the other seizure types seen in the epileptic encephalopathies in which AASs commonly occur, nor is there a strong reflection of the associated encephalopathies.

Moving forward

With all this information on hand, we can move on to assess two mutations in the $\beta 3$ subunit of the GABA_A receptor that are thought to be causative of epilepsy: D120N and P11S. D120N is associated with Lennox-Gastaut syndrome and P11S is associated with both childhood absence epilepsy and autism spectrum disorder. We generated two knock-in strains, *Gabrb3^{+/D120N}* mice and *Gabrb3^{+/P11S}* mice, and assessed them for seizure phenotypes and behavioral abnormalities reflective of their associated epilepsy. Our findings suggest that both mice serve as robust models for their associated epilepsy and will provide ample opportunity for discovery of epileptogenesis mechanisms and novel therapeutic strategies.

Bibliography

1. Shneker, B.F. and N.B. Fountain, *Epilepsy*. Dis Mon, 2003. **49**(7): p. 426-78.
2. Sirven, J.I., *Epilepsy: A Spectrum Disorder*. Cold Spring Harb Perspect Med, 2015. **5**(9): p. a022848.
3. Huff, J.S. and N. Murr, *Seizure*, in *StatPearls*. 2020: Treasure Island (FL).
4. Panayiotopoulos, C.P., in *The Epilepsies: Seizures, Syndromes and Management*. 2005: Oxfordshire (UK).
5. Berg, A.T., et al., *Revised terminology and concepts for organization of seizures and epilepsies: report of the ILAE Commission on Classification and Terminology, 2005-2009*. Epilepsia, 2010. **51**(4): p. 676-85.
6. Khan, S. and R. Al Baradie, *Epileptic encephalopathies: an overview*. Epilepsy Res Treat, 2012. **2012**: p. 403592.
7. McTague, A., et al., *The genetic landscape of the epileptic encephalopathies of infancy and childhood*. Lancet Neurol, 2016. **15**(3): p. 304-16.
8. Nariai, H., S. Duberstein, and S. Shinnar, *Treatment of Epileptic Encephalopathies: Current State of the Art*. J Child Neurol, 2018. **33**(1): p. 41-54.
9. Dulac, O., *Epileptic encephalopathy*. Epilepsia, 2001. **42 Suppl 3**: p. 23-6.
10. Stafstrom, C.E. and E.H. Kossoff, *Epileptic Encephalopathy in Infants and Children*. Epilepsy Currents, 2016. **16**(4).
11. Depienne, C., et al., *Mechanisms for variable expressivity of inherited SCN1A mutations causing Dravet syndrome*. J Med Genet, 2010. **47**(6): p. 404-10.
12. Kitamura, K., et al., *Mutation of ARX causes abnormal development of forebrain and testes in mice and X-linked lissencephaly with abnormal genitalia in humans*. Nat Genet, 2002. **32**(3): p. 359-69.
13. Kato, M., *A new paradigm for West syndrome based on molecular and cell biology*. Epilepsy Res, 2006. **70 Suppl 1**: p. S87-95.
14. O'Connell, B.K., D. Gloss, and O. Devinsky, *Cannabinoids in treatment-resistant epilepsy: A review*. Epilepsy Behav, 2017. **70**(Pt B): p. 341-348.
15. Elmali, A.D., N. Bebek, and B. Baykan, *Let's talk SUDEP*. Noro Psikiyatr Ars, 2019. **56**(4): p. 292-301.

16. Massey, C.A., et al., *Mechanisms of sudden unexpected death in epilepsy: the pathway to prevention*. Nat Rev Neurol, 2014. **10**(5): p. 271-82.
17. Volpe, J.J., *Volpe's Neurology of the Newborn*, ed. N.S. Abend, F.E. Jensen, and T.E. Inder. 2018, Philadelphia, PA El Sevier.
18. Ibrahim, W. and S. Sharma, *Myoclonus*, in *StatPearls*. 2020: Treasure Island (FL).
19. Tenney, J.R. and T.A. Glauser, *The current state of absence epilepsy: can we have your attention?* Epilepsy Curr, 2013. **13**(3): p. 135-40.
20. Cortez, M.A., C. McKerlie, and O.C. Snead, 3rd, *A model of atypical absence seizures: EEG, pharmacology, and developmental characterization*. Neurology, 2001. **56**(3): p. 341-9.
21. van Luijtelaar, G., F.Y. Onat, and M.J. Gallagher, *Animal models of absence epilepsies: what do they model and do sex and sex hormones matter?* Neurobiol Dis, 2014. **72 Pt B**: p. 167-79.
22. Albuja, A.C. and P.B. Murphy, *Absence Seizure*, in *StatPearls*. 2020: Treasure Island (FL).
23. D'Ambrosio, R. and J.W. Miller, *What is an epileptic seizure? Unifying definitions in clinical practice and animal research to develop novel treatments*. Epilepsy Curr, 2010. **10**(3): p. 61-6.
24. Perucca, E., *Cannabinoids in the Treatment of Epilepsy: Hard Evidence at Last?* J Epilepsy Res, 2017. **7**(2): p. 61-76.
25. Thiele, E.A., et al., *Cannabidiol in patients with seizures associated with Lennox-Gastaut syndrome (GWPCARE4): a randomised, double-blind, placebo-controlled phase 3 trial*. Lancet, 2018. **391**(10125): p. 1085-1096.
26. Shields, W.D., *Infantile spasms: little seizures, BIG consequences*. Epilepsy Curr, 2006. **6**(3): p. 63-9.
27. Wylie, T., et al., *Status Epilepticus*, in *StatPearls*. 2020: Treasure Island (FL).
28. Seinfeld, S., H.P. Goodkin, and S. Shinnar, *Status Epilepticus*. Cold Spring Harb Perspect Med, 2016. **6**(3): p. a022830.
29. Cherian, A. and S.V. Thomas, *Status epilepticus*. Ann Indian Acad Neurol, 2009. **12**(3): p. 140-53.
30. Tsuchida, T.N., et al., *Childhood status epilepticus and excitotoxic neuronal injury*. Pediatric Neurology, 2007. **36**(4): p. 253-257.

31. Meldrum, B., *Excitotoxicity and Epileptic Brain-Damage*. Epilepsy Research, 1991. **10**(1): p. 55-61.
32. Husain, A.M., G.J. Horn, and M.P. Jacobson, *Non-convulsive status epilepticus: usefulness of clinical features in selecting patients for urgent EEG*. J Neurol Neurosurg Psychiatry, 2003. **74**(2): p. 189-91.
33. Holtkamp, M. and H. Meierkord, *Nonconvulsive status epilepticus: a diagnostic and therapeutic challenge in the intensive care setting*. Ther Adv Neurol Disord, 2011. **4**(3): p. 169-81.
34. Sutter, R., S. Ruegg, and P.W. Kaplan, *Epidemiology, diagnosis, and management of nonconvulsive status epilepticus: Opening Pandora's box*. Neurol Clin Pract, 2012. **2**(4): p. 275-286.
35. Beal, J.C., K. Cherian, and S.L. Moshe, *Early-onset epileptic encephalopathies: Ohtahara syndrome and early myoclonic encephalopathy*. Pediatr Neurol, 2012. **47**(5): p. 317-23.
36. Demarest, S.T., et al., *The impact of hypsarrhythmia on infantile spasms treatment response: Observational cohort study from the National Infantile Spasms Consortium*. Epilepsia, 2017. **58**(12): p. 2098-2103.
37. Trevathan, E., *Infantile spasms and Lennox-Gastaut syndrome*. J Child Neurol, 2002. **17** **Suppl 2**: p. 2S9-2S22.
38. Jahngir, M.U., M.Q. Ahmad, and M. Jahangir, *Lennox-Gastaut Syndrome: In a Nutshell*. Cureus, 2018. **10**(8): p. e3134.
39. Stommel, E.W., et al., *Cryptogenic epilepsy: an infectious etiology?* Epilepsia, 2001. **42**(3): p. 436-8.
40. Amrutkar, C. and R.M. Riel-Romero, *Lennox Gastaut Syndrome*, in *StatPearls*. 2020: Treasure Island (FL).
41. Kerr, M., G. Kluger, and S. Philip, *Evolution and management of Lennox-Gastaut syndrome through adolescence and into adulthood: are seizures always the primary issue?* Epileptic Disord, 2011. **13** **Suppl 1**: p. S15-26.
42. Battaglia, D., et al., *Cognitive decline in Dravet syndrome: is there a cerebellar role?* Epilepsy Res, 2013. **106**(1-2): p. 211-21.
43. Guzzetta, F., *Cognitive and behavioral characteristics of children with Dravet syndrome: an overview*. Epilepsia, 2011. **52** **Suppl 2**: p. 35-8.
44. Mullen, S.A., S.F. Berkovic, and I.G. Commission, *Genetic generalized epilepsies*. Epilepsia, 2018. **59**(6): p. 1148-1153.

45. Gassmann, M. and B. Bettler, *Regulation of neuronal GABA(B) receptor functions by subunit composition*. Nat Rev Neurosci, 2012. **13**(6): p. 380-94.
46. Macdonald, R.L. and R.W. Olsen, *GABAA receptor channels*. Annu Rev Neurosci, 1994. **17**: p. 569-602.
47. Taylor, P.M., et al., *Identification of amino acid residues within GABA(A) receptor beta subunits that mediate both homomeric and heteromeric receptor expression*. J Neurosci, 1999. **19**(15): p. 6360-71.
48. Yuan, H., et al., *Ionotropic GABA and Glutamate Receptor Mutations and Human Neurologic Diseases*. Mol Pharmacol, 2015. **88**(1): p. 203-17.
49. Wu, C. and D. Sun, *GABA receptors in brain development, function, and injury*. Metab Brain Dis, 2015. **30**(2): p. 367-79.
50. Tanaka, M., et al., *GABRB3, Epilepsy, and Neurodevelopment*, in *Jasper's Basic Mechanisms of the Epilepsies*, th, et al., Editors. 2012: Bethesda (MD).
51. Sigel, E. and M.E. Steinmann, *Structure, function, and modulation of GABA(A) receptors*. J Biol Chem, 2012. **287**(48): p. 40224-31.
52. Ben-Ari, Y., et al., *Interneurons set the tune of developing networks*. Trends Neurosci, 2004. **27**(7): p. 422-7.
53. Sarto-Jackson, I. and W. Sieghart, *Assembly of GABA(A) receptors (Review)*. Mol Membr Biol, 2008. **25**(4): p. 302-10.
54. Nguyen, Q.A. and R.A. Nicoll, *The GABAA Receptor beta Subunit Is Required for Inhibitory Transmission*. Neuron, 2018. **98**(4): p. 718-725 e3.
55. Goetz, T., et al., *GABA(A) receptors: structure and function in the basal ganglia*. Prog Brain Res, 2007. **160**: p. 21-41.
56. Miller, P.S. and A.R. Aricescu, *Crystal structure of a human GABAA receptor*. Nature, 2014. **512**(7514): p. 270-5.
57. Connolly, C.N. and K.A. Wafford, *The Cys-loop superfamily of ligand-gated ion channels: the impact of receptor structure on function*. Biochem Soc Trans, 2004. **32**(Pt3): p. 529-34.
58. Sine, S.M. and A.G. Engel, *Recent advances in Cys-loop receptor structure and function*. Nature, 2006. **440**(7083): p. 448-55.
59. Unwin, N., *Refined structure of the nicotinic acetylcholine receptor at 4A resolution*. J Mol Biol, 2005. **346**(4): p. 967-89.

60. Miyazawa, A., Y. Fujiyoshi, and N. Unwin, *Structure and gating mechanism of the acetylcholine receptor pore*. Nature, 2003. **423**(6943): p. 949-55.
61. Thompson, A.J., H.A. Lester, and S.C. Lummis, *The structural basis of function in Cys-loop receptors*. Q Rev Biophys, 2010. **43**(4): p. 449-99.
62. Luscher, B., T. Fuchs, and C.L. Kilpatrick, *GABAA receptor trafficking-mediated plasticity of inhibitory synapses*. Neuron, 2011. **70**(3): p. 385-409.
63. Mulligan, M.K., et al., *Complex control of GABA(A) receptor subunit mRNA expression: variation, covariation, and genetic regulation*. PLoS One, 2012. **7**(4): p. e34586.
64. Chen, C.H., et al., *Genetic analysis of GABRB3 as a candidate gene of autism spectrum disorders*. Mol Autism, 2014. **5**: p. 36.
65. Macdonald, R.L., J.Q. Kang, and M.J. Gallagher, *Mutations in GABAA receptor subunits associated with genetic epilepsies*. J Physiol, 2010. **588**(Pt 11): p. 1861-9.
66. Rudolph, U. and H. Mohler, *GABAA receptor subtypes: Therapeutic potential in Down syndrome, affective disorders, schizophrenia, and autism*. Annu Rev Pharmacol Toxicol, 2014. **54**: p. 483-507.
67. Delahanty, R.J., et al., *Beyond Epilepsy and Autism: Disruption of GABRB3 Causes Ocular Hypopigmentation*. Cell Rep, 2016. **17**(12): p. 3115-3124.
68. Stagni, F., et al., *Timing of therapies for Down syndrome: the sooner, the better*. Front Behav Neurosci, 2015. **9**: p. 265.
69. Protein [Internet]. Bethesda (MD): National Library of Medicine (US), National Center for Biotechnology Information; [1988] - . Accession No. NP_068712.1, Homo sapiens gamma-aminobutyric acid receptor subunit beta-3 isoform 2 precursor; [cited 2020 February 6]. Available from: https://www.ncbi.nlm.nih.gov/protein/NP_068712.
70. Protein [Internet]. Bethesda (MD): National Library of Medicine (US), National Center for Biotechnology Information; [1988] - . Accession No. NP_001033790.1, Mus musculus gamma-aminobutyric acid receptor subunit beta-3 isoform b precursor; [cited 2020 February 6]. Available from: https://www.ncbi.nlm.nih.gov/protein/NP_001033790.1.
71. Chen, C.H., C.C. Huang, and D.L. Liao, *Association analysis of GABRB3 promoter variants with heroin dependence*. PLoS One, 2014. **9**(7): p. e102227.
72. Bajrami, E. and M. Spiroski, *Genomic Imprinting*. Open Access Maced J Med Sci, 2016. **4**(1): p. 181-4.
73. Ferguson-Smith, A.C. and D. Bourc'his, *The discovery and importance of genomic imprinting*. Elife, 2018. **7**.

74. Homanics, G.E., et al., *Mice devoid of gamma-aminobutyrate type A receptor beta3 subunit have epilepsy, cleft palate, and hypersensitive behavior*. Proc Natl Acad Sci U S A, 1997. **94**(8): p. 4143-8.
75. Letts, V.A., B.J. Beyer, and W.N. Frankel, *Hidden in plain sight: spike-wave discharges in mouse inbred strains*. Genes Brain Behav, 2014. **13**(6): p. 519-26.
76. Jarre, G., et al., *Genetic Models of Absence Epilepsy in Rats and Mice*. Models of Seizures and Epilepsy, 2nd Edition. 2017: Elsevier. 455-471.
77. Vrielynck, P., *Current and emerging treatments for absence seizures in young patients*. Neuropsychiatr Dis Treat, 2013. **9**: p. 963-75.
78. Avoli, M., *A brief history on the oscillating roles of thalamus and cortex in absence seizures*. Epilepsia, 2012. **53**(5): p. 779-89.
79. Huntsman, M.M., et al., *Reciprocal inhibitory connections and network synchrony in the mammalian thalamus*. Science, 1999. **283**(5401): p. 541-3.
80. Delahanty, R.J., et al., *Maternal transmission of a rare GABRB3 signal peptide variant is associated with autism*. Mol Psychiatry, 2011. **16**(1): p. 86-96.
81. Rodriguez, C.I., et al., *High-efficiency deleter mice show that FLPe is an alternative to Cre-loxP*. Nat Genet, 2000. **25**(2): p. 139-40.
82. Stewart, L.S., et al., *Daily rhythms of seizure activity and behavior in a model of atypical absence epilepsy*. Epilepsy Behav, 2006. **9**(4): p. 564-72.
83. Diaz-Negrillo, A., *Influence of sleep and sleep deprivation on ictal and interictal epileptiform activity*. Epilepsy Res Treat, 2013. **2013**: p. 492524.
84. Stewart, L.S., et al., *Severity of atypical absence phenotype in GABAB transgenic mice is subunit specific*. Epilepsy Behav, 2009. **14**(4): p. 577-81.

Chapter 2

Materials and Methods

The materials and methods here apply to both chapters 3 and 4. Any chapter-specific details were included in the applicable chapter.

Mouse husbandry and data fidelity

All animals were cared for and used in accordance with the policies of the Vanderbilt University Medical Center Institutional Animal Care and Use Committee, and to the National Institutes of Health Guide for Care and Use of Laboratory Mice. Mice were maintained in cages of up to 5 adults, except after EEG headmount surgery when mice were single-housed with enrichment. Mice were housed in either the VU Level 5 (not specific-pathogen-free) breeding facility or the Level 7 Neurobehavioral Core, both of which were maintained by the Department of Animal Care. Facilities used a 12-hour light/dark cycle, corn-cob bedding, and ad libitum food and water. Power analyses were conducted with preliminary data to determine final sample sizes. Mice used for data were discrete groups in every case except EEG surgeries and subsequent drug testing were performed on some mice after behavioral testing. Where possible, the observer was blinded to the genotype until after analysis was complete.

Video-EEG recordings and analysis

Synchronized video-EEGs were recorded from 4.5 to 6.5-month-old wild-type littermate and KI mice after electrode implantation (#8201, Pinnacle Technology) with a video-EEG monitoring system from Pinnacle Technology [1], and following published protocols [2]. Prior to surgery, mice were weighed and anesthetized using 2-4% isoflurane and placed into a stereotactic frame. The headmount was placed on the skull with the front edge 3.0-3.5 mm anterior of the bregma and secured with four screws (#8209, Pinnacle Technology) such that all four screws rested on the cerebral cortex, providing electrical contact between the brain surface and the headmount (Figure 1). Two EMG leads were inserted into the nuchal muscles (Figure 2). Mice were allowed to recover for a minimum of 7 days before testing. Video-EEG and EMG data were analyzed offline with Sirenia® Seizure software using a widely-used approach of visual inspection. The entire 24-hour recording was analyzed. Mice were maintained for several months post-operative with headmounts in place and were checked daily for signs of infection or irritation. Power spectra were generated using EDF browser.

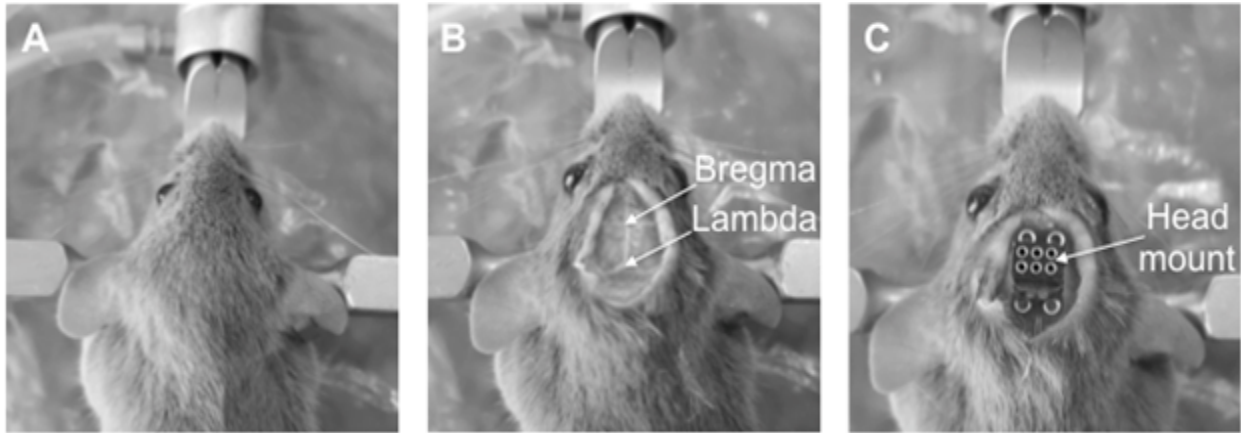


Figure 1: Headmount implantation location

Bregma and Lambda were used as landmarks to ensure consistent headmount placement for each mouse. The front edge of the headmount was placed 3.0-3.5 mm anterior of the bregma.

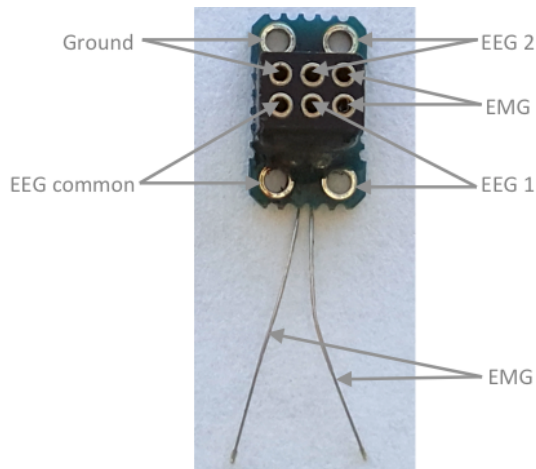


Figure 2: Headmount diagram.

The Pinnacle headmount allows for 4 screw holes, 2 EEG channels, and 1 EMG channel via the two nuchal muscle leads. This headmount enabled acquisition of data from 2 EEG and 1 EMG channels at 400 Hz.

Behavioral testing

The mouse behavioral experiments were performed in the Vanderbilt University Mouse Neurobehavioral Core Laboratory (VUMC MNBCL). Each cohort was subjected to the full suite of behavioral tests, and they were performed in the order in which they were described below. If mice displayed obvious seizures, they were allowed to recover to normal behavior before further testing. Additionally, behavioral tests were conducted between 9 AM and 5 PM to minimize seizure occurrence, as KI mice have increased seizure incidence during the light-to-dark transition. Some mice were observed having stress-related seizures with handling. To eliminate this confound, extensive handling was done by the experimenter prior to any behavioral testing. No one besides this experimenter interacted with the mice, including animal care staff, during testing. Additionally, mice were monitored throughout testing for seizures. If seizures were observed in the home cage, all mice in the cage were left alone until all mice resumed normal activity in the cage. No seizures were observed during behavioral testing. Statistical tests were performed to identify gender differences in each behavior test, and none indicated a significant difference between males and females, so the behavioral data for both genders were combined.

Behavioral tests were selected to investigate behavioral comorbidities with specific encephalopathies associated with each epilepsy syndrome such as LGS or CAE. Some tests were selected to highlight specific abnormal behaviors observed in the two knock-in lines. Tests were selected and conducted from the perspective of Belovicova et al.: "Increased understanding of rodent behavior in a test may be achieved by studying natural rodent behavior, evaluating the ethological validity of the test, determining the source of motivation in the test and using the knowledge of the rodents' sensory capacity to view the test from a rodent's perspective [3]."

Elevated zero maze

The elevated zero maze test was used for assessing anxiety-related behaviors, following a previously described protocol [4]. The elevated circular platform was divided into equal fourths, with two enclosed arenas opposite each other and two open arenas between the enclosed arenas (Figure 3). Each mouse explored the maze for 300 sec. Activity was monitored via an overhead camera using ANY-maze software (Stoelting, Wood Dale, IL).

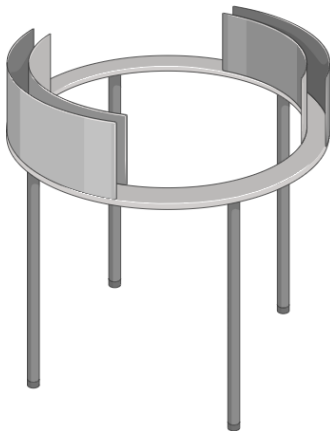


Figure 3: Elevated zero maze

The maze has two enclosed arenas and two open arenas, with each arena making up 25% of the maze. Lumens were measured in the open and closed arenas to make sure they were the same in each pair and to ensure consistency across multiple experimental days.

Locomotor activity tests

The locomotor activity tests were performed as previously described [4-6] using the standard protocol in the VUMC MNBCL. Each mouse was placed for 60 min in an open field activity chamber (Med Associates, 27 x 27 x 20.3 cm) (Figure 4A). Each activity chamber was housed in a light- and sound-controlled box. Location and movement were detected by interruption of infrared beams by the mouse (in each horizontal direction and elevated by 4 cm to measure rearing/jumping) and were measured by the Med Associates Activity Monitoring program. For anxiety analysis, the arena was separated into two equal areas: the center 50% and the perimeter 50% (Figure 4B).

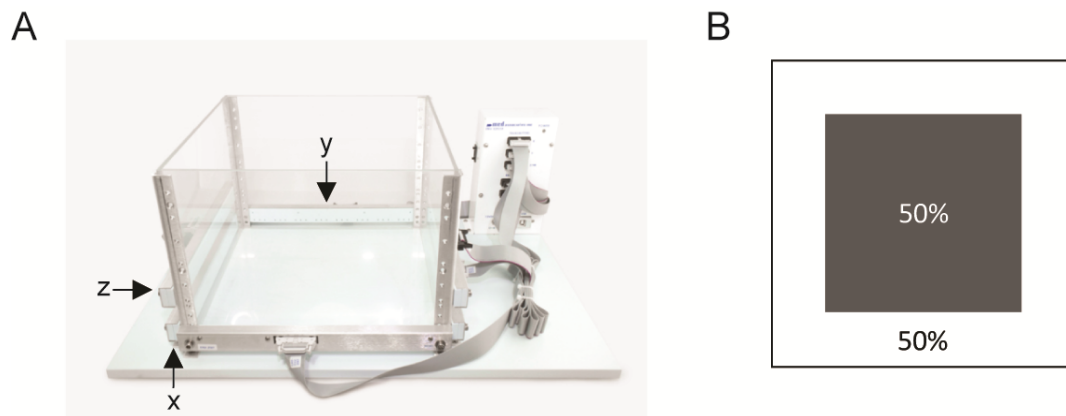


Figure 4: Locomotor activity chambers diagram (image adapted from Med Associates)

The chambers contain three pairs of infrared beams to detect movement in the x, y, and z directions. The floor of the chambers was divided into two equal portions for anxiety analysis: the center 50% and the perimeter 50%.

3-chamber socialization test (3CST)

The 3CST protocol followed that of a previous study [7]. **Habituation:** Subject mouse freely explored the empty apparatus for 10 minutes (Figure 5A). **Sociability:** Subject mouse freely explored a stranger mouse (novel mouse) and empty pencil cup (novel object) for 10 minutes (Figure 5B). **Social Novelty:** Subject mouse freely explored a novel mouse and familiar mouse for 10 minutes (Figure 5C). Mice, excluding the subject mouse, were contained in inverted pencil cups. The time subject mouse spent actively investigating each stimulus was recorded live and by hand using ANY-maze.

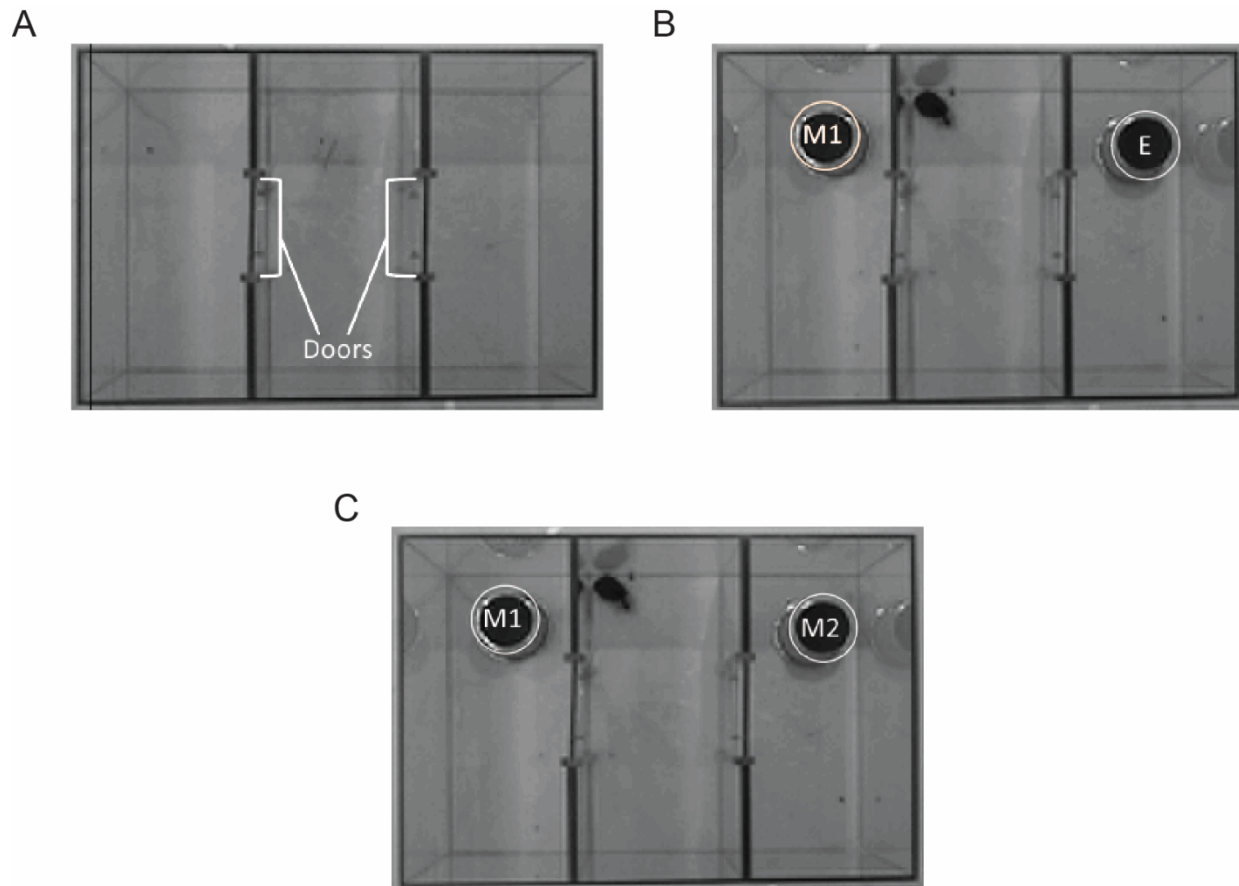


Figure 5: 3CST diagram

The three stages of the 3CST were diagrammed. There was a door in the each of the interior walls through which the mouse could freely pass but which the observer can close between each stage. The experimental mouse was gently guided back to the middle chamber and the doors were closed between each stage. The apparatus was not cleaned, and the experimental mouse was not removed between stages. A) Stage 1: The apparatus was empty. B) Stage 2: Two pencil cups were inverted and placed in the side chambers. One contained a novel age-matched wild-type female C57Bl6 mouse, and one was empty. Cups were cleaned between each animal. The position of the initial mouse (right chamber or left chamber) was alternated to avoid any external biases (proximity to the door or brighter light, for example). C) Stage 3: The novel female mouse from stage 2 remained where she was. A new novel age-matched wild-type female C57Bl6 mouse was placed under the previously empty cup.

Barnes maze

The Barnes maze test was based on a protocol described in detail in a previous study [8]. All data were collected using ANY-maze. The procedure included three stages: pretraining, training, and a memory probe. Every trial regardless of the stage was capped at 300 seconds (5 minutes). All trials began with a 30 second time-out in the start box, a black box placed in the middle of the maze. This gave the mouse time to settle after being handled and randomized the start position. After these 30 seconds, the box was removed, and the mouse was free to explore. All trials ended with a 30 second time-out in the escape box with the entrance blocked. This allowed the mouse to associate the box with a positive space (dark, enclosed). Pretraining trials occurred on day 1 and consisted of each mouse undergoing four consecutive trials in which the maze was not cleaned or moved, and the mouse was able to learn to find the escape box under the target hole (Figure 6). If the mouse was unable to find the escape box in any of the pretraining trials, it was gently guided to the escape box. The maze was cleaned between each animal. These trials were not recorded.

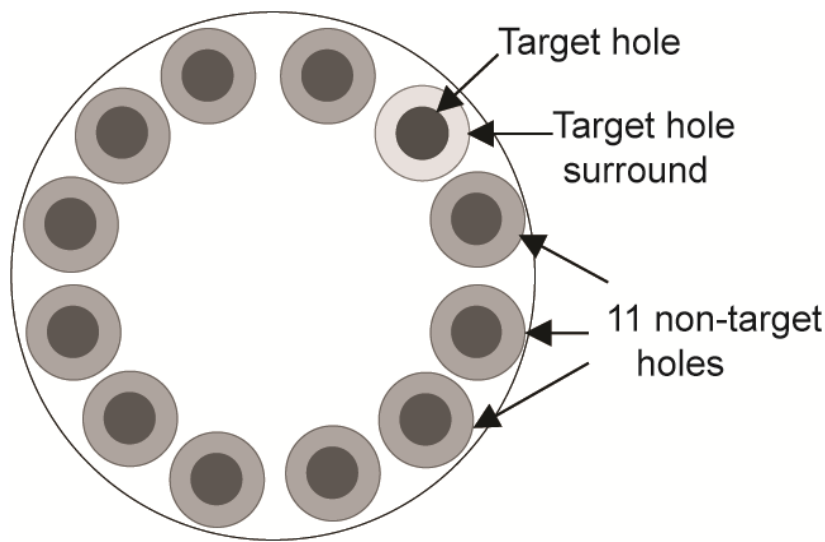


Figure 6: Barnes maze diagram

The Barnes maze consisted of 12 holes, all of which appeared identical from the starting point in the center of the maze. One of these holes, always in the same location relative to the room, had an escape box attached beneath it. The hole-surround extended beyond each hole a distance that was roughly the length of the body of an adult C57Bl6 mouse.

Following pretraining, the maze was rotated 90°. The position of the new target hole was aligned using ANY-maze such that the target hole never changed position with respect to the room. This ensured that the mice must use extra-maze clues in the room, such as a sink, a large whiteboard, the door, a large hose, etc.; instead of intra-maze clues, such as scratches on the maze surface. Four training trials were run on each day with the entire cohort completing training trial 1 before moving on to trial 2. The maze was cleaned between each animal and was rotated 90° after each trial. The four training trials were averaged to make a daily value for each animal. Days of training were repeated until the animals maximized their learning potential, or more technically, until a plot of “latency to escape” reached an asymptote.

On the last day after the training trials were complete, the mice underwent a 60-minute time-out. After this, the escape box was removed from the target hole and was replaced with a cover identical to those under the other 11 holes. Each mouse was given 300 seconds to explore the maze.

Additionally, where differences in learning were observed, search strategies were manually scored for each training trial to elucidate how learning was different for each genotype. Search strategies were scored as A) **a direct path**: the mouse travels either directly to the target hole or to a hole on either side before immediately going to the target hole, worth 0 points (Figure 7A); B) **a serial path**: the mouse visits two or more non-target holes in a sequential order before entering the target hole, also known as a thigmotaxic strategy, worth 1 point (Figure 7B); or C) **a random path** (the mouse used a non-direct or non-sequential method, worth 2 points (Figure 7C). This analysis was based on the strategies outlined in Harrison, et al. 2006.

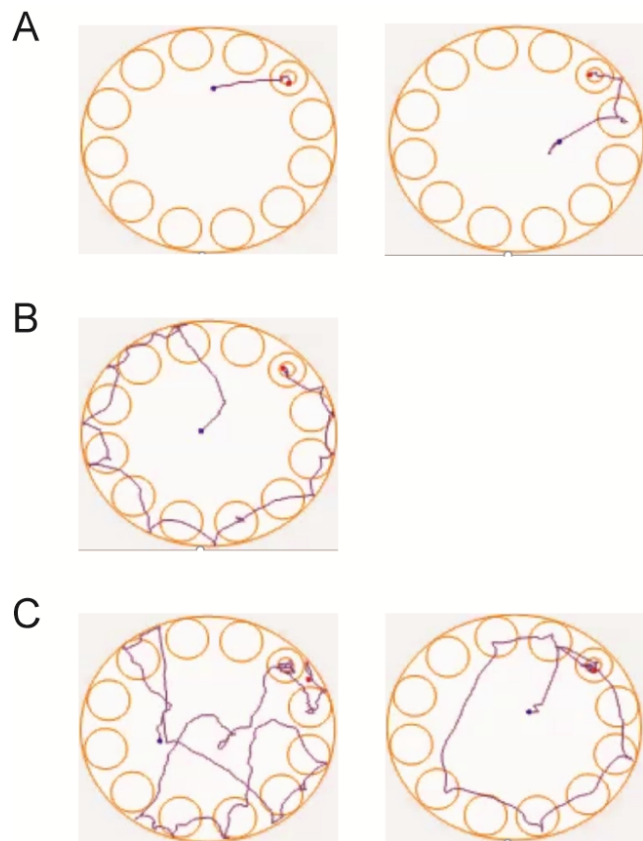


Figure 7: Search strategy examples

Examples for each type of search strategy were shown. Search strategies were manually scored from the ANY-maze mouse path videos. **A)** Direct search strategy: mouse went directly to the target hole, or to either adjacent hole before going to the target hole. **B)** Indirect search strategy: mouse visited several holes in sequential order before arriving at the target hole. **C)** Indirect search strategy: mouse visited holes randomly until finding the target hole. There may be an indirect component to this strategy but it was interrupted by non-sequential visits.

Sense of smell

There were five stages to testing sense of smell. 1) A mouse was placed into a clean cage and allowed 5 minutes of novel-environment exploration. Following this, stimuli were presented by inserting two sterile cotton swabs into the cage through an empty wire rack, one on each side of the cage along the long side, for 2 minutes. There were 2 minutes of rest in the empty cage between each test. Swabs were suspended above the floor by approximately 2 cm and were maintained an equal distance from each of the three walls on that side of the cage (Figure 8). Stimuli were presented alongside a plain control swab in the following order: 2) control (two plain swabs to reduce the novelty of the swabs themselves), 3) mineral oil, 4) home cage, 5) tangerine essential oil. Tangerine oil was chosen as it was not reported to be aversive to mice but would serve as a potent yet novel scent stimulus. Time spent investigating each stimulus compared to control was manually timed. Gloves were changed between each stimulus presentation to prevent scent contamination. The side of each stimulus was randomized throughout the experiment (left or right half of the cage). The timing observer was blind to genotype and to which swab contained the stimulus or the control scent. Mice were returned to the home cage after all mice in that cage completed testing to avoid stimuli scent transfer.

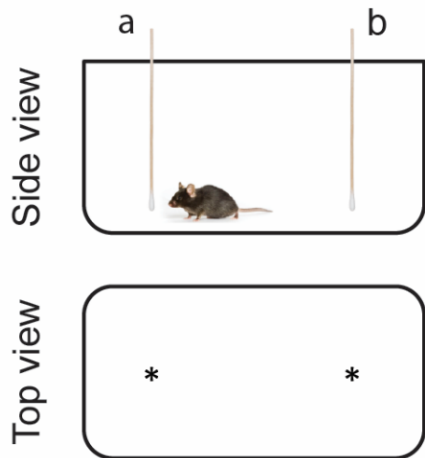


Figure 8: Sense of smell

Swabs were suspended above the floor by approximately 2 cm and were maintained at an equal distance from each of the three walls on that side of the cage. Each stimulus was presented for 2 minutes alongside a control swab. The location of the stimulus (location a or b) was randomized between trials.

TreadScan

The TreadScan apparatus (CleverSys Inc) consists of a transparent treadmill belt that slowly increased in rotation speed. Mice acclimated to the TreadScan apparatus until they were able to walk at 8 m/min. A camera below the belt captured the movement of each paw as the mouse walked (Figure 9). Twenty seconds of walking time was analyzed per animal. The parameters assessed were stance, swing, and stride in ms for each of the four paws, as well as overall average speed. Analysis was conducted using the TreadScan software.

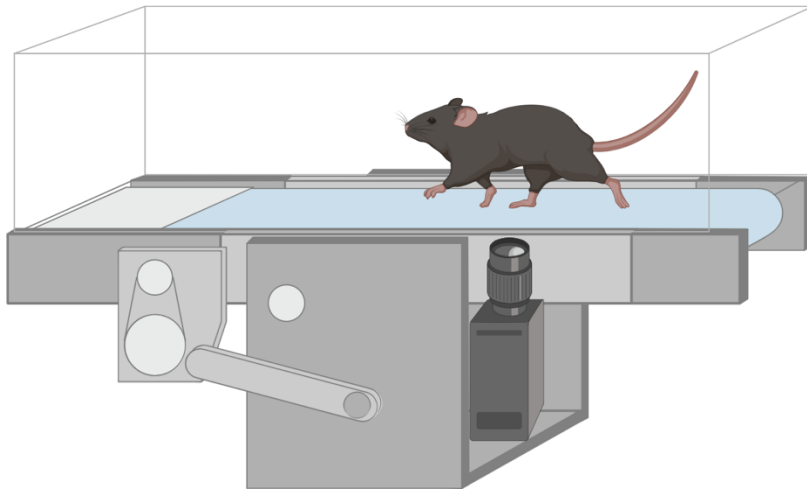


Figure 9: TreadScan

The mouse walked on a clear treadmill, while a camera below the treadmill captured paw movement and placement.

Rotarod

During this test, mice had to balance and walk on a rotating rod (Figure 10). Mice were tested for up to 5 minutes; during the first 2.5 minutes the rotational speed of the rod steadily increased from 4 to 40 rpm, and during the second 2.5 minutes a rotating rod speed of 40 rpm was maintained. Time until each mouse either fell off the rod or held onto and spun around the rod was recorded. Thus, only successful walking as the rod spun was recorded as a successful behavior. This was repeated in triplicate every day for 3 days with a 30-minute rest between each trial.

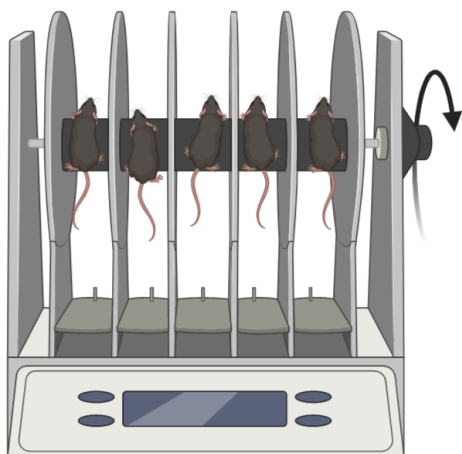


Figure 10: Rotarod

Five mice were tested simultaneously, with walls between them to physically separate each mouse from adjacent mice. The rod spun in the natural direction of forward movement for the mice.

Tail suspension test

Mice were individually suspended onto the apparatus sensor by adhesive tape placed approximately 4 cm from the base of the tail (Figure 11). The sensor detected movement by the mice, and mice were considered immobile when detected motion fell below the lower threshold of 7. Test duration was 6 minutes.

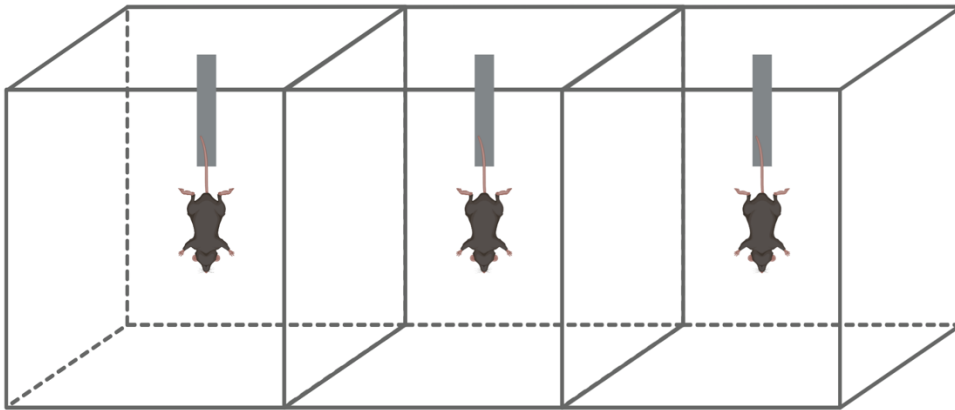


Figure 11: Tail suspension test (TST) schematic

Mice were suspended from the force sensor by their tails. This sensor can record even minute movement. Each sensor was located within a white cube with no front face (for experimenter access).

Analysis

Behavioral data were analyzed with GraphPad Prism software. Independent-sample Student's t-tests were used in the analyses of locomotor activity, elevated zero maze, and the probe trials of the Barnes maze. Two-way ANOVA was used for the 3CST for both sociability and social novelty. Repeated-measures ANOVA was used to analyze the training trials of the Barnes maze. Post hoc and *a priori* Bonferroni comparisons were conducted to evaluate individual mean comparisons where appropriate. All analyses used an alpha level of 0.05 to determine statistical significance.

Biochemistry

Cerebellum, cortex, hippocampus, and thalamus were dissected from 1-3-month-old mouse brains and homogenized with RIPA buffer (50 mM Tris-Cl, pH 8.0, 150 mM NaCl, 1% Nonidet P-40, 0.5% sodium deoxycholate and 0.1% SDS) to obtain lysates. Proteins were fractionated by SDS/PAGE and immunoblotted with following antibodies: ATPase (1:2000, a6F, DSHB), GABA_A receptor α 1 subunit (1:500, 75-136, NeuroMab), GABA_A receptor β 3 subunit (1:500, B300-199, Novus Biologicals), GABA_A receptor γ 2 subunit (1:500, AB 5559, Millipore), gephyrin (1:1000, 3B11, Cedarlane), and GAPDH (1:6000, MAB374, Millipore) antibodies.

Surface expression of GABA_A receptor subunits was evaluated by extraction of plasma membrane proteins from brain. Plasma membrane proteins were isolated by using 101Bio kit (101bio.com) with minor modification. Proteins were fractionated by SDS/PAGE and subjected

to immunoblot analyses. ATPase was used as membrane protein loading control, whereas GAPDH was cytoplasmic proteins contamination control.

Electrophysiology

Whole-cell slice recording

Brain slices were prepared according to previously published methods [9]. Coronal brain slices (300 μm) taken from 30-day-old mice (males and females) were cut using a LEICA VT-1200S vibratome (Leica Inc) with oxygenated dissection solution (mM: 2.5 KCl, 0.5 CaCl₂, 10 MgSO₄, 1.25 NaH₂PO₄, 24 NaHCO₃, 11 Glucose, 214 Sucrose; pH 7.4 and perfused with 95% O₂/5% CO₂ at 4°C). The brain slices were transferred into a glass chamber with oxygenated artificial cerebrospinal fluid (ACSF) (mM: 126 NaCl, 2.5 KCl, 2 CaCl₂, 2 MgCl₂, 26 NaHCO₃, 10 Glucose, pH 7.4) and then recovered at room temperature for 1 hour before experiments.

With an upright Eclipse FN-1IR-DIC microscope (Nikon) and a MultiClamp 700B amplifier and Digidata 1440A (Molecular Devices), whole-cell recordings of layer V/VI pyramidal neurons (with typical apical dendrites within SS cortex) were obtained according to previously published methods [9]. Layer V pyramidal neurons were distinguished by their large soma size with apical dendrites, and layer VI pyramidal neurons were distinguished by their position right above white matter within coronal section brain slices. We did not notice any significant morphological difference (IR-DIC imaging) in pyramidal neurons from wt or KI

mice. The mIPSCs were isolated pharmacologically by including 10-20 μM NBQX and 1 μM tetrodotoxin in the ACSF. The chloride ion reversal potential with the external ACSF and internal solution used (mM: 135 CsCl, 10 HEPES, 10 EGTA, 5 QX-314, 5 ATP-Mg; 290-295 mOsm, pH = 7.3) was 0 mV, and neurons were voltage-clamped at -60 mV. Access resistances during recording were continuously monitored and confirmed to be less than 25 M Ω . Data were collected using the Clampex program 10.2 (Molecular Devices) [9, 10]. Histograms and cumulative graphs were constructed using Clampfit (Molecular Devices).

Thalamocortical oscillations

Horizontal thalamocortical brain slices (350-400 μm) were prepared [11] from P30 mice to maintain thalamocortical and corticothalamic circuit projections. Slices were placed on a self-made nylon mesh interface (only one side of the slice contacted the ACSF solution flowing below). One unipolar tungsten electrode (MultiClamp 700B, current-clamp mode) was placed in the VBn of the thalamus to record spontaneous multi-unit activity, which was band-filtered between 100 Hz and 3 kHz [11]. Experiments were performed at 31 – 32°C for 1-2 hours to collect sufficient spontaneous multi-unit activity. Data were filtered (2 kHz) and digitized (20 kHz) using a Digidata 1440A AD converter. Data were analyzed using both Clampfit and Matlab. Oscillation indices and duration for the spontaneous multi-unit activity in thalamocortical slices from wt and KI mice were calculated and compared [12, 13].

Statistical analysis

Statistical analyses were performed, and graphs were generated using GraphPad Prism. Tests performed on each data set were outlined in the corresponding figure legend. All analyses used an alpha level of 0.05 to determine statistical significance.

Bibliography

1. Arain, F.M., K.L. Boyd, and M.J. Gallagher, *Decreased viability and absence-like epilepsy in mice lacking or deficient in the GABAA receptor alpha1 subunit*. *Epilepsia*, 2012. **53**(8): p. e161-5.
2. Warner, T.A., et al., *Heat induced temperature dysregulation and seizures in Dravet Syndrome/GEFS+ Gabrg2(+/Q390X) mice*. *Epilepsy Res*, 2017. **134**: p. 1-8.
3. Belovicova, K., et al., *Animal tests for anxiety-like and depression-like behavior in rats*. *Interdiscip Toxicol*, 2017. **10**(1): p. 40-43.
4. Kang, J.Q., et al., *The human epilepsy mutation GABRG2(Q390X) causes chronic subunit accumulation and neurodegeneration*. *Nat Neurosci*, 2015. **18**(7): p. 988-96.
5. Fukada, M., et al., *Loss of deacetylation activity of Hdac6 affects emotional behavior in mice*. *PLoS One*, 2012. **7**(2): p. e30924.
6. McLaughlin, B., et al., *Haploinsufficiency of the E3 ubiquitin ligase C-terminus of heat shock cognate 70 interacting protein (CHIP) produces specific behavioral impairments*. *PLoS One*, 2012. **7**(5): p. e36340.
7. Carter, M.D., et al., *Absence of preference for social novelty and increased grooming in integrin beta3 knockout mice: initial studies and future directions*. *Autism Res*, 2011. **4**(1): p. 57-67.
8. Harrison, F.E., et al., *Spatial and nonspatial escape strategies in the Barnes maze*. *Learn Mem*, 2006. **13**(6): p. 809-19.
9. Huang, X., et al., *Overexpressing wild-type gamma2 subunits rescued the seizure phenotype in Gabrg2(+/Q390X) Dravet syndrome mice*. *Epilepsia*, 2017. **58**(8): p. 1451-1461.
10. Zhou, C., et al., *Hypoxia-induced neonatal seizures diminish silent synapses and long-term potentiation in hippocampal CA1 neurons*. *J Neurosci*, 2011. **31**(50): p. 18211-22.
11. Huguenard, J.R. and D.A. Prince, *Intrathalamic rhythmicity studied in vitro: nominal T-current modulation causes robust antioscillatory effects*. *J Neurosci*, 1994. **14**(9): p. 5485-502.
12. Sohal, V.S., et al., *Dynamic GABA(A) receptor subtype-specific modulation of the synchrony and duration of thalamic oscillations*. *J Neurosci*, 2003. **23**(9): p. 3649-57.

13. Sugihara, I., E.J. Lang, and R. Llinas, *Serotonin modulation of inferior olivary oscillations and synchronicity: a multiple-electrode study in the rat cerebellum*. Eur J Neurosci, 1995. 7(4): p. 521-34.

Chapter 3

A Knock-in Mouse Harboring a Patient-Derived Disease-Associated Mutation, *Gabrb3*^{+D120N}, Recapitulates the Full Triad of Features of the Lennox-Gastaut Syndrome

This chapter is adapted from a published work with permission of the authors [1]. The dissertation author was involved in many aspects of this work but focused heavily on the behavioral analysis, spectral frequency analysis, and therapeutic interventions.

Introduction

Lennox-Gastaut syndrome (LGS) is a severe epilepsy that is classified by the International League Against Epilepsy (ILAE) as one of eight early-onset epileptic encephalopathies. Epileptic encephalopathies are associated with abnormal brain activity during development and a progressive decline of cerebral function and cognition and behavioral regression or deterioration after onset of the disorder [2]. LGS has a range of onset between 1-9 years of age [2-4] and accounts for 5-10% of childhood epilepsies [4, 5], although it frequently persists and worsens through adolescence and adulthood [3]. LGS is characterized by a triad of features including epilepsy with multiple seizure semiologies, a generalized slow spike wave discharge (SSWD) pattern on EEG, and cognitive and behavioral abnormalities [6]. The most

common seizure types include atypical absence, atonic, and tonic seizures, and less common types include clonic, myoclonic, and generalized tonic-clonic (GTC) seizures. Most LGS patients experience behavioral abnormalities that can include varying degrees of developmental delay, intellectual disability (ID), and other behavioral problems such as hyperactivity and autism spectrum disorder (ASD). LGS can be genetic or secondary to an underlying brain disorder.

There is no reliably effective treatment for LGS, and up to 10% of LGS patients die before the age of 11. LGS prognosis is generally poor as seizures are often refractory to antiepileptic drugs (AEDs) [6]. It is difficult to address the cause and underlying mechanisms of genetic LGS in human studies, and lack of animal models has hindered progress in understanding the pathophysiology and development of treatment for this devastating disease. While the etiopathology of LGS is largely unknown at cellular and molecular levels, next-generation DNA sequencing has identified mutations in genes implicated in its pathogenesis [7]. The *de novo* mutation (c.G358A, p.D120N) was one of several *GABRB3* mutations found in LGS patients by whole exome sequencing of familial triads (child affected, parents unaffected) [8]. *GABRB3* encodes the human $\beta 3$ subunit of the heteropentameric GABA type A (GABA_A) receptors that mediate fast inhibitory synaptic neurotransmission. Dysfunction of GABA_A receptors can lead to a variety of seizure types [9], and in addition, to LGS. *GABRB3* mutations are implicated in several other childhood epilepsies including childhood absence epilepsy, infantile spasms, and other early onset epileptic encephalopathies [3, 10]. The $\beta 3$ subunit plays an important role during brain development, with expression of $\beta 3$ subunits being widespread and abundant in embryonic and neonatal brains, especially in the cerebral cortex, thalamus, hippocampus, and other regions involved in generating seizures [11, 12].

Amino acid sequence alignment analysis showed that an aspartic acid residue at position 120 (D120) was invariant across all GABA_A receptor subunits, and structural modeling revealed that the D120N amino acid substitution was in a conserved domain of the GABA_A receptor β 3 subunit near the GABA binding pocket. We previously demonstrated *in vitro* in transfected HEK293T cells that the mutant β 3 subunit not only significantly reduced GABA_A receptor currents, but also altered their kinetic properties without affecting receptor assembly or trafficking [13]. However, a major question remains; does the single point mutation in the mutant β 3(D120N) subunit cause the multiple LGS seizure types and behavioral abnormalities, and if so, how? Although these *in vitro* results strongly suggest that the mutant β 3(D120N) subunit contributes to generation of LGS seizure types and behavioral abnormalities, its causal role can only be established directly by determining its effect on behavior and brain excitability *in vivo*. To do this we generated and characterized a mouse model of LGS (the heterozygous *Gabrb3*^{+/*D120N*} KI mouse), which has the human *GABRB3* mutation, c.G358A, p.D120N, that was identified in an LGS patient. Currently, there are no reports of mouse models exhibiting the triad features of LGS and no mouse models carrying LGS-associated human mutations. Here we show that heterozygous *Gabrb3*^{+/*D120N*} KI mice recapitulated both the seizure and behavioral abnormalities associated with LGS. While expression and trafficking were unaltered, cortical mIPSCs in thalamocortical coronal slices had reduced amplitude, and prolonged spontaneous thalamocortical oscillations in horizontal thalamocortical slices were recorded. Finally, AEDs commonly used to treat LGS were similarly effective at reducing seizures in the KI mice. Therefore, *Gabrb3*^{+/*D120N*} KI mice are an excellent model for LGS and should be useful for further characterization of LGS pathophysiology and for development of novel therapies. Importantly, *Gabrb3*^{+/*D120N*} KI mice show that it is possible to fully recapitulate a complex

human epilepsy syndrome in rodents with a single point mutation, indicating overlap of the seizure syndrome and behavioral comorbidity circuitry.

Lennox-Gastaut syndrome

General information

The age of onset of LGS is between ages 1 and 9, with a mean age of onset around the 3rd birthday [2]. LGS represents 1-2% of all epilepsies and 1-10% of childhood epilepsies [2]. In a study of 38 adult LGS patients, those with a previous diagnosis of West syndrome (WS) had a mean age of seizure onset of 3.9 ± 2.1 months ($n = 11$), while those that did not have a WS diagnosis experienced seizure onset at 40 ± 47 months ($n = 27$) [14]. In general, the age of onset is lower in patients with cryptogenic cause than those with an identifiable etiology [2]. Patients experience frequent seizures that are commonly drug resistant [2]. Most patients experience multiple types of seizures, including tonic, atypical absence (AAS), generalized tonic-clonic, and myoclonic seizures [2, 4]. LGS patients can also experience severe sleep abnormalities including tonic seizures in sleep, sleep pattern disorganization, and increase in both SSWD and fast rhythms [14]. Outcomes for LGS patients are considered quite poor [2].

Genetics of LGS

In 67-75% patients, the cause of LGS is identifiable and can include brain damage, perinatal complications (~25% of patients), congenital central nervous system malformations (e.g. tuberous sclerosis), infections (e.g. meningitis, sepsis), or metabolic disorders [2]. The remainder of patients have a cryptogenic or genetic cause [2]. Only about 5% of LGS patients have a family history of epilepsy [2], which is higher than the epilepsy occurrence in the general population (1-2%) [15]. The National Institutes of Health lists eight genes as having mutations associated with LGS, including *GABRB3* [16]. In addition to the *GABRB3* mutation discussed here, Epi4k identified 9 mutations in *SCN1A* alone, and mutations in 16 other genes thought to be causative of LGS [8]. Other genes commonly containing LGS-associated mutations include forkhead box G1 (*FOXG1*), chromodomain helicase DNA-binding protein 2 (*CHD2*), and dynamin 1 (*DNMI*) [2, 17]. Additionally, copy number variations have been found in 3-19% of patients [2]. Therefore, when accounting for genetic risks, *de novo* mutations could have the highest contribution to disease risk [14, 17]. Due to the genetic heterogeneity of patients, it is evident that LGS is a disorder of polygenic origin, in which disruptions in multiple genes may lead to the same disorder [2].

Seizures associated with LGS

At the time of diagnosis, most LGS patients are having multiple types of seizures [2]. LGS patients can experience all of the seizure types discussed in Chapter 1 as presenting in epileptic encephalopathies of childhood [14], except for epileptic spasms, which resolve around 2-3 years of age [3, 4]. However, recall that some 30% of LGS patients previously had a diagnosis of WS [18], which includes epileptic spasms. The most prevalent types of seizures

were tonic seizures and AASs (66-74% of patients each) [2, 4]. These were followed by GTC (45%), focal (29%), and myoclonic (11-28%) seizures [2, 4]. All of these patients had at least 3 types of seizures and drug-resistant seizures [2], both common features of LGS. AASs are not observed in most epilepsy syndromes but are very common in LGS [4]. AASs are more complex than typical absence seizures (TASs) and are usually associated with significant cognitive impairment [19]. Features of each seizure type are discussed in more detail in Chapter 1.

Cognitive dysfunction in LGS

One of the principle features of LGS is that patients have abnormal behaviors such as ID and behavioral problems in conjunction with seizures [2]. The most common of these abnormal behaviors include impaired cognition, attention deficit hyperactivity disorder (ADHD), ASD, mood instability and conduct problems such as agitation or aggression severe enough to require neuroleptic treatment [14, 20]. In one clinical assessment, 47% of LGS patients had diagnosed psychiatric disorders [14]. In LGS these conditions are considered part of the disorder, not comorbidities, and while they are commonly seen in other epilepsy syndromes [21-23], they are particularly impactful to LGS patients and are often associated with poor outcomes [14]. For many patients, while seizures are the prominent problem, the burden of behavioral problems is heavy and increases with aging, sometimes becoming the primary treatment concern [14]. Interestingly, there are no differences seen in seizure severity or cognitive dysfunction between patients with genetic/unknown etiology and those with symptomatic LGS [14].

Impaired cognition is present in 80-90% of LGS patients [3, 24], with an estimated 20-60% having severe ID at the time of seizure onset, which increases to 75-95% five years after seizure onset [2]. Concurrent EEG-fMRI studies have shown that in LGS patients, seizures

engage known cognitive networks including brainstem and thalamocortical pathways. LGS patients have less within-network integration, weaker connectivity in the default-mode network, and increased between-network activity (decreased network segregation), changes that were evident during both ictal and interictal periods [25]. Abnormal connectivity patterns are thought to compete with normal developmental mechanisms, which may result in subsequent cognitive impairment. Furthermore, the SSWD that is a hallmark feature of LGS has been proposed to encourage the brain to focus on antiseizure mechanisms thereby diverting away from normal developmental processes [4, 26]. SSWDs are also associated with increased BOLD signal on fMRI in primary cortical areas [14], which may indicate a direct disruption of cortical processing with SSWDs. In one clinical assessment of 38 adult LGS patients, all had ID, with 18% of LGS patients having mild ID, 40% having moderate ID, and 42% having severe ID [14]. There are several factors that increase the risk of having severe ID, including a history of non-convulsive status epilepticus (NCSE), a previous WS diagnosis, and an early age of seizure onset [2].

There are other common behavioral abnormalities outside of ID in the LGS population. While the percentage of patients with both LGS and ASD is not specifically known, the coincidence is often referenced, with 5-37% of primary epilepsy patients also having an ASD diagnosis [27], and 30-40% of ASD patients having an epilepsy diagnosis [28, 29]. Hyperactivity, one of the hallmark features of ADHD [30], is one of the most common comorbidities diagnosed in patients with LGS [23, 31]. Finally, while cognitive decline and ID are common in LGS patients, it is difficult to distinguish cognitive decline and ID secondary to epilepsy from that due to abnormal neuronal connectivity, severe seizures or AED side effects [2].

Treatments used in LGS

Treatment of LGS is complicated, difficult and generally unsuccessful. The primary treatment option is AED therapy. Most patients with epileptic encephalopathies are resistant to AED therapy and most patients are on more than 2 AEDs [2]. LGS patients take between two and six AEDs, with an average number of 3.4 AEDs [2, 14]. After 18 months of AED treatment, 72% of LGS patients continue to have seizures [2]. Patients had been treated with an average of 9 AEDs (range 4 to 20) [14] during their life-time. The range of seizure types in LGS makes them particularly difficult to treat and some drugs run the risk of improving one seizure type while worsening others [2, 4]. All AEDs used to treat LGS have serious possible side effects including pancreatitis, liver damage or failure, renal stones, aplastic anemia, anorexia, and cognitive impairment [2]. Some medications, such as felbamate and topiramate, carry heavy side effects risks, but LGS is often considered debilitating enough to warrant this risk [32].

The first line of AED therapy includes sodium valproate, lamotrigine, and topiramate [2]. Sodium valproate is specifically beneficial if the primary seizure types are atonic seizures, tonic seizures, and AASs. Ethosuximide, a common medication used in the treatment of TAS, is useful for treatment of AAS, myoclonic, and atonic seizures in LGS patients [4]. Other commonly used AEDs include clobazam, felbamate, and rufinamide [2]. A newer AED, lacosamide, is specifically effective at reducing tonic seizures [14], one of the most common seizure types associated with LGS [2]. Despite recent development of new AEDs, seizure control in LGS patients is still problematic [14], and their doses and safety have yet to be identified for LGS patients [2]. Resistance to AEDs is a constant and persistent problem despite multiple drug trials and polytherapy [14]. Seizures in sleep are the hardest seizures to treat, and AED therapy often causes sedation, which further increases the risk of seizures [4].

Due to the difficulty of controlling seizures in LGS with AEDs, several other therapeutic options have been developed. There are several surgical options including implanting a vagal nerve stimulator (VNS), performing a corpus callosotomy or focal cortical resection, and deep brain stimulation. The mechanism of the anticonvulsant activity of VNS is not known, although it has been proposed to interrupt electrical synchrony or to change metabolism or blood flow in seizure-involved brain regions. VNS is effective for all types of seizures, and while it has side-effects, they are less severe than a corpus callosotomy. Corpus callosotomy can lead to a cortical disconnection syndrome in which specialized brain regions are unable to communicate with each other to jointly perform a task. [2]

Non-surgical alternatives include the ketogenic diet, intravenous immunoglobulin therapy, and gene therapy. The mechanism by which the ketogenic diet works to reduce seizures is unknown, but it can be very effective at reducing NCSE. The ketogenic diet can have side effects, although not generally severe, but it is very difficult for families to strictly follow the diet. [2] Gene therapy is a novel modality, which has yet to be explored in LGS patients but which is an exciting avenue for further research.

Cannabinoid therapy is a new and very interesting therapy for LGS patients. Cannabinoid signaling has been implicated in the pathophysiology of epilepsy and several studies have shown disruptions in endocannabinoid signaling in seizure and epilepsy models. The endocannabinoids anandamide and 2-arachidonoyol glycerol (2-AG), are important for synaptic transmission control and neuronal firing rate. There are two cannabinoid receptors widely distributed in the central nervous system, CB1 and CB2. Both receptors are $G_{i/o}$ -coupled receptors. Neuronal expression is primarily comprised of CB1, which is expressed

presynaptically at both glutamatergic and GABAergic synapses. Activation of CB1 leads to inhibition of synaptic transmission at either type of synaptic terminal. [33]

The three main species of *Cannabis* contain over 100 cannabinoids, with tetrahydrocannabinol (THC) and cannabidiol (CBD) being the most abundant and best characterized and the two main compounds of interest for exogenous cannabinoid therapy [33]. In the United States, the Drug Enforcement Agency classifies CBD as a schedule V drug while THC is a schedule I drug [34] and thus CBD is much easier to obtain for therapeutic and research purposes. Products with high THC content have undesired side effects, whereas cannabidiol has minimal to no psychoactive effect [33]. CBD also has anti-convulsant, analgesic, anxiolytic, antiemetic, anti-inflammatory, neuroprotectant, and anti-tumorigenic properties [33]. Unlike THC, there is no evidence for developing tolerance to CBD, and there are no withdrawal symptoms [33]. Prolonged exposure to marijuana during development can negatively impact neuronal connectivity [33], leading to cognitive impairment and chronic psychiatric concerns [35]. Marijuana also poses concerns in pregnant women [33]. All things considered, CBD is the cannabinoid of choice when considering epilepsy therapy.

There exist several examples of changes in CB1 related to epilepsy, including downregulation of CB1 in glutamatergic regions of the hippocampus in surgical samples from epileptic patients. Additionally, many population surveys indicated CBD and THC efficacy in epilepsy treatment, but these are likely biased and have been hard to confirm. The anti-seizure properties of THC are likely due to its action on the CB1 receptor. [33] CBD is known to act on at least 22 entities; however, it has weak affinity for CB1 and CB2 receptors. The anti-seizure effect of CBD is more likely due to agonism or antagonism of G-protein coupled receptors, ion channels, or neurotransmitter transporters [33, 34]. CBD has been found to be protective in

multiple (but not all) animal seizure models, including pentylenetetrazol induction in rodents and in pilocarpine-induced TLE in rats [33]. CBD has a very low bioavailability (6%), is lipophilic, and readily crosses the blood brain barrier [34]. The half-life of CBD is around 60 hours [34].

There have been three high-quality placebo-controlled adjunctive-therapy CBD trials in Dravet syndrome (DS) and LGS [33]. The initial study on the anti-seizure activity of CBD was conducted in 11 epilepsy centers in the United States [33]. This was done as an adjunctive-therapy trial as it was deemed unethical to take patients off their other AEDs. The study contained 33 DS and 31 LGS patients aged 1-30 years [33]. LGS patients reported a 36% reduction in median seizure occurrence while DS patients reported a 43% reduction. CBD was effective at reducing the frequency of convulsive seizures (tonic, clonic, tonic-clonic, atonic) in DS, and the frequency of drop attacks in LGS [33]. CBD was found to be twice as effective at reducing seizures in patients also taking clobazam (27% vs 51%) [33]. These studies found that the active metabolite of clobazam increases around 5-fold after 4 weeks of CBD; however, there were no evident effects on the other AEDs tested, including valproic acid, topiramate, stiripentol, and levetiracetam [33]. In addition to a reduction in seizure frequency, patients on CBD also reported that several other factors improved, including overall quality of life, energy, memory, cognitive function, social interaction, and general behavior. These factors were not correlated with changes in seizure frequency, indicating that they were direct effects of CBD, not indirect effects of seizure reduction. In another study at the same center, LGS patients had a 48% reduction in the convulsive seizure rate and a reduction in atonic seizures (which often lead to injury) of 71% [33]. Of note, placebo effects were an important component of these studies because of social and political implications of cannabinoid therapy, and individually-held beliefs that “natural” remedies are better [35].

Two double-blind placebo-controlled trials studying the efficacy of CBD therapy in LGS patients followed these initial studies. Both were paid for by the manufacturer, GW Research Ltd., and are therefore limited by their funds, long-term data, and qualitative outcome measures [34]. The first trial, GWPCARE4, enrolled 171 patients between 2 and 55 years of age (average 15 years of age) with uncontrolled atonic seizures occurring at an average rate of 74 per month [36]. The median number of AEDs in these patients was 3, consistent with the LGS population average. 20 mg/kg/day of CBD for 12 weeks was twice as effective at reducing drop attacks than placebo was (44% vs 22%). 44% of the CBD group had an over 50% reduction in all seizures, compared to 24% in the placebo group. Patients in the CBD group reported significant improvements in all secondary outcomes, which included any metric besides atonic seizure frequency. In the second trial, GWPCARE3, 225 patients were enrolled with similar attributes as the first trial [37]. Patients were given CBD either 20 mg/kg/day as before or at 10 mg/kg/day. Both doses resulted in similar seizure control as seen in the first trial, with weaker improvement in the placebo group. In both studies, a high proportion of patients in both the CBD and placebo group reported adverse effects, usually of somnolence or a decrease in appetite. These adverse effects were mild compared to the severity of the effects seen in regularly prescribed AEDs. Of the 212 patients that completed the trial, 99% entered an open-label extension study, which is ongoing [33, 34]. Following the publication of these data, in September of 2018 CBD was approved in the United States for the treatment of both LGS and DS [34].

Outcomes for patients with LGS

There are many comorbidities associated with LGS, which include urinary incontinence, osteoporosis, GI symptoms, renal and pulmonary dysfunction, and severe and treatment-resistant insomnia [14]. All seizure types present in LGS persist into adulthood [14]; however, the features of LGS (seizures types, frequency, severity) evolve over time [2]. Total seizure-freedom is considered unattainable [4]. Cognitive and behavioral problems persist in most patients independent of the level of seizure control [2]. Rarely, some patients may function independently, but up to 76% of patients need special home or institutional care [2].

The D120N patient

The patient in which the *GABRB3* c.G358A, p.D120N mutation was identified experienced AA, atonic, myoclonic, and GTC seizures. In regard to cognitive ability, the patient had an adaptive test score of less than 20. [8] Adaptive skills are defined as “the effectiveness with which the individual copes with the natural and social demands of his environment” [38]. Adaptive behavior is assessed on the same scale as IQ (mean 100, standard deviation 15) and is often used when an IQ assessment is unable to be performed, which is common in individuals with low ranges of IQ [39]. The patient was also diagnosed with ADHD and experienced mood instability and impulsive behavior. Before his LGS diagnosis, the patient had a diagnosis of WS early in childhood. [8]

The D120N mutation

D120N is in loop A on the $\beta 3$ (+) subunit interface of the GABA binding pocket (Figure 1A, B). We predicted that this would not interfere with trafficking or assembly of the receptor but would greatly impact function of the receptor in regards to GABA binding and perhaps receptor/channel coupling.

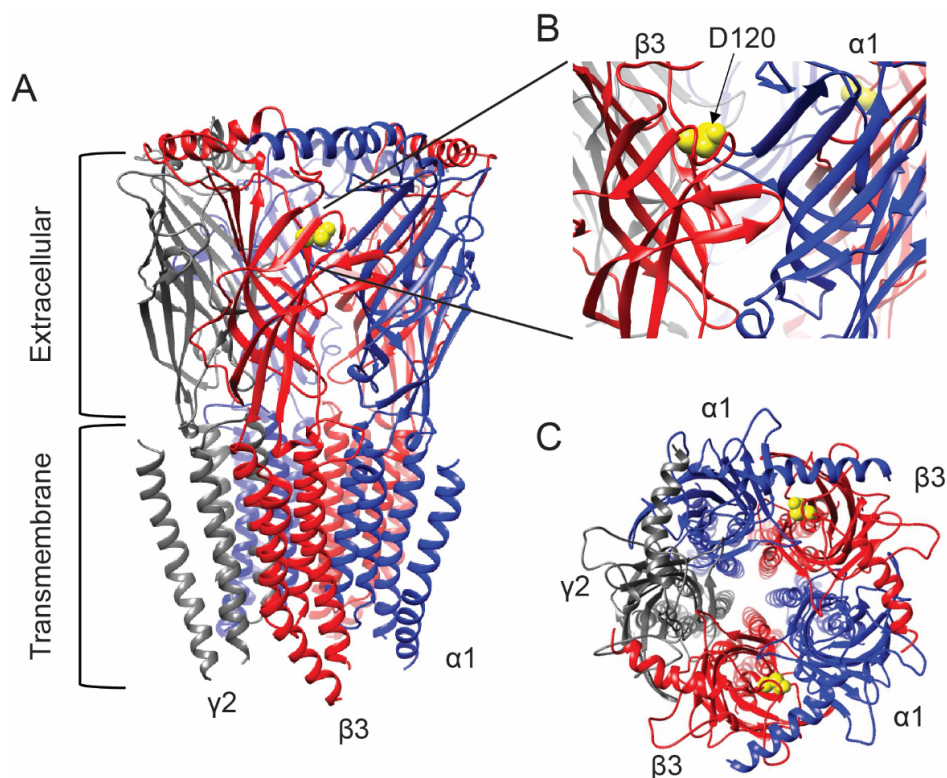


Figure 1: GABA_A receptor structure with D120 highlighted

This structure is based on the published crystal structure of the $\beta 3$ subunit homomer [40]. The location of D120 is highlighted in yellow. **A)** A lateral view of the assembled receptor with the TM3-TM4 ICD removed. **B)** Zoomed in view of the location of D120. D120 is located in the GABA binding pocket at the β - α interface. **C)** Top-down view of the receptor. D120N could be present in one, both, or neither of the two GABA binding pocket.

In vitro data

It is useful to first assess the impact of a mutation in a model system, such as transfected HEK293T cells that do not form synapses and do not express GABA_A receptors [41]. This allows for analysis of the impact of just those subunits that are transfected without having to consider the complicated dynamics of synaptogenesis and varied subunit composition. It is therefore possible to assess the changes in biochemistry and channel properties produced by the mutation. This work was performed in our laboratory and published by Janve et al. (2016).

β 3(D120N) subunit expression was not observed to affect either total or surface expression of the β 3 subunit or its assembly partners, α 1 and γ 2, when these subunits were transfected into HEK-293T cells (Figure 2A). However, when GABA was applied at a saturating concentration of GABA for wild type receptors (1 mM) to similarly transfected HEK-293T cells, β 3(D120N) subunit expression resulted in about a one-third reduction in the current density of mIPSCs in whole-cell recordings (Figure 2B). When the concentration of GABA was increased 10-fold (10 mM), the current density nearly recovered to wild type levels (Figure 2C). Microscopic properties of β 3(D120N) subunit-containing receptor single channel currents were also altered. The open probability, opening frequency, and burst duration of spontaneous activity were all reduced and mean open time was unchanged (Figure 2D). [13] These data are consistent with the hypothesis that the D120N amino acid substitution disrupts the GABA binding pocket due to its location in loop A. Interestingly, while structural modeling comparing a wild-type receptor to a receptor containing D120N indicated that the positioning of loop A was disrupted by $\sim 1\text{\AA}$ by the mutation, both loop B and the β 4- β 5 sheet loop were shifted $>2\text{\AA}$ from their endogenous locations (Figure 2E) [13].

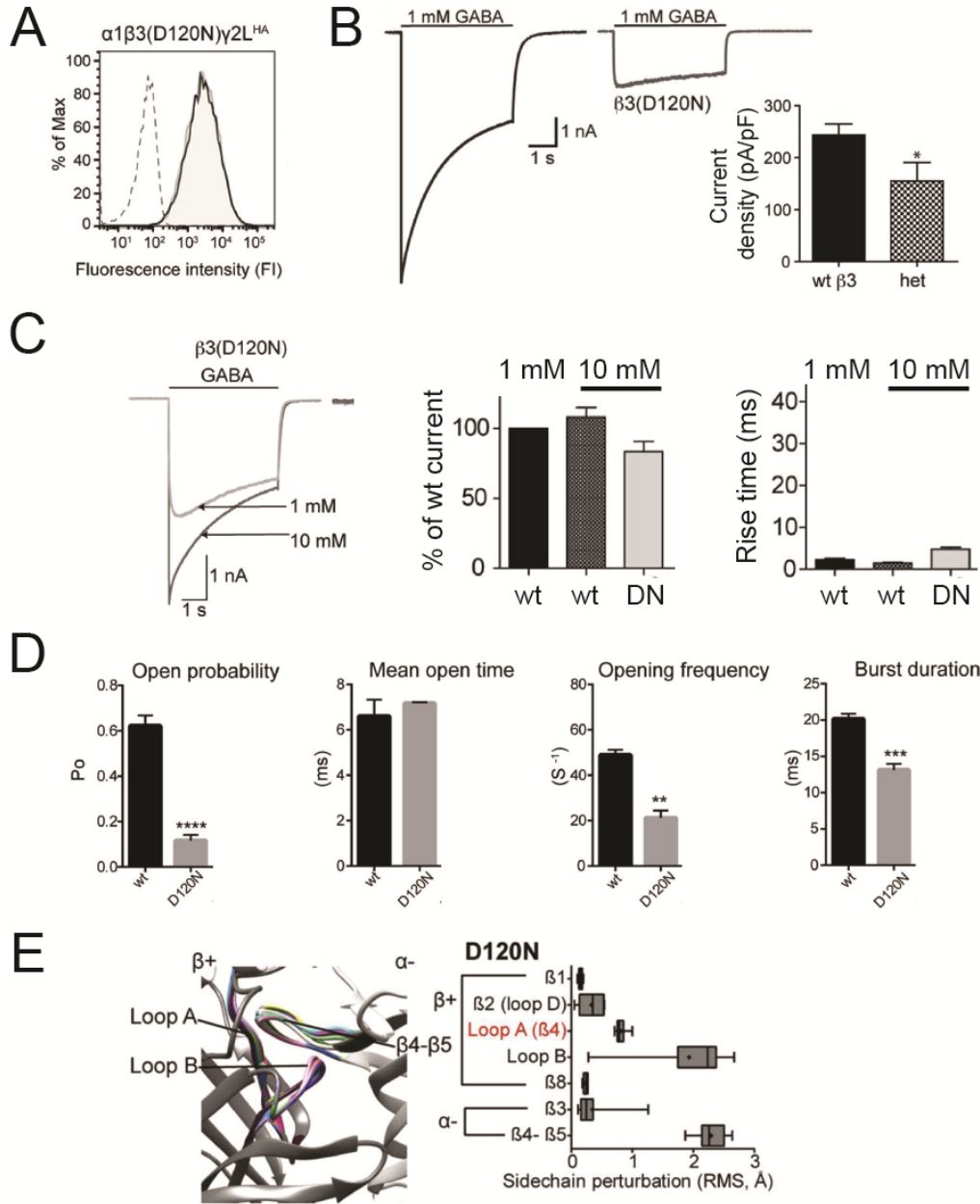


Figure 2: The $\beta 3(D120N)$ subunit amino acid substitution disrupts GABA_A receptor function and tertiary structure.

This work was done in HEK-293T cells transfected with human cDNA for $\alpha 1$, $\beta 3$, and $\gamma 2$ subunits. **A**) Flow cytometry showed no difference in total or surface expression of $\beta 3$, $\alpha 1$, or $\gamma 2$ subunits. **B**) The $\beta 3(D120N)$ mutation in decreased peak amplitude and current density of mIPSCs with application of 1 mM of GABA. **C**) 10 mM GABA rescued the impairments seen at 1 mM. **D**) Spontaneous single channel recordings indicated some properties of GABA_A receptors were disrupted while others were not. **E**) Modeling shows how the $\beta 3(D120N)$ subunit amino acid substitution perturbs the 3-dimensional location of various components of the $\beta 3$ subunit ECD. Figure adapted from Janve et al. (2016) [13].

Materials and methods

See Chapter 2 for additional materials and methods.

Generation of the *Gabrb3*^{+D120N} KI mouse

The *Gabrb3* G358A mutation changes a GAC codon to AAC in exon 4, thus converting an aspartate to an asparagine (D120N) in the $\beta 3$ subunit. The KI mouse was generated in collaboration with the Vanderbilt Transgenic Mouse/ES Cell Shared Resource by using conventional homologous recombination methods. The replacement targeting vector was constructed by cloning an upstream 5.4 kb 5' and a downstream 4.6 kb 3' homology arms into an FRT-flanked PGK-Neo cassette, in a vector with the negative selection marker MC1-thymidine kinase cassette. ES cells (C57BL/6N-PRX-B6N) with a correctly targeted locus, identified first by long range PCR with one of primers located outside of homology arms and followed by PCR/sequencing, were micro-injected into the C57BL/6J albino blastocysts to produce chimeric mice. Chimeric mice were bred with Actin-F1pe C57BL/6J transgenic mice [42] to screen for germline transmission and to excise the PGK-Neo selection cassette. The KI mice were genotyped by using a pair of primers (Forward 5'-GTGCACTGGCATTGAGTTTCTCAC-3' and backward 5'-CTTCATAGAGCACCAATGAGACTGTACC-3'). Mice were further backcrossed to C57BL/6J, which differs from C57BL/6N by only 0.8% [43], for a minimum of 6 generations.

RT-PCR

Total RNAs were extracted from brain tissues of P10-P12 mice by using Direct-zol™ RNA MiniPrep Plus kit (Zymo Research, Irvine, CA, USA). RT-PCR was carried out by using QIAGEN OneStep RT-PCR kit. Forward primer 5'-GTAGAGTGGAGCAGTTCCTCCACTCAG-3' (upstream of the start codon), and backward primer 5'-GACAGGCAGGGTAATATTTCACTCAGTG-3' (downstream of the stop codon). GAPDH primers were 5'-GTGAAGGTCGGTGTGAACGGATTTG-3' and 5'-GATGGCATGGACTGTGGTCATGAG-3'.

Postnatal spasm observations

Pups from P1-6 were observed in their home cage with their mother to reduce separation-induced stress and rejection. P6-P11 and P12-18 pups were separated from the home cage for 5 and 10 minutes, respectively, and observed and videotaped individually for general behaviors and spontaneous seizures. Pups were genotyped at weaning.

Behavioral testing

Tests in which behavioral anomalies were observed were conducted at two ages, in three cohorts per age, with an approximately equal number of males and females per age. These ages were P35-P55 (called P49) and P180-P240 (called P200). These ages reflect ages of significance for LGS, being childhood (onset of LGS) and adulthood (persistence or worsening of LGS). Preliminary behavior tests deemed insignificant were conducted only in one cohort of adult mice (male and female, sample sizes provided in figure legends). Based on data gathered in the first cohort of P200 mice, a power analysis was performed on data collected in the 3CST which indicated that to achieve power of 0.8 with 4 groups, an n of 17 must be used. Therefore, a

minimum of 17 animals were utilized for each behavioral test, as each animal was subjected to the same battery of tests for consistency. In some cases, where more than 17 mice were available, they were also used for behavioral testing. Where significance failed to be achieved, such as in the probe trial of the Barnes maze at P200, an additional power analysis was conducted to determine if the group size should be increased. However, additional power analyses did not indicate there was just cause to increase sample size so additional cohorts were not added.

AED treatment of LGS KI mice

Head mounts were surgically implanted on the skull surface of adult KI mice (6-8 months old). The following classic AEDs were tested: ethosuximide (200 mg/kg in saline), clobazam (2.5 mg/kg in 30% PEG 400 solution), and topiramate (30 mg/kg in saline). Experiments began at 10am, with AEDs given at 12 pm. Two hours prior to drug injection, animals were injected with the AED diluent to serve as control observations. A single dose of AED was injected intraperitoneally in a solution volume of about 200 μ L. Mice were monitored by synchronized video-EEG recording for 2 hours after vehicle administration and for 2 hours after AED injection. WIN 55,212-2, a CB1 agonist, was given daily for 7 days at a dose of 0.1 mg/kg dissolved in DMSO. Video-EEGs were recorded from 12pm to 2 pm on the 1st day for baseline (prior to the first injection) and on the 8th day also from 12 pm to 2 pm. For drugs with published mouse data, dosing was based on available information. For drugs without published mouse data, dosing was based on either the mid-range of human dosing or previous experimental knowledge of the lab. Mice were sacrificed after drug treatment.

Statistical analysis and data availability

Statistical analyses were performed, and graphs were generated using GraphPad Prism. Tests performed on each data set are outlined in the corresponding figure legend. All analyses used an alpha level of 0.05 to determine statistical significance. The naïve EEG profile was scored and analyzed by V.J., while R.K.H. scored and analyzed the drug data. There may be subtle differences between their scoring strategies, but their data were not cross-analyzed to avoid any observer-specific effects.

Generating the mouse

Genetic approach

To establish a LGS mouse model with the specific mutation in *GABRB3* (c.G358A, p.D120N) reported in a human with LGS, we generated mice with a targeted G358A mutation at the endogenous *Gabrb3* locus using conventional homologous recombination in B6N embryonic stem (ES) cells (Primogenix, Inc) derived from the C57BL/6N mouse (Figure 3). The G358A mutation located in the 5' homologous arm was generated by site-directed mutagenesis, resulting in substitution of asparagine for aspartic acid at residue 120. The correctly targeted ES cell clones were identified by long-range PCR with one of the primers (A or D) located outside the homologous arms to exclude the clones with random vector insertion (Figure 3A). PCR fragments were digested with the Hind III (H3) enzyme to confirm further correctly targeted recombination (Figure 3B). Chimeric mice were bred with Flpe transgenic mice to screen for

germline transmission and to excise the PGK-Neo selection cassette. The leftover FRT site allowed convenient genotyping (Figure 3C).

The presence of the G358A mutation was further confirmed by PCR/sequencing. The sequencing chromatogram of the RT-PCR products of total RNA isolated from the heterozygous KI mice showed similar intensity of peak G (wild type mRNA) and peak A (mutant mRNA) nucleotides (Figure 3D), indicating that both alleles were transcribed identically. Additionally, to determine if the gene editing affected *Gabrb3* expression at the transcriptional level, semi-quantitative RT-PCR was carried out with total RNAs isolated from whole brain (Figure 3E1). The results revealed that expression levels of *Gabrb3* mRNA from total brain were equivalent in KI and wild type littermate mice (Figure 3E2). Sequence analysis using RT-PCR that included the entire coding region of the *Gabrb3* transcript from *Gabrb3^{+D120N}* mouse brain confirmed that there were no DNA sequence changes other than the intended G358A mutation. At the translation level, western blots with whole brain lysates (Figure 3F1) showed expression of $\beta 3$ subunits in brain of *Gabrb3^{+D120N}* mice was the same as that of wild type littermate mice (Figure 3F2).

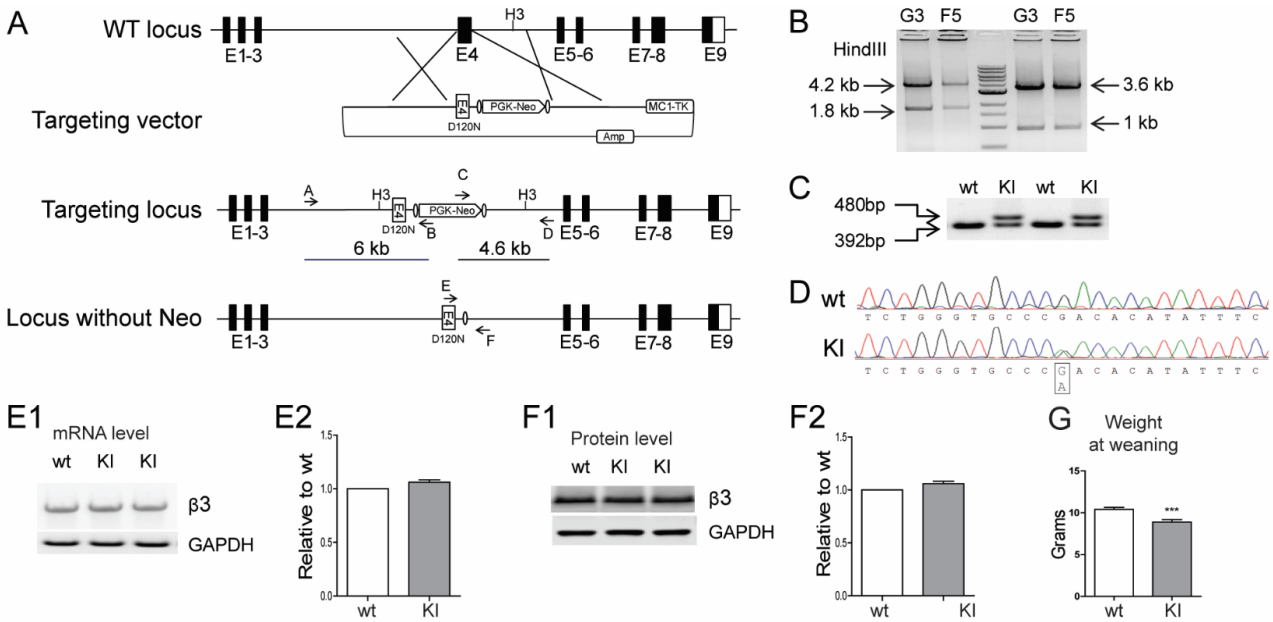


Figure 3: Generating the *Gabrb3*^{+D120N} mouse

A) Scheme for targeted KI of the *Gabrb3* locus. A vector was constructed to replace *Gabrb3* exon 4 genomic DNA with an exon 4 containing the G358A mutation and the positive selection cassette (PGK-Neo). **B)** Long-range PCR was used to identify the correctly targeted clones, G3 and F5. 6 kb and 4.6 kb fragments were amplified from correctly targeted clones using primers A/B and C/D, respectively. The PCR fragments were digested with the HindIII restriction enzyme (to generate the predicted 4.2 and 1.8 kb fragments for the 5' end, and 3.6 and 1 kb fragments for the 3' end) to further confirm correct homologous recombination. **C)** The KI mice were genotyped. PCR amplified a 392 bp fragment from the wild type $\beta 3$ subunit allele and a 480 bp fragment from the $\beta 3$ subunit KI allele due to the insertion of FRT sequences and other modifications. **D)** Sequencing chromatogram of RT-PCR derived from total brain RNA showed the presence of the G358A mutation and corresponding equal level of wild type and mutant nucleotide expression. **E1)** Semi-quantitative RT-PCR showed that the KI allele did not affect *Gabrb3* gene expression, using GAPDH as a loading control. **E2)** Band intensities of the RT-PCR products were first normalized to GAPDH for quantification and then to wild type levels. **F1)** Immunoblotting showed equal $\beta 3$ subunit expression in KI and wild type littermate mouse brain whole cell lysates. GAPDH served as a loading control. **F2)** Protein levels were normalized first to internal GAPDH and then to wild type levels. **G)** The body weight of KI and their littermate mice at weaning were plotted (n = 22 wt, 18 KI).

***Gabrb3*^{+D120N} mice had increased mortality, reduced body weight, and other abnormalities.**

P18.5-P19.5 homozygous *Gabrb3*^{D120N/D120N} embryos collected from heterozygous KI intercrossed timed-pregnant mice were viable, and there were no apparent differences at this embryonic age among homozygous KI, heterozygous KI, and wild type littermates. However, no homozygous pups survived to the three-week weaning and genotyping age, indicating that homozygous D120N mutations were neonatal lethal.

While heterozygous KI mice achieved normal body weight by adulthood, at P21 KI pups weighed significantly less than wild type pups (Figure 3G). No major differences were observed between wild type and KI pups in the neonatal (P0-P5) period. From P6-11, KI pups had delays in development of skin pigmentation and in righting when they were placed on their backs. Adult male KI mice did not fight when combined from different cages. Males had a limited reproductive time window that was restricted to when they were relatively young, so breeding was done primarily between female KI and male wild type mice. Additionally, first-time KI dams failed to nurture their offspring irrespective of pup genotype; the nurturing behavior improved for subsequent litters after KI dams were housed with wild type foster dams.

Mating of female KI mice with male wild type mice revealed a ratio of KI to wild type offspring at weaning that was inconsistent with Mendel's law. Out of 525 weanlings genotyped, 294 were wild type and 231 were KI, suggesting that KI mice had increased mortality. Surviving KI mice had a life-span similar to that of wild type mice. Using Nissl stain, there were no apparent differences in brain cross sectional anatomy between KI mice and their wild type littermates (data not shown), suggesting that the increased death rate of heterozygous mice was likely related to seizures.

Seizure phenotype of the mouse

***Gabrb3*^{+D120N} mice had seizure semiologies and ictal EEG patterns consistent with LGS.**

We next determined if the KI mice had LGS seizure semiologies and ictal EEGs by home cage observation and synchronized video-EEG analyses. In adult mice, EEG head mounts were implanted around 4 months of age in both wild type and KI mice, and after one week of recovery, the mice were monitored by synchronized video-EEG across a range of ages. We observed multiple types of spontaneous seizures in the KI mice, but not in wild type littermates (except for infrequent, brief, typical absence-like seizures, as is expected in C57BL6 mice [44]).

TASs in humans are classified by 1) generalized, symmetrical spike wave discharge (SWD) with a peak ictal spectral frequency higher than 2.5 Hz, usually around 3 Hz; 2) duration average of 9.4 s (range 1-44 s); and 3) abrupt onset and offset loss of consciousness that is time-locked with the SWD. Additionally, they are common in different epilepsies, can occur at any age (though typically onset is at 6 to 12 years of age), are generally considered benign, and have a high remission rate (57-74% for childhood absence epilepsy) [45]. Wild type littermates had rare, brief absence seizures (Figure 4A, B) characterized by 1) generalized SWD with a high peak frequency (peak 7.6 Hz, range 6-8 Hz), 2) a short duration (mean 9.9 ± 0.1 s, range 1.3–30.7 s), and 3) behavioral arrest with sudden onset and offset time-locked to the SWD. These seizures reflect TASs in humans and those reported in absence epilepsy mouse models where duration is 0.3-10 seconds, and the predominant frequency range is 6-8 Hz [44, 46].

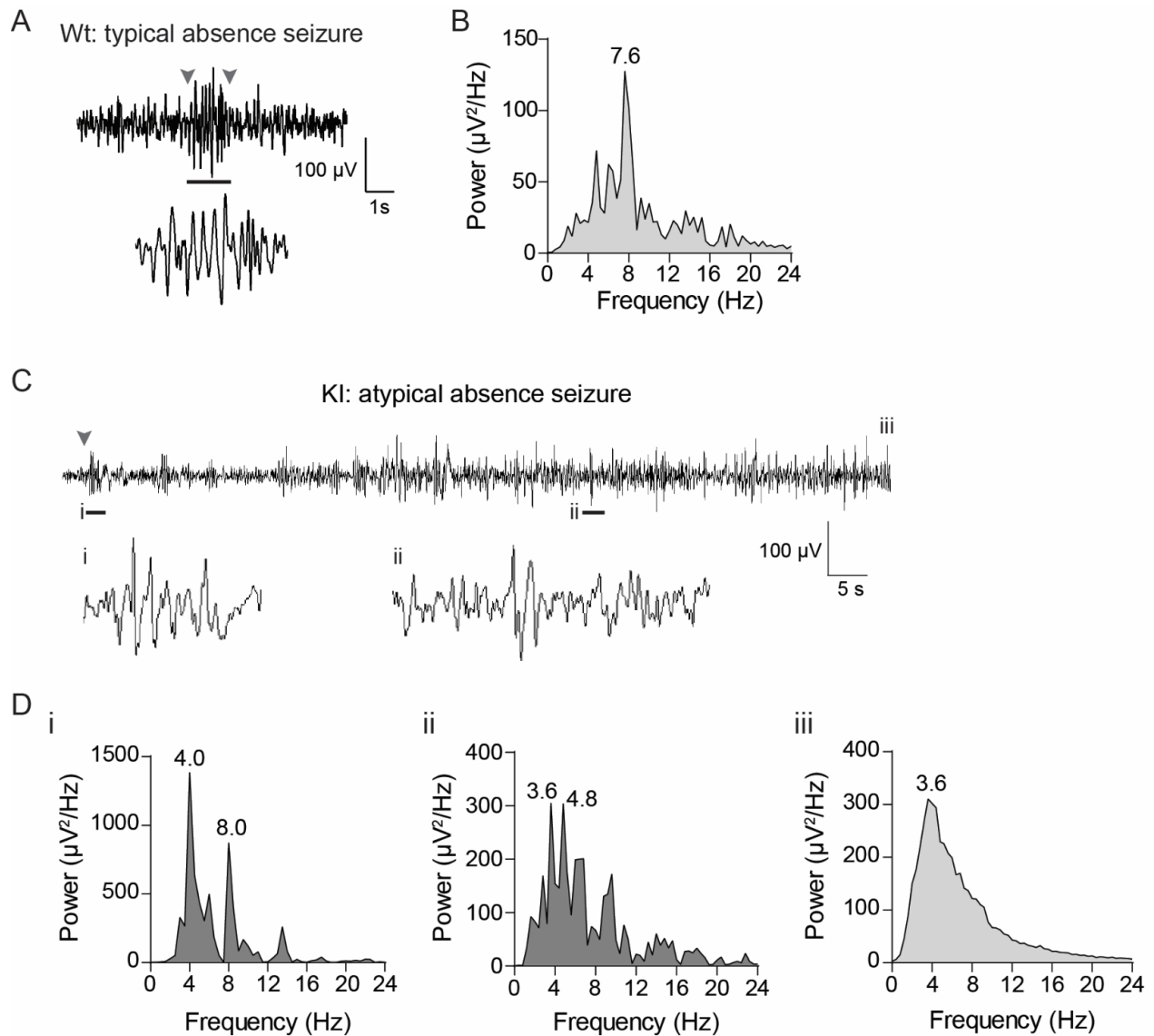


Figure 4: Spontaneous TAS in wild type mice and AASs in *Gabrb3*^{+/*D120N*} mice.

Representative EEG traces for TASs seen in wild type mice and AASs seen in KI mice. The arrowheads indicate the start and end of the seizure. Note that the AAS extends beyond the selected time frame, so no endpoint is shown. **A**) TASs in wild type mice were brief and behavioral arrest was time-locked to SWD onset and offset. **B**) Power spectral density for TASs EEGs in wild type mice with peak frequency at 7.6 Hz. **C**) AAS EEG trace; AASs were not always time-locked with the behavioral onset and/or had brief movements during the seizure (see Video 1 for full seizure). **D**) Power spectral density of AAS EEGs often started with **(i)** higher frequency components which **(ii)** decreased over time; however, the frequency over the entire seizure **(iii)** was low.

AASs in humans are classified by 1) generalized, diffuse, irregular slow SWD (SSWD) with a frequency of less than 2.5 Hz with or without irregular diffuse fast activity; 2) a longer duration than typical absence; and 3) impairments of consciousness that are variable in severity and may not be time-locked to the SSWD. Additionally, they are more rare and more difficult to control pharmacologically than TASs, and while they are often considered minor seizures as they are not directly life-threatening, they are believed to contribute to the severe learning disabilities associated with disorders like LGS [45, 47]. KI mice expressed frequent AASs (Figure 4C, D) that were characterized by 1) an ictal EEG containing slow SWDs that were primarily poorly formed high-voltage, low frequency events (3-7 Hz), which is closer in range to AASs observed in the rat AY-9944 induction model and the GABA_BR1a overexpression mouse model (5-6 Hz [19, 48]); 2) a longer duration than typical absence (mean 20.3±10.2 s; range 0.5–363.5 s); and 3) behavioral arrest and loss of consciousness that were necessarily tightly time-locked to seizure onset or offset, and behavioral arrest which not always complete. These events were only identified as seizures if the mouse was clearly awake (visibly open eyes or a sudden interruption of a high level of activity at event onset). It was possible to distinguish AASs from non-REM sleep based on behavior and spectral density (Figure 5). Peak SSWD frequency was often higher at the beginning of the seizure (Figure 4Di; 4.0 Hz peak, strong 8.0 Hz contribution) and developed a lower frequency as the seizures progressed and became less organized (Figure 4Dii; 3.6 Hz peak, strong 4.8 Hz contribution). Because of the characteristics of these seizures, including appropriate peak spectral frequency, time, and behavioral dynamics, we classified them as AASs, the hallmark seizures of LGS.

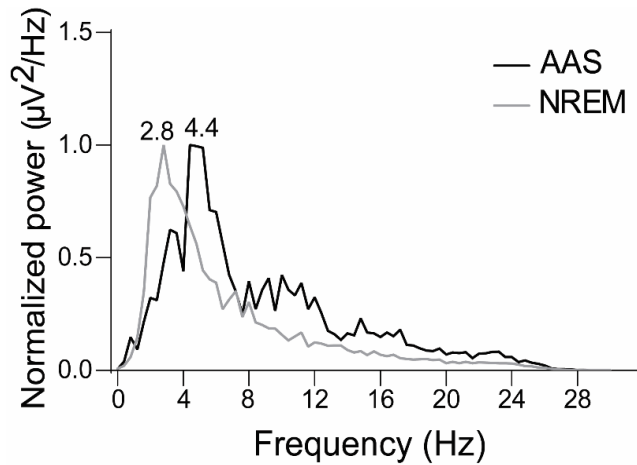


Figure 5: AASs were distinguishable from NREM sleep by power spectral density analysis.

Due to the similar shape of non-REM (NREM) sleep and AASs EEGs, a power spectral density analysis was performed on sample NREM sleep and AASs to ensure we could adequately separate the two. This analysis consistently showed NREM sleep has a slower peak spectral density than AASs, and therefore, we were able to exclude NREM sleep from the AAS analysis.

Myoclonic seizures in humans are characterized by sudden, brief (< 350 ms) shock-like movements with a high-amplitude spike on EEG [49]. Myoclonic seizures in KI mice were moderately frequent and brief (around 300 ms), with sudden muscle contraction involving whole-body extension and flexion associated with a single, high-amplitude sharp wave (~200-400 μ V) on EEG and EMG channels (Figure 6A).

Tonic seizures in humans are characterized by either unilateral or bilateral contraction of one or more muscle groups. This contraction is sustained, lasting for a few seconds to up to a minute, and may be asymmetrical resulting in turning to one side [50, 51]. Tonic seizures in KI mice involved a sudden and prolonged (up to several seconds) contraction of the limbs, with or without tail stiffening, that was associated with either no change in EEG amplitude or with low-

amplitude, high-frequency activity, as previously described [52] (Figure 6B). Tonic seizures often resulted in the “rolling” of the animal, similar to how humans may turn to one side. Tonic seizure incidence may be underestimated because the KI mice did not have an obvious or characteristic EEG pattern. Thus, we were conservative in identifying tonic seizures since the EEG pattern was variable, and unless the mice were moving prior to the seizure, it was difficult to confirm a behavioral event.

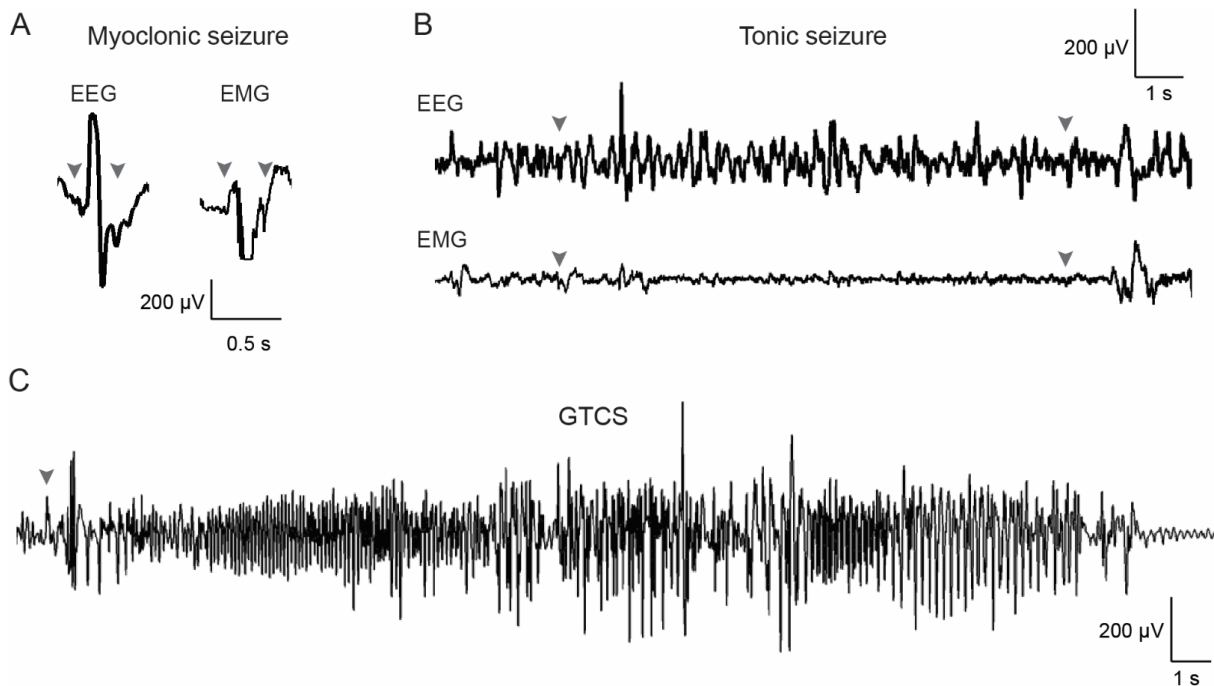


Figure 6: Myoclonic, tonic, and GTC seizures in *Gabrb3^{+/D120N}* mice.

Representative EEG traces for myoclonic, tonic, and GTC seizures. The arrowheads indicate the start and end of the seizure. **A)** Myoclonic seizure EEG discharges were brief (~300 µs) and both EEG and EMG traces had prominent spikes. **B)** EEG during tonic seizures did not stand out from the baseline in amplitude, but showed an increased frequency compared to the baseline. **C)** GTCS EEGs were striking with the largest increase in EEG amplitude. The tonic phases during GTCS had slightly lower amplitude but higher waveform frequencies compared to the clonic phase, which was followed by electrodecrement. See Video 1 for examples of KI video-EEG recordings for each seizure type.

Generalized tonic-clonic seizures (GTCSs) in humans are characterized by an abrupt seizure onset with loss of consciousness, a high-amplitude high-frequency tonic phase, and finally a lower frequency clonic phase characterized by myoclonic and clonic jerking. The EEG may also show background suppression interrupted by polyspike-wave discharges [51, 53]. The postictal state encompasses a gradual recovery of the background EEG, consciousness, and physical movement. In KI mice, GTCSs started with limb stiffening and extension, followed by rapid clonic movements of the limbs, and proceeded to strong tonic-clonic activity with abrupt jumps and Straub tail, ending in postictal behavioral arrest (Figure 6C). The GTCSs were mostly observed in older mice. The ictal EEG showed a high-amplitude, high-frequency discharge followed by a low amplitude base line rhythm, followed by a low-activity postictal state lasting up to several minutes.

In adult KI mice, atypical absence and myoclonic seizures were observed most frequently, while tonic and GTCSs were observed much less frequently (Figure 7A). TAS (wt) and AAS (KI) occurrences were graphed together for visual comparison; however, the absence seizures in wild type mice were 100% TASs (6-8 Hz), while the absence seizures in the KI mice were approximately 97% low frequency AASs (3-5.5 Hz). Because a random sampling of absence seizures in KI mice yielded an average peak frequency of 4.4 Hz, despite the presence of a small percentage of higher-frequency (possibly typical) absence seizures, all absence seizures in KI mice have been grouped together as “atypical” due to the overwhelming majority of these seizures, yielding a range in peak spectral frequency of 3-7 Hz. AASs in KI mice peaked at the light-to-dark transition (Figure 7B), and KI mice had more AASs overall during the dark hours (Figure 7C). Finally, atonic seizures were observed extremely rarely and were difficult to verify, so they were not quantified; however, an example is available in the supplementary video.

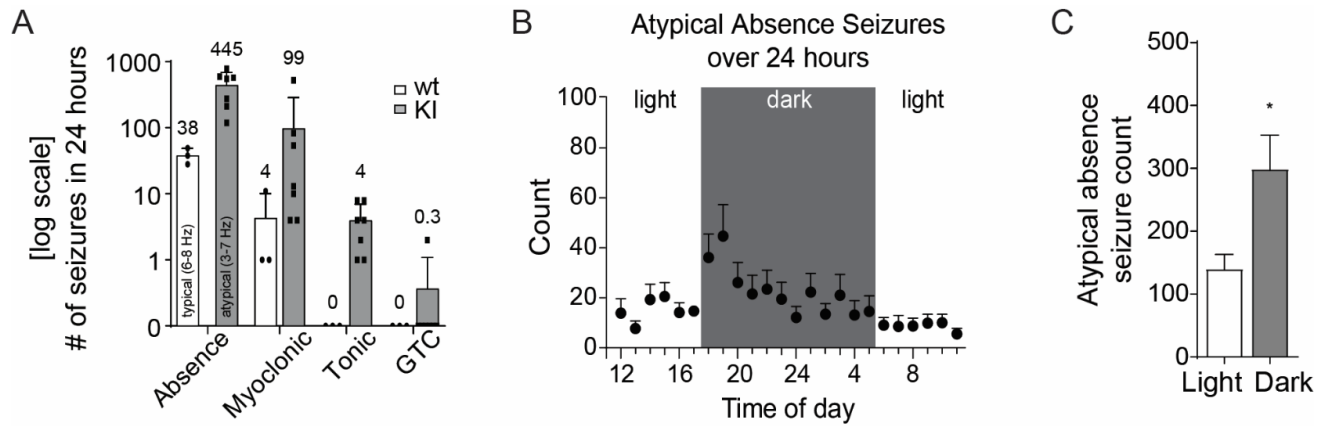


Figure 7: Quantification of seizure incidence and timing in *Gabrb3*^{+/*D120N*} mice.

A) Bar graph showing average number seizures in wild type and KI mice in a 24-hour period (note: y-axis is log scale). AASs and myoclonic seizures were the dominant seizures in KI mice. **B, C)** Most AASs in KI mice occurred during the dark (active) period with a peak incidence at the light-to-dark period transition (paired *t*-test, *n* = 7, light mean = 142, dark mean = 297.7, **p* = 0.011). As the light cycle does not change with daylight savings, all times are set to the appropriate non-daylight savings time (6:00-18:00 light, 18:00-6:00 dark). Video-EEG recordings (for panels A-J) were done in *n* = 4 wt (2 male, 2 female) and 7 KI (3 male, 4 female) mice at age 4.5-6.5 months.

Additionally, while we could not implant our EEG head mounts on pups, blinded observations of young mice, aged P1 to P21, showed epileptic spasms in KI mice from age P13 to P17 (Figure 8). Approximately 20% of patients with LGS had a diagnosis of infantile spasms prior to developing LGS [54], including the D120N patient. Spasms in humans last 0.5-2 seconds, with neck and trunk flexion and arm abduction in a jack-knife pattern, and they often occur in clusters [51]. In KI mice, spasms were brief, around one second, with rapid flexion-extension movements accompanied by behavioral arrest, staring, and loss of responsiveness. While a fraction of wild-type pups was scored to have spasms (< 30%) from age P13 to P17, all of the KI mice had spasms at that age range. Additionally, we observed more seizures during

pregnancy and nursing, suggesting female hormones may affect the epilepsy phenotype [55]. Taken together, the seizure semiologies and ictal EEGs were consistent with a diagnosis of LGS, representing the first time the LGS seizure semiology has been faithfully replicated in a genetic model system.

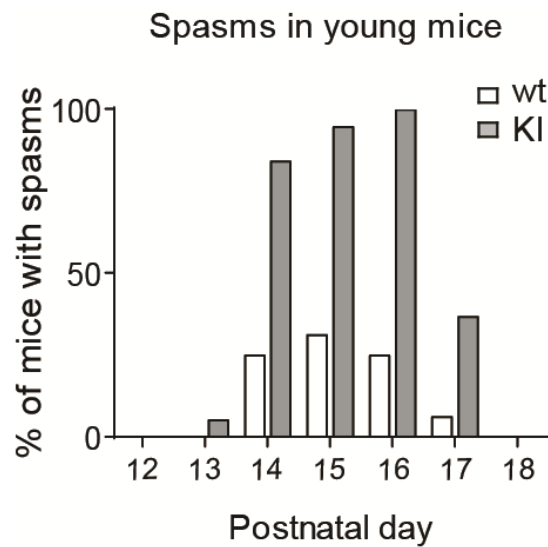


Figure 8: Spontaneous spasms in young *Gabrb3^{+/-D120N}* mice.

Spontaneous spasms in wt and KI mice were observed in pups between P12 and P18. Shown are the percentages of wt and KI pups that exhibited spasms at each age. Observers were blind (5 litters, with n = 16 wt and n = 19 KI mice).

Behavioral phenotype of the KI mouse

Patients with LGS have behavioral abnormalities, which can severely impact the quality of their life, are sometimes the feature of the disorder that is the most difficult to treat and most negatively impacts the patient [14]. These are outlined in more detail above in the section *Cognitive dysfunction in LGS*, but abnormalities can include mildly to severely impaired cognition, ADHD, and ASD [20]. We conducted a series of studies to assess whether the abnormal behavior in KI mice recapitulated the behavioral abnormalities seen in humans with LGS. These tests were conducted in both male and female mice around two ages, juvenile to young adulthood (P30-55, called P49) and mature adulthood (P180-220, called P200).

***Gabrb3*^{+D120N} mice had impaired spatial learning and memory.**

To assess cognitive deficiencies of KI mice, spatial learning and memory were assayed using the Barnes maze. In the first cohort, in order for KI mice to reach the same level of learning as their wild-type littermates, 8 days (more than the standard 5 days [56]) of learning trials were necessary (Figure 9). At P49, KI mice displayed a spatial learning deficit in the Barnes maze as measured by the latency to find the target hole (Figure 10A) and the number of errors committed (non-target holes visited) before entering the target hole (Figure 10B). Additionally, P49 KI mice displayed a less effective search strategy overall (Figure 10C) and had persistently worse search strategies on the final day. P200 KI mice displayed a similar spatial learning deficit, with notable spatial learning delays (Figure 10D), a significant number of errors made (Figure 10E), and worse search strategies (Figure 10F).

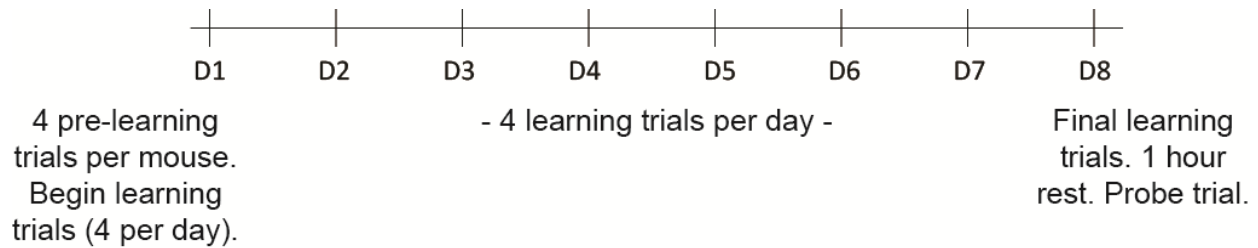


Figure 9: Barnes maze timeline

A schematic showing when each of the three stages of the Barnes maze were performed.

In the memory trial, P49 KI mice spent less time investigating the target hole area (Figure 11A) and made an increased number of errors (Figure 11B), showing that young KI mice have a spatial memory deficit. P200 KI mice showed a similar phenotype, with a trend towards a decrease in amount of time spent investigating the target hole area (Figure 11C), and a significant increase in the number of errors made (Figure 11D). Together these data showed that both spatial learning and spatial memory deficits in KI mice began early in life and persisted across their lifespan.

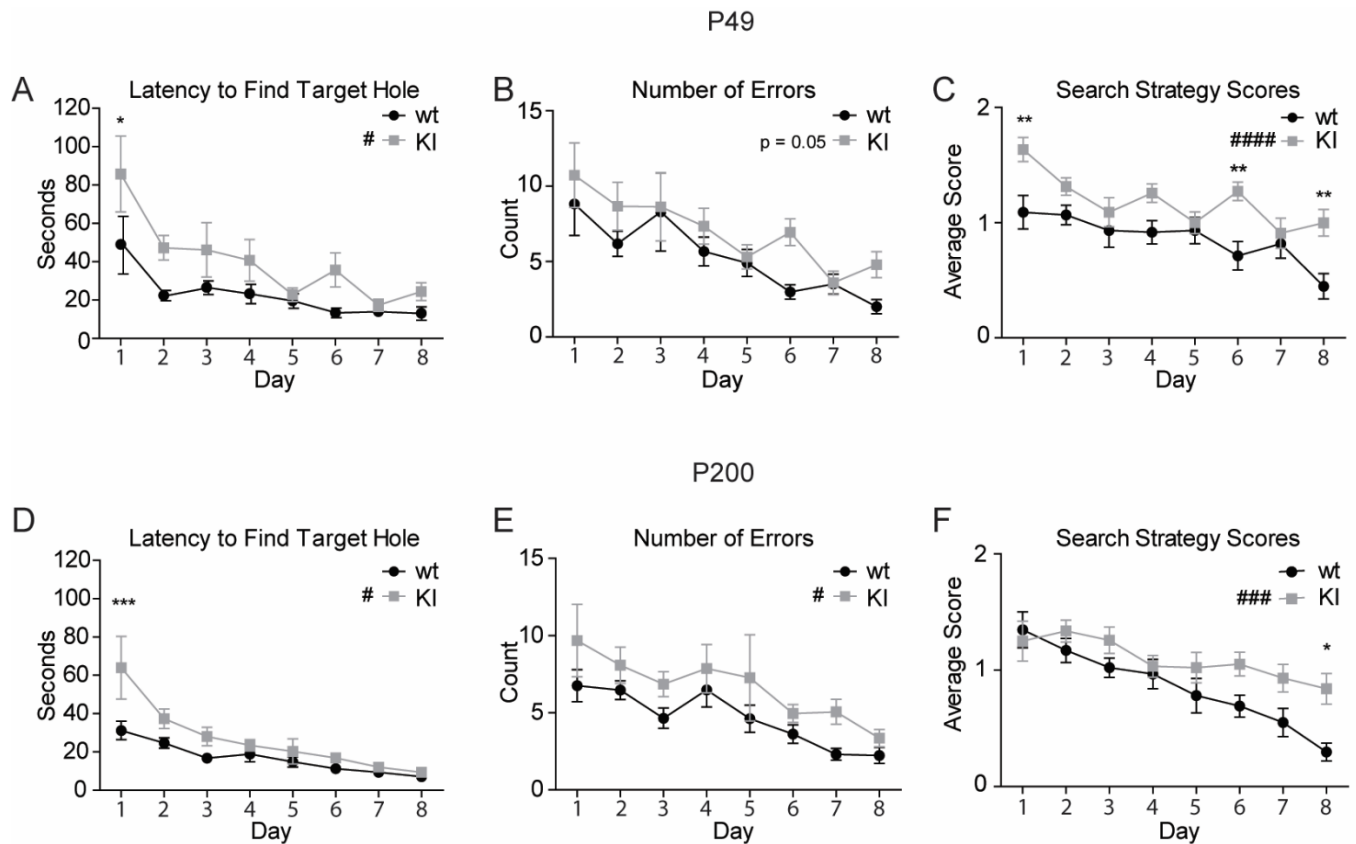


Figure 10: *Gabrb3*^{+/*D120N*} mice had spatial learning deficits.

8 days of learning trials depict spatial learning abilities in P49 **A-C)** and P200 **D-F)** wt and KI mice. Each day represents the average across all mice of each genotype with the data point of each mouse being the average of the four trials conducted that day. For the search strategy scores, mice earned 0 points for a direct path to the target hole, 1 point for a serial path, and 2 points for a random path. Higher scores represented less efficient searching. **A)** At P49, the time it takes each animal (latency) to find the target hole for each day was increased in KI mice (interaction $F_{7,294} = 1.138$, $p = 0.3394$; genotype main effect $F_{1,294} = 5.999$, $p = 0.0186$ #). **B)** At P49, the number of non-target hole zones entered (errors) was not significantly increased in KI mice (interaction $F_{7,294} = 0.5226$, $p = 0.8173$; genotype main effect $F_{1,294} = 4.009$, $p = 0.0518$). **C)** At P49, search strategy scores were increased in KI mice (interaction $F_{7,294} = 1.836$, $p = 0.0802$; genotype main effect $F_{1,294} = 26.35$, $p < 0.0001$ #####). **D)** At P200, the time it takes each animal (latency) to find the target hole for each day was increased in KI mice (interaction $F_{7,301} = 2.142$, $p = 0.0393$ #; genotype $F_{1,301} = 7.625$, $p = 0.0084$ ##). **E)** At P200, the number of non-target hole zones entered (errors) was increased in KI mice (interaction $F_{7,301} = 0.2108$, $p = 0.9828$, genotype $F_{1,301} = 4.009$, $p = 0.0257$ #). **F)** At P200, search strategy scores were increased in KI mice (interaction $F_{7,301} = 1.410$, $p = 0.2006$, genotype $F_{1,301} = 13.59$, $p = 0.0006$ ###). **(A-F)** Two-way ANOVA for repeated measures: genotype effect # $p < 0.05$, ### $p < 0.001$, ##### $p < 0.0001$. Bonferroni post-tests: * $p < 0.05$, ** $p < 0.01$, *** $p < 0.001$.

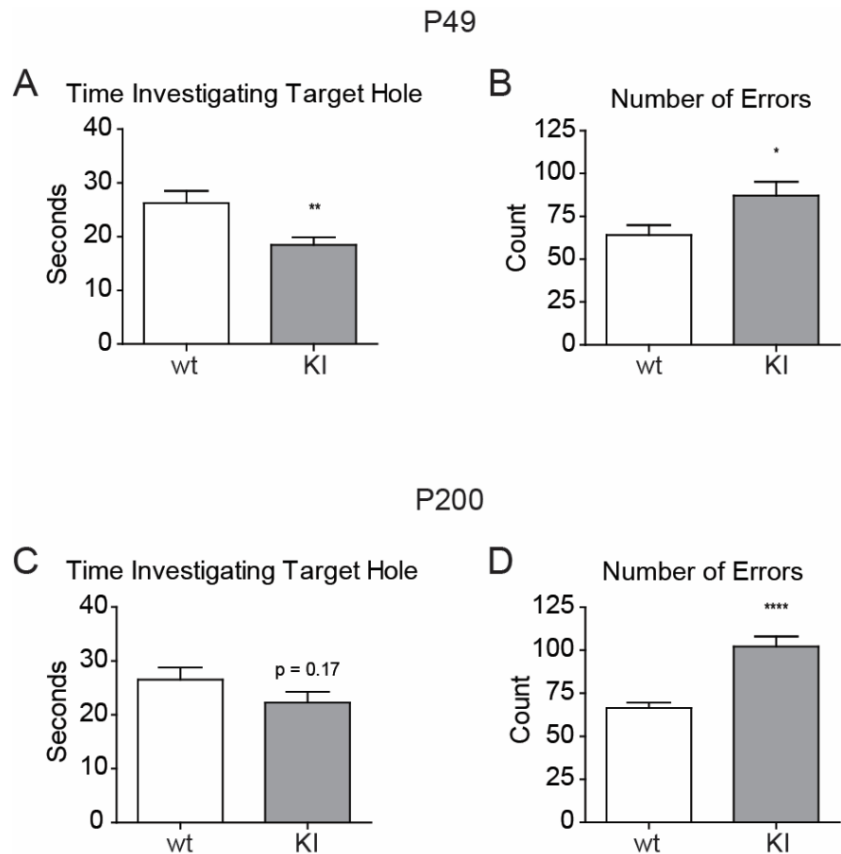


Figure 11: *Gabrb3*^{+/*D120N*} mice had spatial memory deficits.

5-minute probe trial for spatial memory performed on day 8 after the learning trials were plotted for **A, B)** P49 and **C, D)** P200 mice. The target hole was then covered and appeared identical to the other 11 holes. **A)** At P49, time spent near the target hole was decreased in KI mice ($t_{42} = 2.897$, $p = 0.0060$ **). Group means: wt 26.25 ± 2.27 seconds, $n = 21$; KI 18.44 ± 1.5 seconds, $n = 22$). **B)** At P49, the number of errors committed by KI mice was increased ($t_{42} = 2.46$, $p = 0.018$ *). Group means: wt = 64.05 ± 5.48 , $n = 21$; KI 87.27 ± 7.68 , $n = 22$). **C)** At P200, time spent near the target hole was not significantly decreased in KI mice ($t_{42} = 1.390$, $p = 0.172$). Group means: wt 26.50 ± 2.28 seconds, $n = 21$; KI 22.27 ± 2.015 seconds, $n = 22$). **D)** The number of errors committed at P200 was increased in KI mice ($t_{42} = 5.314$, $p < 0.0001$ ****). Group means: wt 66.36 ± 3.287 , $n = 21$; KI 102.1 ± 5.875 , $n = 22$). **(A-D)** Values expressed as mean \pm SEM. Unpaired two-tailed Student's t -test, * $p < 0.05$, ** $p < 0.01$, **** $p < 0.0001$. $n = 21-22$ for all panels.

***Gabrb3*^{+D120N} mice were hyperactive.**

ADHD is one of the most common comorbidities diagnosed in patients with LGS [23, 31], and hyperactivity is one of the primary characteristics of ADHD [30]. We assessed hyperactivity using locomotor activity chambers. At P49, KI mice had a mild hyperactive phenotype with an increased number of vertical counts (jumps in which the feet leave the floor, a phenotype often observed in the home cage which we sought to quantify) (Figure 12A) and a trend towards an increase in the total distance traveled in the chamber (a more traditional measure of hyperactivity) compared to wild type mice (Figure 12B). P200 mice displayed a more robust hyperactive phenotype, with significant increases in both parameters (Figure 12C) and in total distance traveled (Figure 12D). Together, these data demonstrate KI mice had hyperactivity which worsened with age.

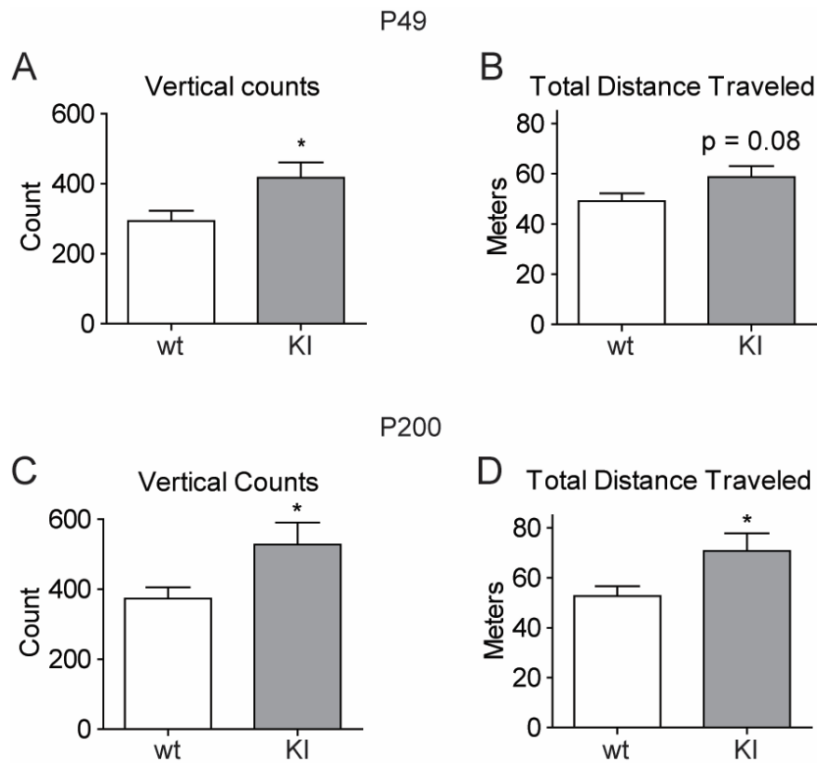


Figure 12: *Gabrb3^{+/-D120N}* mice had a mild hyperactive phenotype at P49, which became more pronounced at P200.

Data shown were collected from 60 minutes in the locomotor activity chambers. **A)** Vertical counts, or the number of rearings, detected at P49 were plotted ($t_{40} = 2.323$, $p = 0.0253$ *. Group means: wt 293.6 ± 29.10 , $n = 21$; KI 417.0 ± 44.42 , $n = 21$). **B)** Total distance traveled (center and surround included) in the locomotor activity chambers at P49 ($t_{48} = 1.779$, $p = 0.0815$. Group means: wt 49.03 ± 3.224 meters, $n = 25$; KI 58.71 ± 4.383 meters, $n = 25$). (Note that the n for B is higher than A; this is due to the z-axis infrared beams not functioning on one set of the chambers in one cohort so $n = 4$ was lost from each genotype.) **C)** Vertical counts at P200 ($t_{39} = 2.209$, $p = 0.0331$ *. Group means: wt 373.3 ± 32 , $n = 21$; KI 527.5 ± 63.17 , $n = 20$). **D)** Total distance traveled at P200 ($t_{39} = 2.526$, $p = 0.0157$ *. Group means: wt 52.68 ± 3.971 meters, $n = 21$; KI 72.93 ± 7.077 meters, $n = 20$). Graphed values are expressed as median \pm SEM. Unpaired two-tailed Student's t -test, * $p < 0.05$.

***Gabrb3*^{+D120N} mice had impaired social interaction.**

The overlap between epilepsy and ASD is profound. 30-40% of ASD patients also have epilepsy [28, 29], and up to a third of epilepsy patients also have ASD [27]. The exact percentage of LGS patients with ASD is not known though the coincidence is often referenced [8, 23, 31]. Therefore, an ASD-like phenotype may be an important attribute when phenotyping the KI mouse. One of the principal diagnostic criteria for ASD is altered social interaction [30], and so we tested socialization using the three-chamber socialization test (3CST). Independent of age, wild type littermate mice showed a preference for novel socialization over exploration of a novel object (Figure 13). P49 KI mice showed this preference as well (Figure 13A); however, by P200, KI mice had reduced exploratory behavior overall (total time spent investigating targets), and the preference for novel socialization over a novel object was lost (Figure 13C).

A wild type littermate mouse at both ages preferred socializing with the novel mouse over the familiar mouse (Figure 14). At P49, KI mice did show this preference, although there was a significant reduction in overall exploratory behavior (Figure 14A). P200 KI mice lost the preference for novel over familiar socialization, and also had a reduction in overall exploration (Figure 14C). Together, the 3CST indicated that P49 mice had reduced socialization, which evolved into completely aberrant socialization by P200, at which time KI mice showed none of the social preferences of their wild type littermates.

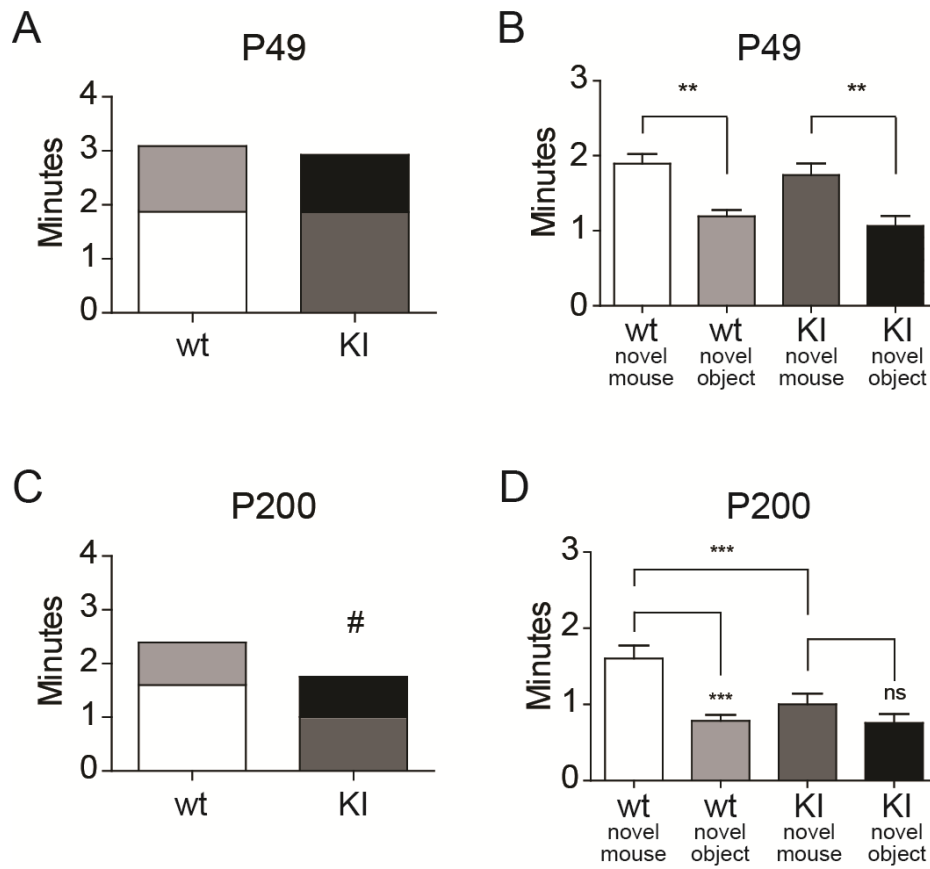


Figure 13: Stage 2 of the 3CST: *Gabrb3*^{+/*D120N*} mice had mild social deficits.

Not shown is Stage 1, a 10-minute familiarization stage for the test mouse to acclimate to the set up. Stage 2 of the 3CST was a 10-minute trial in which subject mice had two socialization options: 1) an empty inverted pencil cup in one side chamber, or 2) an inverted pencil cup containing a novel age-matched female mouse in the other side chamber. Panels A and C represent the two-way ANOVA for each age, while B and D represent the post-tests for each age. Four comparisons were made in both B and D; however, only significant or otherwise relevant results were shown. **A)** Two-way ANOVA was not significant for a genotype effect at P49 (interaction $F_{1,84} = 0.0064$, $p = 0.9363$ ns; genotype $F_{1,84} = 1.202$, $p = 0.277$ ns. Group means – novel mouse: wt 1.89 ± 0.13 min, KI 1.86 ± 0.18 min; novel object: wt 1.19 ± 0.08 min, KI 1.06 ± 0.14 min; total exploration: wt 3.00 ± 0.24 min, KI 2.64 ± 0.18 min). **C)** Genotype effect was significant at P200, as well as the interaction between genotype and target. (interaction $F_{1,87} = 4.140$, $p = 0.0449$ #; genotype $F_{1,84} = 7.727$, $p = 0.0067$ ##. Group means – novel mouse: wt 1.60 ± 0.17 min, KI 1.00 ± 0.14 min; novel object: wt 0.79 ± 0.08 min, KI 0.76 ± 0.11 min; total exploration: wt 2.39 ± 0.21 min, KI 1.73 ± 0.22 min). Statistical tests shown on graphs are *a priori* Bonferroni post-tests after two-way ANOVAs. Bonferroni multiple-comparison correction significance levels for B, D were: * $p < 0.0125$, ** $p < 0.001$, *** $p < 0.0001$. n = 21-23.

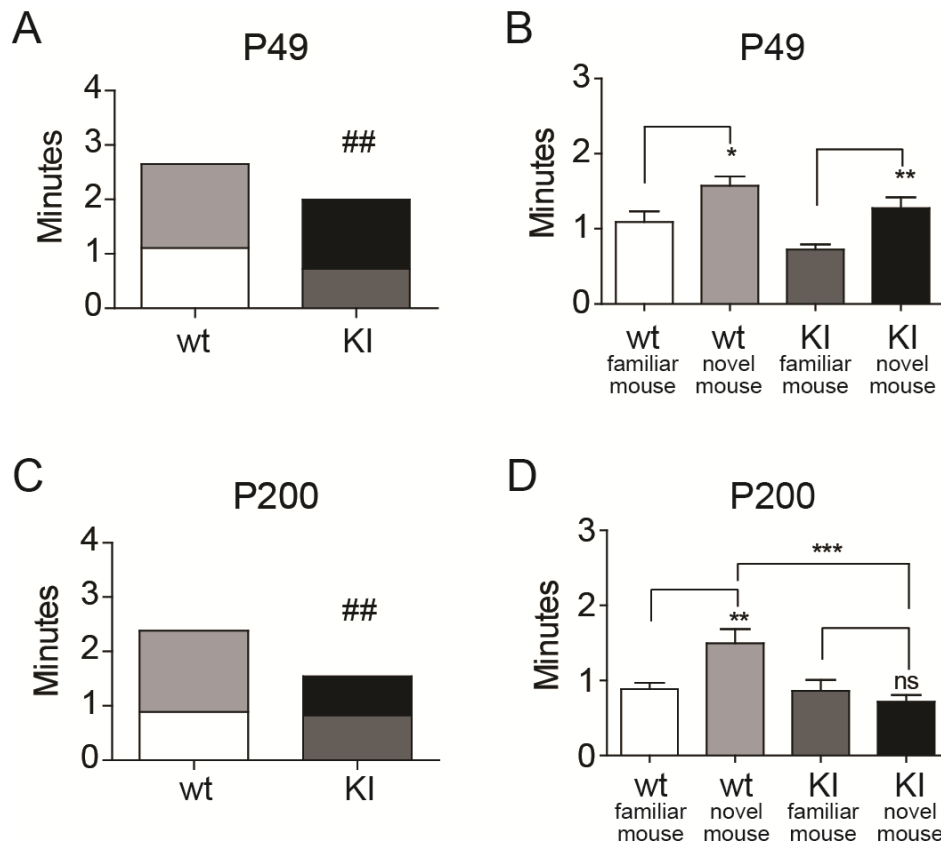


Figure 14: Stage 3 of the 3CST: *Gabrb3*^{+/*D120N*} mice had severe social deficits.

Stage 3 of the 3CST was a 10-minute trial in which test mice had two socialization options: 1) familiar socialization, in which the novel mouse from stage 2 remained where she was, or 2) novel socialization, in which a new novel mouse was placed under the previously empty pencil cup. Panels A and C represent the two-way ANOVA for each age, while B and D represent the post-tests for each age. Four comparisons were made in both B and D; however, only significant or otherwise relevant results were shown. **A)** Two-way ANOVA showed a significant genotype effect at P49 (interaction $F_{1,84} = 0.2347$, $p = 0.6293$ ns; genotype $F_{1,84} = 7.219$, $p = 0.0087$ ##. Group means – familiar mouse: wt 1.11 ± 0.14 min, KI 0.72 ± 0.07 min; novel mouse: wt 1.54 ± 0.12 min, KI 1.27 ± 0.14 min; total exploration: wt 2.65 ± 0.21 min, KI 2.00 ± 0.17 min). **C)** There was a significant genotype effect at P200, as well as a significant interaction between genotype and target (interaction $F_{1,87} = 7.039$, $p = 0.0095$ ##; genotype $F_{1,87} = 9.778$, $p = 0.0024$ ##. group means – familiar mouse: wt 0.89 ± 0.08 min, KI 0.82 ± 0.14 min; novel mouse: wt 1.49 ± 0.19 min, KI 0.72 ± 0.09 min; total exploration: wt 2.38 ± 0.21 min, KI 1.58 ± 0.17 min). Statistical tests shown on graphs are *a priori* Bonferroni post-tests after two-way ANOVAs. Bonferroni multiple-comparison correction significance levels for B, D were: * $p < 0.0125$, ** $p < 0.001$, *** $p < 0.0001$. $n = 21-23$.

***Gabrb3*^{+D120N} mice had elevated anxiety.**

The final behavioral comorbidity of LGS that we assessed was elevated anxiety [57]. To test for anxiety, we took data from two tests: the locomotor activity chambers and the elevated zero maze (EZM). When in the locomotor activity chambers, a more anxious mouse will spend more time on the perimeter of the chamber, avoiding the center (called thigmotaxis) [58]. At both P49 and P200, KI mice traveled less through the center of the chamber (Figure 15A, B). On the EZM, a more anxious mouse will spend more of its time in the closed arms, avoiding the open arms [59]. At P49, KI mice did not have a significant change in the time spent in the open arms of the maze (Figure 15C), while at P200, KI mice spent significantly less time in the open arms of the maze (Figure 15D). Together these data indicated young KI mice had a mild anxiety phenotype that became worse with age.

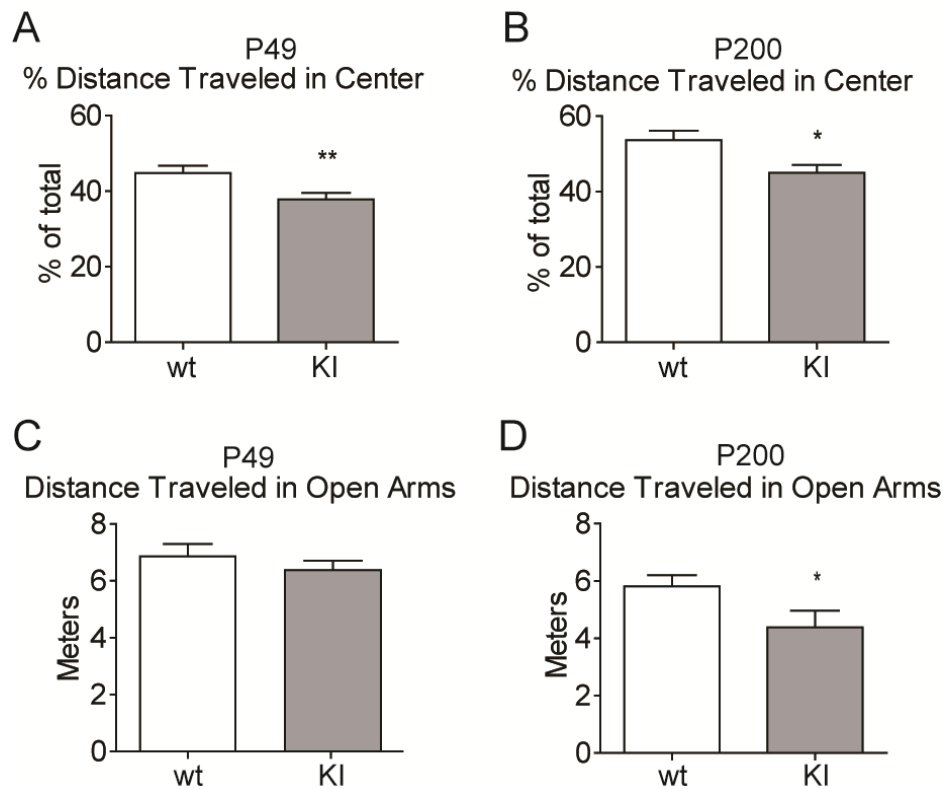


Figure 15: *Gabrb3*^{+/*D120N*} mice had elevated anxiety that worsened with age.

KI mice displayed elevated anxiety in both the locomotor activity chambers and the elevated zero maze, with a mild anxiety phenotype at P49 and more pronounced anxiety at P200. **A, B)** Each subject spent 60 min in the locomotor activity chamber. The chamber was divided into two 50% sections by area: the center, and the surround. Distance traveled within the surround (edge) area was calculated as a percentage of total distance traveled as total distance traveled was significantly different: see Figure 12B, D. **A)** At P49, the % distance traveled in the center 50% was reduced in KI mice ($t_{48} = 2.737$, $p = 0.0087$ **). Group means: wt 44.80 ± 1.921 %, $n = 25$; KI 37.84 ± 1.665 %, $n = 25$). **B)** At P200, the % distance traveled in the center 50% was reduced in KI mice ($t_{39} = 2.674$, $p = 0.0109$ *). Group means: wt 53.63 ± 2.490 %, $n = 21$; KI 44.59 ± 2.274 %, $n = 20$). **C, D)** Each subject spent 5 min in the elevated zero maze. **C)** At P49, the distance traveled in the open arms was not significantly changed ($t_{55} = 0.8854$, $p = 0.3798$ ns. Group means: wt 6.866 ± 0.4310 meters, $n = 28$; KI 6.388 ± 0.3280 meters, $n = 29$). **D)** At P200, KI mice did travel less time in the open arms ($t_{43} = 2.070$, $p = 0.0445$ *). Group means: wt 5.815 ± 0.3877 meters, $n = 23$; KI 4.386 ± 0.5780 meters, $n = 22$). Data not shown: total distance traveled was not changed for the KI mice at either age in the zero maze (P49: $t_{55} = 1.633$, $p = 0.1082$ ns. Group means: wt 16.12 ± 0.7513 meters, $n = 28$; KI 14.54 ± 0.6115 meters, $n = 29$. P200: $t_{43} = 1.435$, $p = 0.1584$ ns. Group means: wt 14.59 ± 0.5908 meters, $n = 23$; KI 12.93 ± 1.011 meters, $n = 22$). Unpaired two-tailed Student's t -test for all panels, * $p < 0.05$, ** $p < 0.01$. $n = 22-28$.

Addressing potential confounding factors in behavioral testing

It is possible that acute seizures were confounding factors in all behavioral tests except for hyperactivity. Except for AASs, all seizure types would be observable without EEG. During all tests except for during the open field test in which mice were in an enclosed chamber, mice were constantly observed. Because the KI mice were hyperactive in the open field chambers, it does not appear as if prolonged seizures occurred, and if they did mice still had ample time to over-explore the chamber. No seizures were observed during any testing, except for one mouse which had a fatal GTCS and was excluded from the data set. KI mice were observed having seizures in their home cages on testing days. When this occurred, the entire cage was left undisturbed until all mice in the cage resumed normal activity, plus an additional five-minute delay. During the Barnes maze and elevated zero maze testing, mice did not display any prolonged motor arrests indicative of AASs. With our testing structure, it is not possible to know if KI mice were experiencing AASs seizures during the 3CST, and they were often immobile for several minutes. However, at the end of each stage, immobile mice were never non-responsive to the stimulus of the observer reaching into the apparatus, indicating there were at least not very prolonged AASs during the test.

The Barnes maze assays hippocampal learning and memory [60], which is of interest in a disorder with AASs as hippocampal involvement in those seizures has been proposed [47]. This test was selected over the Morris water maze due to concerns of seizures occurring during a swim test and due to minor motor abnormalities observed with TreadScan (see below, Figure 19). It is possible that an anxiety (the mouse could freeze on the maze) or hyperactivity (the mouse may have trouble focusing and might be more inclined to run around the maze) phenotype could be confounding factors in the Barnes maze. Low anxiety has been shown to decrease

performance in spatial learning tasks by increasing both latency and accuracy, while high anxiety increased performance by decreasing latency but with no effect on the number of errors committed [61]. Because KI mice have elevated anxiety but decreased spatial learning performance in both latency and error measures, it appears that anxiety is not responsible for the changes seen in Barnes maze testing. Furthermore, this was addressed by assessing the search strategy employed by mice to find the target hole. Harrison et al. [56] developed this technique and showed that decreased hippocampal learning and memory processing leads to an elevated (by the scoring adaptation shown here) search strategy score. KI mice do show a persistent elevation in search strategy score, indicating that hippocampal learning and memory is associated with decreased performance in the Barnes maze despite potential confounding factors. Finally, KI mice were not observed having seizures during the Barnes maze testing.

Anxiety has been shown to confound hyperactivity; however, it is low anxiety that increases activity levels [61]. The jumping (vertical counts) phenotype was also included as a less-traditional hyperactivity measure that has not been shown to be associated with anxiety. Therefore, the anxiety phenotype does not appear to be responsible for hyperactivity in KI mice. Additionally, where hyperactivity was present (open field test, not elevated zero maze) % change in activity was calculated for assessing anxiety as the raw values would no longer be valid. This is based on the assumption that hyperactivity would not change the anxiety response in the open field test, which is not necessarily true. For example, a hyperactive mouse may run repetitive circles around the perimeter of the chamber (thigmotaxis) instead of a chaotic travel pattern across the center of the chamber. This is why the elevated zero maze was included, in which there was no change in total distance traveled but the anxiety phenotype was still present, albeit mild. To summarize, hyperactivity may contribute to the anxiety phenotype seen in the open

field chambers; however, the elevated zero maze confirms there is an isolated anxiety phenotype in KI mice. Furthermore, highly anxious mice have been reported to be less aggressive [61], which is consistent with the low aggression we have observed in the KI colony. KI male mice from different litters could be housed together without incident, and KI males did not fight back when attacked by wild type males.

It is possible that the 3CST was confounded by several factors, including anxiety, hyperactivity, sense of smell, and spatial reasoning. Low anxiety has been shown to decrease the exploration of a testing environment [61], whereas KI mice had elevated anxiety but decreased exploration. Additionally, both high and low anxiety led to increased social time [61], whereas KI mice had decreased social time. Therefore, anxiety does not explain the social deficits seen in KI mice. KI mice did not appear to be hyperactive during the 3CST, possibly due to the introduction of other factors (socialization, novel objects), or possible due to the complicated nature of the apparatus. When not socializing or exploring a novel object, KI mice were typically stationary, whether they were grooming or immobile. These behaviors occurred either adjacent to a target with their back to the target, or with their back to a corner of the apparatus. Sense of smell is very important for socialization in mice, and *Gabrb3* is highly expressed in the olfactory bulb of mice [12]. It was necessary to exclude a deficit in the sense of smell as being a factor in the observed socialization deficits. KI mice spent more time investigating each of the target smells than the control swab, even more-so than wild type mice, indicating there is not a loss of olfaction in KI mice that would explain the social deficits (Figure 16). Additionally, as KI mice do have a properly functioning olfactory system, it does not seem that spatial deficits would explain the socialization deficits as the KI mice would be able to navigate the chamber using olfaction as a guide. Additionally, investigation of the non-novel social stimulus (be it

novel object or familiar socialization) was unchanged in comparison to wild type mice, indicating that KI mice could adequately find the non-social stimulus.

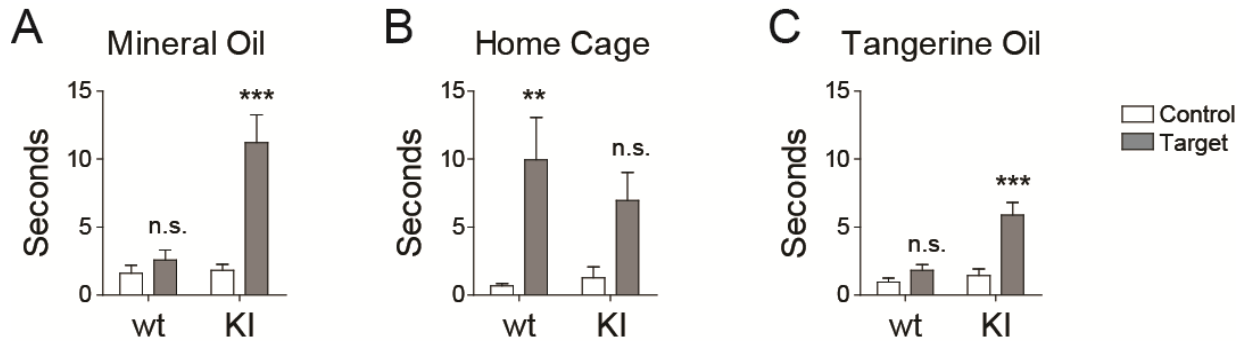


Figure 16: *Gabrb3*^{+/*D120N*} mice did not show any deficits in the sense of smell.

Mice were exposed to three scent stimuli, but they did not display any deficits in their ability to detect these odors. **A)** Mineral oil (interaction $F_{1,12} = 16.32$, $p = 0.0037$ ###; genotype $F_{1,12} = 12.91$, $p = 0.0016$ ##). **B)** Home cage (interaction $F_{1,12} = 1.170$, $p = 0.3007$; genotype $F_{1,12} = 0.3106$, $p = 0.5876$ ns). **C)** Tangerine oil (interaction $F_{1,12} = 19.42$, $p = 0.0009$ ###; genotype $F_{1,12} = 10.38$, $p = 0.0073$ ##). KI mice did display an elevated interest in these novel objects over wild type mice. Two-way ANOVA with Bonferroni post-tests comparing means within each genotype. $n = 7$ KI, males and females, P200.

When performing behavioral tests in mice, it is important to separate depression-like symptoms from anxiety-like symptoms [62]. The tail suspension test (TST) has been used traditionally to model antidepressant activity in mice based on the test inducing an inescapable stressor to the mice [63] and may also be used to screen for depression-like behavior in mice

[64]. A depression-like phenotype was assessed using the tail suspension test (TST). KI mice did not display a depressive-like phenotype (Figure 17).

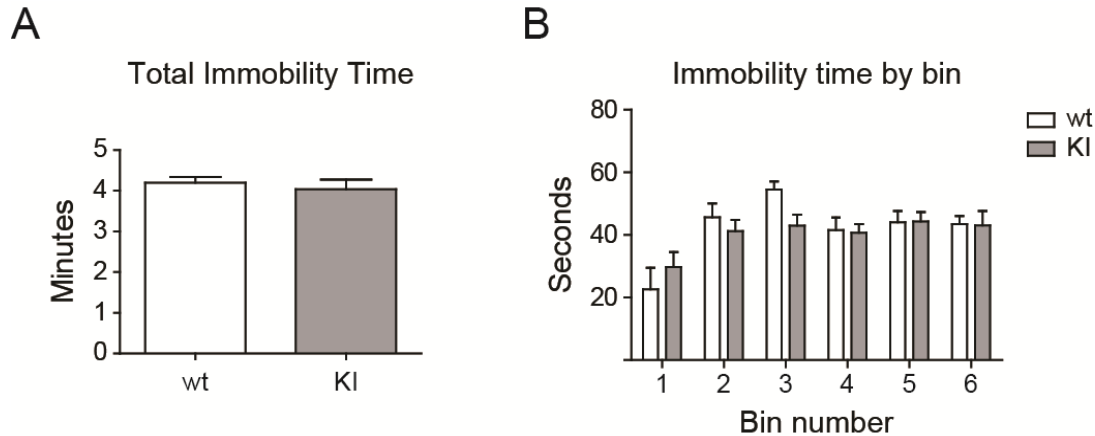


Figure 17: *Gabrb3*^{+/*D120N*} mice did not exhibit a depression-like phenotype.

The TST was used to test for a depression-like phenotype. Mice were suspended on the pressure-sensitive bars for 6 minutes. The lower threshold detects differences between immobility and very slight movement. **A)** KI mice did not show a difference in overall immobility time (unpaired Students' *t*-test: $t_{11} = 0.61$, $p = 0.55$ ns. Group means: wt 4.1 ± 0.142 minutes, KI 4.04 ± 0.24 minutes). **B)** KI mice did not show a difference when the test was separated into six 1-minute bins (two-way repeated measures ANOVA: interaction $F_{5,55} = 1.18$, $p = 0.33$; genotype $F_{1,55} = 0.55$, $p = 0.37$). wt $n = 7$, KI $n = 6$.

Finally, despite seeing an overall phenotype of increased movement (hyperactivity) in KI mice, we sought to ensure that mobility was not compromised in the mice as they have reduced distance traveled in some components of the EZM and locomotor activity chambers. Separation of motor ability from cognitive and behavioral function is of great importance for validating the

severity and specificity of cognitive and behavioral effects [65]. Additionally, $\beta 3$ subunits are highly expressed in the cortex including the motor cortex (Chapter 1, Figure 5). Mobility was tested using both the Rotarod and TreadScan. The accelerating rod of the rotarod evaluates maximal motor performance and motor coordination [66]. TreadScan uses a high-speed digital camera below a clear treadmill to detect individual footprints and calculates several motor and gait characteristics [67]. KI mice did not show any motor deficits on the Rotarod test (Figure 18) but did display minor abnormalities using the TreadScan system (Figure 19). Alongside the rest of the motor data, we do not feel this minor abnormality has substantial impact on the other behavioral data; however, it is something to consider when performing motor-based tasks on these mice. This did help inform the decision to use the Barnes maze over the Morris water maze.

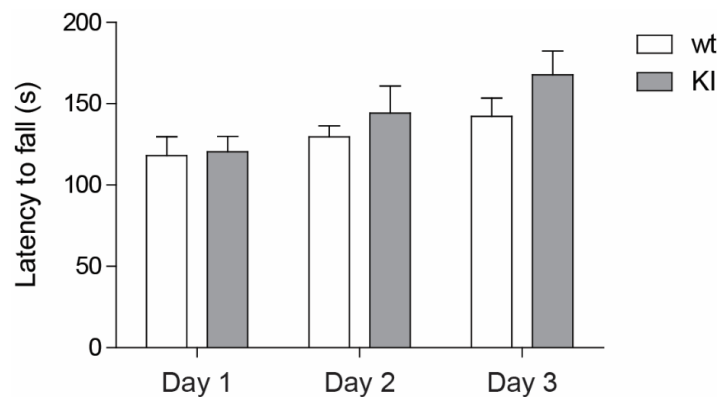


Figure 18: *Gabrb3*^{+/*D120N*} mice did not display motor deficits on the Rotarod.

Mice underwent three days of testing on the rotarod. Three trials per day were averaged into one daily value for each mouse. The latency to fall (or to spin twice, which is marked as a fall) is shown. KI mice did not show a deficit on the Rotarod test (interaction $F_{2,22} = 0.65$, $p = 0.53$; genotype $F_{1,22} = 1.32$, $p = 0.27$ ns). Two-way repeated measures ANOVA. P200, $n = 7$.

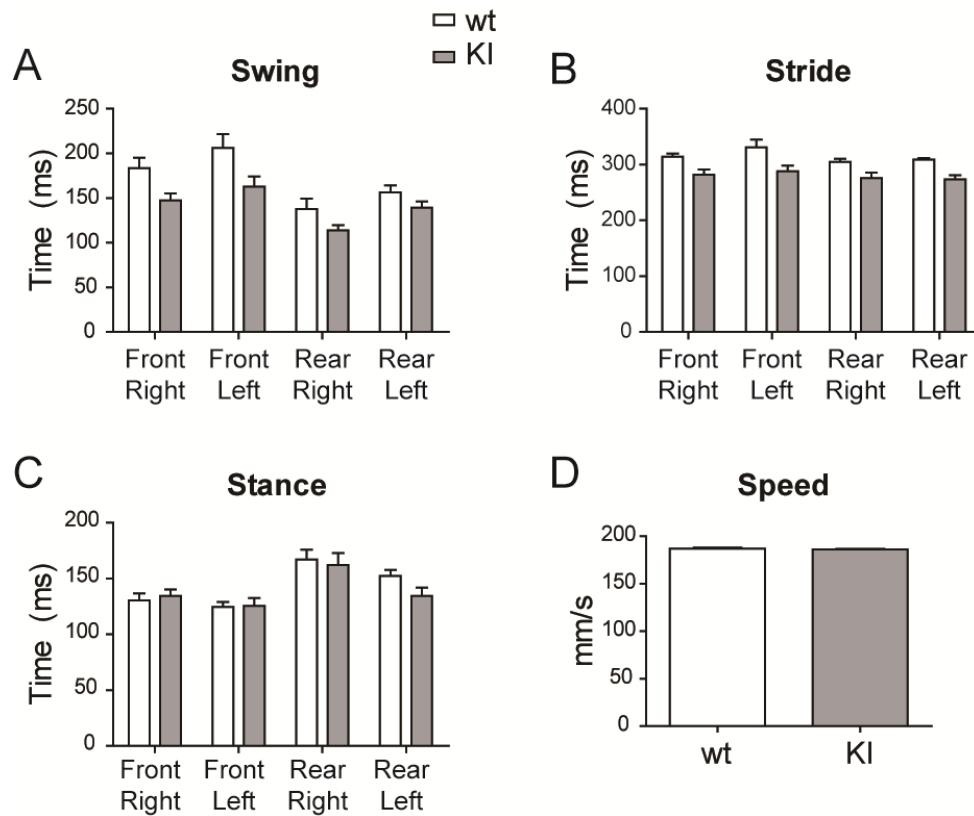


Figure 19: *Gabrb3*^{+/*D120N*} mice displayed minor motor abnormalities using TreadScan.

The TreadScan system automatically calculates several motor and gait characteristics. KI mice displayed minor abnormalities in the following parameters: **A**) Swing (interaction $F_{3,30} = 1.02$, $p = 0.396$; genotype $F_{1,30} = 8.37$, $p = 0.0160$ #) and **B**) Stride (interaction $F_{3,30} = 0.58$, $p = 0.63$; genotype $F_{1,30} = 10.93$, $p = 0.0079$ ##). KI mice did not show any abnormalities in **C**) Stance (interaction $F_{3,30} = 1.51$, $p = 0.23$; genotype $F_{1,30} = 0.33$, $p = 0.58$ ns) or **D**) Speed: $t_{10} = 1.16$, $p = 0.27$, wt 187.2 ± 0.73 mm/s, KI 186.0 ± 0.66 mm/s). wt n = 6, KI n = 6. P200.

Cellular profile in wild type and KI mice

Having confirmed that KI mice had the seizure and behavioral phenotypes of LGS, we next examined the underlying mechanisms for the seizures. The majority of *GABR* epilepsy mutations produce subunits with impaired biogenesis, leading to altered cell surface expression [68]. To determine if the effects of the mutant $\beta 3(D120N)$ subunits on $GABA_A$ receptor currents were related to its expression and trafficking *in vivo*, we assayed total expression of wild type and KI $\beta 3$ subunits in cerebellum (Ce), cortex (Co), hippocampus (Hi), and thalamus (Th) (Figure 20A, B), surface expression in whole brain (Figure 20C, D), and synaptosomal content from regions of interest (Ce, Co, Hi, and Th) (Figure 20E, F) but found no differences between KI and wild type littermate mice (see methods). These results demonstrated that mutant $\beta 3(D120N)$ subunits did not affect $GABA_A$ receptor biogenesis, trafficking, or synaptic distribution, and suggested that the mutant $\beta 3$ subunits can effectively compete with wild type subunits to form intact, but functionally impaired, $GABA_A$ receptors in brain, which leads to decreased GABAergic inhibition and seizures.

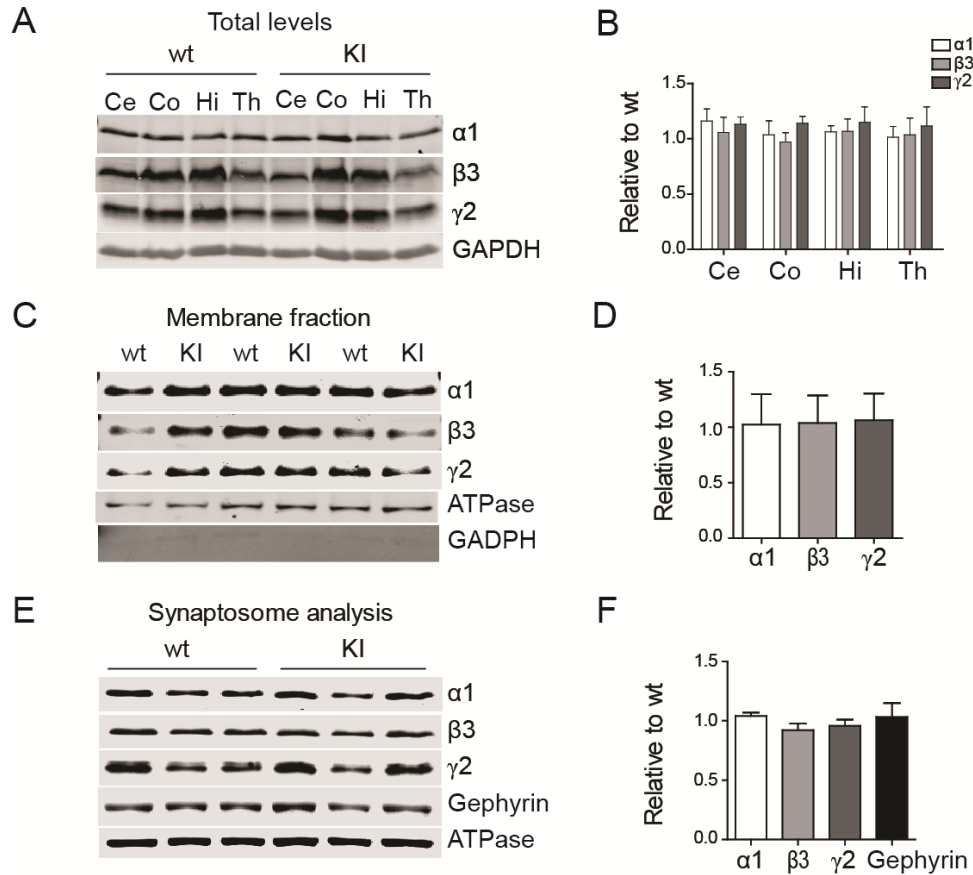


Figure 20: Biogenesis and trafficking of receptors containing mutant $\beta 3(D120N)$ subunits were unaltered in $Gabrb3^{+/D120N}$ KI mice.

The mutant $\beta 3(D120N)$ subunits did not affect expression, surface trafficking, or synaptosomal distribution of either their own or other GABA_A receptor subunits. **A)** Whole cell lysates from different brain regions [cortex (Co), cerebellum (Ce), hippocampus (Hi) and thalamus (Th)] were collected from KI and wild type littermate mice and subjected to SDS-PAGE and immunoblotted with anti- $\alpha 1$, $\beta 3$, and $\gamma 2$ subunit antibodies. GAPDH served as a loading control. **B)** Band intensities of $\alpha 1$, $\beta 3$, and $\gamma 2$ subunits were normalized to the GAPDH signal and then KI was compared to wild type ($n = 3$ KI:wt pairs). One-way ANOVA followed by the Dunnett's multiple comparison test was used to determine significance, however, no changes were identified. **C)** Plasma membrane proteins from mouse brain were isolated, analyzed by SDS-PAGE and immunoblotted with anti- $\alpha 1$, $\beta 3$, and $\gamma 2$ subunit antibodies. Na^+/K^+ ATPase served as a loading control, and GAPDH served as a cytosolic protein contamination control. **D)** Band intensities of $\alpha 1$, $\beta 3$, and $\gamma 2$ subunits were normalized to ATPase signal, and then KI bands were compared to wild type bands ($n = 3$ KI:wt pairs). **E)** Proteins from synaptosomes were analyzed by SDS-PAGE and immunoblotted with anti- $\alpha 1$, $\beta 3$, and $\gamma 2$ subunit and gephyrin antibodies. Na^+/K^+ ATPase served as a loading control. The distribution of GABA_A receptor subunits was not changed in KI or wild type littermate mice. **F)** Band intensities of $\alpha 1$, $\beta 3$, and $\gamma 2$ subunits and gephyrin were normalized to the ATPase signal and then KI bands were compared to wild type bands ($n = 3$ KI:wt pairs). Student's *t*-tests were used in D and F with a significance level of $\alpha = 0.05$.

Electrophysiological findings

mIPSCs recorded from SS cortex layer V/VI pyramidal neurons of *Gabrb3*^{+D120N} mice had reduced amplitude

Having confirmed that KI mice had the seizure and behavioral phenotypes of LGS, we next examined the underlying mechanisms for the seizures. During brain development, $\beta 3$ subunits are a major constituent of GABA_A receptors and are widely expressed in the brain, especially highly in the cerebral cortex, amygdala, olfactory bulb, nucleus reticularis of the thalamus and hippocampus [12]. Our previous *in vitro* results assessing $\alpha 1\beta 3(D120N)\gamma 2$ GABA_A receptor currents in transfected HEK293T cells showed that the mutant subunits significantly reduced peak amplitude and altered kinetic properties including decreased open probability, opening frequency, and burst duration [13]. Here, using western blots of wild type littermate and KI mouse brain tissue, the expression and trafficking of $\beta 3(D120N)$ subunits were confirmed to be normal *in vivo*. We saw no evidence for a decrease in $\beta 3$ subunits in assembled receptors or in the overall expression of $\beta 3$ subunits, and $\beta 2$ subunits have been shown to be unable to substitute for $\beta 3$ subunits. Since their expression is generally quite limited [10], we do not expect to detect a change in receptor composition, quantity, or localization even if a change in $\beta 3$ subunits exists.

Next, we determined whether the D120N amino acid substitution affected the functional properties of GABAergic inhibitory interneuron synapses on cortical layer V/VI pyramidal neurons. We targeted SS cortex layer V/VI pyramidal neurons as they participate in the thalamocortical feedback loop [69]. Using the whole-cell patch-clamp technique and acute coronal thalamocortical slices, we recorded mIPSCs in the pyramidal neurons from wild type

littermate and KI mice (Figure 21A, B). In KI mice we observed decreased GABA_A receptor-mediated mIPSC amplitude (Figure 21C-E), and increased mIPSC decay time constant (Figure 21F), with no change to mIPSC frequency. Consistent with the decrease in mIPSC amplitudes, mIPSC charge transfer was also decreased in neurons from het KI mice compared with that from wild type mice (wt 617.12 ± 89.89 pA*ms, n = 5 mice; KI 363.14 ± 38.04 pA*ms, n = 5 mice; Student's *t*-test $p = 0.040$). The reduced current amplitudes and charge transfer of mutant GABA_A receptors containing $\beta 3(D120N)$ subunits in layer V/VI SS cortical pyramidal neurons would be predicted to decrease interneuron phasic GABAergic inhibition and lower the seizure threshold by promoting neuronal hyperexcitability, resulting in epilepsy.

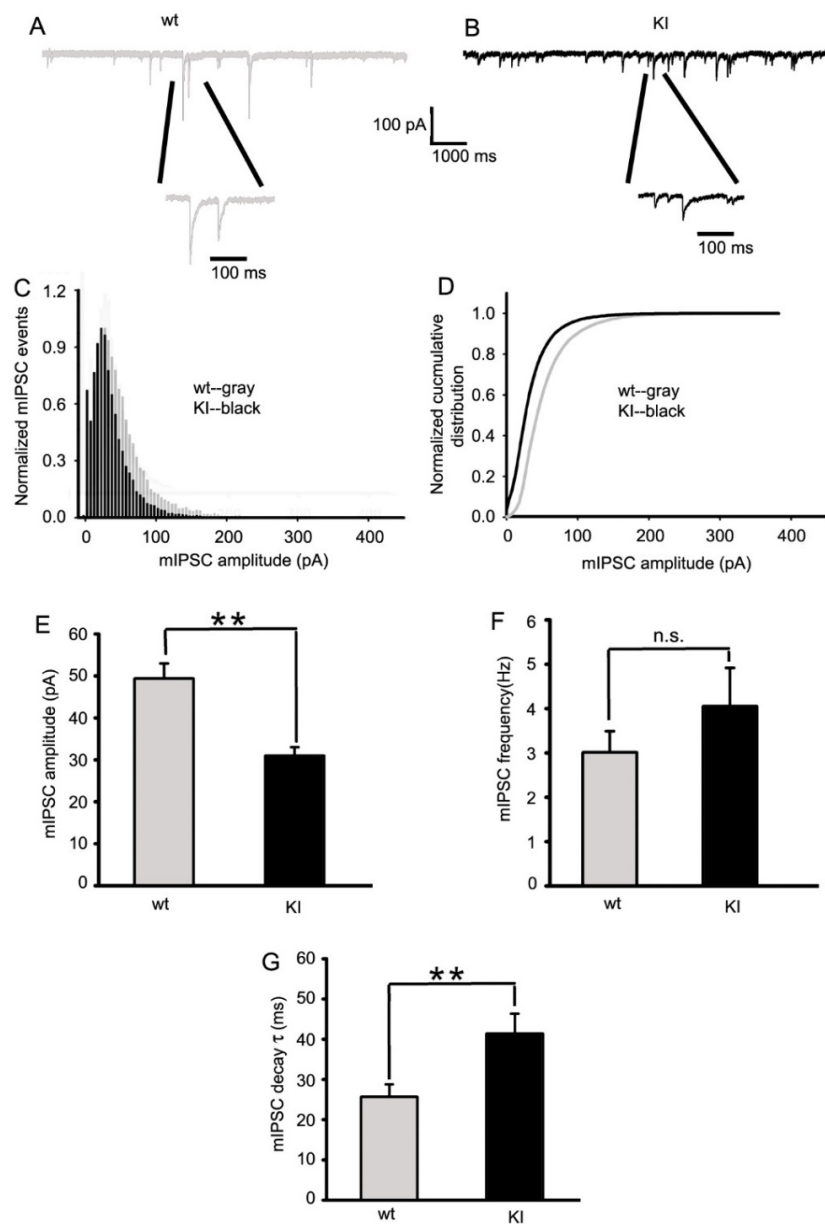


Figure 21: mIPSCs recorded from KI mouse SS cortex layer V/VI neurons were altered.

mIPSCs were recorded from SS cortex layer V/VI neurons (voltage-clamped at -60 mV with equal chloride concentration inside and outside cells) in thalamocortical slices from littermate A) wt and B) KI mice. C) Normalized mIPSC events for wt and KI mice showed the frequency of mIPSCs in each amplitude bin. D) Normalized cumulative distributions were plotted for wt and KI mouse mIPSCs. Compared with mIPSCs recorded from wt littermate mice, those from SS cortex layer V/VI neurons in KI mice had E) significantly reduced amplitudes (wt -49.67 ± 2.71 pA; KI -31.48 ± 1.76 pA) and F) slowed mIPSC decay (wt 25.05 ± 2.87 msec; KI 39.13 ± 2.72 msec). Wild type, n = 6 mice; KI, n = 5 mice. Student's *t*-test, * $p < 0.05$, ** $p < 0.01$, *** $p < 0.001$.

Thalamocortical oscillations recorded from VBn neurons of *Gabrb3*^{+D120N} mice had prolonged duration

Excitatory-inhibitory balance critically regulates cortical network function and activity, and an imbalance is the basis for pathogenesis for seizures and other neuropsychiatric disorders [70-73]. Additionally, as AASs with SSWD are the predominant seizure type in LGS KI mice, and thalamocortical hypersynchrony is known to be the primary cause of SWD, we asked whether mutant $\beta 3$ (D120N) subunits affected neural network activity at the cellular level in the thalamocortical circuit. Spontaneous thalamocortical network oscillations were measured in the thalamic ventrobasal nucleus (VBn) in horizontal slices from wild type littermate and KI mice that retained the thalamocortical circuitry (Figure 22A, B). Multiunit recordings from VBn in slices from KI mice exhibited prolonged and high amplitude, spontaneous network oscillations compared to the very short, spontaneous network bursts in thalamocortical slices from wild type littermate mice (Figure 22C), consistent with the notion that excessive thalamocortical synchronization and hyperexcitability occur during seizures, particularly absence seizures. However, these results do not exclude a role for other brain areas such as hippocampus from participating in the spontaneous oscillations.

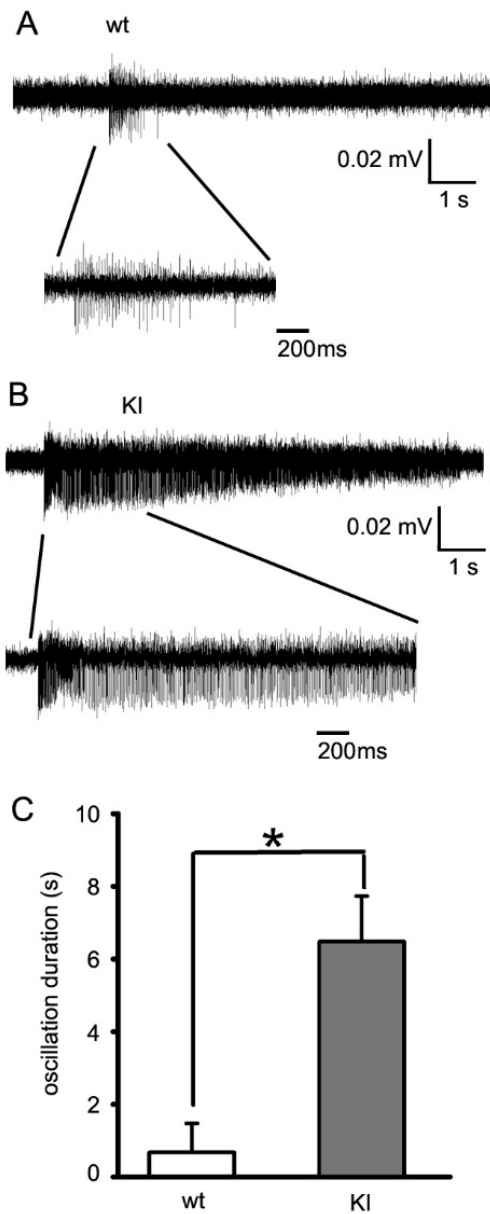


Figure 22: Spontaneous thalamocortical network oscillations from KI mice were longer and more frequent than those from wild type littermate mice.

Representative extracellular multiple unit recordings from VBn in slices showing **A)** spontaneous brief thalamocortical bursts in wt mice and **B)** spontaneous prolonged thalamocortical oscillations in KI mice. One short burst from a wt and one oscillation from a KI mouse were expanded in each panel to show the multiple spikes in the burst or oscillation. Scale bars are as indicated. **C)** Average duration of spontaneous bursts for P42 wt mice (0.78 ± 0.71 secs, $n = 6$ mice) and spontaneous oscillations from P42 KI mice (6.88 ± 1.39 secs, $n = 9$ mice) were plotted (** $p < 0.01$, Student's t -test).

Therapeutics in mice

To further assess the validity of the *Gabrb3*^{+/*D120N*} mouse as an LGS model, we evaluated the effectiveness of several AEDs, ethosuximide, clobazam, and topiramate, used to treat LGS in the KI mice. Ethosuximide is the primary drug of choice for treatment of TASs and is also used in LGS treatment when other treatments are ineffective, or as an adjunct to other AEDs to increase efficacy [74, 75]. Ethosuximide can also reduce AAS occurrence, and in some patients it may reduce tonic and myoclonic seizures as well [74, 76]. Clobazam and topiramate are both commonly used for treatment of LGS [74]. Additionally, as cannabidiol has been shown recently to be effective in treatment-resistant epilepsies such as LGS, we assessed the effectiveness of the cannabinoid receptor 1 (CB1)-specific agonist WIN 55,212-2 for treatment of LGS seizures. While these drugs are all used in treatment of LGS, the AEDs sometimes have significant side effects. These AEDs are often not efficacious in every patient or may require a specific combination of several drugs unique to each patient to achieve efficacy, making drug therapy difficult. We sought to determine whether any of these drugs were effective in treating the seizures in the KI mice.

For evaluation of AED efficacy, KI mice were injected with solvent and video-EEG was recorded for two hours to establish a seizure baseline. Seizure time and count were found to be stable during these two hours, so an average of ‘per hour’ was used for baseline for each animal. Mice were then injected with the AED dissolved in solvent, and another two hours of video-EEG were recorded (Figure 23A). These two hours were split into one-hour bins as AEDs have a plasma half-life that is shorter in mice than that in humans, often as short as one hour. Here we quantified only total AAS duration as other seizures were much less frequent and thus would not

provide useful information for the short experimental protocol used here. Two AEDs, ethosuximide and clobazam, showed main effects by one-way ANOVA. Bonferroni post-tests indicated a significant decrease in cumulative AAS duration in the hour after injection for both drugs (Figure 23B). Ethosuximide and clobazam resulted in a decrease in AAS time of around 50%. Ethosuximide showed a full return to baseline by the second hour after injection, while clobazam showed a partial return to baseline. Topiramate was not effective in reducing AAS cumulative time.

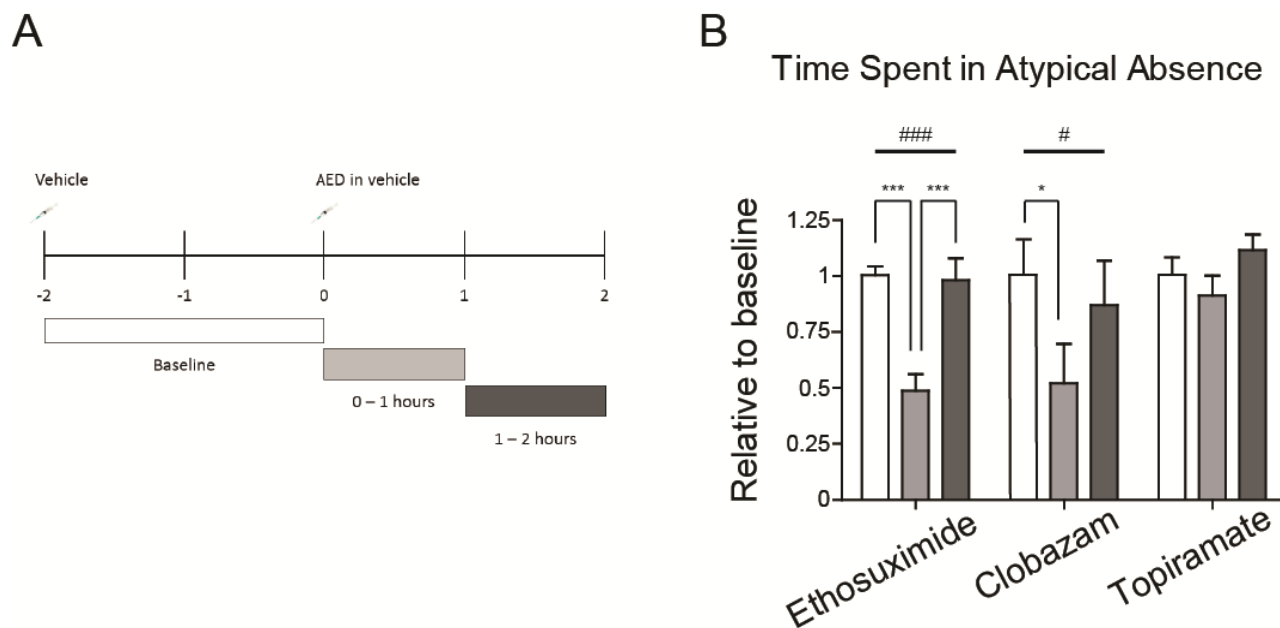


Figure 23: The AEDs ethosuximide and clobazam, but not topiramate, reduced total AAS duration in KI mice.

A) Total observation period by video-EEG for each AED lasted 4 hours. At hour 0, an injection of each drug's respective vehicle was given as a control observation. Vehicle and vehicle washout were found to be stable and were therefore averaged as a baseline for each animal. Drug + vehicle were administered at hour 2. The two hours after the drugs were administered were split into single hour observations, the first hour after administration and the second hour after administration. **(B)** Three AEDs were administered individually to KI mice. A one-way ANOVA was performed on each drug individually (shown above each drug set), and Tukey's multiple comparison tests were conducted comparing all three pairs of time points (shown on bar graphs where significant). Both ethosuximide and clobazam, but not topiramate, significantly reduced the relative time spent in atypical absence seizures as compared to the baseline for each animal. Ethosuximide: ($F_{2,16} = 17.53$ $p < 0.0001$ ###. A to B: $q = 7.408$ ***, mean diff 0.5125. A to C: $q = 0.323$ ns. B to C: $q = 7.084$ ***, mean diff = 0.490), Clobazam: ($F_{2,14} = 5.077$, $p = 0.022$ #. A to B: $q = 4.447$ *, mean diff = 0.5019. A to C: $q = 1.592$ ns. B to C: $q = 2.855$ ns), Topiramate: ($F_{2,14} = 1.575$, $p = 0.242$ ns. A to B: $q = 1.339$ ns. A to C: $q = 1.169$ ns. B to C: $q = 2.508$ ns). $n = 8-9$, 6-8 months old, males and females. Repeated measures one-way ANOVA # $p < 0.05$, ### $p < 0.001$; Tukey's multiple comparison test adjusted p value * $p < 0.05$, *** $p < 0.001$.

Cannabinoids may require long-term dosing to achieve an effect; therefore, WIN 55,212-2 was given to mice daily for 7 days and cumulative AAS duration and count within a two-hour window on day 8 were compared to the baseline state for each mouse recorded on day 1 (Figure 24A). Administration of WIN 55,212-2 produced a decrease by 75% in the time spent in AASs (Figure 24B) as well as a reduction in the number of these seizures (Figure 24C).

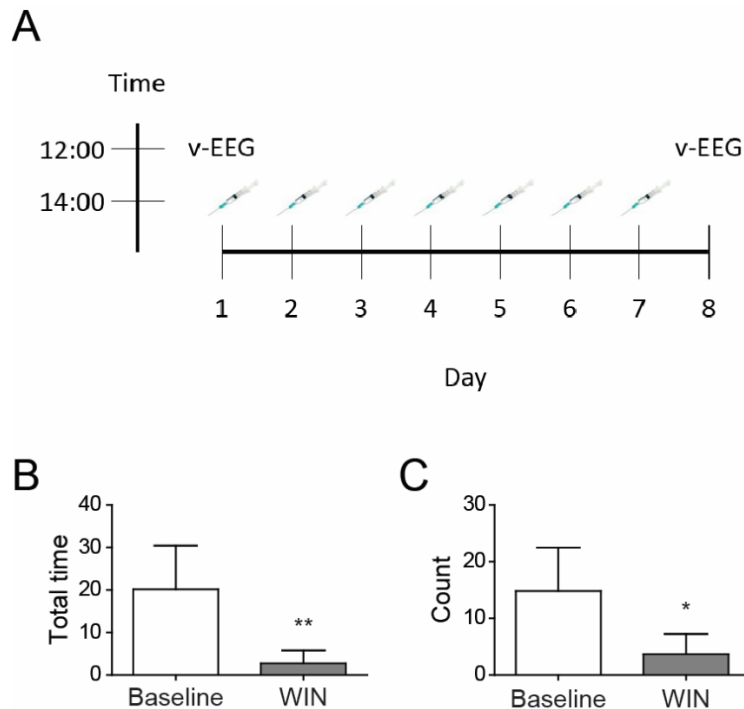


Figure 24: Cannabinoid therapy was effective at reducing AASs.

A) Win 55,212-2 was administered daily for one week. KI mice had a significant reduction in both **(B)** cumulative time spent in AASs ($t_5 = 5.00$, $p = 0.0041$ **). Group means: baseline = 20.16 minutes, WIN = 2.716 minutes), and **(C)** AAS seizure count after one week of dosing. ($t_5 = 3.159$, $p = 0.0251$ *). Group means: baseline = 14.83, WIN = 3.667). $n = 6$, paired Student's t -test, 5-8 months old, males and females, * $p < 0.05$, ** $p < 0.01$.

An analysis of peak spectral frequency was performed on random samples of AASs before and after each AED (data not shown). Not only was peak spectral frequency unchanged, indicating that while incidence or duration of AASs was able to be impacted, the core features of the AASs themselves were unchanged. Additionally, this analysis allowed us to verify that the AASs recorded in these short windows were true AASs and not the NREM sleep, which has a slower peak spectral frequency (Figure 5).

Discussion

The *Gabrb3*^{+D120N} KI mouse is a model of human LGS

LGS is a severe form of early onset epileptic encephalopathy, which has multiple genetic and symptomatic structural causes. LGS is characterized by seizures with multiple semiologies, a generalized SSWD pattern on EEG, and cognitive and behavioral abnormalities [6]. In each case of genetic LGS, it is unclear whether the multiple seizures and behavioral abnormalities are caused by mutations of several genes and varying genetic background or are the result of a single mutation in a key gene. To answer this question, it would be useful to have an animal model of LGS caused by a single gene mutation and with a uniform genetic background to determine if the animal model develops the multiple seizures and behavioral comorbidities.

The *GABRB3* (c.G358A, p.D120N) mutation was shown to be associated with LGS by its presence only in the proband of an LGS triad, but its causal role in development of LGS can be established directly by generating a mouse model with the corresponding mutation. Generation of a genetic mouse model with a human LGS mutation displaying the LGS phenotype is an

important advance for understanding the pathophysiology of LGS and for potential development of new treatments for LGS and associated behavioral abnormalities. The *Gabrb3*^{+D120N} KI mouse generated for this study recapitulated both the occurrence and semiologies of LGS seizures (spontaneous atypical absence, GTC, myoclonic, and tonic seizures with appropriate ictal EEG correlates) and the behavioral phenotypes (cognitive disability, hyperactivity, social deficits, and anxiety) seen in both the proband and broadly in LGS patients. Together, these results show that we have generated a mouse model for LGS based on a human genetic mutation.

***Gabrb3*^{+D120N} mice had seizure semiologies like those of LGS patients.**

Home-cage monitoring revealed that KI mice had modest developmental delay in the infantile period, and video-EEG monitoring in adult KI mice showed atypical absence and myoclonic seizures as the most prominent seizure types, with tonic seizures being observed less frequently, although all of these seizures were observed throughout adulthood. GTCs were observed infrequently and were seen more often in older mice (> 6 months of age). Additionally, we observed spontaneous epileptic spasms in young KI mice between P13 and P17. These flexion-extension spasms, accompanied by behavioral arrest, staring, and loss of responsiveness, were similar to spasms reported in models of infantile spasms [77], a disorder whose diagnosis often precedes the diagnosis of LGS, as it did in the patient bearing the D120N mutation. Seizure semiologies observed at all ages in the KI mice were consistent with those of LGS and demonstrated a worsening of seizure semiology from an early-life onset to late-life persistence. It is worth noting that while tonic seizures were observed in the majority of LGS patients [78], they were infrequently observed in the KI mice. This could be the result of scoring difficulties, or due to different underlying genetics or genetic modifiers in idiopathic LGS patients compared

to our inbred KI mice. Nonetheless, the KI mice recapitulated LGS-associated seizures.

LGS patients are reported to have AASs (1-2.5 Hz SSWDs) [79]. There are several rodent models of TASs (6-8 Hz), but AASs have been reported only after administration of AY-9944 (a cholesterol biosynthesis inhibitor) to young rats [19] or by overexpressing the GABA_BR1a receptor in mice [48], neither of which reflect human genetics or result in a complete LGS phenotype. AASs are a hallmark symptom of LGS and are thought to contribute significant cognitive impairment [79] that is more severe than that seen in patients with TASs. This KI mouse offers an opportunity to identify neural circuits underpinning AASs and to determine if worsening of seizures with age can be prevented by blocking them as soon as they are observed.

Gabrb3^{+D120N} mice exhibited behavioral comorbidities like those of LGS patients.

LGS is known to have several comorbidities, including cognitive disability, ADHD, ASD, and anxiety. Treatment of LGS necessitates not only a reduction in seizures, but also management of the complex behavioral abnormalities that accompany the disorder [20, 80]. Thus, the KI mice were assessed for comorbid conditions seen in LGS patients. Because onset of LGS occurs early in life but often persists throughout adulthood, mice were studied at young adult (P49) and older adult (P200) ages. While the Barnes Maze test is traditionally thought to require hippocampal processing, evidence suggests that the cortex is also required for spatial navigation and spatial memory formation [60]. Additionally, although we have largely studied the thalamocortical circuit in this study, which is the primary circuit involved in TASs [81, 82], at least one model of AASs indicated that the hippocampus is also involved [47]. We decided that the Barnes maze test would be an effective low-stress method of assessing cognitive ability

in this model. Both adolescent and adult KI mice displayed deficits in spatial learning and spatial memory as assessed in the Barnes maze test, consistent with involvement of hippocampus in AASs.

Social impairment is a hallmark symptom of ASD, a condition commonly associated with epilepsy [8, 23, 31], and in the 3CST, KI mice were shown to have mild social impairment in adolescence that evolved into a profound social deficit by adulthood. Because *Gabrb3* is highly expressed in the olfactory bulb [12] and because olfactory cues are important for socialization in mice [83], we tested for differences in olfaction between wild type littermate and KI mice. We did not find any olfactory deficits in KI mice (data not shown).

KI mice were also more hyperactive than their wild type littermates, a phenotype that reflects human ADHD and which began in adolescence and worsened with age. Finally, while adolescent KI mice showed a mild anxiety phenotype, adult KI mice were substantially more anxious. While we assessed motor deficiencies using Rotarod and TreadScan tests and for depression using the tail suspension test, we did not find significant effects in any of these tests (data not shown). Together, these comorbidities recapitulate the symptoms observed in many LGS patients. Of note, while it is possible that some of the comorbid conditions may impact each other, there is no evidence that any one of the conditions explains any other condition. The data suggest that each abnormality is a distinct condition associated with the LGS mutation.

Cortical layer V/VI neurons in thalamocortical slices from *Gabrb3*^{+/*D120N*} mice showed decreased inhibition

After establishing that the KI mice recapitulated the salient features of LGS, the molecular mechanism of the mutation was assessed. Our previous work *in vitro* demonstrated

that there was no change in assembly or trafficking of $\alpha 1\beta 3(D120N)\gamma 2$ GABA_A receptors in transfected HEK293T cells [13]. Here, using western blots of wild type littermate and KI mouse brain tissue, the expression and trafficking of $\beta 3(D120N)$ subunits were confirmed to be normal in brain *in vivo*. We saw no evidence for a decrease in the presence of $\beta 3$ subunits in assembled receptors or in the overall expression of $\beta 3$ subunits, and $\beta 2$ subunits have been shown to be unable to substitute for $\beta 3$ subunits. Since their expression is generally limited [10], we do not predict a change in receptor composition, quantity, or localization. Previously, whole-cell recordings from HEK293T cells transfected with $\alpha 1\beta 3(D120N)\gamma 2$ GABA_A receptor subunits showed a decrease in current amplitude with 1 mM GABA applied, and single channel recordings from transfected HEK293T cells showed decreased open probability, opening frequency, and burst duration with 1 mM GABA applied [13]. In adult mice, $\beta 3$ subunits are highly expressed in cortical layers V/VI, which plays a role in thalamocortical oscillations. We recorded mIPSCs from SS cortical layer V/VI pyramidal cells that result from release of GABAergic vesicles from local interneurons. In KI mice the amplitudes of mIPSCs were reduced 37%, and the decay times were increased 53% with no change in frequency, and an overall reduction in net charge transfer of 44%.

These results suggest a change in postsynaptic function without a change in presynaptic neurotransmitter release [84], which is consistent with our finding that surface levels and synaptic quantity of $\beta 3(D120N)$ subunits were unchanged by the mutation. This indicates that network wiring resulted in similar patterns of GABAergic synaptic inputs in KI as in wild type littermate mice, and the changes we report were due instead to dysfunction of postsynaptic GABA_A receptors. Generation of TASs is known to involve both cortex and thalamus; however, there is conflicting evidence about whether TASs occur due to an increase or a decrease in

activity in thalamocortical activity [85], and how this differs in AASs is not well understood. Our data suggest this is due to an increase in network activity and a reduction in interneuronal inhibition. GTCSs also involve increases in cortical activity [85], among other regions, but the networks involved in tonic, atonic, clonic, and myoclonic seizures are less-well understood. The $\beta 3$ subunit is highly expressed in selective locations in the brain such as the cortex where we observed substantial mIPSC changes, yet this mutation had profound effects on brain function. This mouse offers the opportunity to further study and understand the networks involved in these types of seizures.

Existing relevant mouse models

The Epi4k consortium also discovered two *de novo* mutations in dynamin 1 (*DNMI*) thought to be causative of LGS in patients [17] and the fitful mouse containing a spontaneous murine *Dnm1* mutation has been reported to have seizures. While this mouse is certainly a useful model, the fitful mouse was not derived from a human mutation and exhibits only a partial set of the seizure profile observed in patients [86]. Additionally, the fitful mouse has a limited expression of human comorbidities, with no observed social deficits, and cognitive tests that showed either no deficit or were confounded by severe hyperactivity. Separately, *Gabrb3* knock-out (KO) mice were shown to recapitulate some of the features of Angelman syndrome, including a subset of the common seizure and comorbid phenotypes of Angelman syndrome patients [87, 88]. This does not appear to be an LGS-like phenotype, suggesting that LGS in the KI mouse is not caused by haploinsufficiency only.

As AASs are an important feature of LGS, it is pertinent to discuss existing rodent models of AASs. The cholesterol biosynthesis inhibitor AY-9944 (AY) causes AASs in rats

when administered repeatedly during the first month of life [19]. AY-treated rats show occasional voluntary ictal movement as is seen in patients with AASs, and these AASs display a characteristic asynchrony in that AASs EEG signatures and behavioral arrest are not time-locked to each other at the onset and termination of the seizure, [89]. Ethosuximide, which is used to treat TASs, successfully abolished AASs in rats, with AASs returning after ethosuximide was eliminated. However, these rats do not have increased susceptibility to other seizures in the LGS profile, such as GTCS [19]. Behaviorally, AY-treated mice display minor social deficits in the 3CST that are similar to those seen at P49 in D120N mice, with a social deficit only seen in stage 3 of testing, hyperactivity in the locomotor activity chambers, but no increase in anxiety in the elevated plus maze [89]. Additionally, direct application of AY to acute mouse brain slices has been shown to induce AASs-like activity by increasing membrane excitability in hippocampal neurons via voltage-gated sodium channels [90]. Notably, TASs are constrained to the thalamocortical circuit and do not involve the hippocampus [89], so hippocampal involvement in addition to thalamocortical disruptions in AASs is unique and valuable information.

The GABA receptor type B ($GABA_B$) is a metabotropic receptor with three subunits: R1a, R1b, and R2. $GABA_B$ receptors activate calcium and potassium channels and act to inhibit activity. Overexpression of R1a results in AASs with 3-6 Hz SSWD, reduced synaptic plasticity, and cognitive impairment. [48] In both models of AASs, $GABA_B$ receptor agonists exacerbate the seizures while antagonists suppress the seizures, indicating that both models function through increased $GABA_B$ receptor activity. Neither model represents a model of human genetics that may be causative of LGS, and neither recapitulates the full seizure profile or full behavioral profile of LGS.

How this mouse fits into future of LGS therapies

Our KI mice mirror the seizure types and behavioral abnormalities associated with LGS. Mechanistically, LGS was shown to occur at least in part via a reduction in mIPSC amplitude in cortical layer V/VI pyramidal neurons and development of thalamocortical oscillations. LGS is a disorder that is notoriously difficult to treat, and seizures are poorly controlled with AEDs. The need for novel therapeutic strategies is great. In the KI mice, we found that ethosuximide, clobazam, and a CB1 agonist were all effective at reducing AASs, the most-frequent seizure type observed in KI mice. However, topiramate was not effective, and none of the drugs were effective at stopping all seizures. Ethosuximide is primarily prescribed to target the thalamocortical oscillations of TASs [4] as it antagonizes the T-type calcium channels [91] present in the VBn which enable a bursting firing pattern [92]. However, treatment with ethosuximide resulted in only a 50% reduction in the time spent in AAS in the LGS mouse for the first hour after administration, followed by a complete return to baseline seizure activity. WIN 55,212-2 was able to reduce the time spent in AAS by over 80% and in a long-term dosing strategy in which observation occurred 24 hours after the last dose of the CB1 agonist. CB1 receptors are highly expressed pre-synaptically on interneurons of the cortex and pre-synaptically on the intra-nuclear projections of the GABAergic neurons in the nRT. Additionally, in young rodents, CB1 is highly expressed in the CA1 of the hippocampus and is expressed, albeit less, in the excitatory projection neurons of the hippocampus. Overall, hippocampal and entorhinal cortex expression increases with age. [93, 94] CB1 receptors are expressed in other regions as well but these regions have been established as being of particular interest to AASs. In addition to the therapeutic data, deficits in the Barnes maze established that hippocampal processing is disrupted in KI mice. Together, these data suggest that hippocampal

dysfunction may be associated with AASs as expanding treatment from just the thalamocortical circuit with ethosuximide to include the hippocampus with WIN 55,212-2, led to a substantially increased therapeutic benefit. The hippocampus is connected primarily to the entorhinal cortex as an intermediate, but also has projections directly to cortical regions such as the medial prefrontal cortex [95]. It is possible that these connections are responsible for the differences seen between TASs and AASs both in how they present and in how they are best treated.

While the KI mouse represents one mutation in one gene that is causative for LGS, we believe that the strong similarity between the mouse and the human seizure types and behavioral phenotypes will enable future studies of the mechanisms of and treatments for LGS. It is evident that the circuitry enabling the seizure phenotype of LGS overlaps heavily with the circuitry enabling the behavioral abnormalities associated with LGS. This one mutation is able to influence all relevant circuitry causing the full gamut of LGS symptoms, which will enable further study of what circuits are involved, how they are disrupted, and hopefully how they may be repaired. Of further interest, 20% of patients with LGS have a history of prior infantile spasms [54]. The proband patient in which the *GABRB3* G358A mutation was discovered had a diagnosis of IS prior to the LGS diagnosis, and here we report epileptic spasms in young LGS KI mice. The LGS KI mice will also serve as a tool to elucidate the changes that occur between infancy and the juvenile period, on to adulthood, which may reflect this progression from IS to LGS and the age-related worsening of LGS, offering another tool for future therapeutic exploration.

Network disturbances in *Gabrb3*^{+D120N} mice provide opportunities for discovery

The above data suggested that network wiring resulted in similar patterns of GABAergic synaptic inputs in KI and wild-type littermate mice, and the changes we report were due instead to dysfunction of postsynaptic GABA_A receptors. Because the GABA_A receptor β 3 subunit is highly expressed in selective locations in the brain such as the cortex where we observed substantial mIPSC changes, D120N had profound effects on brain function. These data indicate that a reduction in interneuronal inhibition likely is the cause of the LGS. Generation of absence seizures is known to involve both cortex and thalamus; however, there is conflicting evidence about whether absence seizures occur due to an increase or a decrease in activity in thalamocortical activity [85]. Our data suggest that for AASs, this is due to an increase in network activity in the LGS mouse. GTCS also are associated with increases in cortical activity [85], among other regions, but the networks involved in tonic, atonic, clonic, and myoclonic seizures are less well understood. This mouse offers the opportunity to further study and understand the networks involved in these types of seizures. Of particular value, a single point mutation in the β 3 subunit that was observed in a human with LGS was able to recapitulate both the seizure and behavioral comorbidity profiles seen in this complex disorder when expressed in this rodent model. This fact also indicates that the circuitry involved in the LGS seizure profile overlaps with that which is involved in the observed behavioral abnormalities. Therefore, future work may elucidate the connections between seizure circuitry and behavioral circuitry.

Bibliography

1. Qu, S., et al., *GABAA receptor $\beta 3$ subunit mutation D120N causes Lennox–Gastaut syndrome in knock-in mice*. Brain Communications, 2020. **2**(1).
2. Jahngir, M.U., M.Q. Ahmad, and M. Jahangir, *Lennox-Gastaut Syndrome: In a Nutshell*. Cureus, 2018. **10**(8): p. e3134.
3. McTague, A., et al., *The genetic landscape of the epileptic encephalopathies of infancy and childhood*. Lancet Neurol, 2016. **15**(3): p. 304-16.
4. Panayiotopoulos, C.P., in *The Epilepsies: Seizures, Syndromes and Management*. 2005: Oxfordshire (UK).
5. Abu Saleh, T. and L. Stephen, *Lennox gastaut syndrome, review of the literature and a case report*. Head Face Med, 2008. **4**: p. 9.
6. Trevathan, E., *Infantile spasms and Lennox-Gastaut syndrome*. J Child Neurol, 2002. **17** Suppl 2: p. 2S9-2S22.
7. Euro, E.-R.E.S.C., P. Epilepsy Phenome/Genome, and K.C. Epi, *De novo mutations in synaptic transmission genes including DNMI cause epileptic encephalopathies*. Am J Hum Genet, 2014. **95**(4): p. 360-70.
8. Epi, K.C., et al., *De novo mutations in epileptic encephalopathies*. Nature, 2013. **501**(7466): p. 217-21.
9. Macdonald, R.L., J.Q. Kang, and M.J. Gallagher, *Mutations in GABAA receptor subunits associated with genetic epilepsies*. J Physiol, 2010. **588**(Pt 11): p. 1861-9.
10. Homanics, G.E., et al., *Mice devoid of gamma-aminobutyrate type A receptor beta3 subunit have epilepsy, cleft palate, and hypersensitive behavior*. Proc Natl Acad Sci U S A, 1997. **94**(8): p. 4143-8.
11. Laurie, D.J., W. Wisden, and P.H. Seeburg, *The distribution of thirteen GABAA receptor subunit mRNAs in the rat brain. III. Embryonic and postnatal development*. J Neurosci, 1992. **12**(11): p. 4151-72.
12. Hortnagl, H., et al., *Patterns of mRNA and protein expression for 12 GABAA receptor subunits in the mouse brain*. Neuroscience, 2013. **236**: p. 345-72.
13. Janve, V.S., et al., *Epileptic encephalopathy de novo GABRB mutations impair GABAA receptor function*. Ann Neurol, 2016.

14. Vignoli, A., et al., *Lennox-Gastaut syndrome in adulthood: Long-term clinical follow-up of 38 patients and analysis of their recorded seizures*. *Epilepsy Behav*, 2017. **77**: p. 73-78.
15. Singh, A. and S. Trevick, *The Epidemiology of Global Epilepsy*. *Neurol Clin*, 2016. **34**(4): p. 837-847.
16. *Lennox-Gastaut syndrome*. 2018 February 26, 2019 February 28, 2019]; Available from: <https://ghr.nlm.nih.gov/condition/lennox-gastaut-syndrome>.
17. Allen, A.S., et al., *De novo mutations in epileptic encephalopathies*. *Nature*, 2013. **501**(7466): p. 217-21.
18. Amrutkar, C. and R.M. Riel-Romero, *Lennox Gastaut Syndrome*, in *StatPearls*. 2020: Treasure Island (FL).
19. Cortez, M.A., C. McKerlie, and O.C. Snead, 3rd, *A model of atypical absence seizures: EEG, pharmacology, and developmental characterization*. *Neurology*, 2001. **56**(3): p. 341-9.
20. Kerr, M., G. Kluger, and S. Philip, *Evolution and management of Lennox-Gastaut syndrome through adolescence and into adulthood: are seizures always the primary issue?* *Epileptic Disord*, 2011. **13 Suppl 1**: p. S15-26.
21. Ettinger, A.B., et al., *Attention-deficit/hyperactivity disorder symptoms in adults with self-reported epilepsy: Results from a national epidemiologic survey of epilepsy*. *Epilepsia*, 2015. **56**(2): p. 218-24.
22. Holmes, G.L., *Cognitive impairment in epilepsy: the role of network abnormalities*. *Epileptic Disord*, 2015. **17**(2): p. 101-16.
23. Hamiwka, L.D. and E.C. Wirrell, *Comorbidities in pediatric epilepsy: beyond "just" treating the seizures*. *J Child Neurol*, 2009. **24**(6): p. 734-42.
24. Widdess-Walsh, P., et al., *Lennox-Gastaut syndrome of unknown cause: phenotypic characteristics of patients in the Epilepsy Phenome/Genome Project*. *Epilepsia*, 2013. **54**(11): p. 1898-904.
25. Warren, A.E., et al., *Abnormal cognitive network interactions in Lennox-Gastaut syndrome: A potential mechanism of epileptic encephalopathy*. *Epilepsia*, 2016. **57**(5): p. 812-22.
26. Blume, W.T., *Lennox-Gastaut syndrome: potential mechanisms of cognitive regression*. *Ment Retard Dev Disabil Res Rev*, 2004. **10**(2): p. 150-3.
27. Jeste, S.S. and R. Tuchman, *Autism Spectrum Disorder and Epilepsy: Two Sides of the Same Coin?* *J Child Neurol*, 2015. **30**(14): p. 1963-71.

28. Jacob, J., *Cortical interneuron dysfunction in epilepsy associated with autism spectrum disorders*. *Epilepsia*, 2016. **57**(2): p. 182-93.
29. Pickett, J., et al., *Mortality in individuals with autism, with and without epilepsy*. *J Child Neurol*, 2011. **26**(8): p. 932-9.
30. Association, A.P., *Diagnostic and statistical manual of mental disorders (5th ed.)*. 2013, Arlington, VA: American Psychiatric Publishing.
31. Hancock, E.C. and J.H. Cross, *Treatment of Lennox-Gastaut syndrome*. *Cochrane Database Syst Rev*, 2013(2): p. CD003277.
32. Shneker, B.F. and N.B. Fountain, *Epilepsy*. *Dis Mon*, 2003. **49**(7): p. 426-78.
33. Perucca, E., *Cannabinoids in the Treatment of Epilepsy: Hard Evidence at Last?* *J Epilepsy Res*, 2017. **7**(2): p. 61-76.
34. Chen, J.W., L.M. Borgelt, and A.B. Blackmer, *Cannabidiol: A New Hope for Patients With Dravet or Lennox-Gastaut Syndromes*. *Ann Pharmacother*, 2019. **53**(6): p. 603-611.
35. O'Connell, B.K., D. Gloss, and O. Devinsky, *Cannabinoids in treatment-resistant epilepsy: A review*. *Epilepsy Behav*, 2017. **70**(Pt B): p. 341-348.
36. Thiele, E.A., et al., *Cannabidiol in patients with seizures associated with Lennox-Gastaut syndrome (GWPCARE4): a randomised, double-blind, placebo-controlled phase 3 trial*. *Lancet*, 2018. **391**(10125): p. 1085-1096.
37. Devinsky, O., et al., *Effect of Cannabidiol on Drop Seizures in the Lennox-Gastaut Syndrome*. *N Engl J Med*, 2018. **378**(20): p. 1888-1897.
38. Heber, R., *A manual on terminology and classification in mental retardation*. *Am J Ment Defic*, 1959. **Suppl 64**(2): p. 1-111.
39. Hamburg, S., et al., *Assessing general cognitive and adaptive abilities in adults with Down syndrome: a systematic review*. *J Neurodev Disord*, 2019. **11**(1): p. 20.
40. Miller, P.S. and A.R. Aricescu, *Crystal structure of a human GABAA receptor*. *Nature*, 2014. **512**(7514): p. 270-5.
41. Brown, L.E., et al., *gamma-Aminobutyric Acid Type A (GABAA) Receptor Subunits Play a Direct Structural Role in Synaptic Contact Formation via Their N-terminal Extracellular Domains*. *J Biol Chem*, 2016. **291**(27): p. 13926-42.
42. Rodriguez, C.I., et al., *High-efficiency deleter mice show that FLPe is an alternative to Cre-loxP*. *Nat Genet*, 2000. **25**(2): p. 139-40.
43. Mekada, K., et al., *Genetic differences among C57BL/6 substrains*. *Exp Anim*, 2009. **58**(2): p. 141-9.

44. Letts, V.A., B.J. Beyer, and W.N. Frankel, *Hidden in plain sight: spike-wave discharges in mouse inbred strains*. *Genes Brain Behav*, 2014. **13**(6): p. 519-26.
45. Tenney, J.R. and T.A. Glauser, *The current state of absence epilepsy: can we have your attention?* *Epilepsy Curr*, 2013. **13**(3): p. 135-40.
46. Jarre, G., et al., *Genetic Models of Absence Epilepsy in Rats and Mice*. *Models of Seizures and Epilepsy*, 2nd Edition. 2017: Elsevier. 455-471.
47. Vrielynck, P., *Current and emerging treatments for absence seizures in young patients*. *Neuropsychiatr Dis Treat*, 2013. **9**: p. 963-75.
48. Stewart, L.S., et al., *Severity of atypical absence phenotype in GABAB transgenic mice is subunit specific*. *Epilepsy Behav*, 2009. **14**(4): p. 577-81.
49. Striano, P. and V. Belcastro, *Treatment of myoclonic seizures*. *Expert Rev Neurother*, 2012. **12**(12): p. 1411-7; quiz 1418.
50. Werhahn, K.J., et al., *Tonic seizures: their significance for lateralization and frequency in different focal epileptic syndromes*. *Epilepsia*, 2000. **41**(9): p. 1153-61.
51. Daroff, R.B. and W.G. Bradley, *Bradley's neurology in clinical practice / [edited by] Robert B. Daroff... [et al.]*. 6th ed. 2012, Philadelphia, PA: Elsevier/Saunders.
52. Gohma, H., et al., *Absence-like and tonic seizures in aspartoacylase/attractin double-mutant mice*. *Exp Anim*, 2007. **56**(2): p. 161-5.
53. Seneviratne, U., M.J. Cook, and W.J. D'Souza, *Electroencephalography in the Diagnosis of Genetic Generalized Epilepsy Syndromes*. *Front Neurol*, 2017. **8**: p. 499.
54. Shields, W.D., *Diagnosis of infantile spasms, Lennox-Gastaut syndrome, and progressive myoclonic epilepsy*. *Epilepsia*, 2004. **45 Suppl 5**: p. 2-4.
55. Tauboll, E., L. Sveberg, and S. Svalheim, *Interactions between hormones and epilepsy*. *Seizure*, 2015. **28**: p. 3-11.
56. Harrison, F.E., et al., *Spatial and nonspatial escape strategies in the Barnes maze*. *Learn Mem*, 2006. **13**(6): p. 809-19.
57. Fisher, P.L. and A.J. Noble, *Anxiety and depression in people with epilepsy: The contribution of metacognitive beliefs*. *Seizure*, 2017. **50**: p. 153-159.
58. Simon, P., R. Dupuis, and J. Costentin, *Thigmotaxis as an index of anxiety in mice. Influence of dopaminergic transmissions*. *Behav Brain Res*, 1994. **61**(1): p. 59-64.
59. Shepherd, J.K., et al., *Behavioural and pharmacological characterisation of the elevated "zero-maze" as an animal model of anxiety*. *Psychopharmacology (Berl)*, 1994. **116**(1): p. 56-64.

60. Negron-Oyarzo, I., et al., *Coordinated prefrontal-hippocampal activity and navigation strategy-related prefrontal firing during spatial memory formation*. Proc Natl Acad Sci U S A, 2018. **115**(27): p. 7123-7128.
61. Yen, Y.C., et al., *Co-segregation of hyperactivity, active coping styles, and cognitive dysfunction in mice selectively bred for low levels of anxiety*. Front Behav Neurosci, 2013. **7**: p. 103.
62. Erhardt, A., et al., *TMEM132D, a new candidate for anxiety phenotypes: evidence from human and mouse studies*. Mol Psychiatry, 2011. **16**(6): p. 647-63.
63. Cryan, J.F., C. Mombereau, and A. Vassout, *The tail suspension test as a model for assessing antidepressant activity: review of pharmacological and genetic studies in mice*. Neurosci Biobehav Rev, 2005. **29**(4-5): p. 571-625.
64. Miller, B.H., et al., *Phenotypic characterization of a genetically diverse panel of mice for behavioral despair and anxiety*. PLoS One, 2010. **5**(12): p. e14458.
65. Brooks, S.P., R.C. Trueman, and S.B. Dunnett, *Assessment of Motor Coordination and Balance in Mice Using the Rotarod, Elevated Bridge, and Footprint Tests*. Curr Protoc Mouse Biol, 2012. **2**(1): p. 37-53.
66. Shiotsuki, H., et al., *A rotarod test for evaluation of motor skill learning*. J Neurosci Methods, 2010. **189**(2): p. 180-5.
67. Beare, J.E., et al., *Gait analysis in normal and spinal contused mice using the TreadScan system*. J Neurotrauma, 2009. **26**(11): p. 2045-56.
68. Macdonald, R.L. and J.Q. Kang, *mRNA surveillance and endoplasmic reticulum quality control processes alter biogenesis of mutant GABAA receptor subunits associated with genetic epilepsies*. Epilepsia, 2012. **53 Suppl 9**: p. 59-70.
69. Ledergerber, D. and M.E. Larkum, *Properties of layer 6 pyramidal neuron apical dendrites*. J Neurosci, 2010. **30**(39): p. 13031-44.
70. Magloczky, Z. and T.F. Freund, *Impaired and repaired inhibitory circuits in the epileptic human hippocampus*. Trends Neurosci, 2005. **28**(6): p. 334-40.
71. Marin, O., *Interneuron dysfunction in psychiatric disorders*. Nat Rev Neurosci, 2012. **13**(2): p. 107-20.
72. McCormick, D.A. and D. Contreras, *On the cellular and network bases of epileptic seizures*. Annu Rev Physiol, 2001. **63**: p. 815-46.
73. Penzes, P., et al., *Developmental vulnerability of synapses and circuits associated with neuropsychiatric disorders*. J Neurochem, 2013. **126**(2): p. 165-82.
74. Schmidt, D. and B. Bourgeois, *A risk-benefit assessment of therapies for Lennox-Gastaut*

- syndrome*. Drug Saf, 2000. **22**(6): p. 467-77.
75. Gomez, M.R. and D.W. Klass, *Epilepsies of infancy and childhood*. Ann Neurol, 1983. **13**(2): p. 113-24.
 76. van Rijckevorsel, K., *Treatment of Lennox-Gastaut syndrome: overview and recent findings*. Neuropsychiatr Dis Treat, 2008. **4**(6): p. 1001-19.
 77. Dulla, C.G., *Utilizing Animal Models of Infantile Spasms*. Epilepsy Curr, 2018. **18**(2): p. 107-112.
 78. Crumrine, P.K., *Management of seizures in Lennox-Gastaut syndrome*. Paediatr Drugs, 2011. **13**(2): p. 107-18.
 79. Gastaut, H., et al., [*Epileptic encephalopathy of children with diffuse slow spikes and waves (alias "petit mal variant") or Lennox syndrome*]. Ann Pediatr (Paris), 1966. **13**(8): p. 489-99.
 80. Archer, J.S., et al., *Conceptualizing lennox-gastaut syndrome as a secondary network epilepsy*. Front Neurol, 2014. **5**: p. 225.
 81. Bomben, V.C., et al., *Isolated P/Q Calcium Channel Deletion in Layer VI Corticothalamic Neurons Generates Absence Epilepsy*. J Neurosci, 2016. **36**(2): p. 405-18.
 82. Barad, Z., D.R. Grattan, and B. Leitch, *NMDA Receptor Expression in the Thalamus of the Stargazer Model of Absence Epilepsy*. Sci Rep, 2017. **7**: p. 42926.
 83. Arakawa, H., et al., *A new test paradigm for social recognition evidenced by urinary scent marking behavior in C57BL/6J mice*. Behav Brain Res, 2008. **190**(1): p. 97-104.
 84. Choi, S. and D.M. Lovinger, *Decreased frequency but not amplitude of quantal synaptic responses associated with expression of corticostriatal long-term depression*. J Neurosci, 1997. **17**(21): p. 8613-20.
 85. Blumenfeld, H., *Consciousness and epilepsy: why are patients with absence seizures absent?* Prog Brain Res, 2005. **150**: p. 271-86.
 86. Asinof, S.K., et al., *Independent Neuronal Origin of Seizures and Behavioral Comorbidities in an Animal Model of a Severe Childhood Genetic Epileptic Encephalopathy*. PLoS Genet, 2015. **11**(6): p. e1005347.
 87. DeLorey, T.M., et al., *Mice lacking the beta3 subunit of the GABAA receptor have the epilepsy phenotype and many of the behavioral characteristics of Angelman syndrome*. J Neurosci, 1998. **18**(20): p. 8505-14.
 88. Fiumara, A., et al., *Epilepsy in patients with Angelman syndrome*. Ital J Pediatr, 2010. **36**: p. 31.

89. Jung, S., et al., *Social deficits in the AY-9944 mouse model of atypical absence epilepsy*. Behav Brain Res, 2013. **236**(1): p. 23-9.
90. Jung, S., Y. Jeong, and D. Jeon, *Epileptic activity during early postnatal life in the AY-9944 model of atypical absence epilepsy*. Cell Calcium, 2015. **57**(5-6): p. 376-84.
91. Hanrahan, B. and R.P. Carson, *Ethosuximide*, in *StatPearls*. 2020: Treasure Island (FL).
92. Avoli, M., *A brief history on the oscillating roles of thalamus and cortex in absence seizures*. Epilepsia, 2012. **53**(5): p. 779-89.
93. Busquets-Garcia, A., J. Bains, and G. Marsicano, *CBI Receptor Signaling in the Brain: Extracting Specificity from Ubiquity*. Neuropsychopharmacology, 2018. **43**(1): p. 4-20.
94. Marsicano, G. and B. Lutz, *Expression of the cannabinoid receptor CBI in distinct neuronal subpopulations in the adult mouse forebrain*. Eur J Neurosci, 1999. **11**(12): p. 4213-25.
95. Tannenholz, L., J.C. Jimenez, and M.A. Kheirbek, *Local and regional heterogeneity underlying hippocampal modulation of cognition and mood*. Front Behav Neurosci, 2014. **8**: p. 147.

Chapter 4

A Knock-in Mouse Harboring a Patient-Derived Disease-Associated Mutation, *Gabrb3*^{+P11S}, Recapitulates Both Childhood Absence Epilepsy and Autism Spectrum Disorder

This text was adapted from a manuscript that is in preparation at the time that this dissertation is being completed. This work is presented here by permission of all authors. Some work or analysis by others in the lab is still in progress, which is indicated in the applicable figure legends. Behavior collection and analysis is complete. The dissertation author was involved in many aspects of this work but focused heavily on the behavioral analysis and spectral frequency analysis.

Introduction

Childhood absence epilepsy (CAE) is the most common genetic childhood-onset epilepsy syndrome, occurring in 10-17% of genetic epilepsy cases [1-5]. CAE onset peaks at 6-7 years of age, and patients with CAE have frequent, intrusive (up to 200 daily) typical absence seizures (TAS) that are characterized by >3 seconds (average of 9.4 seconds in duration) impairment of consciousness and behavioral arrest [4, 6]. The ictal EEG of a typical absence seizure has bilateral, synchronous and symmetrical generalized spike wave discharges (SWDs) occurring at

>2.5 Hz, typically at 3-4.5 Hz, which are time-locked to the impairment of consciousness and behavioral arrest [1-3, 5, 6]. The seizures are not associated with aura or postictal symptoms but may be accompanied by one or more features including staring, behavioral arrest, eyelid fluttering or hand/face automatisms and are often (12-60% of patients) associated with generalized tonic-clonic seizures (GTCSs) later in life [1].

CAE is classified by the International League Against Epilepsy (ILAE) as a generalized genetic epilepsy (GGE) [5, 7], which is defined by associated seizure types and ages of seizure onsets, and patients typically have normal intellect and normal imaging. GGE's themselves are common, accounting for one-third of all epilepsies in the general population and an even high frequency of occurrence in children [8]. Despite the formal definition, over half of children with GGEs, including CAE, have associated cognitive disorders and multiple behavioral comorbidities including autism spectrum disorder (ASD), hyperactivity, depression, anxiety, and attentional, emotional and conduct problems [9-11].

While symptomatic therapies are available for many patients with CAE, up to half of patients are refractory and treatments for the comorbid conditions are generally ineffective. In short, there are no therapies for CAE that treat intractable absence seizures and prevent development of the behavioral comorbidities. While much excellent work has been done on the basis for SWDs and absence seizures using mutant rodent strains and chemoconvulsants [12], less has explored the pathophysiology of CAE and the basis for CAE comorbidities associated with human mutations. An animal model of human CAE for use in elucidating disease pathogenesis and for antiepileptic drug (AED) development would be extremely useful.

We have developed a knock-in mouse, the *Gabrb3*^{+/*PIIS*} mouse, which contains a mutation in the human GABA_A receptor β 3 subunit gene (*GABRB3*) that has been identified in

both CAE and ASD patients [6, 13]. The codon for P11 is located in exon 1A of *GABRB3*, an area of important transcriptional control (see Chapter 1, *Genomic interactions* for more detail on transcriptional regulation of *GABRB3*) [14]. Exon 1A encodes the signal peptide of the β 3-version 2 (V2) subunit, which is cleaved to form the mature peptide [15]. Several papers have been published by both our laboratory and others including patient data and *in vitro* effects of this mutation. Since the *GABRB3*(P11S) mutation is located in the β 3-V2 subunit signal peptide, it was unclear how it would impair GABA-evoked current. It could alter processing and/or signal peptide cleavage, or it could decrease expression of the subunit from the mutant allele. To explore this further, we generated a het *Gabrb3*^{+/*P11S*} knock-in (KI) mouse and determined if the P11S mutation caused CAE and behavioral comorbidities such as ASD in the KI mice.

Childhood absence epilepsy

Overview

CAE is characterized by frequent and obtrusive TAs [2] and accounts for 10-12% of epilepsy in children under 16 years of age [6]. TAs are generalized, non-convulsive seizures [2] that have an abrupt onset and offset during which behavioral arrest is time-locked with the SWD seen on EEG [1]. The ictal SWD of TAs has a peak spectral frequency higher than 2.5 Hz, usually 3-4.5 Hz, and the seizures last an average of 9-10 seconds (with a range of 1-44 seconds) [1, 2]. TAs are not preceded by an aura or followed by a postictal state as other seizures often are [2]. CAE is often labeled as a “benign epilepsy” despite somewhat poor seizure control and incomplete remission [1].

Development is generally undisturbed in CAE patients [3], although up to half [3] of people with CAE experience behavioral, psychiatric, language, cognitive comorbidities [1, 2]. Cognitive comorbidities may include problems with executive function, attention, anxiety, ADHD, ASD, depression, social dysfunction, verbal skills, and visuospatial memory [1, 2]. Comorbidities usually appear at or after the onset of seizures and often must be addressed separately from seizure management. Some of these comorbidities, such as attention deficits, do not often improve even seizures are well controlled. Importantly, children with CAE are more likely to require special classes or to repeat a grade and are less likely to graduate high school than children without neurologic chronic disease. They are also more likely to be under-employed, have an unplanned pregnancy, and to have diagnosed psychiatric problems [3]. Management of all aspects of CAE, including both the seizures and comorbidities, is therefore of great importance to the quality of life for these patients.

Genetics of CAE

Genetic factors are believed to play a very important role in the etiology of CAE [5], as they do in all GGEs [2]. Early family studies indicated an inherited risk of 50% for SWD, 12% for GTCs, and 12% for absence seizure for either siblings or offspring [6]. Twin studies showed 74% concordance in monozygotic twins and 27% concordance in dizygotic twins of inheriting SWD traits [6]. Perturbations in many genes have since been implicated in inheritance of CAE, particularly in ion channels including voltage-gated T-type calcium channels (discussed in detail in Chapter 1, *Typical absence models*) as being expressed in the ventrobasal nucleus of the thalamus) and several GABA_A receptor subunits ($\alpha 1$, $\beta 3$, $\gamma 2$, $\gamma 3$, and δ) [1, 2, 6, 8]. Specifically, at least 13 single nucleotide polymorphisms (SNPs) in *GABRB3* have been

associated with CAE patients.

ASD in CAE

ASD is an important comorbidity to examine as it relates both to epilepsy broadly, and specifically to CAE, as these populations greatly overlap. Approximately 30% of children with ASD also have epilepsy (up to 75% have EEG abnormalities with or without epilepsy), and similarly up to 30% of children with epilepsy also have ASD [6, 8]. ASD affects approximately 1 in 150 children and is characterized by impaired development of communication, impaired social behaviors, and the presence of restricted and repetitive behaviors [13]. When ASD and epilepsy co-exist, patients are statistically more likely to have other neuropsychiatric disorders or intellectual disabilities [8]. It is unclear how epilepsy and ASD can both evolve from the same set of genetic factors. Both ASD and epilepsy are heterogeneous disorders with complex etiologies or susceptibilities factors which often affect neural development, synaptic transmission, or brain network activity. Many synaptic protein genes (including synaptogenesis and synaptic function) have been identified as being associated with an elevated risk of autism. Of these genes, GABA_A receptor subunit genes *GABRs* have frequently appeared. [8]

GABA_A receptors: an overlap between ASD and CAE genetics

GABAergic signaling was first identified two decades ago as being perturbed in ASD, indicating that inhibitory dysfunction may be involved in ASD pathogenesis. Brain specimens of ASD and epilepsy patients from multiple investigators have indicated disruptions in GABA_A receptor expression, including several GABA_A receptor subunits that are not well-explored in the field of epilepsy: $\gamma 1$, $\gamma 3$, $\alpha 2$, $\alpha 4$, $\alpha 5$, and $\beta 1$. Not only have *GABRs* themselves been identified as

risk-factors for ASD, but genes that modulate GABAergic signaling (MET, Plaur, neuropilin 2) are also associated with ASD. [8] SNPs in *GABRB3* have not only been heavily associated with CAE, but at least 7 laboratories studying multiple ethnic groups have identified SNPs in either *GABRB3* or the surrounding chromosomal cluster, 15q11-13 (see Chapter 1, *Genomic interactions*) [8]. One of these SNPs, which encodes GABRB3(P11S), was identified in both CAE and ASD populations and is the subject of this chapter.

Treatment of CAE

Ethosuximide is the first-line treatment for CAE in patients with no history of GTCS, with a success rate of 53% at 18 weeks in treatment of TASs [1-3]. Ethosuximide fails in 47% of patients either due to continuing seizures or side effects [1]. This is followed by valproic acid, which has a higher success rate of 58% at 18 weeks in treatment of TASs and is also capable of treating GTCSs, but does carry a higher risk of attention problems [1-3]. Both ethosuximide and valproic acid suppress the T-type calcium channels expressed in the ventrobasal nucleus of the thalamus (see Chapter 1, Figure 5 for more information on these channels) [2, 3]. Lamotrigine used to be the first-line medication but ethosuximide and valproic acid have been found to be more effective with fewer side effects [1-3]. If a third AED is needed, clobazam, a benzodiazepine (see Chapter 1, *Drug binding domains* for more information on AEDs), may be effective and less sedative than the other two medications [3]. 60-95% of patients respond well to medication; however, some patients are left with treatment-resistant seizures [3]. In some of these patients, a ketogenic diet may be effective.

Outcome and prognosis of CAE

If CAE is the sole phenotype present, prognosis is improved and up to 95% of cases

remit; however, when patients have other conditions such as cognitive comorbidities, prognosis is worsened [6]. The overall remission rate for CAE is around 60% (21%-74%) [1, 2]. GTCSs develop in 40% of CAE patients, typically 5-10 years after CAE onset between the ages of 8 and 15 years old [1]. If GTCSs do develop, patients will not respond well to the initial ethosuximide therapy and often will have persistent seizures and no long-term remission [2]. Additionally, injury is a concern in CAE, and 20% of patients will suffer a severe injury during a TAS or due to problems in the areas of attention, executive function, or verbal and visuospatial memory [1, 2]. Finally, even if cognitive abilities are normal, patients may struggle academically as frequent seizures can interfere with learning [2].

Thalamocortical circuitry in TASs and CAE

Thalamocortical circuitry plays a major role in the pathophysiology of TASs. The SWD associated with TASs is produced by reciprocally connected neurons in both the cortex and the thalamus [1]. Pyramidal cells in layer V/VI of the cortex send excitatory projections to both the nucleus reticularis (nRT) and the ventrobasal nucleus (VBN) of the thalamus. The GABAergic neurons comprising the nRT project both to the nRT and to the VBN [2]. The nRT can switch between two modes of firing: an oscillatory pattern (associated with the generation of sleep spindles), or single spikes (tonic firing during wakefulness). These two firing modes are controlled by the activity of the thalamocortical circuit and by the low-threshold T-type calcium channels in the VBN, which are in turn affected by both GABA_A and GABA_B receptors. [2] The mechanism by which these calcium channels function is explained in more detail in Chapter 1, Figure 5. Alterations in any of these domains affecting normal thalamocortical rhythms can contribute to the pathophysiology of TASs [3].

Patient background

Several studies have identified multiple families that carry the P11S mutation. Tanaka et al. (2008) identified the presence of P11S in 4 of 48 families with CAE residing in Central America [6] (Figure 1). In one family, M120, four members of the family had both CAE and carried P11S. 630 healthy controls from Mexico and Honduras were screened for the mutation but it was not found. In one family, HMO10, the father carried the mutation but did not have an epilepsy phenotype; however, the paternal grandfather (unable to be sequenced) had a CAE diagnosis. [6] This information indicates that P11S may be considered a rare variant that is potentially disease-causing.

Lachance-Touchette et al. (2010) screened 183 French-Canadians with GGE, including 88 persons with CAE, for SNPs in *GABRB3*. Nine SNPs were found, five of which were in patients with CAE, including P11S (Figure 2). The mutation was present in three members of one family that also have seizures, as well as one unaffected individual (as of age 14). One of the 378 control individuals in this study was found to harbor P11S. [5]

Kang and Barnes (2013) reported 17 families with ASD that also carried P11S (1.47% of families tested) (Figure 3). Five individuals with P11S also had seizures and varying degrees of ASD traits. No family members without the mutation had seizures. [8]

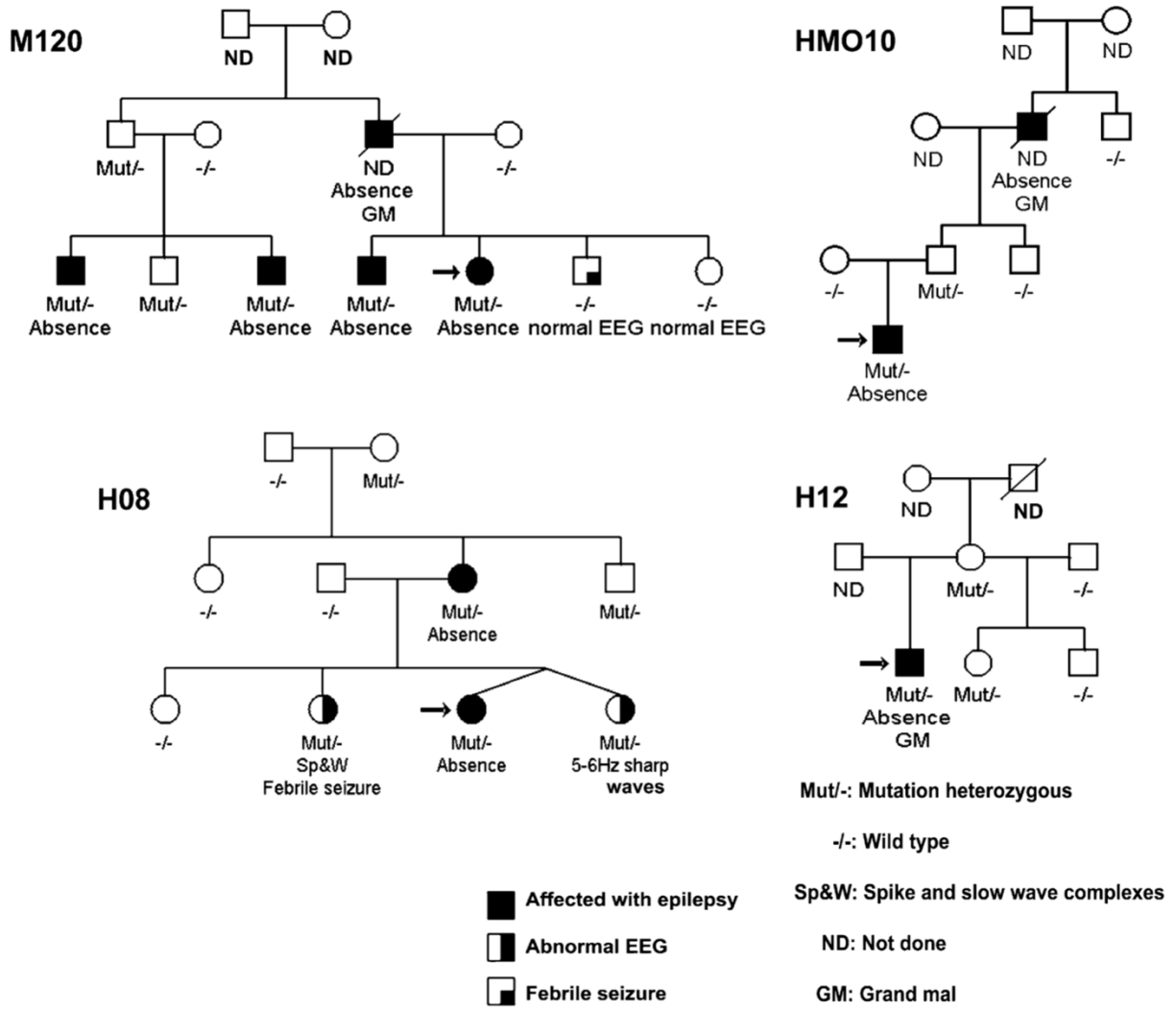


Figure 1: P11S was found in four families with CAE in Central America.

Eight individuals were found to have both TASs and P11S. Figure adapted from Tanaka et al. 2008 [6].

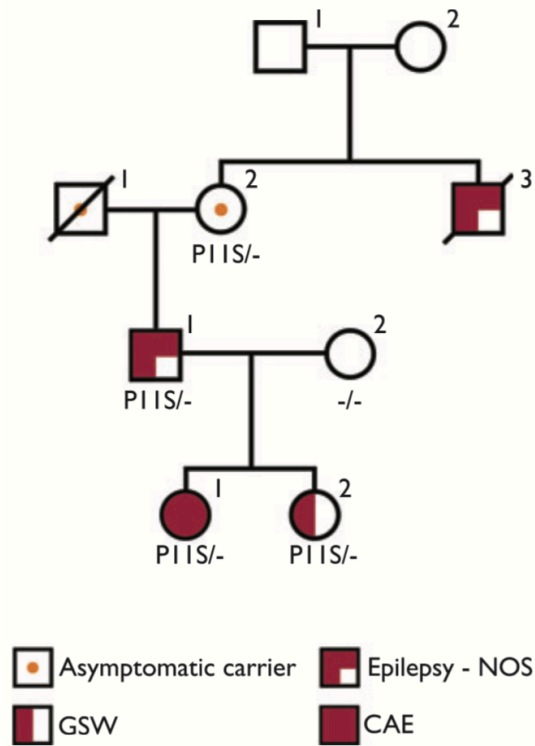


Figure 2: P11S is found in a French-Canadian family with a history of CAE.

Legend: GSW = generalized spike-and-wave discharges. IGE = idiopathic generalized epilepsy (now known as GGE). NOS = not otherwise specified. Figure adapted from Lachance-Touchette et al. (2010) [5].

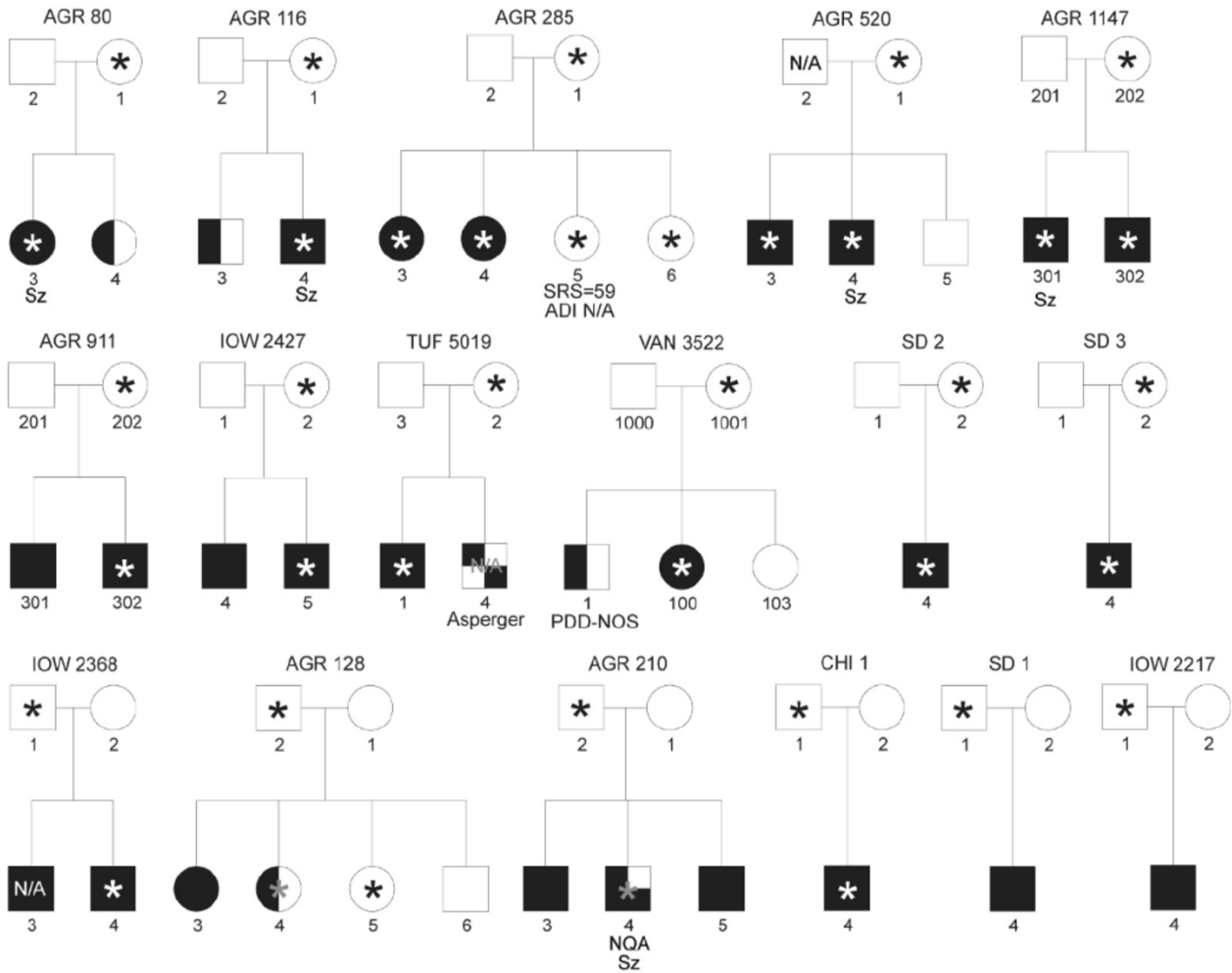


Figure 3: P11S was found in 17 families with ASD.

Five individuals were found to have varying degrees of ASD characteristics, seizures, and the P11S mutation. Legend: Asterisks: individuals carrying P11S. N/A: individuals for whom DNA was not available. Filled in black and half-filled black: individuals who meet varying criteria for ASD. Unfilled: ASD or seizure status is considered unknown. SRS scores: individuals did not meet ASD criteria but a social responsiveness scale (SRS) value is given if available (60-75 = moderate to mild for ASD, 55-59 = “high functioning” ASD). SZ = 2: individuals with definite seizures. SZ = 1: individuals with suspected seizures. Figure adapted from Kang and Barnes (2013) [8].

Materials and methods

See Chapter 2 for more information on materials and methods. Only information specific to this chapter is present here.

Generation of *Gabrb3*^{+/*P11S*} knock-in mice

The *Gabrb3*^{+/*P11S*} knock-in mice were generated in a mixed DBA/2JxC57BL/6J background in collaboration with the Vanderbilt Transgenic Mouse/Embryonic Stem Cell Shared Resource by using CRISPR/Cas9 technology. Potential gRNAs targeting the P11S allele were screened by using the program developed in the Zhang laboratory (zlab.bio/guide-design-resources). To avoid re-cutting by Cas9 after editing, a gRNA (gAGGCCCTGCTGCTGCCAATC) targeting the *Gabrb3* c.C31T, p.P11S site (cleavage site was 2 bp away from the intended KI site) with a good quality score was selected. The double strand oligonucleotides encoding the gRNA were cloned into the pX330 vector, and the resulting vector was co-microinjected (5 ng/ul) into mouse zygotes at the pronuclei stage with a 187 nucleotides homology directed repair template (10 ng/ul) with the C31T mutation in the middle. The injected zygotes were cultured until the blastocyst stage (3.5 days). Thereafter, 15 – 25 blastocysts were transferred into the uterus of pseudo pregnant females at 2.5 days post conception. Three out of 22 live birth mice containing mixed mutations were identified by PCR-sequencing from their tail DNAs. These founders were backcrossed with C57B6 mice to screen for germline transmitted mutations.

The germline transmitted mutations were identified by tail DNA PCR/sequencing. The heterozygous mouse with a *GABRB3* (c.C31T, p.P11S) mutation was named the *Gabrb3*^{+/*P11S*} KI

mouse. The whole-genome search for sequences similar to the guide target sequence showed there were 222 possible off-target sites with at least 2 mismatches and among them only five off-target sites located outside of the seed region (the 12 bp to the PAM) with two to four mismatches (<http://crispor.tefor.net/crispor>). These data strongly suggested the presence of a very low off-target possibility. Nonetheless, these mice were back-crossed with C57BL/6J mice for 12 generations to breed out possible off-target mutations.

Published *in vitro* data

Several labs including our own have explored the impact that P11S has on $\beta 3$ biochemistry and GABAergic function. Using a cell-free *in vitro* translation and translocation system, preproteins (still containing the signal peptide) of the same size were translated from both wild-type and mutant cRNA. Both wild type and mutant signal peptides were determined to appropriately orient towards the plasma membrane indicating that P11S did not disrupt the plasma membrane signal. Interestingly, even though P11S was not predicted to affect N-glycosylation, P11S was observed to result in a hyper-glycosylated protein. This is important because N-glycosylation is highly conserved and is essential in processes such as modifying protein folding, transport, and cell-surface trafficking. Glycosylation of the $\beta 3$ subunit is known to be critical for protein maturation and overall GABA_A receptor trafficking from the endoplasmic reticulum to the cell surface. [6] Hyper-glycosylation could therefore contribute to abnormal processing or assembly of GABA_A receptors and contribute to CAE etiology.

HEK293T cells were transfected with either wild type $\beta 3$ or $\beta 3$ (P11S), and the assembly partners $\alpha 1$ and $\gamma 2$ subunits. When a saturating concentration of GABA was applied (1 mM, 4 seconds), receptors containing $\beta 3$ (P11S) subunits had reduced peak amplitude (Figure 5A) and mean current density (Figure 5B). [6]

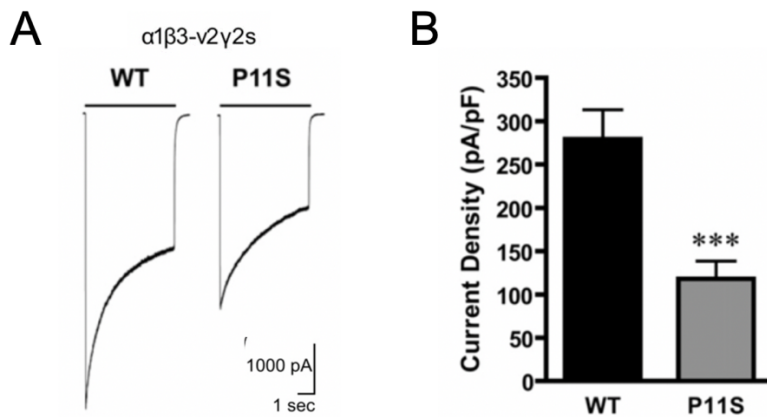


Figure 5: P11S reduced peak current amplitude and current density in HEK cells.

1 mM GABA was applied to transfected HEK cells for whole-cell recording. Figure adapted from Tanaka et al. (2008) [6].

Seizure phenotype of the P11S KI mouse

The *GABRB3* (c.C31T, p.P11S) mutation has been shown to be associated with CAE and ASD [6, 13], and we sought to determine if the *Gabrb3*^{+P11S} KI mouse reflected these disorders. We first used synchronized video-EEG analyses and observed that *Gabrb3*^{+P11S} KI mice had generalized TASs. The TASs were associated with ictal high-amplitude 5-7 Hz SWDs and were time locked to sudden behavioral arrest that lasted from a few seconds to several minutes (Figure 6). We also observed infrequent myoclonic seizures, which were associated with sudden, brief generalized muscle contractions accompanied by a single, high-amplitude sharp wave on EEG. Overall, TASs were the most prominent seizure type seen in *Gabrb3*^{+P11S} KI mice. 24 hours of video-EEG were analyzed for TASs in both wild-type and KI mice. KI mice had TASs more

often than wild-type mice, which are known to have rare, brief TASs [17] (Figure 7A). TASs in KI mice were also significantly longer than in wild-type mice (Figure 7B). These results clearly demonstrated that the *GABRB3*(c.C31T, p.P11S) mutation caused a robust TAS phenotype indicative of CAE in *Gabrb3*^{+/*P11S*} KI mice.

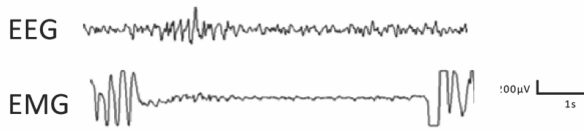


Figure 6: *Gabrb3*^{+/*P11S*} mice had frequent TASs.

A sample TAS in a KI mouse is shown. Video-EEG data are still being analyzed for information such as peak spectral density.

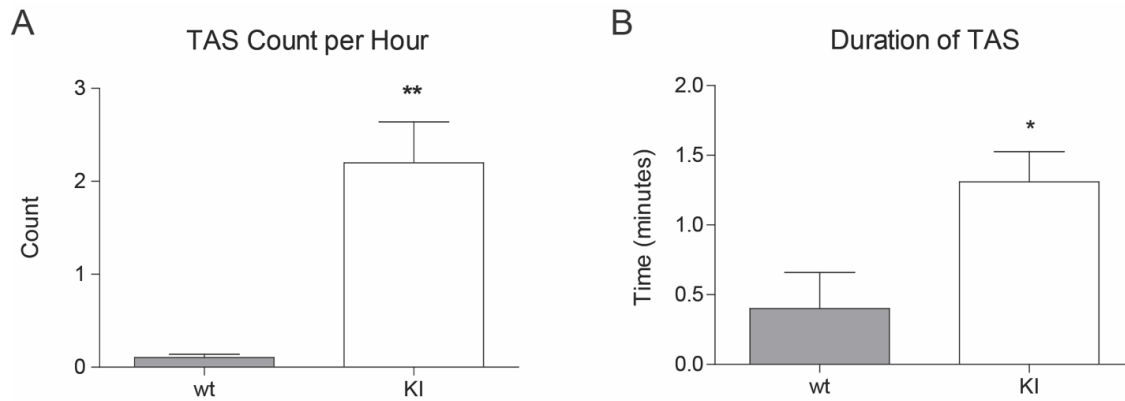


Figure 7: *Gabrb3*^{+/*P11S*} mice had more TASs per hour as well as longer TASs than wild type.

TAS were counted over a 24-hour window. **A)** the number of TASs observed in both wt and KI mice plotted per hour. **B)** The average duration of TASs for wt and KI. Wt n = 6, KI n = 11. P200, males and females. Data are still being collected and analyzed.

Behavioral phenotype of mouse

The P11S mutation specifically has been associated with autism [13], and patients with CAE often experience disrupted development or behavioral and cognitive comorbidities including ASD, mild cognitive impairment, linguistic difficulties, attention deficit hyperactivity disorder (ADHD), and anxiety [1-3]. We therefore assessed *Gabrb3^{+P11S}* mice for social deficits (a hallmark diagnostic criterion in ASD [18]), cognitive impairment, hyperactivity (a hallmark diagnostic criterion in ADHD [18]), and anxiety. All tests were performed on every mouse in the following order: elevated zero maze (EZM), locomotor activity chambers, 3 chamber socialization test (3CST), and Barnes maze. Mice were 6-8 months old at the time of behavior testing, and male and female mice were approximately equally represented. See Chapter 2 for details on each test.

***Gabrb3^{+P11S}* mice displayed abnormal social preferences**

We performed the 3CST to assess social preference and observed abnormal socialization in *Gabrb3^{+P11S}* mice compared to wild type littermates. In stage 2 of the 3CST, genotype did not have an effect on variance overall, and *Gabrb3^{+P11S}* mice spent a similar amount of time investigating both targets as wild type mice did (Figure 8A). However, *Gabrb3^{+P11S}* mice did not have the same preference for socialization over novel object exploration as wild type mice did, and *Gabrb3^{+P11S}* mice spent both less time investigating the novel mouse and more time investigating the novel object than wild type littermates did (Figure 8B).

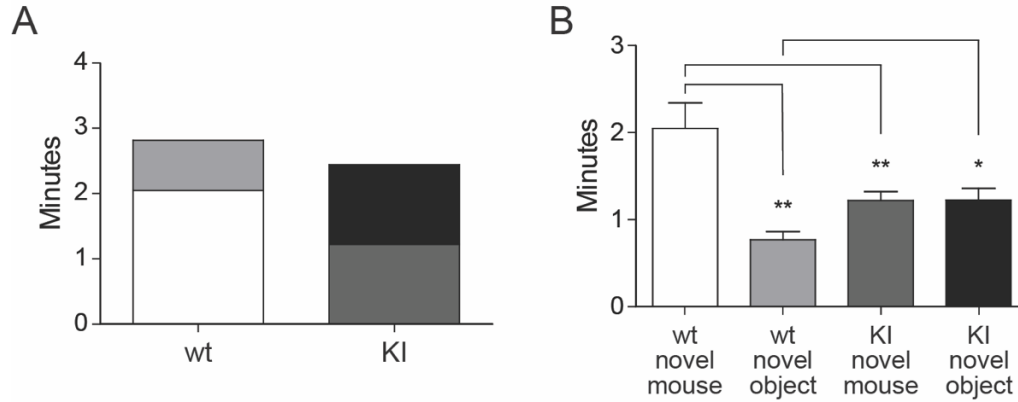


Figure 8: Stage 2 of the 3CST: *Gabrb3*^{+P11S} mice had mild social deficits.

Not shown is Stage 1, a 10-minute familiarization stage for the test mouse to acclimate to the set up. Stage 2 of the 3CST was a 10-minute trial in which subject mice had two socialization options: 1) an empty inverted pencil cup in one side chamber, or 2) an inverted pencil cup containing a novel age-matched female mouse in the other side chamber. **A**) Two-way ANOVA was not significant for a genotype effect (interaction $F_{1,46} = 7.452$, $p = 0.0002$ ###; genotype $F_{1,46} = 1.336$, $p = 0.2537$ ns. Group means – novel mouse: wt 2.050 min, KI 1.219 min; novel object: wt 0.7675 min, KI 1.226; total exploration: wt 3.269 min, KI 2.445 min). **B**) Bonferroni post-tests. Four comparisons were made, however only significant or otherwise relevant results were shown. * $p < 0.0125$, ** $p < 0.01$. $n = 8$ wt, 17 KI.

In stage 3 of the 3CST, genotype had a very significant effect on overall variance and *Gabrb3*^{+P11S} mice spent less time socializing overall (Figure 9A). *Gabrb3*^{+P11S} mice spent less time investigating the novel mouse and did not prefer novel socialization over familiar socialization, as wild type mice do (Figure 9B). Together these data suggest that *Gabrb3*^{+P11S} mice have substantially altered socialization which reflects autistic-like behavior.

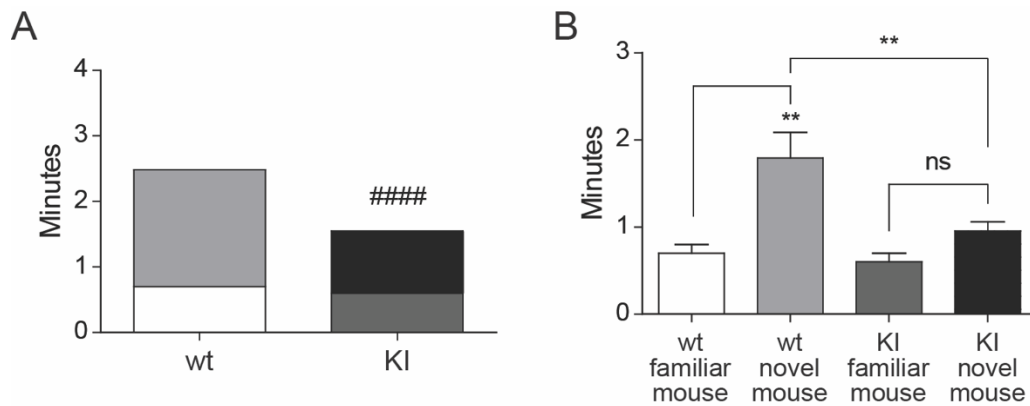


Figure 9: Stage 3 of the 3CST: *Gabrb3*^{+P11S} mice had severe social deficits.

Stage 3 of the 3CST was a 10-minute trial in which test mice had two socialization options: 1) familiar socialization, in which the novel mouse from stage 2 remained where she was, or 2) novel socialization, in which a new novel mouse was placed under the previously empty pencil cup. **A)** Two-way ANOVA was very significant for a genotype effect (interaction $F_{1,46} = 5.986$, $0.0183 \#$; genotype $F_{1,46} = 9.779$, $p < 0.0001$ #####. Group means – familiar mouse: wt 0.6975 min, KI 0.5955 min; novel mouse: wt 1.788 min, KI 0.9523; total exploration: wt 2.4855 min, KI 1.5478 min). **B)** Bonferroni post-tests. Four comparisons were made, however only significant or otherwise relevant results were shown. * $p < 0.0125$, ** $p < 0.01$, *** $p < 0.001$. $n = 8$ wt, 17 KI.

***Gabrb3*^{+/*P11S*} mice did not have additional cognitive deficits.**

Beyond abnormal socialization, we did not observe any additional behavioral abnormalities in *Gabrb3*^{+/*P11S*} mice. We tested for hyperactivity using locomotor activity chambers but found no significant difference in vertical counts (reflective of rearing behavior we have often observed in other hyperactive epilepsy mouse models; Figure 10A) or in the total distance traveled over the 60-minute trial (a more traditional measure of hyperactivity, Figure 10B).

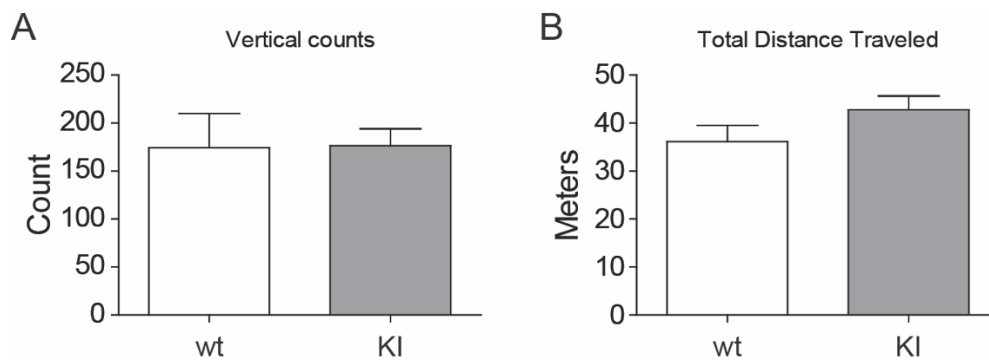


Figure 10: *Gabrb3*^{+/*P11S*} mice were not hyperactive.

Data shown was collected from 60 minutes in the locomotor activity chambers. **A)** Vertical counts, or the number of rearings ($t_{27} = 0.568$, $p = 0.9552$ ns. Group means: wt 174.3 ± 35.70 , $n = 10$; KI 176.3 ± 17.81 , $n = 19$). **B)** Total distance traveled (center and surround included) in the locomotor activity chambers ($t_{26} = 1.397$, $p = 0.1741$ ns. Group means: wt 36.13 ± 3.403 meters, $n = 9$; KI 42.79 ± 2.845 , $n = 19$). Values expressed as mean \pm SEM. Unpaired two-tailed Student's t -test, * $p < 0.05$.

To test for anxiety, we took data from two tests: the locomotor activity chambers and the EZM. When in the locomotor activity chambers, a more anxious mouse will spend more time on the perimeter of the chamber, avoiding the center (called thigmotaxis) [19]. KI mice traveled a similar amount through the center of the chamber (Figure 11A). On the EZM, a more anxious mouse will spend more of its time in the closed arms, avoiding the open arms [20]. KI mice did not have a significant change in the time spent in the open arms of the maze (Figure 11B). Together these data indicated KI mice do not have an anxiety phenotype.

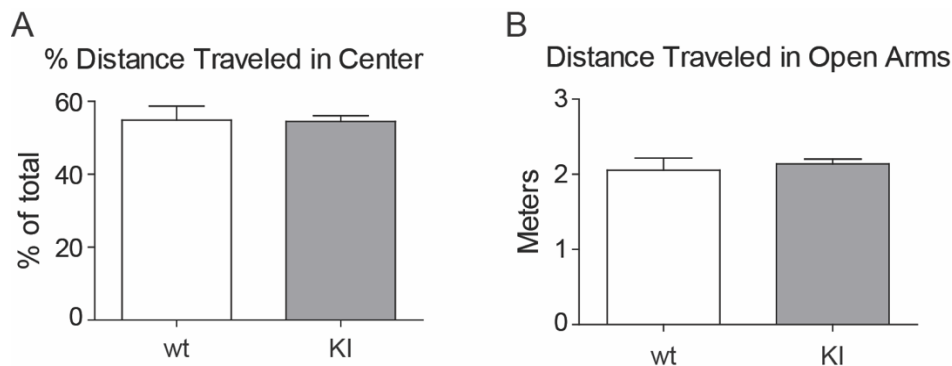


Figure 11: *Gabrb3*^{+/*P11S*} mice did not have elevated anxiety.

KI mice did not display elevated anxiety in either the locomotor activity chambers or the elevated zero maze. **A)** Each subject spent 60 min in the locomotor activity chamber. The chamber was divided into two 50% sections by area: the center, and the surround. Distance traveled within the surround (edge) area was calculated as a percentage of total distance traveled as total distance traveled. ($t_{26} = 0.1132$, $p = 0.9107$ ns. Group means: wt 54.86 ± 3.865 %, $n = 9$; KI 54.47 ± 1.602 %, $n = 19$) **B)** Each subject spent 5 min in the elevated zero maze. ($t_{27} = 0.6099$, $p = 0.5472$ ns. Group means: wt 2.054 ± 0.1628 meters, $n = 9$; KI 2.140 ± 0.06113 , $n = 19$). Values expressed as mean \pm SEM. Unpaired two-tailed Student's t -test, * $p < 0.05$.

Finally, to assess cognitive deficiencies of KI mice, spatial learning and memory were assayed using the Barnes maze. Mice underwent 5 days of learning trials followed by a probe trial on day 5. KI mice did not display a spatial learning deficit in the Barnes maze as measured by the latency to find the target hole (Figure 12A) or the number of errors committed (non-target holes visited) before entering the target hole (Figure 12B). In the memory trial, KI mice spent the same amount of time investigating the target hole area (Figure 13A) and made a similar number of errors (Figure 13B) showing that KI mice do not have a spatial memory deficit.

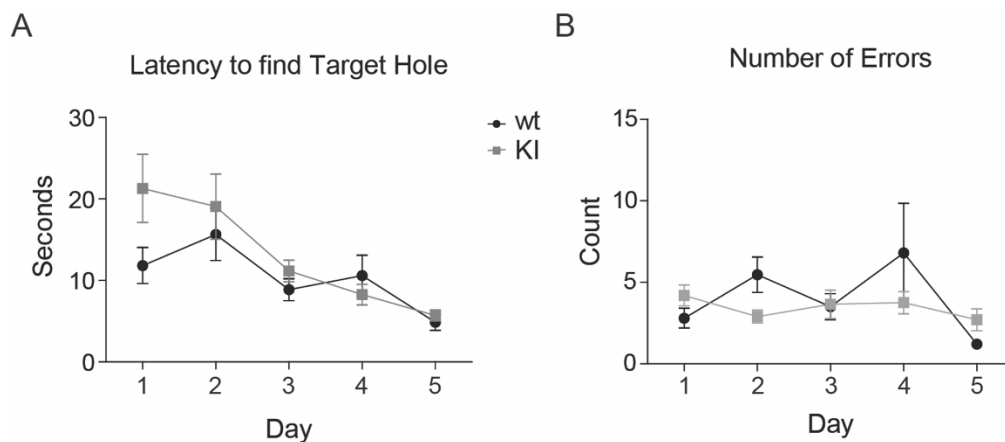


Figure 12: *Gabrb3*^{+/*P11S*} mice did not have spatial learning deficits.

5 days of learning trials depict spatial learning abilities. Each day represents the average across all mice of each genotype with the data point of each mouse being the average of the four trials conducted that day. **A)** The time it takes each animal (latency) to find the target hole for each day was unchanged in KI mice (interaction $F_{4,112} = 1.040$, $p = 0.3901$; genotype main effect $F_{1,112} = 2.461$, $p = 0.1279$ ns). **B)** The number of non-target hole zones entered (errors) was not significantly increased in KI mice (interaction $F_{4,112} = 2535$, $p = 0.8173$; genotype main effect $F_{1,112} = 0.4800$, $p = 0.4941$ ns). Two-way ANOVA for repeated measures: genotype effect $\#p < 0.05$. Bonferroni post-tests: $*p < 0.05$. $n = 10$ wt, 20 KI.

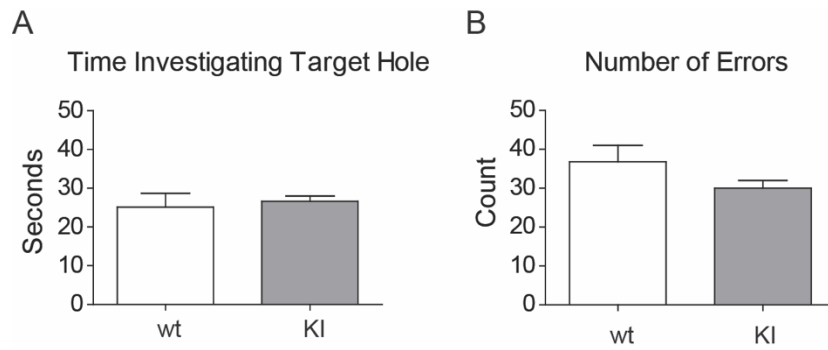


Figure 13: *Gabrb3*^{+/*P11S*} mice did not have impaired spatial memory.

5-minute probe trial for spatial memory performed on day 5 after the learning trials. **A)** Time spent near the target hole was unchanged in KI mice ($t_{28} = 0.4704$, $p = 0.6417$ ns. Group means: wt 25.16 ± 3.524 seconds, $n = 10$; KI 26.63 ± 1.362 seconds, $n = 20$). **B)** The number of errors committed by KI mice was not different from wild-type ($t_{28} = 1.663$, $p = 0.1075$ ns. Group means: wt 36.80 ± 4.203 , $n = 10$; KI 30.00 ± 2.008 , $n = 20$). Values expressed as mean \pm SEM. Unpaired two-tailed Student's t -test, * $p < 0.05$.

Cellular profile in mouse

The results from previous *in vitro* studies suggested that the P11S substitution decreased $\beta 3$ -v2 subunit expression on the cell surface due to impaired intracellular subunit processing [13]. To determine the *in vivo* effects of the mutant $\beta 3$ (P11S) subunits on GABA_A receptor-biogenesis, total and surface proteins from adult mice were blotted for $\alpha 1$, $\beta 3$ and $\gamma 2$ subunits and quantified. The total expression of GABA_A receptor subunits in cortex (Co), hippocampus (Hi), thalamus (Th) and cerebellum (Cb) of KI mice was similar to corresponding regions of wild-type mouse brains (Figure 14A, B). The surface expression of GABA_A receptor subunits was evaluated by using the membrane fraction of whole brain tissue. The results again showed no significant difference between KI and wild-type mice (Figure 14C, D). These results appeared to be consistent with our previous *in vitro* studies in transfected HEK293T cells that showed no differences in surface levels of wild-type and mutant $\beta 3$ subunits. This result was not surprising given the fact that in the *in vivo* experiments, 90% of $\beta 3$ subunit mRNA was the $\beta 3$ -v1 variant [21], and thus most of the *in vitro* subunits were $\beta 3$ -v2 subunits. The small contribution from the mutant $\beta 3$ (P11S) subunit would be difficult to detect. A $\beta 3$ -v2 subunit specific antibody would be helpful for future studies.

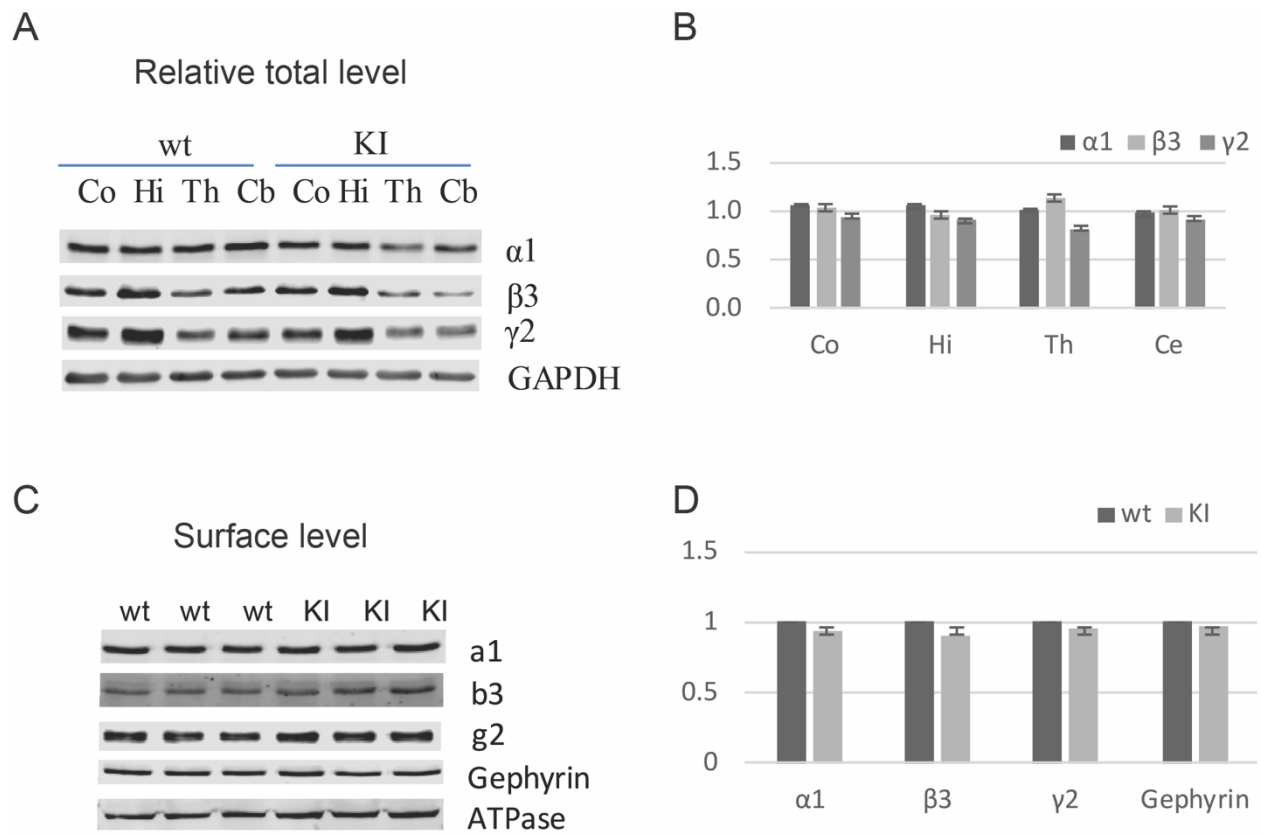


Figure 14: Neither total nor surface expression of GABA_A receptor subunits was changed in *Gabrb3^{+P11S}* mice

The mutant β3(P11S) subunits did not affect expression, surface trafficking, or distribution in synaptosomes of either their own or other GABA_A receptor subunits. **A)** Whole cell lysates from different brain regions [cortex (Co), hippocampus (Hi), thalamus (Th), and cerebellum (Ce)] were collected from KI and wild type littermate mice and subjected to SDS-PAGE and immunoblotted with anti-α1, β3, and γ2 subunit antibodies. GAPDH served as a loading control. **B)** Band intensities of α1, β3, and γ2 subunits were normalized to GAPDH signal and then KI was compared to wild type (n = 3 KI:wt pairs). One-way ANOVA followed by the Dunnett's multiple comparison test was used to determine significance, however no changes were identified. **C)** Plasma membrane proteins from mouse brain were isolated, analyzed by SDS-PAGE and immunoblotted with anti-α1, β3, and γ2 subunit antibodies. Na⁺/K⁺ ATPase served as a loading control, and GAPDH served as cytosolic protein contamination control. **D)** Band intensities of α1, β3, and γ2 subunits were normalized to ATPase signal and then KI bands were compared to wild type bands (n = 3 KI:wt pairs).

Electrophysiology in *ex vivo* slices

***Gabrb3*^{+/*P11S*} mice had reduced mIPSC amplitudes in SS cortex layer V/VI pyramidal neurons**

The thalamocortical circuitry, which includes SS cortical layer V/VI pyramidal neurons, has been suggested to be involved in generalized epilepsy/seizures in several animal models [12, 22, 23]. To characterize GABAergic synaptic transmission in wt and *Gabrb3*^{+/*P11S*} mice, miniature inhibitory postsynaptic currents (mIPSCs), were recorded from cortical layer V/VI pyramidal neurons at a -60 mV holding potential. In wild type mice, mIPSC amplitude was 52.89 ± 4.78 pA, and frequency was 4.51 ± 1.28 Hz (n = 6 neurons, 4 mice) and mIPSCs exhibited fast rising and slow decaying phases (Figure 15A). Compared with mIPSCs from wild type littermates, mIPSCs from het *Gabrb3*^{+/*P11S*} mice showed no difference in amplitudes (52.41 ± 4.17 pA, n = 8 neurons, 4 mice, p = 0.941) (Figure 15B) and a reduction in frequency (2.20 ± 0.34 Hz, n = 8 neurons, 4, mice, p= 0.07), suggesting that mIPSCs in layer VI pyramidal neurons from het *Gabrb3*^{+/*P11S*} mice were reduced. We did not observe a significant difference in mIPSC decay constants between wild type and *Gabrb3*^{+/*P11S*} mice. Thus, it is likely that presynaptic mechanisms are involved in the reductions of mIPSC frequency in het *Gabrb3*^{+/*P11S*} mice.

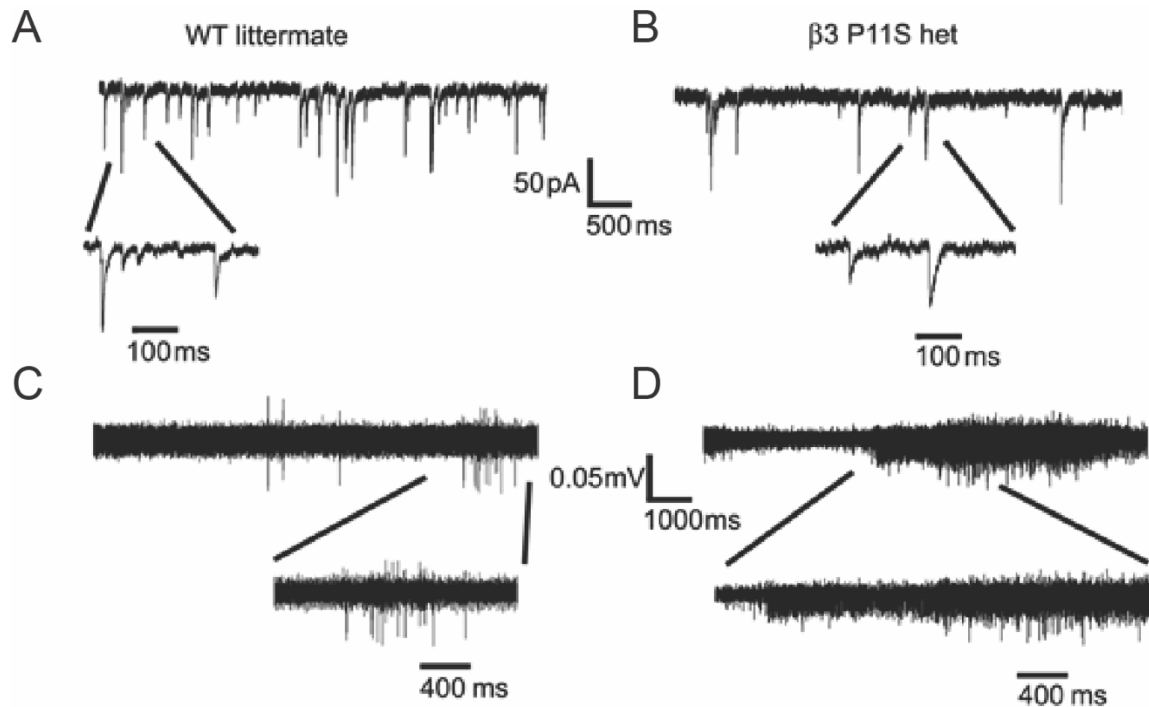


Figure 15: *Gabrb3*^{+/*P11S*} mice had mIPSCs with decreased amplitude and increased spontaneous thalamocortical network oscillations.

A, B) mIPSCs were recorded from SS cortex layer V/VI neurons (voltage-clamped at -60 mV with equal chloride concentration inside and outside cells) in thalamocortical slices from littermate wt and KI mice. Representative extracellular multiple unit recordings from VBn in 32°C slices showing **C)** spontaneous brief thalamocortical bursts in wt mice and **D)** spontaneous prolonged thalamocortical oscillations in KI mice. Scale bars are as indicated. One short burst from a wt and one oscillation from a KI mouse were expanded in each panel to show the multiple spikes in the burst or oscillation. Data are still being collected and analyzed.

Network oscillations in thalamocortical circuitry underlies epilepsy and epileptogenesis in animal models [24]. Thus, we examined ventrobasal nucleus (VBn) multi-unit activity in thalamocortical slices from WT and het *Gabrb3*^{+/*P11S*} mice. The network oscillation exhibits different spike waveforms and amplitude in its multi-unit recordings, suggesting involvement of

multiple types of neurons. In slices from WT mice (32°C), spontaneous, short bursts of multiunit firing were recorded and often these multiunit bursts exhibited similar amplitudes, suggesting that short bursts (0.31 ± 0.18 s, $n = 7$ slices) (Figure 15C) were from the same population of neurons in the corticothalamic circuitry. In contrast, in slices from het *Gabrb3*^{+/*P11S*} mice (32°C), spontaneous long duration multiunit firing of oscillations with different amplitudes (3.53 ± 0.71 s, $n = 11$ slices, t-test $p = 0.002$) (Figure 15D) were recorded, implying that these multiunit oscillations were from different types of neurons in the corticothalamic circuitry and that neuronal loops were involved to generate this network oscillation. All these results indicated that het *Gabrb3*^{+/*P11S*} mice might have more and longer network oscillations in corticothalamic circuitry, which would lead to more cortical hyperactivity/oscillations (seizures/epileptogenesis).

Discussion

The P11S mutation is involved in the pathogenesis of CAE

Mutations in the GABA_A receptor $\beta 3$ subunit have been associated with a variety of disorders including Angelman Syndrome, ASD, insomnia, and CAE [21, 25-27]. Additionally, $\beta 3$ subunit KO mice express absence-like, ethosuximide-sensitive seizures [21]. Here we have demonstrated the importance of the signal peptide of the developmentally regulated $\beta 3$ -V2 subunit splice variant and the role of the P11S mutation in this subunit on the function of the GABA_A receptor and its relationship to the pathogenesis of CAE. GABA_A receptor subunit oligomerization occurs in the ER and is associated with chaperone proteins such as calnexin and

BiP [28, 29]. The fundamental role of the signal peptide in secretory pathway proteins such as GABA_A receptor subunits is direction of the nascent peptide to translocation into the endoplasmic reticulum via the signal recognition particle [30].

Functional analysis of the P11S mutation in the signal peptide of the β 3-V2 subunit of the GABA_A receptor in CAE demonstrated reduced function of α 1 β 3-v2(P11S) γ 2S receptors [6]. While it was unlikely that the mutation altered the signal peptide cleavage point, it may have altered the efficiency of translocation into the ER or the efficiency of cleavage by signal peptidase, which might impair folding and ultimately oligomerization of the GABA_A receptor. The mutation may also alter the function of the receptor itself. Such findings contribute to the growing body of evidence implicating genetic alterations of ion channels in GGEs. Furthermore, they demonstrate an important role of the signal peptide of a developmentally regulated splice variant of the β 3 subunit of the GABA_A receptor in childhood epilepsy.

The *GABRB3*^{+P11S} mouse is strongly associated with ASD since it has been found in six families that also have seizures or epilepsy, and ASD is a common comorbidity of CAE. CAE patients often suffer from additional comorbidities that are intractable and contribute to poor outcomes, such as ADHD, cognitive impairment, and anxiety [1-3, 31]. Through behavioral testing, we found that the *Gabrb3*^{+P11S} mice display substantial social deficits, a hallmark feature of ASD [18], but the other comorbidities for which we tested were not present (spatial learning and memory, hyperactivity, anxiety). While CAE is generally considered a “benign” epilepsy, there is a group of patients for whom seizures and/or neurobehavioral conditions persist throughout life, contributing to poor outcomes for these patients [1, 31]. Only 23% of children with CAE receive any intervention targeted at comorbidities [32], indicating a need for improved understanding and characterization of these deficits. Because cognitive abnormalities variably

effect the patient population with the severity of these impairments related to the severity of the disorder in each individual, we suggest that the presence of only a severe socialization deficit and no other potentially CAE-associated comorbidities still make this mouse a strong model for CAE and reflective of the *GABRB3*^{+P11S} patient population.

Bibliography

1. Tenney, J.R. and T.A. Glauser, *The current state of absence epilepsy: can we have your attention?* *Epilepsy Curr*, 2013. **13**(3): p. 135-40.
2. Albuja, A.C. and P.B. Murphy, *Absence Seizure*, in *StatPearls*. 2020: Treasure Island (FL).
3. Kessler, S.K. and E. McGinnis, *A Practical Guide to Treatment of Childhood Absence Epilepsy*. *Paediatr Drugs*, 2019. **21**(1): p. 15-24.
4. Sadleir, L.G., et al., *Electroclinical features of absence seizures in childhood absence epilepsy*. *Neurology*, 2006. **67**(3): p. 413-8.
5. Lachance-Touchette, P., et al., *Screening of GABRB3 in French-Canadian families with idiopathic generalized epilepsy*. *Epilepsia*, 2010. **51**(9): p. 1894-7.
6. Tanaka, M., et al., *Hyperglycosylation and reduced GABA currents of mutated GABRB3 polypeptide in remitting childhood absence epilepsy*. *Am J Hum Genet*, 2008. **82**(6): p. 1249-61.
7. Mullen, S.A., S.F. Berkovic, and I.G. Commission, *Genetic generalized epilepsies*. *Epilepsia*, 2018. **59**(6): p. 1148-1153.
8. Kang, J.Q. and G. Barnes, *A common susceptibility factor of both autism and epilepsy: functional deficiency of GABA A receptors*. *J Autism Dev Disord*, 2013. **43**(1): p. 68-79.
9. Sundelin, H.E., et al., *Autism and epilepsy: A population-based nationwide cohort study*. *Neurology*, 2016. **87**(2): p. 192-7.
10. Loughman, A., N.A. Bendrups, and W.J. D'Souza, *A Systematic Review of Psychiatric and Psychosocial Comorbidities of Genetic Generalised Epilepsies (GGE)*. *Neuropsychol Rev*, 2016. **26**(4): p. 364-375.
11. Mazarati, A.M., M.L. Lewis, and Q.J. Pittman, *Neurobehavioral comorbidities of epilepsy: Role of inflammation*. *Epilepsia*, 2017. **58 Suppl 3**: p. 48-56.
12. Beenhakker, M.P. and J.R. Huguenard, *Neurons that fire together also conspire together: is normal sleep circuitry hijacked to generate epilepsy?* *Neuron*, 2009. **62**(5): p. 612-32.
13. Delahanty, R.J., et al., *Maternal transmission of a rare GABRB3 signal peptide variant is associated with autism*. *Mol Psychiatry*, 2011. **16**(1): p. 86-96.
14. Tanaka, M., et al., *GABRB3, Epilepsy, and Neurodevelopment*, in *Jasper's Basic Mechanisms of the Epilepsies*, th, et al., Editors. 2012: Bethesda (MD).

15. Kirkness, E.F. and C.M. Fraser, *A strong promoter element is located between alternative exons of a gene encoding the human gamma-aminobutyric acid-type A receptor beta 3 subunit (GABRB3)*. J Biol Chem, 1993. **268**(6): p. 4420-8.
16. Chen, C.H., et al., *Genetic analysis of GABRB3 as a candidate gene of autism spectrum disorders*. Mol Autism, 2014. **5**: p. 36.
17. Letts, V.A., B.J. Beyer, and W.N. Frankel, *Hidden in plain sight: spike-wave discharges in mouse inbred strains*. Genes Brain Behav, 2014. **13**(6): p. 519-26.
18. Association, A.P., *Diagnostic and statistical manual of mental disorders (5th ed.)*. 2013, Arlington, VA: American Psychiatric Publishing.
19. Simon, P., R. Dupuis, and J. Costentin, *Thigmotaxis as an index of anxiety in mice. Influence of dopaminergic transmissions*. Behav Brain Res, 1994. **61**(1): p. 59-64.
20. Shepherd, J.K., et al., *Behavioural and pharmacological characterisation of the elevated "zero-maze" as an animal model of anxiety*. Psychopharmacology (Berl), 1994. **116**(1): p. 56-64.
21. DeLorey, T.M., et al., *Mice lacking the beta3 subunit of the GABAA receptor have the epilepsy phenotype and many of the behavioral characteristics of Angelman syndrome*. J Neurosci, 1998. **18**(20): p. 8505-14.
22. McCormick, D.A. and D. Contreras, *On the cellular and network bases of epileptic seizures*. Annu Rev Physiol, 2001. **63**: p. 815-46.
23. Kang, J.Q., et al., *The human epilepsy mutation GABRG2(Q390X) causes chronic subunit accumulation and neurodegeneration*. Nat Neurosci, 2015. **18**(7): p. 988-96.
24. Huguenard, J.R. and D.A. Prince, *Intrathalamic rhythmicity studied in vitro: nominal T-current modulation causes robust antioscillatory effects*. J Neurosci, 1994. **14**(9): p. 5485-502.
25. Liljelund, P., et al., *GABAA receptor beta3 subunit gene-deficient heterozygous mice show parent-of-origin and gender-related differences in beta3 subunit levels, EEG, and behavior*. Brain Res Dev Brain Res, 2005. **157**(2): p. 150-61.
26. Buhr, A., et al., *Functional characterization of the new human GABA(A) receptor mutation beta3(R192H)*. Hum Genet, 2002. **111**(2): p. 154-60.
27. Handforth, A., et al., *Pharmacologic evidence for abnormal thalamocortical functioning in GABA receptor beta3 subunit-deficient mice, a model of Angelman syndrome*. Epilepsia, 2005. **46**(12): p. 1860-70.
28. Connolly, C.N., et al., *Assembly and cell surface expression of heteromeric and homomeric gamma-aminobutyric acid type A receptors*. J Biol Chem, 1996. **271**(1): p. 89-96.

29. Gelman, M.S., et al., *Role of the endoplasmic reticulum chaperone calnexin in subunit folding and assembly of nicotinic acetylcholine receptors*. J Biol Chem, 1995. **270**(25): p. 15085-92.
30. Stevens, F.J. and Y. Argon, *Protein folding in the ER*. Semin Cell Dev Biol, 1999. **10**(5): p. 443-54.
31. Barnes, G.N. and J.M. Paolicchi, *Neuropsychiatric comorbidities in childhood absence epilepsy*. Nat Clin Pract Neurol, 2008. **4**(12): p. 650-1.
32. Glynn, P., et al., *Feasibility of a Mobile Cognitive Intervention in Childhood Absence Epilepsy*. Front Hum Neurosci, 2016. **10**: p. 575.

Chapter 5

Conclusions and Future Directions

Summary of findings

Chapters 3 and 4 present the stories of two mutations in the gene *GABRB3*, which encodes the $\beta 3$ subunit of the GABA_A receptor. These mutations lead to two different mutant proteins associated with two different epilepsy syndromes: D120N, associated with Lennox-Gastaut syndrome (LGS), and P11S, associated with childhood absence epilepsy (CAE). D120N is located in loop A of the GABA_A receptor $\beta 3$ subunit, which forms part of the GABA binding pocket at the interface of the $\beta 3$ and alpha subunits. P11S is located in the signal peptide, which is important for transcription factor binding; however, it is not incorporated into the mature subunit since it is cleaved to form the mature protein. Knock-in mice containing each of the mutations were generated, yielding the *Gabrb3*^{+/*D120N*} and *Gabrb3*^{+/*P11S*} mice. Both strains were assessed for their validity in replicating the seizure, cognitive, and behavioral phenotypes associated with each epilepsy syndrome.

LGS is an epileptic encephalopathy [1] that is characterized by childhood onset of persistent and difficult to treat seizures, including atypical absence, tonic, clonic, myoclonic, atonic, and generalized tonic-clonic seizures [1-4]. Additionally, patients experience cognitive and behavioral abnormalities including moderate to severe intellectual disability, hyperactivity or attention deficit hyperactive disorder (ADHD), autism spectrum disorder (ASD), and mood

instability [5]. We characterized spontaneous atypical absence, myoclonic, tonic, atonic, and generalized tonic clonic seizures in the *Gabrb3*^{+D120N} mice, as well as spatial learning and memory deficits, hyperactivity, social deficits, and elevated anxiety. We did not observe any deficits in expression or subcellular localization of mutant β 3(D120N) subunits. Slices from *Gabrb3*^{+D120N} mice did show reduced miniature postsynaptic current (mIPSC) amplitudes and prolonged thalamocortical oscillations. Our previous *in vitro* data indicated that GABA_A receptors containing β 3(D120N) subunits were not saturated by 1 mM GABA as wild-type receptors were, but rather they required a 10-fold higher concentration of GABA to produce currents with amplitudes similar to those of wild-type receptors [6]. Finally, *Gabrb3*^{+D120N} mice had variable responses to traditional anti-epileptic drugs (AEDs), but the newly approved cannabinoid therapy was quite successful.

CAE, a genetic generalized epilepsy [7, 8], also has childhood onset. Patients experience multiple daily typical absence seizures (TASs) [9, 10] and some have GTCSs later in life [11]. Development is not usually impaired by onset of CAE [12], but patients experience behavioral, psychiatric, language, and cognitive deficits including poor executive function, attention deficits, anxiety, ADHD, ASD, depression, social dysfunction, and poor verbal skills [11, 13]. Direct socioeconomic impacts of CAE include under employment, unplanned pregnancy, and poor school performance [3]. We documented frequent TASs and social dysfunction in *Gabrb3*^{+P11S} mice. Interestingly, the β 3 subunit P11S mutation has been identified also in many families with ASD, which highlights the importance of the observed social dysfunction phenotype. The β 3 subunit P11S mutation has been shown to increase subunit glycosylation *in vitro*, and glycosylation state is critical for protein maturation and overall GABA_A receptor trafficking from the endoplasmic reticulum to the cell surface [14].

We did not observe any changes in trafficking of GABA_A receptor subunits in *Gabrb3*^{+P11S} mice; however, slices from these mice showed decreased mIPSC amplitudes and spontaneous thalamocortical oscillations.

The role of GABA_A receptor β 3 subunits

The GABA_A receptor β 3 subunit is abundantly expressed in the developing brain, and disruptions in *GABRB3* have been associated with epilepsy and developmental abnormalities such as ASD [15, 16]. For several years it has been known that the β 3 subunit is important for thalamocortical circuitry due to work done using the *Gabrb3* knock-out mouse. Mice lacking one copy of *Gabrb3* showed frequent absence-like behavioral arrests, which were successfully treated with ethosuximide [14], a drug commonly used to treat absence seizures in humans [1]. Spike wave discharges (SWDs), an important feature of absence seizures, have been associated with abnormal synchronous firing in thalamocortical circuitry [9, 14, 17], indicating that β 3 subunits play an important role in this circuitry. Thalamocortical oscillatory synchrony was increased in *Gabrb3* null mice, which indicated that β 3 subunit-containing receptors may function to de-synchronize this circuit [14]. Thalamocortical circuitry is discussed in more detail in Chapter 1 (*Typical absence models*) and is shown here as a component of Figure 1. Rodent models of TAS have indicated that SWDs emanate from the cortex and thalamus but do not involve the hippocampus or temporal lobe [9, 17], likely initiating in the somatosensory cortex and propagating to the ventrobasal nucleus (VBn) of the thalamus [9], with the nucleus reticularis (nRT) playing a role in synchrony [18]. Importantly, while β 3 subunit expression is high during brain development throughout the brain, especially in the cerebral cortex,

amygdala, olfactory bulb, nRT, and hippocampus [19], $\beta 3$ subunit expression in adulthood remains high in the nRT [20] and the hippocampus and is moderate in the cortex [21]. It is possible that mutations in $\beta 3$ subunits may affect circuitry formation in all regions where $\beta 3$ subunits are expressed during development, and these disruptions may continue to drive disease processes in adulthood by $\beta 3$ subunit expression remaining high in key regions involved in epilepsy pathology.

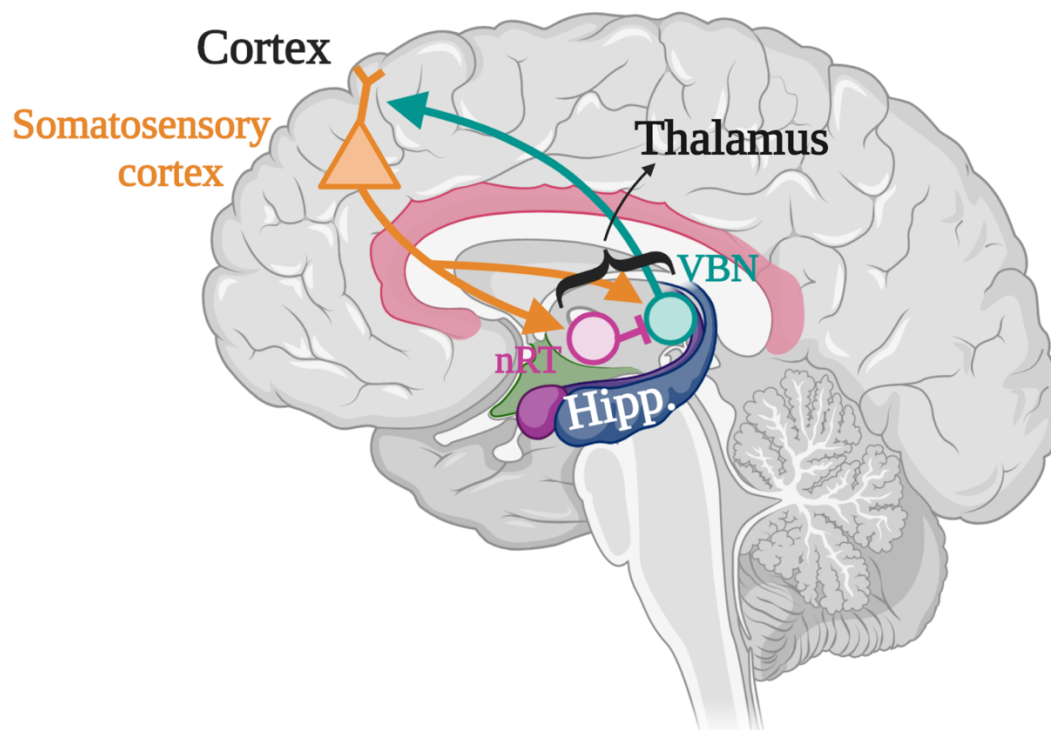


Figure 1: What role does the hippocampus play in thalamocortical circuitry?

An expansion of Figure 5 (Chapter 1). Cortical pyramidal neurons (orange) project to the thalamus, synapsing on both nRT (pink) and VBn (green). GABAergic neurons in nRT send inhibitory projections to VBn. Normal firing patterns are disrupted in this circuit by mutations in $\beta 3$ subunits, resulting in hypersynchrony and TASSs. It remains unclear how the hippocampus (Hipp., blue structure) is related to this circuit in AASs.

While the $\beta 3$ subunit D120N mutation was associated with the severe disorder LGS, the $\beta 3$ subunit P11S mutation was associated with the less severe disorders CAE and ASD. The $\beta 3$ subunit P11S mutation was expressed only in variant 2 of the $\beta 3$ subunit while the $\beta 3$ subunit D120N mutation was present in both splice variants. The $\beta 3$ subunit, particularly variant 2, is expressed highly early and throughout development in many brain regions [19, 22]. However, in adulthood, variant 2 expression declines relative to variant 1 [21], and $\beta 3$ subunit expression is decreased overall except in a few key regions [20, 21]. McTague et al. (2016) discussed the concept of phenotypic heterogeneity in epilepsy, in which different mutations in one gene can result in different epilepsy syndromes [4]. Here this is evident with *GABRB3*, in which $\beta 3$ subunit mutation P11S results in CAE and the $\beta 3$ subunit D120N mutations results in Lennox-Gastaut syndrome. These two mutations represent two very different points on the spectrum of severity of disease-causing mutations in *GABRB3*.

Thalamocortical circuitry and the hippocampus

Many studies have examined the roles of the thalamus and cortex in generating SWD and TAsSs. Much less is known about atypical absence seizures (AAsSs). AAsSs are frequently associated with significant cognitive and neurodevelopmental deficits [9, 17] and are difficult to control even with drugs commonly effective at reducing TAsSs [9]. There are several reasons to suspect that involvement of the hippocampus may be responsible for some of the differences between AAsSs and TAsSs. First, at least one model of AAsSs reported disruptions in hippocampal synaptic plasticity [23]. Additionally, direct application of AY-9944, a chemical used to induce AAsSs in rats (see Chapter 1, *Atypical absence seizure models*), to brain slices

increases membrane excitability in hippocampal neurons [24]. Finally, we observed deficits in spatial learning and memory in *Gabrb3*^{+/*D120N*} mice. These processes, and the Barnes maze specifically, have been shown to assay hippocampal processing of learning and memory [25]. Importantly, we still observed frequent and prolonged thalamocortical oscillations in *Gabrb3*^{+/*D120N*} mice indicating that this circuitry is still highly relevant for AASs.

While the *Gabrb3* knock-out mouse has been thoroughly studied and serves as a useful comparison for the *Gabrb3*^{+/*D120N*} mouse, we generated a *Gabrb3*^{+/*var2*} heterozygous $\beta 3$ subunit splice variant 2 (var 2) knock-out mouse to study the effects of removing $\beta 3$ splice variant 2 for comparison to the *Gabrb3*^{+/*P11S*} mouse. Variants 1 and 2 are differentially expressed both by location and over time [21], indicating that they may play unique roles in development, synapse formation, or circuitry. The *Gabrb3*^{+/*var2*} mouse will allow us to determine which phenotypes of the *Gabrb3*^{+/*P11S*} mouse are a result of the mutation and how these differ from loss of variant 2.

Future directions: viral gene therapy

Further development of traditional AEDs is unlikely to have great impact on LGS patients or on those CAE patients that remain afflicted by seizures and cognitive dysfunction such as ASD, particularly if the disorder is caused by a mutation. There does appear to be a promising future for cannabinoid therapy as is discussed in detail in Chapter 3, *Treatments used in LGS*. However, as drug therapies have associated side effects and often only remain effective for a short period of time [1], alternative approaches may be preferred. Gene therapy entails manipulating DNA, which could be used for the purpose of repairing a disease-causing

genetic alteration such as a mutation [26]. Viral gene therapy has grown into a promising field as safety, vector engineering, and delivery have all improved [27]. Additionally, the clustered regularly interspaced short palindromic repeats (CRISPR) and CRISPR associated nuclease9 (Cas9) system allows for even more precisely targeted gene therapy [26]. While gene therapy would not repair circuitry that had developed abnormally, it would enable replacing malfunctioning receptors such as those seen in the *Gabrb3^{+D120N}* and *Gabrb3^{+P11S}* mice with fully functioning receptors.

Introduction to lentivirus (LV) and adeno-associated virus (AAV)

Gene therapy is the process of delivering DNA encoding a gene of interest into a cell for the purpose of treating a disease, such as those caused by genetic mutations [28]. Viral gene therapy was approved for human use in the United States in 2017 for the treatment of acute lymphoblastic leukemia [28]. There have been over 3000 clinical trials using gene therapy, about 70% of which used viruses [27]. While there were initially some setbacks regarding the safety of viral gene therapy in which some patients developed leukemia [27], safety has greatly improved. Animal models of several neurological disorders including Huntington's disease, Rett syndrome, and Parkinson's disease have all shown promise with viral gene therapy [27], indicating that success in treating other neurological diseases may be possible. There are several viruses that are viable as candidates for human viral gene therapy, chiefly lentivirus (LV) and adeno-associated virus (AAV). The characteristics of these viruses will first be discussed, and then several strategies for using viruses in the LGS and CAE knock-in mice will be proposed. Some traits of each virus family may be either an advantage or a disadvantage depending on the research goals.

AAV offers several advantages, which led to their initial popularity. First, AAV is easy to handle and does not require BSL-2 safety precautions as it is not a retrovirus [29]. Retroviruses like LV were derived from the human immunodeficiency virus (HIV) and have a genome made of RNA, which is converted to DNA after entering the cell [28]. AAV has a DNA genome and offers a low risk of pathogenicity and toxicity in the host, yet can provide long-term expression of the foreign DNA [27, 30]. AAV has a small diameter, around 20 nm, which enables it to diffuse relatively far after injection [30]. Both afferent and efferent neurons are infected in the region where AAV is injected, although a novel AAV variant, rAAV2-retro vector, greatly increases the rate of retrograde infection (infection along the axon from the terminal towards the soma) [31]. One major drawback of AAV is that it leads to a substantial immune response from the host, particularly after repeated injections [27]. It is possible to reduce the immune response by changing the serotype of AAV; however, immune responses are not abolished [27]. AAV is still considered to be relatively safe for use in humans [30].

Despite its initial drawbacks, LV is becoming more widely used in both research and clinical trials [32]. LV is a retrovirus, which is derived from HIV and has an RNA genome. The RNA genome is converted to DNA after entering the host cell by the LV-encoded enzyme reverse transcriptase [28]. LV allows for a much larger insert of foreign DNA than AAV, about 9 kilobases (kb) versus 4 kb, respectively [29, 30]. Regardless of the host virus, however, the larger the insert size, the lower the titer and infection potential of the virus [27]. The diameter of LV is about 5-fold larger than AAV (~100 nm), which restricts the movement of LV through the extracellular space of the host tissue [30]. This can be a great advantage if spatial specificity of infection is desired [30]. While the first generation of LV vectors did retain a significant portion of the HIV genome, by the third generation of LV the viral genome

had been split into separate plasmids to reduce the likelihood of replication as occurred in the first viral gene therapy trial in which patients developed cancer [28]. Third generation LV provides stable, long-term expression of the introduced sequence, is considered non-pathogenic and does not result in an immune response in the host [30, 32]. Not only was the viral genome separated into multiple plasmids, but two-thirds of the LV genome was removed including all replication genes, and self-inactivation properties were introduced to prevent genes from being repackaged [29, 32].

Unlike many viruses that depend on cell division to access the host genome, LV is able to enter the nucleus of post-mitotic cells [28, 30], where it will integrate the foreign genetic material into the host DNA at random [30]. This further reduces oncogenic potential of LV by allowing for the targeting of non-dividing cells [28], which reduces the potential for oncogene activation [30]. LV tropism is the profile of glycoproteins on the surface of the viral envelope and can be changed to preferentially bind to host cell receptors, thereby increasing the likelihood of infected target cells, which is called viral pseudotyping [30]. A common LV pseudotype contains the envelope protein of another virus, VSVg. LV-VSVg diffuses only 1-2 mm from the injection site [30] and has a low efficiency for retrograde gene transfer [31], and thus it is a good tool for targeting a specific region of the brain.

Introduction to CRISPR

Once an appropriate viral vector is identified, what is the best approach to modify the host DNA? CRISPR provides an excellent option. CRISPR is a naturally occurring adaptive immune response used by some prokaryotes to protect themselves against threats such as viruses in which a DNA sequence from the virus is incorporated into the prokaryotic genome.

The prokaryote is then able to detect that the same virus in the future contains non-native DNA, thereby activating the degradation processes. Prokaryotes use Cas9, an RNA-guided endonuclease, to cleave DNA at sequences that are complimentary to the associated RNA sequence. The DNA can be repaired by either nonhomologous end-joining (NHEJ), which results in an indel mutation and may disrupt gene function, or homology-directed repair (HDR), which can use a template provided by researchers to alter the DNA. Both NHEJ and HDR are likely to produce undesired indels in the repaired DNA. Cas9 can be directed to a specific site using designed guidance RNA sequences, however there are guidance RNA sequence and length requirements for Cas9 to function appropriately. Specifically, the sequence must be 20 nucleotides long and adjacent to the DNA motif “NGG”, in which N can be any nucleotide. Within these 20 nucleotides, the closer the targeted cleavage site is to the NGG motif the more accurate the splicing will be. Both Cas9 and the guidance RNA must be provided in a research-directed CRISPR experiment in eukaryotic cells. Off-target effects in which the Cas9 edits DNA regions in addition to the target location can be predicted with online software and may or may not predict possibly damaging effects such as an off-target effect in a critical gene for cell function. [33] One group has generated a modified Cas9 system that also contains a mechanism for self-degradation of Cas9. This would allow Cas9 to target the DNA sequence it can most efficiently bind and cleave, ideally the target location, but degrade Cas9 before it can have detrimental off-target effects [28]. There are several ethical issues to consider when utilizing the CRISPR/Cas9 system, including deciding which genetic diseases warrant being corrected [33] and the history that this editing system has led to deadly inflammatory responses or to oncogene activation and subsequent leukemia in a small number of cases [34].

Viral gene therapy

Both LV and AAV vectors have been used to deliver Cas9 and guidance RNA to target tissues [28, 34]. One experimental option would be to repeatedly inject different serotypes of AAV containing both Cas9 and a guidance RNA into the ventricles of KI mice. The guidance RNA would contain the wild-type DNA sequence for the region around either D120N or P11S in *Gabrb3* to allow for HDR of the Cas9 cleaved DNA to incorporate the wild-type nucleotide at the site of the point mutation. The combination of this injection location and the small size of AAV would allow for broad diffusion of the virus into many brain regions. Changing the serotype would reduce the immune response to each injection. Repeated injections would be desired to infect as much tissue as possible. It would also be possible to deliver a continuous dose of AAV into the ventricle for several days via an osmotic pump. Such pumps are not currently approved for use in humans; however, there are both oral and peripherally implantable osmotic pumps that are safe for humans [35]. Oral pumps deliver a continuous dose for 8-24 hours while implantable pumps can function for up to 1 year. While traditional AAV does not cross the blood-brain-barrier (BBB), new variations of AAV have shown promise at crossing the BBB [36]. A peripherally implanted osmotic pump could be used to deliver this new BBB-crossing AAV containing both Cas9 and appropriate guidance RNAs for several weeks while immune response is monitored. This would reduce the risk of a direct injection into the central nervous system and the associated infection potential. Additionally, the brain's blood supply would enable delivery of AAV throughout the entire brain. This type of technology is likely far from being approved for use in humans; however, proof-of-principle experiments in rodents would promote further safety adaptations and technology development.

Both seizure activity and behavioral abnormalities would be monitored at 1, 3, 6, and 12 months from beginning any of the above therapies to identify how long the therapies need to take effect and to determine the longevity of their impact.

An interesting variation on these experiments would be to use Cas9 to generate indels in the mutated gene only leaving the wild-type gene intact. Appropriate homologous recombination using the guidance RNA is not always efficient, which is why the virus would be delivered on a long-term schedule. Indels, however, are more easily achieved and may result in the mutated gene no longer producing stable a RNA or protein [34]. This would effectively result in a heterozygous knock-out, which appears to be substantially less severe in animal models [37, 38]. While a complete recovery of gene function would be ideal, this could serve as a back-up method for treating severe cases, which would yield incomplete but substantial recovery when homologous recombination to fully repair the mutated DNA proved difficult.

Future directions: using viruses to further scientific knowledge

Aside from use of gene therapy as a therapeutic tool, it can also be used experimentally to provide better understanding of the circuitry involved in the pathology of epilepsy and associated cognitive dysfunction. Targeting gene therapy to specific brain regions such as the nRT or hippocampus could help elucidate the specific roles of those regions in disease presentation. Additionally, the mutations themselves could be introduced in a region-specific manner using a Cre/loxP system, or in a time-specific manner, such as after normal circuitry

development, using an inducible Cre/loxP system. There are several existing animal models of neurological diseases that have successfully treated with viral therapy, including the treatment of Huntington's disease, Rett syndrome, and Parkinson's disease. Therefore, the use of viruses to explore the disease processes behind epilepsy and potentially discover new therapeutic approaches has great potential. Overall, there are several research questions that can be addressed with the help of viral gene therapy. First, is any brain region either necessary or sufficient for any one seizure or behavioral phenotype, or for any combination of them? Second, after development is allowed to proceed normally, what is the result of either globally or regionally inducing a mutation? Alternatively, after abnormal development, is eliminating the mutation either globally or regionally capable of rescuing the epilepsy? Before constructing experiments to address these questions, several concepts need to be introduced, including rabies virus, the Cre/loxP system, and genetic promoters.

Introduction to rabies virus

The rabies virus (RV) is a negative-strand RNA virus, which infects neurons exclusively in a retrograde direction. After entering axon terminals, RV spreads throughout the neuron and crosses conventional synapses in a retrograde fashion to infect additional cells [39]. This property makes RV both a very useful and a very dangerous tool. RV glycoprotein (G) is required for RV packaging and trafficking retrogradely across synapses. Deletion of the G gene from the RV genome (G-deleted RV) disables its ability to spread beyond the initially infected cell population unless an alternative form of G gene is provided. If the G is provided *trans* in cells infected with G-deleted RV (G-*trans* RV), RV is able to cross synapses a single time, allowing it to infect cells mono-synaptically connected to the initially infected

population. These two recombinant versions of RV are also able to carry exogenous DNA for any gene of interest. [39] Therefore, genes of interest, including those for fluorescent labels and genetic tools such as Cre (discussed in detail below), are able to be delivered to 1) cells whose axons project to the injection site, 2) cells mono-synaptically connected to the initially infected cells, or 3) all cells in any circuit connected to cells projecting to the immediate injection area.

There are two major drawbacks to consider when using any form of RV aside from the level of personal protection that is required. First, RV will induce cytotoxicity in infected neurons within 4 to 11 days of infection [39], providing a narrow time window within which to work. Second, because RV is an RNA virus and never in its lifecycle produces DNA, researchers cannot employ promoter-specific expression of transgenes using RV infection [39].

As was true for AAV, the glycoprotein signature on the envelope of RV is important and able to be varied beyond just its deletion in the G-deleted RV. EnvA and EnvB are envelope proteins identified in avian sarcoma leucosis viruses, and they bind to TVA and TVB receptors, respectively, which are not natively expressed in mammals. Using the G-deleted RV described above, G is replaced by a chimera consisting of the ectodomain of either EnvA or EnvB and the cytoplasmic domain of G. The chimera-containing virus is then only able to infect cells that have been made to express TVA or TVB, which is primarily achieved through either a transgenic knock-in approach or using the Cre/loxP system described below. [39]

Introduction to the Cre/loxP system

There are two main components to the Cre/loxP system: a transgene encoding Cre recombinase and a section of DNA flanked by two loxP sequences. Each loxP sequence contains two 13-base pair palindromic sequences around an 8-base pair core sequence. Cre recombinase recognizes these two loxP sequences and canonically catalyzes permanent excision of the DNA between the two loxP sites. In the absence of Cre, expression of the loxP-flanked (or “floxed”) DNA is normal. [29]

There are several common manipulations of the Cre/loxP system, often in conjunction with each other. The first method uses pairs of loxP and lox511, a mutated form of loxP, together to invert a section of DNA simultaneously turning off one gene (by inverting a critical exon) and turning on another gene (often a reporter gene that was previously inverted and is now able to be transcribed) [40]. In this case, only one loxP and one lox511 site remain, rendering the change irreversible as this combination is unable to trigger another Cre-mediated event. Second, STOP codons preceding a gene for a reporter such as LacZ or green fluorescent protein (GFP) will express the reporter once the stop codon is excised by Cre [29]. Alternatively, an internal ribosomal entry site (IRES) can be inserted between the gene for Cre and a reporter gene such that in any cell where Cre is expressed the reporter will also be expressed [41].

The remaining methods fall under two main categories: spatial control and temporal control. Spatial control, often referring to cellular-subtype specificity, is best exerted through the use of genetic promoters. Genetic promoters are DNA sequences usually located nearby and upstream of transcription start sites [42]. Promoters allow for highly regulated transcriptional control, and the promoters for many genes have been identified. By inserting a DNA sequence containing a characterized promoter followed by *Cre*, *Cre* transcription is able

to be controlled in the same temporal and spatial manner as the genes canonically controlled by that promoter. There are many available mouse lines that contain such sequences, and relevant lines are listed in Table 1.

| Common name or abbreviated name | Full name | Specificity |
|----------------------------------------|------------------|--------------------|
|----------------------------------------|------------------|--------------------|

| | | |
|-----------------|----------------------------------------------------|---------------------------------------------------------------------------|
| Arc | Activity regulated cytoskeletal-associated protein | Activated neurons in the hippocampus during memory encoding and retrieval |
| Cal | Calretinin, also called calbindin 2 | Cal+ GABAergic neurons |
| CaMKII α | Calcium/calmodulin-dependent protein kinase II | Glutamatergic neurons |
| CMV | Cytomegalovirus enhancer/promoter element | All cell types |
| Drd1a | Type 1a dopamine receptor gene | Pyramidal cells in cortical layer 6 that project to thalamus |
| GAD67 | Glutamate decarboxylase 67 | GABAergic neurons |
| Grik4 | Ionotropic glutamate receptor kainate 4 | Pyramidal cells and CA3 of the hippocampus |
| Nest | Nestin | Neuronal and glial cell precursors |
| NPY | Neuropeptide Y | NPY+ GABAergic neurons |
| POMC | Pro-opiomelanocortin-alpha | Granule cells of the dentate gyrus of the hippocampus |
| PV | Parvalbumin | PV+ GABAergic neurons |
| Sst | Somatostatin | Sst+ GABAergic neurons |
| Syn | Synapsin 1 | Neurons |
| Vgat | Vesicular inhibitory amino acid transporter | GABAergic neurons |
| Vglut2 | Vesicular glutamate transporter 2 | Glutamatergic neurons |
| VIP | Vasoactive intestinal polypeptide | VIP+ GABAergic neurons |
| WFS1 | Wolframin | Glutamatergic neurons in hippocampus CA1 |

Table 1: Commercially available (via Jackson Labs, www.jax.org) promoter-driven Cre mouse lines relevant to the LGS and CAE mouse models, listed according to the gene canonically controlled by that promoter.

There are several tools for exerting temporal control. First, Cre may be substituted for CreER, a chimeric protein consisting of Cre fused to the tamoxifen-binding domain of the human estrogen receptor α , which is able to be activated only by tamoxifen, often administered intraperitoneally for several consecutive days [30, 43]. Alternatively, Cre can be delivered directly into the brain using stereotactic injections of Cre packaged into either LV [44] or AAV [43]. There are also promoters that may be induced by drugs, metal ions, heat shock, or hormones [30]. The Tet-On/Off system is one of the most widely used inducible promoter systems and is derived from antibiotic-resistant *E. coli* and the herpes simplex virus [30]. In this system, the exogenous DNA is downstream of a promoter containing a Tet response element (TRE) to which the interchangeable antibiotics tetracycline or doxycycline (DOX) can bind. DOX is typically provided in daily water or food and can be administered indefinitely. In the Tet-On system, the Tet repressor is fused to a portion of virion protein 16 of the herpes simplex virus (VP16), which contains the tetracycline-controlled transactivator (tTA). When tTA binds to the TRE, DOX is able to activate the promoter. In the Tet-Off system, tTA binds to the TRE when DOX is not present. Therefore, when DOX is administered it represses the promoter and stops transcription of downstream genes. [30] Each of these methods have different advantages or disadvantages allowing researchers to craft experiments best suited to the study design or goals.

Proposed experiments

As was mentioned above, the principle experimental questions are, briefly: is any brain region sufficient or necessary for restoring function in an epilepsy model, or is any brain region sufficient or necessary for causing epilepsy in a wild-type mouse? Additionally, viruses can be

used to aid in the discovery of how circuitry and biochemical processing are affected in KI mice. As was discussed in the previous chapters, circuitry relating to the development of LGS is poorly understood. Thalamocortical circuitry has been established as being heavily involved in absence seizures, but how this relates to the behavioral comorbidities associated with CAE is not understood. Further experiments could help identify what circuits are involved in these disorders, which could allow for even further experiments into the specific dysfunction of those circuits. This would significantly advance the field not only in basic understanding, but also in identification of new therapeutic targets. First, experiments using mice that we already have generated or mice readily available for purchase will be proposed, followed by experiments that would require generation of a new variation of the knock-in mice.

1. Using CRISPR to restore function.

We have not had success with injection of wild-type guidance RNA for *Gabrb3*^{+/*D120N*} and Cas9 packaged into AAV and injected into the temporal vein at P0, so the following is a modification of that experiment to attempt to increase the chance of success. KI mice will be crossed with Cas9 mice available from Jackson Laboratories to generate *Gabrb3*^{+/*D120N*;Cas9} and *Gabrb3*^{+/*P11S*;Cas9} mice. The benefit of taking the time to generate these crossed mice is that the *Cas9* gene is quite large and limits the size of additional genetic material that can be packaged into LV or AAV, which may also reduce the titer and therefore the efficacy of the virus to infect many cells. Guidance RNA will be prepared containing the wild-type *Gabrb3* sequence that flanks either D120 or P11 and packaged into LV (β 3-LV or β 3-AAV referring to either condition, or β 3^{*P11*}-LV or -AAV and β 3^{*D120*}-LV or -AAV referring to the individual

conditions). Where Cas9 and the guidance RNA are both present, the mutation will be replaced with the wild-type $\beta 3$ sequence.

a. Global restoration from birth.

Using a globally expressed CMV-Cas9 will allow for all cells to obtain the wild-type *Gabrb3* sequence. The $\beta 3$ -AAV would be modified to also contain the sequence for mCherry, a red fluorescent protein, to allow for post-mortem identification of positively infected cells ($\beta 3$ -mCherry-AAV). Injection of $\beta 3$ -mCherry-AAV into the temporal vein in the first two days of life allows for sustained, whole body-wide expression of the virus [45]. AAV was chosen for this experiment due to its relatively small size. The virus will hopefully penetrate the entire brain and will enable a substantial number of cells to express wild-type *Gabrb3*. This experiment will show if this method of genetic modification is effective, serving as a comparison for the following experiments.

- i. **Assessment strategy:** In-person monitoring, video monitoring, electrophysiological, and behavioral experiments are fairly quick assessments of whether or not the epilepsy phenotype has been abolished or reduced. Video-EEG will also be valuable; however, it is more time consuming so an indication that the experiment has worked first would be valuable. These assessments would take place 1-3 months following injection. Experimental mice will be compared to littermates of the same genotype that received an injection of empty viral vector and identical treatment otherwise.

b. Global restoration after birth.

Using the same CMV-Cas9 as in experiment 1a but instead injecting $\beta 3$ -mCherry-AAV at different ages bilaterally into the ventricles would indicate whether normal function can be restored after abnormal development and onset of seizures. Again, this is useful before probing specific areas to see if they are capable of restoring function on their own. Ages of interest include P18 (marks the end of cortical neuron maturation), P30 (puberty, also the weaning age for *Gabrb3*^{+/*D120N*} mice), P60 (sexual maturity, beginning of adulthood), P200 (later-stage adulthood). These ages would help determine how far disease progression could occur and still be ameliorated with a genetic strategy. The same assessment strategy as is outlined in 1ai would be followed.

c. Regional restoration using promoters.

Mice are available with Cas9 transcription driven by various promoters, but because this strategy would require generation of multiple mouse lines, it is not the optimal way to assess regional restoration of $\beta 3$ function. Instead, Jackson Laboratories carries a Cre-driven Cas9 mouse that would be more practical. These mice (strain #026175) have Cre-dependent expression of Cas9 and GFP driven by the CAG promoter (based on CMV) that expresses in all cell types). Depending on when and where Cre is provided, expression of Cas9 can be regionally and temporally controlled. GFP serves as a marker for cells that also transcribed Cas9. $\beta 3$ -AAV would be packaged with one of the following promoter-driven Cre sequences and injected into either the temporal vein (P0-2) or bilaterally into the ventricles using a stereotax (P18, P30, P60, P200), after

which the animals would be assessed according to the protocol outlined in 1a. Injection into the ventricles is not guaranteed to produce potent infection of the entire brain, so it is possible that only the temporal vein strategy will prove useful for targeting specific brain regions. Importantly, the specificity of promoters is not absolute [30] so assessment of which cells are GFP+ post-mortem would be essential. mCherry is not necessary to package into this virus as GFP is present in the Cas9 animal.

- i. **Layer 6 pyramidal cells.** The *Drd1a* promoter has been shown to selectively express in layer 6 cortical cells that project to the thalamus, a primary component of the thalamocortical circuit that is disrupted in both the LGS and CAE models.
- ii. **Glutamatergic neurons.** The *Vglut2* promoter allows for selective infection of glutamatergic neurons. This would allow for $\beta 3$ subunit restoration in the excitatory cells of both the cortex and thalamus. This experiment would indicate the degree to which the major disruptions observed in both the LGS and CAE mice are due to changes in the inhibitory drive on glutamatergic neurons.
- iii. **GABAergic neurons.** The *Vgat* promoter allows for selective infection of GABAergic neurons. This experiment would be particularly interesting because GABAergic synapses are largely located on glutamatergic neurons; however, the GABAergic cells of the nRT regulate thalamocortical synchrony via their projections back onto the nRT itself. The timing of these feedback projections is thought to be

critical for thalamocortical oscillations so it is possible that restoring function to just the nRT could disrupt the abnormal oscillatory activity seen in both KI mice.

d. Regional restoration using stereotactic injections.

The hippocampus is of particular interest in the LGS model as hippocampal memory was shown to be disrupted in Chapter 3 and other research on atypical absence seizures has indicated that the hippocampus may be involved. Stereotactic injections of $\beta 3$ -mCherry-AAV bilaterally into the hippocampi of *Gabrb3^{+ / D120N}* mice as young as P7 [46] would reveal if it is possible to prevent the development of atypical absence seizures by restoring normal hippocampal function. This could possibly solidify the role of the hippocampus in atypical absence seizures, which are poorly understood and remain difficult to treat.

2. Using CRISPR to induce dysfunction.

The principle advantage to this research strategy is that, because these experiments are conducted in wild-type mice, neuronal development is normal. Additionally, while $\beta 1$ and $\beta 2$ subunits have not been shown to compensate for the loss of $\beta 3$ subunits [38], this variable would be eliminated, as would any changes in synapse or receptor number that occur as compensation for the loss of inhibition. All experiments will be assessed in the same manner as is described in 1ai.

a. Global induction at birth.

This experiment will be performed in the same manner as 1a, using a globally expressed CMV-Cas9 and injecting $\beta 3$ KI-AAV into the temporal vein, but using guide RNA containing the sequence for either mutation (generally

referred to as β 3KI-AAV, or with mCherry as β 3KI-mCherry-AAV). This experiment will shed light on to what extent LGS or CAE is caused in the KI mice by abnormal development that results from having the mutation present from conception. If β 3KI-mCherry-AAV is successful in causing phenotypes similar to those originally described, it would be interesting to continue with the following more specific mutation induction protocols.

b. Global induction after birth.

Using the CMV-Cas9 animal, β 3KI-mCherry-AAV would be injected at different ages bilaterally into the ventricles in the same manner as 1b. It would be best to conduct these experiments no earlier in development than P18, and perhaps not until P30 after more neuronal maturation is complete and mice have been weaned and adjusted to their new housing environment.

c. Regional induction using promoters.

As in 1c, using Cre-dependent Cas9 and promoter-driven Cre packaged into β 3KI-AAV, each mutation can be induced only in select brain regions. As a reminder, GFP is present in the Cas9 animal as a post-mortem marker for positively infected cells.

- i. **Layer 6 pyramidal cells.** Again, using the *Drd1a* promoter as in 1ci, the mutations would be induced in only the corticothalamic projection neurons. Being a large population of neurons, the contribution of this population to LGS and CAE would be clearer.
- ii. **Glutamatergic neurons.** Again, using the *Vglut2* promoter to target glutamatergic neurons, including those in the cortex and thalamus, the

role of the excitatory drivers would be clearer. Additionally, while targeting just the layer 6 pyramidal cells above provides some information, disrupting both the cortical and thalamic excitatory neurons while maintaining the nRT's ability to intervene on thalamocortical oscillations would be interesting.

- iii. **GABAergic neurons.** The *Vgat* promoter allows for selective infection of GABAergic neurons. This experiment would be particularly interesting because GABAergic synapses are largely located on glutamatergic neurons; however, the GABAergic cells of the nRT regulate thalamocortical synchrony via their projections back onto the nRT itself.

3. Using loxP and lox511 to manipulate mutation expression.

This experiment would require generation of new mice. Using one pair of loxP sites and one pair of lox511 sites, the wild-type exon where the mutation site is located would be followed by the inverted mutant exon. This would allow for the wild-type exon to be expressed unless Cre is present, in which case the lox sites work together to first flip the mutant exon and then excise the wild-type exon. This change is permanent, and the mutant exon will now be expressed. For *Gabrb3*^{+/*D120N*} mice this is exon 4, and for *Gabrb3*^{+/*P11S*} mice this is exon 1A. If these mice were crossed with a CMV-Cre mouse, any mouse containing both the mutant allele and Cre would have global expression of the mutation from conception. Alternatively, if Cre is supplied later in life, the mouse can develop normally but the researcher has control over when and where the mutation is expressed.

a. Using RV and LV to explore connectivity.

Using a retrograde virus such as RV to supply Cre would provide unique insight into the relationship between connectivity and function [39]. Due to the toxic nature of RV, LV-RV chimeras have been developed. LV pseudotyped with VSV-G is inefficient at retrograde gene delivery [31] and is limited to a 1-2 mm spread from the injection site [30]. However, if the VSV-g pseudotype is combined with select RV glycoproteins to create the chimera, Rbg-LV, the viral contents are delivered locally and are also efficiently transported to the cell body after transduction at the axon terminal but they cannot progress across additional synapses as the virus will no longer have its envelope [30, 31]. Both high efficiency retrograde gene transfer (HiRet) and neuronal-specific retrograde gene transfer (NeuRet) versions of Rbg-LV have been generated [31]. HiRet is very effective at transducing dividing cells whereas NeuRet only transduces mature cells, highly reducing the risk of oncogenesis [31]. NeuRet can be constructed to deliver promoter-driven Cre to provide not only regional specificity but also cell-type specificity of transduction [39]. The following experiments would be done at similar ages as the other experiments (P7, P18, P30, P60, P200) and would use the same assessment strategy as is outlined in 1ai. All of the following constructs would also carry mCherry for post-mortem identification of infected cells.

i. Infection of glutamatergic neurons of the VBn and cortex.

Stereotactically delivering NeuRet-Vglut-Cre into the VBn would allow for infection and transduction of the glutamatergic cells of the VBn and

the glutamatergic cells of the cortex that project to the VBn, which are two of the three principal components of thalamocortical oscillations. We know that thalamocortical oscillations are an important component of both LGS and CAE mice, but this experiment would indicate to what extent activating the excitatory component of this pathway contributes to each disorder.

- ii. **Infection of GABAergic neurons of the nRT.** Stereotactically delivering NeuRet-Vgat-Cre into the VBn would allow for infection and transduction of the GABAergic cells in the nRT that project to the nRT and which are critical for controlling thalamocortical oscillations. This strategy would be particularly useful as the nRT itself is very difficult to target. The nRT functions to either interrupt or drive thalamocortical oscillations, so while I would not expect full disease development from this experiment, it would still be interesting to see exactly how the two mutations interrupt nRT and thalamocortical function.
- iii. **Infection of the entire thalamocortical circuit.** Stereotactically delivering both NeuRet-Vglut-Cre and NeuRet-Vgat-Cre in the VBn would transduce mutant expression in all three components of the thalamocortical circuitry. This experiment is predicted to cause the full presentation of CAE as thalamocortical abnormalities are so prominent in that disorder. Using the *Gabrb3*^{+/*D120N*} mice, this experiment would show to what extent this circuitry is responsible for the complex phenotype of LGS. This could be further combined or compared to

injections with other promoter-driven Cre constructs to identify what other structures are heavily involved in LGS pathology.

- iv. Infection of the hippocampus.** As an additive to 3aiii above, CMV-Cre LV stereotactically injected into the hippocampus would provide mutant expression of only local hippocampal neurons. With mutation expression only in the thalamocortical circuit and the hippocampus, it is possible that the entire LGS phenotype could be recapitulated. Additionally, as some CAE patients do have cognitive difficulties, perhaps we would find that the hippocampus is indeed critical for CAE pathogenesis.

4. Using HA or quantum dots to yield more precise information.

Because D120N is located inside the GABA binding pocket, it is not predicted to have any major effect on translation, assembly, or trafficking. It is easy to see how D120N disrupts GABAergic signaling, particularly given the experiments showing that with increased GABA concentration, current kinetics can be restored in D120N-containing receptors [6]. However, the location of P11S in the signal peptide domain has left us wondering how, if it is meant to be cleaved, is the mutation causing CAE? I hypothesize that the mutant protein is either inefficiently cleaved, incorrectly cleaved, or that the signal domain behaves inappropriately after cleavage. To determine the mechanistic effect of P11S, it would be helpful to have more information on where the signal peptide is located.

a. Using HA to visualize post-mortem proteins

This experiment would require generation of a new mouse with an HA tag located in the signal peptide. There are some drawbacks to this approach including that the tag could itself disrupt cleavage or function of the subunit, and the process of generating the mouse. However, the specificity of HA tagging the mutant protein would be guaranteed and only standard immunofluorescence would need to be conducted post-mortem. It would be possible to identify the subcellular location of any HA present in the cells [30]. Ideally, cells would show little to no presence of HA as the signal peptide should be degraded after cleavage. However, if its presence is detected at the cell surface, in the cytoplasm, or in the endoplasmic reticulum or in lysosomes, we would have more understanding of how P11S is disrupting normal cell function.

b. Using quantum dots to visualize *in vivo* proteins

If, in the future, better means of live-imaging intracellular proteins *in vivo* are developed, it would be extremely useful to apply to this scenario. For example, if quantum dots were more readily incorporated into living, healthy cells, they could be utilized to specifically tag and visualize movement of the signal peptide. Quantum dots are very small (2-10 nm) with two layers of heavy metal semiconductors each with a very narrow and disparate bandgap (the energy required to excite an electron). Excitation and absorption of energy result in the release of a photon that falls within a narrow wavelength range. Quantum dots are 20 times brighter and 100 times more stable than traditional fluorophores

such as GFP or mCherry. [47] Quantum dots allow for ultrasensitive detection *in vivo* or *in vitro* and can be conjugated to many biomolecules. Quantum dots would be conjugated to GABA (qGABA) and applied to primary neuronal cultures prepared from cortical neurons obtained from either KI mouse model. Synaptic activity would be monitored to determine where the signal peptide is located and how much of it remains.

These experiments will help us identify the relationship between circuitry and disease. By parsing out the roles of various brain regions by either restoring function or inducing dysfunction to observe the impact on epilepsy progression could highlight potential avenues for therapy. For example, if dysfunction in the nRT is shown to be critical for LGS pathogenesis, therapies can be developed to target the nRT. This could include things such as deep brain stimulation to sense and alter nRT activity remotely. There are promising rodent studies that have shown that detection and interruption of thalamocortical oscillations can halt absence seizures [48]. Similar approaches could be employed to target key disrupted circuits in LGS and CAE. Application of that principle here, to more complicated circuitry, could be possible once the disease circuitry is better understood. Once circuits were found to be disrupted, more specific work could be done to identify specific alterations in those circuits. For example, perhaps GABAergic inhibition is disrupted only in neurons that receive input from one of many subtypes of GABAergic interneurons. This would allow for therapies targeted to these connections. Alternatively, we have indicated that the mechanism behind LGS in the *Gabrb3^{+D120N}* mice could be that GABA_A receptors require substantially more GABA to achieve currents with an amplitude similar to non-mutant receptors. Perhaps then a

GABA-reuptake inhibitor targeted to the brain regions identified as impacted in the above experiments could alleviate some of the symptoms. The development of these mice and establishing them as robust models for LGS and CAE provides the epilepsy community with ample opportunity to better understand and treat these chronic disorders, which will hopefully contribute to improving patient care and quality of life.

Bibliography

1. Panayiotopoulos, C.P., in *The Epilepsies: Seizures, Syndromes and Management*. 2005: Oxfordshire (UK).
2. Jahngir, M.U., M.Q. Ahmad, and M. Jahangir, *Lennox-Gastaut Syndrome: In a Nutshell*. Cureus, 2018. **10**(8): p. e3134.
3. Stommel, E.W., et al., *Cryptogenic epilepsy: an infectious etiology?* *Epilepsia*, 2001. **42**(3): p. 436-8.
4. McTague, A., et al., *The genetic landscape of the epileptic encephalopathies of infancy and childhood*. *Lancet Neurol*, 2016. **15**(3): p. 304-16.
5. Kerr, M., G. Kluger, and S. Philip, *Evolution and management of Lennox-Gastaut syndrome through adolescence and into adulthood: are seizures always the primary issue?* *Epileptic Disord*, 2011. **13 Suppl 1**: p. S15-26.
6. Janve, V.S., et al., *Epileptic encephalopathy de novo GABRB mutations impair GABAA receptor function*. *Ann Neurol*, 2016.
7. Lachance-Touchette, P., et al., *Screening of GABRB3 in French-Canadian families with idiopathic generalized epilepsy*. *Epilepsia*, 2010. **51**(9): p. 1894-7.
8. Mullen, S.A., S.F. Berkovic, and I.G. Commission, *Genetic generalized epilepsies*. *Epilepsia*, 2018. **59**(6): p. 1148-1153.
9. van Luijtelaa, G., F.Y. Onat, and M.J. Gallagher, *Animal models of absence epilepsies: what do they model and do sex and sex hormones matter?* *Neurobiol Dis*, 2014. **72 Pt B**: p. 167-79.
10. Shneker, B.F. and N.B. Fountain, *Epilepsy*. *Dis Mon*, 2003. **49**(7): p. 426-78.
11. Tenney, J.R. and T.A. Glauser, *The current state of absence epilepsy: can we have your attention?* *Epilepsy Curr*, 2013. **13**(3): p. 135-40.
12. Kessler, S.K. and E. McGinnis, *A Practical Guide to Treatment of Childhood Absence Epilepsy*. *Paediatr Drugs*, 2019. **21**(1): p. 15-24.
13. Albuja, A.C. and P.B. Murphy, *Absence Seizure*, in *StatPearls*. 2020: Treasure Island (FL).
14. Tanaka, M., et al., *Hyperglycosylation and reduced GABA currents of mutated GABRB3 polypeptide in remitting childhood absence epilepsy*. *Am J Hum Genet*, 2008. **82**(6): p. 1249-61.

15. Kang, J.Q. and G. Barnes, *A common susceptibility factor of both autism and epilepsy: functional deficiency of GABA A receptors*. J Autism Dev Disord, 2013. **43**(1): p. 68-79.
16. Delahanty, R.J., et al., *Maternal transmission of a rare GABRB3 signal peptide variant is associated with autism*. Mol Psychiatry, 2011. **16**(1): p. 86-96.
17. Cortez, M.A., C. McKerlie, and O.C. Snead, 3rd, *A model of atypical absence seizures: EEG, pharmacology, and developmental characterization*. Neurology, 2001. **56**(3): p. 341-9.
18. Avoli, M., *A brief history on the oscillating roles of thalamus and cortex in absence seizures*. Epilepsia, 2012. **53**(5): p. 779-89.
19. Hortnagl, H., et al., *Patterns of mRNA and protein expression for 12 GABAA receptor subunits in the mouse brain*. Neuroscience, 2013. **236**: p. 345-72.
20. Huntsman, M.M., et al., *Reciprocal inhibitory connections and network synchrony in the mammalian thalamus*. Science, 1999. **283**(5401): p. 541-3.
21. Tanaka, M., et al., *GABRB3, Epilepsy, and Neurodevelopment*, in *Jasper's Basic Mechanisms of the Epilepsies*, th, et al., Editors. 2012: Bethesda (MD).
22. Laurie, D.J., W. Wisden, and P.H. Seeburg, *The distribution of thirteen GABAA receptor subunit mRNAs in the rat brain. III. Embryonic and postnatal development*. J Neurosci, 1992. **12**(11): p. 4151-72.
23. Vrielynck, P., *Current and emerging treatments for absence seizures in young patients*. Neuropsychiatr Dis Treat, 2013. **9**: p. 963-75.
24. Jung, S., Y. Jeong, and D. Jeon, *Epileptic activity during early postnatal life in the AY-9944 model of atypical absence epilepsy*. Cell Calcium, 2015. **57**(5-6): p. 376-84.
25. Negron-Oyarzo, I., et al., *Coordinated prefrontal-hippocampal activity and navigation strategy-related prefrontal firing during spatial memory formation*. Proc Natl Acad Sci U S A, 2018. **115**(27): p. 7123-7128.
26. Mollanoori, H. and S. Teimourian, *Therapeutic applications of CRISPR/Cas9 system in gene therapy*. Biotechnol Lett, 2018. **40**(6): p. 907-914.
27. Lundstrom, K., *Viral Vectors in Gene Therapy*. Diseases, 2018. **6**(2).
28. Milone, M.C. and U. O'Doherty, *Clinical use of lentiviral vectors*. Leukemia, 2018. **32**(7): p. 1529-1541.
29. Heldt, S.A. and K.J. Ressler, *The Use of Lentiviral Vectors and Cre/loxP to Investigate the Function of Genes in Complex Behaviors*. Front Mol Neurosci, 2009. **2**: p. 22.

30. Parr-Brownlie, L.C., et al., *Lentiviral vectors as tools to understand central nervous system biology in mammalian model organisms*. *Front Mol Neurosci*, 2015. **8**: p. 14.
31. Kobayashi, K., et al., *Pseudotyped Lentiviral Vectors for Retrograde Gene Delivery into Target Brain Regions*. *Front Neuroanat*, 2017. **11**: p. 65.
32. White, M., et al., *A Guide to Approaching Regulatory Considerations for Lentiviral-Mediated Gene Therapies*. *Hum Gene Ther Methods*, 2017. **28**(4): p. 163-176.
33. Thurtle-Schmidt, D.M. and T.W. Lo, *Molecular biology at the cutting edge: A review on CRISPR/CAS9 gene editing for undergraduates*. *Biochem Mol Biol Educ*, 2018. **46**(2): p. 195-205.
34. Lino, C.A., et al., *Delivering CRISPR: a review of the challenges and approaches*. *Drug Deliv*, 2018. **25**(1): p. 1234-1257.
35. *Drug delivery systems*, in *Strategies to Modify the Drug Release from Pharmaceutical Systems*, M.L. Bruschi, Editor. 2015, Woodhead Publishing. p. 87-194.
36. Deverman, B.E., et al., *Cre-dependent selection yields AAV variants for widespread gene transfer to the adult brain*. *Nat Biotechnol*, 2016. **34**(2): p. 204-9.
37. DeLorey, T.M., et al., *Mice lacking the beta3 subunit of the GABAA receptor have the epilepsy phenotype and many of the behavioral characteristics of Angelman syndrome*. *J Neurosci*, 1998. **18**(20): p. 8505-14.
38. Homanics, G.E., et al., *Mice devoid of gamma-aminobutyrate type A receptor beta3 subunit have epilepsy, cleft palate, and hypersensitive behavior*. *Proc Natl Acad Sci U S A*, 1997. **94**(8): p. 4143-8.
39. Osakada, F. and E.M. Callaway, *Design and generation of recombinant rabies virus vectors*. *Nat Protoc*, 2013. **8**(8): p. 1583-601.
40. Schnutgen, F., et al., *A directional strategy for monitoring Cre-mediated recombination at the cellular level in the mouse*. *Nat Biotechnol*, 2003. **21**(5): p. 562-5.
41. Michael, S.K., J. Brennan, and E.J. Robertson, *Efficient gene-specific expression of cre recombinase in the mouse embryo by targeted insertion of a novel IRES-Cre cassette into endogenous loci*. *Mech Dev*, 1999. **85**(1-2): p. 35-47.
42. Haberle, V. and A. Stark, *Eukaryotic core promoters and the functional basis of transcription initiation*. *Nat Rev Mol Cell Biol*, 2018. **19**(10): p. 621-637.
43. Li, X.G., et al., *Viral-mediated temporally controlled dopamine production in a rat model of Parkinson disease*. *Mol Ther*, 2006. **13**(1): p. 160-6.

44. Heldt, S.A., et al., *Hippocampus-specific deletion of BDNF in adult mice impairs spatial memory and extinction of aversive memories*. Mol Psychiatry, 2007. **12**(7): p. 656-70.
45. Gombash Lampe, S.E., B.K. Kaspar, and K.D. Foust, *Intravenous injections in neonatal mice*. J Vis Exp, 2014(93): p. e52037.
46. Cetin, A., et al., *Stereotaxic gene delivery in the rodent brain*. Nat Protoc, 2006. **1**(6): p. 3166-73.
47. Walling, M.A., J.A. Novak, and J.R. Shepard, *Quantum dots for live cell and in vivo imaging*. Int J Mol Sci, 2009. **10**(2): p. 441-91.
48. Paz, J.T., et al., *Closed-loop optogenetic control of thalamus as a tool for interrupting seizures after cortical injury*. Nat Neurosci, 2013. **16**(1): p. 64-70.